UNIVERSITY OF SOUTHAMPTON

Faculty of Natural and Environmental Sciences

Centre for Biological Sceinces

Improving immunotherapy for Alzheimer's Disease- determining the role of effector function in the clearance of plaques and neuro-inflammatory response

by

James Peter Fuller Bsc. (Hons), Msc. (Hons)

Thesis for the degree of Doctor of Philosophy

September 2015

UNIVERSITY OF SOUTHAMPTON

ABSTRACT

FACULTY OF NATURAL AND ENVIRONMENTAL SCIENCES

Biological Sciences

Thesis for the degree of Doctor of Philosophy

Improving immunotherapy for Alzheimer's Disease- determining the role of effector function in the clearance of plaques and neuro-inflammatory response

James Peter Fuller BSc. (hons) MSc. (hons)

Alzheimer's Disease (AD) initially presents as episodic memory loss, followed by severe cognitive deterioration leaving a patient unable to complete daily tasks. Current therapies for AD are ineffective and can only manage the symptoms in the short term, none can modify the progression of disease. The devastating impact of the disease and the world's ageing population make the development of new therapeutics an urgent unmet clinical need. One of the hallmarks of AD, still used to formally diagnose the disease, is the accumulation of the protein amyloid beta (Aβ) as extracellular deposits called plaques. Immunotherapy is a promising strategy for the treatment of AD, as antibodies directed against Aβ are able to successfully clear plaques and reverse cognitive deficits in transgenic mouse models, and now to a certain extent in humans. One issue has been the development of dose limiting side effects in the brain, where clearance of Aβ is associated with damage to the cerebral vasculature. It is though that these side effects are due to a neuro-inflammatory response, mediated by the activation of Fc gamma receptors (FcγRs) by anti-Aβ antibodies. Therefore engineering of therapeutic antibodies to reduce FcγR affinity may prevent these side effects from occurring. The role of FcγRs in the clearance of Aβ and the neuro-inflammatory response to immunotherapy has not been thoroughly investigated.

The role of antibody effector function in the clearance of plaques and the associated neuro-inflammatory response was investigated by the generation of murine anti-Aβ antibodies with different constant regions, IgG1 and IgG2a, which have different FcγR affinities. These antibodies were administered to transgenic mice via intracerebral and systemic injection, and the neuro-inflammatory response and clearance of Aβ was measured. The potential for systemic inflammation to affect the response to antibodies was investigated by the infection of transgenic APP mice with the bacterium *Salmonella typhimurium*, measuring the expression of activating FcγRs in the brain and vascular changes following infection.

I found that 3 factors that may impact on the ability of anti-Aβ antibodies to clear plaques and the strength of the neuro-inflammatory response. The effector function of antibodies is important, as antibodies with the more pro-inflammatory IgG2a constant region, were better at clearing plaques and caused more neuro-inflammation than the same antibody with an IgG1 constant region. The antibody binding specificity was also important; antibodies binding to the N-terminus of Aβ were better at clearing plaques and caused more inflammation than those binding to different regions. Finally we propose that the inflammatory state of the brain could determine the response to immunotherapy, as I show that peripheral infection is associated with enhanced activating FcγR expression in the brain.

Table of Contents

List of figures

List of Tables

Declaration of authorship

I James Peter Fuller,

declare that this thesis and the work presented in it are my own and has been generated by me as the result of my own original research.

Improving immunotherapy for Alzheimer's Disease- determining the role of effector function in the clearance of plaques and neuro-inflammatory response

I confirm that:

1. This work was done wholly or mainly while in candidature for a research degree at this University;
2. Where any part of this thesis has previously been submitted for a degree or any other qualification at this University or any other institution, this has been clearly stated;
3. Where I have consulted the published work of others, this is always clearly attributed;
4. Where I have quoted from the work of others, the source is always given. With the exception of such quotations, this thesis is entirely my own work;
5. I have acknowledged all main sources of help;
6. Where the thesis is based on work done by myself jointly with others, I have made clear exactly what was done by others and what I have contributed myself;
7. Parts of this work have been published as:

Fuller JP, Stavenhagen J, Christensen S, Kartberg F, Glennie M, Teeling J (2015) Comparing the efficacy and neuroinflammatory potential of three anti-abeta antibodies. Acta neuropathologica 130: 699-711 Doi 10.1007/s00401-015-1484-2
Fuller JP, Stavenhagen JB, Teeling JL (2014) New roles for Fc receptors in neurodegeneration-the impact on lmmunotherapy for Alzheimer's Disease. Frontiers in Neuroscience 8: Doi 10.3389/fnins.2014.00235

Signed:……

Date:……..

Publication and Presention of the work in this thesis

Peer reviewed publications:

Fuller, J. P., Stavenhagen, J. B. and Teeling, J. L. (2014). New roles for Fc receptors in neurodegeneration-the impact on lmmunotherapy for Alzheimer's Disease. *Frontiers in Neuroscience* **8**

Fuller JP, Stavenhagen J, Christensen S, Kartberg F, Glennie M, Teeling J (2015) Comparing the efficacy and neuroinflammatory potential of three anti-abeta antibodies. Acta neuropathologica 130: 699-711 Doi 10.1007/s00401-015-1484-2

Oral presentations:

H Lundbeck AS, Denmark 2012 and 2014

SoNG seminars, 2011-4

CFBS Postgrad symposium, 2015

Pint of science festival, Southampton 2015

3 minute thesis ™ University final, 2015

ARUK Conference London, 2015

Poster presentations

ARUK Conference, Birmingham 2012

ARUK Conference, Belfast 2013

Health and Pharma UIST meeting, 2013

CFBS postgraduate symposium, 2013

SoNG symposium ,2013

Antibodies for neurodegenerative disease ,Uppsala 2013

Glia in health and disease Conference, Cold Spring Harbour 2014

SoNG symposium, 2014

ARUK Conference, London 2015

Awards and Prizes

Max Perutz award 2012-Highly commended

CFBS postgraduate symposium 2013-poster prize winner

Health and Pharma UIST meeting 2013-poster prize winner

SoNG Symposium 2014- poster prize winner

ARUK Conference, London 2015- David Dawburn prize winner

CFBS Postgraduate symposium 2015- 3rd place prize for oral presentation

3 minute thesis ™ 2015-Winner of School and Faculty competition

Acknowledgements

I would like to start by saying thank you to everyone who has made my PhD such an enjoyable and valuable experience, there are so many people that have made the past four years some of the best in my life. Firstly, thank you to my supervisory team: Dr Jessica Teeling, Dr Jeffrey Stavenhagen and Professor Martin Glennie, your expert input and support have been invaluable throughout. I have had a fantastic time in both Southampton and Copenhagen, and this was in no small part due to great supervision. I really appreciate the freedom I have been given to have my own ideas and to learn from my own mistakes, and as a result I have gained so much for the last four years. Thank you in particular to Jessica for always being so positive and supportive in everything I have done, and also to Jeff for making so much effort to help me settle in during my stay in Copenhagen.

I would like to say a massive thank you to all members of the CNS inflammation group past and present. Professor Hugh Perry for feedback and input throughout my PhD and to Ursula Püentener, Patrick Garland and Diego Gomez-Nicola for their help and advice in the lab. Adam Hart, Olivia Larsson, Salomé Murinello, Alex Collcutt, Paul Ibbett and Steve Booth (who taught me everything he knew) I really appreciate the help you have given me, but most of all thank you for your friendship that has made the past four years so much fun. Thank you to Steve, Alex and Sjoerd for everything, you guys kept me sane for large parts of my PhD. From the Cancer Sciences group in Southampton, many people have helped me to produce the antibodies that were vital to my work. In particular I would like to thank Claude Chan and Alison Tutt, whose expertise in all things antibody was completely invaluable to this project. Thank you to all of the BRF staff at the hospital for help with the husbandry and breeding of animals, and to Delphine Boche, Clive Holmes and Sonja Rakic for their help and advice with human studies. Moving to a new country for the first time in my life was exciting but also slightly daunting. This transition was made so much easier by so many friendly and welcoming people at Lundbeck, who made it one of the best experiences I have had. Kasper, Rasmus, Marcel and many others, thank you for the fun times and very expensive beers! Thanks to Fredrik Kartberg, Susanne Lüder and Søren Christensen who helped in the production and characterisation of the antibodies used in chapters 6 and 7. Also to Anna Parachikova and Kate Pedersen who helped with all animal related issues, and to Kasper Larsen who helped with the surgeries.

Thank you for the hard work of undergraduate students Amanda Hyne and Sophie Thornton whose immunohistochemistry has been used in chapters 4 and 8 respectively, and to Alexander Collcutt for the scoring of nesting behaviour, and Paul Ibbett for help with the tissue collection in chapter 8.

Lastly, thanks to Lauren Malcherczyk for all of your love and support over the last four years. Thank you for understanding my grumpiness (particularly in the mornings), for sitting through countless presentations and for just generally being wonderful.

List of abbreviations

AA-Amino acid

AD-Alzheimer's Disease

ADCC-Antibody dependent cellular cytotoxicity

ALS- Amyloid Lateral Sclerosis

ANOVA- Analysis of variance

APO Apolipoprotein

APP-Amyloid Precursor Protein

ARIA E-Amyloid related imaging abnormality (vasogenic edema)

ARIA H- Amyloid related imaging abnormality (micro-haemorrhage)

Aβ –Amyloid beta

BBB-Blood brain barrier

BSA-Bovine serum albumin

CA-Cortical area

CAA-Cerebral amyloid angiopathy

CDR-Complementary determining region

CFA-Complete Freunds Adjuvant

CFU-Colony forming units

CH-Heavy chain constant region

CK-Kappa chain constant region

CNS -Central Nervous System

CSF-Cerebro Spinal Fluid

CVO-Circumventricular organ

DAB-3,3 Diaminobenzidine

ELISA-Enzyme linked imunosorbent assay

EU-Endotoxin units

FcRn- The neonatal Fc receptor

FCS-Fetal calf serum

FcyR- Fc gamma recptor

FDC-Folicular dendritic cell

HC-Hippocampus

HRP-Horseradish peroxidase

I.C.-Intra-cerebral

IFN –Interferon

KC-Keratinocyte chemoattractant

IgG- Immuno gamma globulin

IL-Interleukin

iNOS-Inducible Nitric Oxide Synthase

I.P.-Intraperitoneal

IRR.-Irrelevant

ITAM-Immuno tyrosine activating motif

ITIM-Immuno tyrosine inhibitory motif

I.V.- Intravenous

kDA-Kilo Dalton

LAL-Limulus amebocyte lysate

LPS-Lipopolysaccharide

LRP1-Low density lipo-protein receptor 1

LTP-Long term potentiation

MAC-membrane attack complex

MCI-Mild cognitive impairment

MHC-Major-histocompatability complex

MMP-Matrix metallo-proteinase

MRI-Magnetic resonance imaging

NFT- Neurofibrillary tangle

NO-Nitric oxide

OCT-Optimum cutting temperature

PAMP-Pathogen associated molecular pattern

PRR-Pattern recognition receptor

PBS- Phosphate buffered saline

PD-Parkinsons disease

PET-Positron emission topography

PI3K -Phospho-inositol 3 kinase

PLC-Phospholipase C

PrPc -The cellular prion protein

PrPsc-The scrapie prion protein

ROS-Reactive oxygen species

S. typhimurium-Salmonella enterica typhimurium

S.D. Standard deviation

SYK-Splenic tyrosine kinase

TGF- Transforming Growth Factor

TG-Transgenic

TNF-Tumour necrosis factor

TLR-Toll-like receptor

VH- Heavy chain variable domain

VK-Kappa chain variable domain

WT-Wild type

Chapter 1: General introduction

1.1 1.1 An introduction to the brain

1.1.1 Neurons, the basis of brain function

Neuronal cells enable the rapid transmission of information throughout the body via electrical impulses. In general, neurons have a cell body (soma) which contains the nucleus and other organelles, projections named dendrites which receive signals from other neurons, and an axon which projects and signals to other neurons sometimes metres away from the cell soma (For references to this section see Purves 2008). An electrical potential is created across the plasma membrane of a neuron (-70mV), mediated by continuously pumping Na+ ions across the membrane; this is called "the resting potential". Neurons are able to transmit electrical signals from their dendrites to the end of their axon. This is mediated by voltage-gated ion channels, which open in response to nearby membrane depolarisation, allowing ions to flow across the membrane. Therefore if the membrane is depolarised in a dendrite, this causes the opening of nearby ion channels and the depolarisation of an adjacent part of the membrane. This process is repeated, conducting the electronic signal down the length of the neuron. Individual neurons are connected to one another by structures called synapses, which are found between the axon of one neuron and a dendrite of another. At a synapse, the electronic message that has passed down the axon of the first neuron, causes the release of chemicals called neurotransmitters into the synapse, for example acetylcholine. This neurotransmitter then binds to a receptor on the post synaptic cleft (e.g. glutamate receptors NMDA), which opens an ion channel (i.e., a Na+ channel), and induces the depolarisation of the second neuron. Neurons are organised into networks, which connect together via synapses forming electrical circuits, which form the basis of brain function. Damage or dysfunction of synapses has been implicated in neurodegenerative diseases, including Alzheimer's disease.

1.1.2 Glial cells

Neurons are not the only cell type in the central nervous system (CNS), they are ably supported by a range of neuro-glial cells. There are four different types of glia within the CNS: astrocytes, oligodendrocytes, microglia and pericytes each with highly specialised functions. Microglia are the CNS resident phagocytes and make up 10% of cells in the CNS, which like other tissue

macrophages are derived from myeloid progenitor cells that develop in the yolk sac and enter the CNS in the early stages of development (Ginhoux et al., 2010). Microglia have a wide range of functions, playing an active role in shaping neuronal circuits by pruning of synapses during development and are also important for the regulation of synaptic plasticity by release of soluble factors such as cytokines IL-1β and TNFα (Hulse et al., 2008; Paolicelli et al., 2011). In the healthy CNS microglia have often been described as "resting", however this is misleading as microglia are actually incredibly active. Microglial processes continuously extend and retract, surveying their surrounding microenvironment for damage to the CNS or apoptotic cells (Nimmerjahn et al., 2005a). Microglia express a range of receptors enabling them to sense danger to the CNS, including pattern recognition receptors (PRRs) and cytokine receptors. If invading pathogens or mis-folded proteins are detected, microglia become activated, adopting a more amoeboid like morphology and attempt to remove the threat to the CNS. This activation has been linked with many neurodegenerative conditions such as: Parkinson's Disease, Amyotrophic Lateral Sclerosis (ALS, or Motor Neuron Disease), HIV related dementia and Alzheimer's disease (Garden, 2002; Peress et al., 1993; Rogers et al., 2007). Astrocytes provide trophic and metabolic support to neurons, this is highly important when you consider the distances that neuron projections can travel from the cell soma. Astrocytes also take up and release neurotransmitters aiding synaptic function, and their end feet completely envelop cerebral blood vessels regulating the uptake of ions and water into the brain. Oligodendrocytes myelinate neurons in the brain, surrounding axonal projections in myelin sheaths to increase the speed of electrical transmission. Pericytes partially surround brain endothelial cells, and one of their functions is to maintain the integrity of the blood brain barrier (BBB) (Zlokovic, 2008).

1.1.3 BBB and immune privilege

Neurons require large amounts of energy and oxygen for optimal function, and although the brain only accounts for roughly 2% of body mass, it requires over 20% of total blood flow (Zlokovic, 2008). This means that the CNS requires a rich supply of blood, delivered by a huge network of capillaries spanning around 400 miles. It was observed over 100 years ago, that the brain was protected from pharmacological effects and that histological dyes couldn't penetrate into the brain parenchyma (Zlokovic, 2008). This led to the theory that there was a barrier between peripheral blood flow and the CNS, which was further supported by the brain's protection from the effects of the peripheral immune system- or "immune privilege". This is due to the blood brain barrier

(BBB), a highly complex structure which tightly regulates the entry of cells and proteins into the brain (Zlokovic, 2008). Figure 1.1 shows the structure of the BBB (taken from (Feng et al., 2015)). The BBB is a highly specialised structure, composed of a number of cell types which are adapted to restrict the entry of solutes into the brain and are collectively named the neurovascular unit. Brain endothelial cells are different to those found in peripheral blood vessels, this is due to adaptations at the border between cells-called tight junctions. Tight junctions reduce the transport of solutes through the extracellular pathway, therefore reducing non-specific diffusion into the brain (Hawkins and Davis, 2005). Endothelial cells are then surrounded by the basement membrane which is shared by pericytes, which particularly associate with endothelial tight junctions and regulate capillary permeability (Liu et al., 2012; Tilling et al., 1998). Astrocytes surround the basement membrane of brain capillaries with their end feet and produce factors which maintain the integrity of the neurovascular unit, also regulating the influx of: water, ions and glucose which are all essential for neuronal function (Cabezas et al., 2014). Blood vessels in the brain are also innervated, allowing the control of blood flow based on the levels of neuronal activity (Zlokovic, 2008).

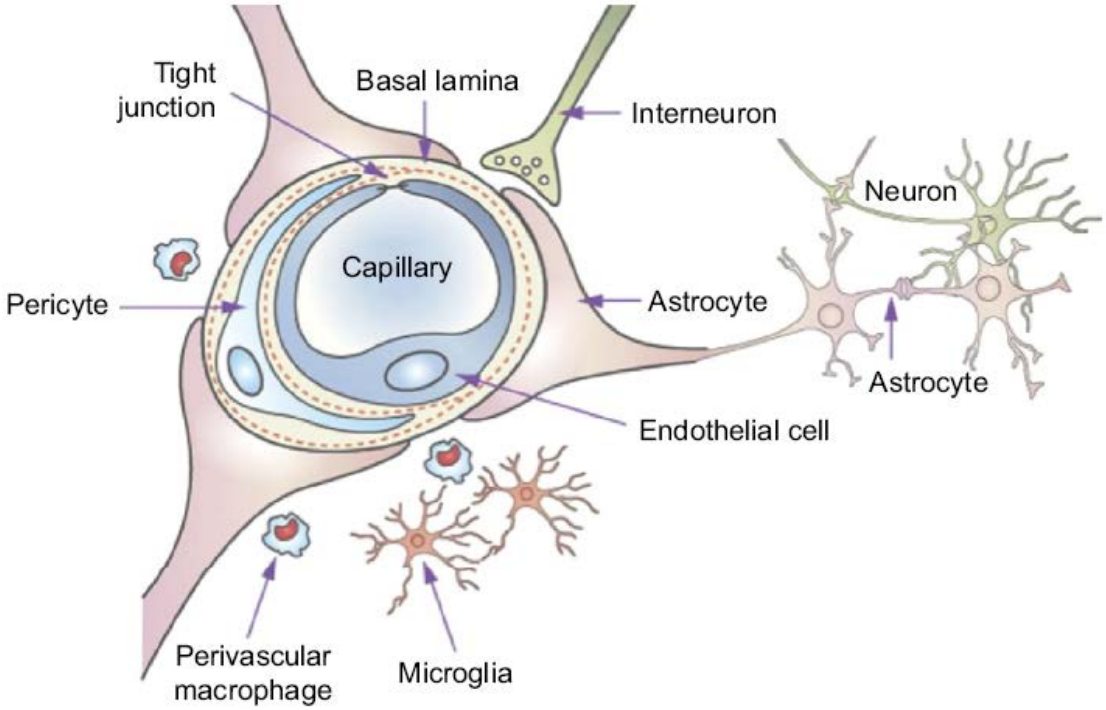

Figure 1. 1The blood brain barrier

The structure of the neurovascular unit, figure taken from (Feng et al., 2015)

1.1.4 Brain structure and organisation

At the most basic level brain regions are classified as grey matter or white matter. Grey matter is composed of neuronal cell bodies and their dendrites which make synaptic connections with the axons of other neurons. Linking different regions of grey matter are bundles of myelinated axons, which are known as white matter due to their appearance in brain sections. Macroscopically the brain can be divided into three regions: the cerebral hemisphere, the cerebellum and the brain stem. The cerebral hemisphere is subdivided into lobes, which are named after the bones of the skull which cover them: frontal, parietal temporal and occipital. The outer layer of the cerebral hemisphere is a highly folded grey matter area known as the cerebral cortex, different cortical regions have specialised functions (Purves 2008). Located in the temporal lobe is the hippocampus, a grey matter region that is very important in the formation and retrieval of memory. Figure 1.2 shows the organisation of neurons and the basic wiring of the hippocampus. In the hippocampus there are three main regions containing densely packed neuronal cell bodies: the dentate gyrus granular layer, the cortical area one (CA1) and cortical area three (CA3) regions. Separating the dentate gyrus and CA1 regions is the hippocampal fissure (or suculus), a region containing large blood vessels. The hippocampus receives sensory information from neurons in the entorhinal cortex, whose axons synapse with dendrites of dentate gyrus granular cells. The granular cell's axons project to the CA3 region, and are called mossy fibres, forming synapses with the dendrites of CA3 pyramidal neurons. The axons of CA3 neurons are called Schaffer collaterals, and form synapses with the dendrites of CA1 neurons, whose axons project back to the entorhinal cortex (Amaral and Lavenex, 2007; Neves et al., 2008). The basis of new memory formation is the ability of this network to change and adapt to incoming signals. This is known as neuronal plasticity and can occur at the level of an individual synapse, or the integration of new neurons into the network. This high plasticity is reflected by the fact that the dentate gyrus is one of only two regions in the human brain which continues to generate new neurons throughout life (Drew et al., 2013).

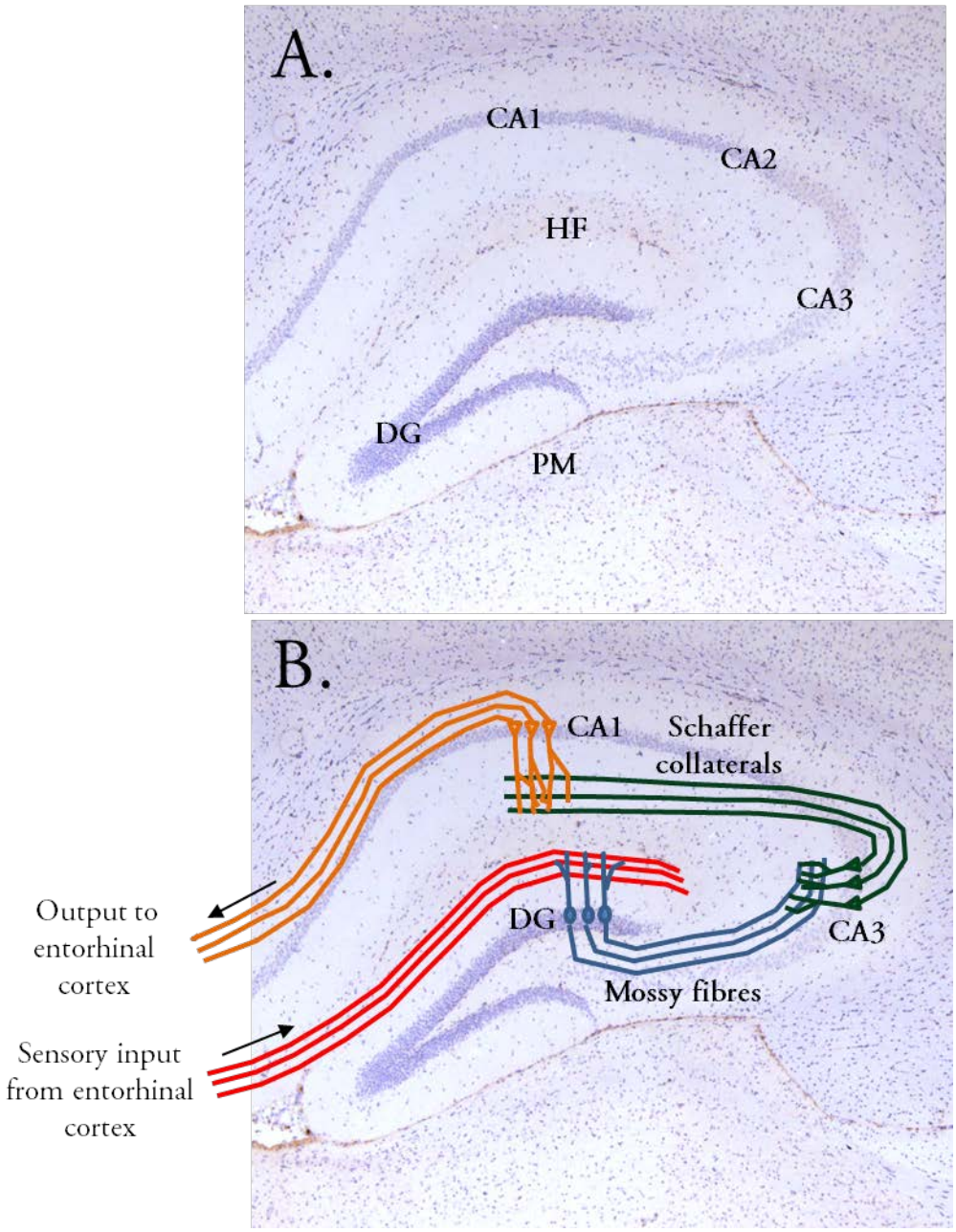

Figure 1. 2 The anatomy and wiring of the mouse hippocampus

A. CA cortical area, DG dentate gyrus, HF Hippocampal fissure, PM pial membrane
B. The wiring of the hippocampus: Sensory inputs from the entorhinal cortex (perforant path) synapse with granular cells of the dentate gyrus. Projections from granular cells called mossy fibres synapse with pyramidal cells in the cortical area 3, which in turn send projections called Schaffer collaterals which synapse with pyramidal neurons of the cortical area 1. Projections from cortical area one travel back to the entorhinal cortex.

1.1.5 Neurodegeneration

Due to the brain's importance to our daily activities, the result of dysfunction is often severe. Diseases that cause the long term dysfunction and death of neurons in the CNS are collectively termed "neurodegenerative diseases". Different neuronal circuits in the brain and spinal cord perform different roles, and therefore the result of neurodegenerative disease is specific to the area affected. For example, Parkinson's disease causes the loss of dopaminergic neurons in the substantia nigra, causing a loss of motor function control. ALS causes death of motor neurons leading to muscle weakness and progressive paralysis, whilst AD causes the dysfunction and loss of neurons in the cortex and hippocampus, which cause memory deficits and cognitive decline termed "dementia"(Martin, 1999). Neurodegenerative conditions are generally associated with ageing and/or genetic factors, and most neurodegenerative diseases are associated with the accumulation and misfolding of specific proteins in specific regions of the CNS. Due to the worlds ageing population, the incidence of dementia is predicted to triple in the next 50 years. Dementia is already a huge problem, estimated to cost the U.K. £26 billion a year, and last year it was the number one cause of death in British women (Office of national statistics 2014). Unfortunately the treatments available to treat dementia are ineffective, and only able to manage the symptoms in the short term.

1.2 The pathology of Alzheimer's disease

AD is the most common cause of dementia, affecting an estimated 18 million people worldwide. Sporadic AD accounts for over 95% of cases and typically presents after 65 years of age, with the likelihood of developing AD doubling every 5 years. AD initially presents as episodic loss of memory and inability to encode new memories, followed by a progressive deterioration of cognitive function until death 3-9 years after diagnosis (Almkvist, 1996). The currently approved treatments for AD are: inhibitors of acetyl-cholinesterase and Memantine® which blocks glutamate binding to its receptor (NMDA). Both therapies are able to transiently improve cognition by increasing synaptic function (Reisberg et al., 2003; Tariot Pn, 2004), but no treatment is available that can modify disease progression. The increasing number of individuals suffering from AD and the burden placed on our healthcare services, makes developing effective AD therapeutics an urgent unmet clinical need.

AD was first described in 1906 by Alois Alzheimer who observed that cognitive deterioration in a patient was associated with two neuro-pathological hallmarks that are still used to diagnose AD today. The first lesions observed were extracellular protein deposits called senile plaques, surrounded by abnormal neuronal processes named dystrophic neurites. The primary constituent of these plaques was found to be amyloid beta (Aβ), a 39-43 amino acid protein cleaved from the amyloid precursor protein (APP) (Allsop et al., 1988). The deposition of plaques in the brain is not unique to AD, as the cognitively normal elderly often possess senile plaques which are not pathological (Perl, 2010). The second lesions observed were intra-neuronal neurofibrillary tangles (NFTs), which are composed of the microtubule associated protein tau. There are many neurodegenerative conditions which share tau pathology-collectively named tauopathies. Some are driven by mutations in tau increasing its propensity to aggregate and/or phosphorylate, however such mutations in tau have not been linked to AD (Tolnay and Probst, 1999). AD is defined as cognitive deterioration which is accompanied by the presence of both Aβ and tau pathology. The neuro-pathological progression of AD was categorised by Braak and Braak into six stages of tau accumulation. During stages I and II, tau pathology begins to accumulate in the trans-entorhinal cortex, before spreading to the hippocampus and other limbic structures during stages III and IV. The final stages V and VI are characterised by wide spread accumulation of tau in the enthorinal cortex, hippocampus and other cortical structures (Braak and Braak, 1991). Synaptic dysfunction is an early event in AD, with patients who have Mild cognitive impairment (MCI) or mild AD

showing marked reduction in synaptophysin immuno-reactivity compared to healthy age-matched controls (Masliah et al., 2001). Synaptophysin is a protein expressed on presynaptic vesicles and reduction of synaptophysin indicates a reduced number of synapses. The level of synaptophysin correlates well with cognitive decline in advanced AD patients (Masliah et al., 1991). In the late stages of AD, large numbers of neurons are lost particularly in the hippocampus and cortex, resulting in a substantial decrease in brain volume and severe dementia. The reduction of synaptic and neuronal function and numbers is accompanied by the activation of the CNS resident macrophages, the microglia; it is currently unclear if activation of these cells contributes to pathology, however depletion of microglia can reverse cognitive deficits in the 3xTG mouse model of AD (Dagher et al., 2015). The two classic neuropathological hallmarks, plaques and tangles, are still utilized to diagnose AD. These lesions are not exclusive to AD, it is presence of both plaques and tangles associated with cognitive decline that defines AD (SantaCruz et al., 2005).

1.2.1 Amyloid beta

1.2.1.1 The processing and accumulation of amyloid beta

Senile Plaques were first described by Alois Alzheimer in 1905 yet it was 80 years before the main constituent of these plaques- Aβ was identified (Masters et al., 1985). Aβ is a 39-43 amino acid protein produced by the cleavage of the APP, which is expressed by neurons. There are two divergent APP processing pathways, which begin when APP is cleaved by either α-secretase or β-secretase. Cleavage of APP by α-secretase cuts through the Aβ domain, producing sAPPα and the c83 peptide; this prevents the production of mature Aβ. β-secretase cleaves a different site in APP leaving the Aβ region intact allowing the production of the mature Aβ peptide by the γ-secretase complex, producing Aβ and Amyloid Intracellular Domain (AICD) (Cole and Vassar, 2008). The processing of APP is summarised in figure 1.3. The exact function of Aβ is unclear, but the levels Aβ are increased in response to peripheral or central inflammation (Lee et al., 2008). There is some evidence that it is an anti-microbial peptide, that is produced as a part of the brain's innate immune response to infection (Soscia et al., 2010). The APP gene has been knocked out in mice, producing viable and fertile offspring who experience age dependent cognitive deficits and metabolic changes

(Senechal et al., 2008). This does not provide insight into the function of Aβ, due to the number of other APP cleavage products.

Aβ is produced in the healthy brain and cleared away, but in the AD brain increased production and/or decreased clearance leads Aβ accumulation. Aβ, in particular the 42 amino acid version ($A\beta_{42}$), is prone to aggregate and can exist in a wide array of different sized species. Monomers of Aβ aggregate to form oligomers which aggregate further to produce protofibrils, fibrils and plaques. A recent study has shown that aggregation of soluble Aβ species is catalysed by proto-fibrils (Cohen et al., 2013).

Plaques were the first Aβ species to be identified in AD, but there is significant heterogeneity in terms of structure and size. Plaques can be categorised based on their morphology, and the ability of histological dyes to label them. Some plaques are classified as "diffuse", these plaques do not bind the histological dye congo red and are amorphous with no visible substructure. Congophillic plaques are named due to their ability to bind the histological dye congo red, they also have a defined central crystalline structure. Congophillic plaques are more likely to be associated with abnormal neuronal processes-named dystrophic neurites, in which case they are named "neuritic plaques" (Dickson and Vickers, 2001; Perl, 2010; Wisniewski et al., 1989). Aβ also exists as soluble oligomeric species-the definition of which is not clear, ranging from dimers of Aβ up to large proto-fibrils. These oligomeric structures are highly promiscuous and bind to a range of neuronal receptors such as: PrPc, FcγRIIb or NMDA expressed at the synapse, and binding to these receptors can induce neuronal dysfunction and/or death (Chung et al., 2010; Kam et al., 2013; Lai and McLaurin, 2010; Um et al., 2012). Blocking these interactions with antibodies against Aβ protects against neuronal dysfunction in vitro and *in vivo*, and APP mice deficient for PrPc or FcγRIIb are protected from cognitive deficits (Kam et al., 2013; Klyubin et al., 2008; Zago et al., 2012). As well as its deposition as plaques, Aβ is often deposited around the cerebral blood vessels of AD patients which is known as cerebral amyloid angiopathy (CAA). This deposition is associated with changes in blood vessel morphology, and an increased incidence of micro haemorrhage to these vessels (Perl, 2010; Zago et al., 2013).

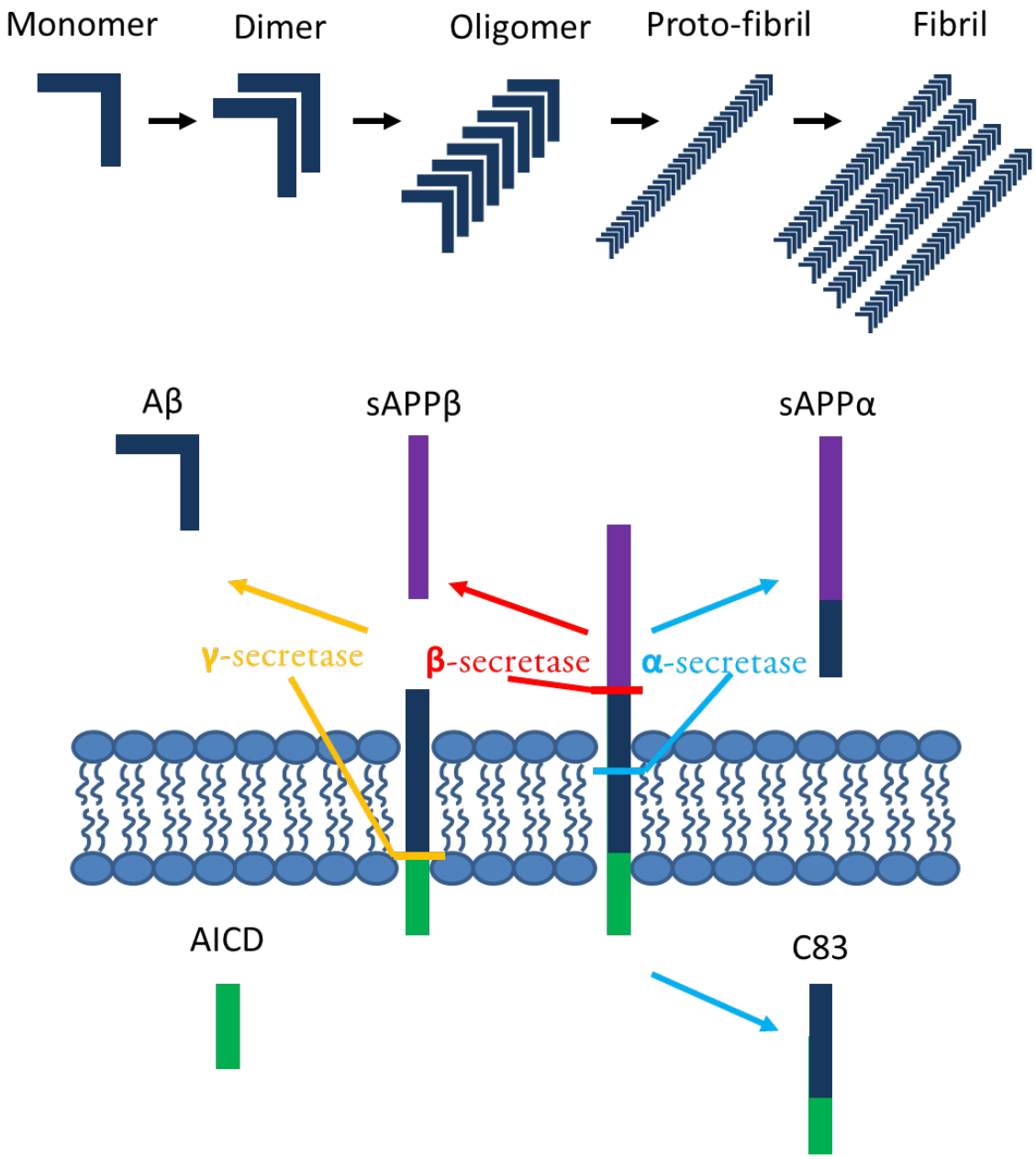

Figure 1. 3 Processing of the amyloid pre cursor protein and Aβ aggregation

The amyloid precursor protein is a 695-723 amino acid trans-membrane protein. Full length APP can be cleaved by α-secretase or β-secretase, cleavage by α-secretase cuts through the Aβ peptide region preventing Aβ production, creating C83 and sAPPα. Cleavage of APP by β-secretase produces sAPPβ and allows cleavage by γ-secretase; mutations in APP such as the Swedish mutation (K670N/M671L) increase β-secretase cleavage. γ secretase cleaves the remainder of APP producing Aβ and AICD, the length of Aβ (39-42) is variable and mutations such as V717F increase the proportion of Aβ42 produced.

1.2.1.2 The Amyloid Cascade Hypothesis

Aβ accumulation is thought to be one of the first pathological changes to occur in AD, with accumulation beginning decades before the onset of clinical symptoms (Jack et al., 2009). The amyloid cascade hypothesis states that accumulation of Aβ in the brain is the driving force behind other aspects of AD pathology (Hardy and Selkoe, 2002). It is proposed that certain species such as oligomers and proto-fibrils are highly synaptotoxic and result in the synaptic dysfunction occurring early on in AD, whilst the accumulation of Aβ as plaques leads to neuro-inflammation and the accumulation of hyper-phosphorylated tau as NFTs. Together these factors drive the progressive neurodegeneration and cognitive decline observed in patients.

The most convincing support for the amyloid cascade hypothesis is the occurrence of early onset familial forms of AD that account for less than 5% of total cases. Mutations that cause early onset AD have been identified in the APP and presynillin genes, the latter is part of the γ-secretase complex that cleaves APP to form Aβ. The mechanisms by which these mutations cause disease are dependent on their location within the APP protein (Cruts and Van Broeckhoven, 1998; Goate et al., 1991). For example, the Swedish double mutation (K670N/M671L) is located around the β-secretase site, and increases the total levels of Aβ produced by increasing the amount of APP processed by β-secretase (Citron et al., 1992; Goate et al., 1991). Mutations which occur around the γ-secretase site of APP such as the London mutation (V717F) or in the presynillin genes, increase the levels of Aβ42 produced in comparison to Aβ40 (Goate et al., 1991; Suzuki et al., 1994). There are a number APP mutations that lead to early onset AD that are not located around the β-secretase or γ-secretase sites, these include the Dutch (E693Q), Flemish (A692G) and Arctic mutations (E693G). A number of different mechanisms have been proposed for these mutations: the Arctic and Dutch mutations appear to cause AD by accelerating the formation of protofibrils of Aβ (Nilsberth et al., 2001), whilst the Flemish mutation appears to influence α-secretase and β-secretase cleavage. Familial AD is caused by mutations affecting the processing Aβ or changing its conformation. Supporting a role for Aβ in the development of AD, the transgenic expression of human APP with these mutants in mice (e.g. TG2576 or APP/PS1), leads to the recapitulation of some elements of AD pathology. These mice exhibit: deposition of Aβ as plaques, cognitive deficits and neuroinflammation as measured by higher cytokine production and microglial phenotype change (Games et al., 1995; Hsiao et al., 1996; SturchlerPierrat et al., 1997). Furthermore Down syndrome sufferers possess an extra copy of APP due to trisomy of chromosome 21, and frequently

develop early onset dementia. This dementia has many pathological hallmarks of AD including: plaque formation, CAA and NFTs (Lubec and Engidawork, 2002). The genetic evidence linking Aβ to the development of early onset AD is convincing, however links to sporadic AD have so far been less robust. Recently a study of the elderly population in Iceland found that a mutation in APP (A673T) adjacent to the β-secretase site is protective against sporadic AD. This mutation reduces the total levels of Aβ produced, not only decreasing the likelihood of carriers developing AD but also reducing the amount of cognitive decline in the elderly population without AD (Jonsson et al., 2012). The strongest genetic risk factor associated with sporadic AD is the e4 allele of the apolipoprotein (*apoe*) gene. Individuals with one or two copies of the e4 allele have a significantly increased risk of developing sporadic AD (Strittmatter and Roses, 1995). ApoE has since been shown to be directly involved in the binding and clearance of Aβ (Bales et al., 1997; Holtzman et al., 2000; Kelly R, 2010).

In recent years the amyloid hypothesis has come under increasing scrutiny, with much evidence contradicting a central role of Aβ in AD pathology. In AD plaque density does not correlate with cognition in anything other than an age dependent manner (Storandt et al.), and does not correlate with the rate of brain atrophy (Josephs et al., 2008). In most APP transgenic mice, increased deposition of Aβ alone is not sufficient to cause NFTs and neuronal loss, and the neuro-inflammation observed in these models is not representative of AD (Wilcock et al., 2011b). Plaque deposition does not correlate spatially with the formation of NFTs, and in fact the presence of NFTs is a better predictor of cognition decline (Giannakopoulos et al., 2003). The role of Aβ in sporadic AD is far from understood, however there is compelling evidence that Aβ is important in the development of AD. As a result the vast majority of recent research and drug development has focussed on the clearance of Aβ.

1.2.1.3 Transgenic APP models of Alzheimer's disease

The discovery of mutations in APP and presynilin genes that cause familial AD have enabled the generation of transgenic rodent models of AD. These models over-express the human APP gene, containing one or more mutation associated with the early onset form of the disease. Typically these mice develop plaques in the brain anywhere between three and twelve months of age, and have an associated neuro-inflammatory response and behavioural changes (Games et al., 1995; Hsiao et al., 1996; SturchlerPierrat et al., 1997). The TG2576 mouse is arguably the most extensively

used model of Aβ deposition, the mice possess a transgene coding for human APP with the Swedish mutation (K670N, M671L) downstream of the hamster prion promoter (Hsiao et al., 1996). Mutant APP is overexpressed resulting in the production of high levels of Aβ40 and Aβ42, which is subsequently deposited in the hippocampus and cortex as plaques similar to plaques found in AD patients. After 7-8 months, diffuse plaques become visible in the hippocampus and cortex of TG2576 mice, by 12-15 months congophilic plaques appear and by 20 months Aβ has accumulated to a similar extent as in AD (Kawarabayashi et al., 2001). The deposition of Aβ is accompanied by a concomitant impairment of memory as measured by spontaneous alternation in the T maze, and activation of microglial cells, as measured by CD45 expression, surrounding the plaques (Benzing et al., 1999; Hsiao et al., 1996). TG2576 mice do not develop substantial tau pathology, and do not suffer extensive neuron loss. These mice therefore do not recapitulate all aspects of AD pathology, and should only be thought of as a model of Aβ deposition. There are many different transgenic APP models, each expressing human APP with different familial mutations. Each model develops varying levels of Aβ deposits in the parenchyma and around the vasculature, and newer models with multiple mutations display accelerated pathology and a more severe phenotype. The TG2576 mouse model is well characterised in the context of immunotherapy, so it provides a good platform for the investigation of the effector function of therapeutic antibodies.

1.3 The immune system and the role of inflammation in Alzheimer's disease

The basis of the immune system is the ability of our body to recognise molecules and cells as "self" and "non-self"; facilitating the removal of potentially harmful pathogens and toxins. The immune system can be divided into two branches: innate immunity and adaptive immunity. Innate immunity allows the rapid recognition of pathogens using pattern recognition receptors (PRRs), by binding to molecules associated with pathogens (pathogen associated molecular patterns, PAMPs). This enables rapid phagocytosis and destruction of invading pathogens, and the presentation of antigens to B and T-cells enabling an adaptive immune response. The response of the adaptive immune system is delayed in comparison, but this allows an antibody and T-cell response that is specific for a particular pathogen. The immune system is of interest to AD research as inflammation plays an important role in both the underlying pathology and exacerbation of cognitive decline in AD. This section will summarise the effect that peripheral inflammation has on the healthy and diseased brain and summarise the evidence that systemic inflammation is important in the underlying pathology of AD. To investigate the effect of peripheral inflammation on the brain, our lab uses the attenuated bacterium *Salmonella Typhimurium* SL3261 (*S. typhimurium*), I will describe the course of the peripheral immune response to infection.

1.3.1 Sickness behaviour

1.3.1.1 Sickness behaviour and immune to brain communication

It was once thought that the brain was isolated from peripheral immune responses, however it is now clear that the brain plays an integral role in the body's response to infection. This is illustrated by changes in behaviour and physiology that the brain orchestrates in response to infection. For example, after contracting an infection you feel lethargic and anti-social, you lose appetite and your temperature increases. These changes in behaviour and metabolism are collectively termed sickness behaviours, which improve pathogen elimination and prevent the spread of illness to other people (Hart, 1988). Therefore inflammation in the periphery is able to directly alter behaviour, and therefore brain function. This is demonstrated by experiments where healthy volunteers were injected with low concentrations of the bacterial lipo-polysaccharide (LPS), and experienced short

term decreases in cognition and increased depressive behaviour (DellaGioia et al., 2013; Krabbe et al., 2005).

The BBB restricts the entry of cytokines and immune cells into the brain, therefore under normal conditions the induction of sickness behaviours does not occur by direct contact between peripheral cytokines and CNS neurons. There are instead three pathways by which the immune system can communicate with the brain. The vagus nerve has afferent fibres located in peripheral tissues, which are able to signal to the brain in response to localised inflammation (Wang et al., 2003). The afferent fibres signal to the nucleus of the solitary tract, which then signals to other brain regions, including the hippocampus and hypothalamus, inducing sickness behaviour and metabolic changes, such as appetite, fever and lethargy. This is illustrated by the abolition of certain sickness behaviours after the vagus nerve is surgically severed (Watkins et al., 1995). Circum-ventricular organs (CVOs), are regions in the brain that have an incomplete BBB. This means that at CVOs, inflammatory mediators and circulating immune cells can access a discrete location in the brain. Microglia and macrophages in CVOs are directly responsive to systemic administration of LPS, up regulating CD14 and influencing proximal neuronal activity (Lacroix et al., 1998; Sagar et al., 1995). Systemic inflammation can also induce de novo cytokine production by activation of brain endothelial cells, which express cytokine receptors and PRRs. Activated endothelial cells produce cytokines and activate cyclooxygenase (COX-1 and COX-2) resulting in prostaglandin (PGE_2) production, which in turn results in microglial activation and sickness behaviour in mice (Teeling et al., 2010). A similar effect is seen when cytokines are directly injected into the brain (Dantzer and Kelley, 2007).

1.3.1.2 Sickness behaviour in neurodegenerative disease

Whilst sickness behaviours are beneficial for people with a healthy CNS, in a diseased or ageing brain the response to peripheral infection can be detrimental and increases the rate of cognitive decline. Elderly individuals who contract a peripheral infection are prone to develop delirium, a condition which results in a severe short term cognitive problems and a long term decline in brain function (Manos and Wu, 1997). Even in the absence of delirium, AD patients who have peripheral immune activation, as measured by higher cytokine levels, exhibit decreased cognition and accelerated cognitive decline (Holmes et al., 2011; Holmes et al., 2009; Holmes et al., 2003). One explanation for the response observed in elderly and AD patients, is that microglia are primed to

respond to a peripheral immune stimuli. Priming is a well described response of macrophages *in vitro*, where an initial treatment of interferon-γ (IFNγ) exacerbates their response to a second stimulus with LPS. Experimental evidence suggest that microglia of mice with a chronic neurodegenerative disease are primed to respond to a secondary immune stimulus, and produce higher levels of pro-inflammatory cytokines after local or peripheral LPS treatment (Combrinck et al., 2002; Cunningham et al., 2005; Lunnon et al., 2011). In the context of AD, microglia may also be primed and then respond to local inflammation or following systemic inflammation in an exaggerated manner producing higher levels of pro-inflammatory cytokines increasing sickness behaviour and inducing cognitive decline.

1.3.2 The role of inflammation on Alzheimer's disease

As well as accelerating the progression of AD, a role for the immune system in the development of disease has also been suggested. Long term non-steroidal anti-inflammatory drugs (NSAIDs) use decreases the risk of developing AD later in life (Szekely et al., 2004), although other studies have not been able to reproduce these results. Recent genome wide association studies (GWAS) have revealed polymorphisms in several immune receptors that confer a higher risk of developing AD (Guerreiro et al., 2013; Hollingworth et al., 2011; Lambert et al., 2009). It has also been found that certain infections such as: chronic periodontitis or C*hlamydia pneumoniae* are associated with increased risk of AD (Hammond et al., 2010; Stein et al., 2012). Recently it was shown that anti-TNFα therapy could slow cognitive deterioration in AD, however this is in the early stages of clinical development (Butchart et al., 2015). The exact mechanisms by which inflammation is involved in AD pathology are still unclear.

To understand the brain's response to peripheral inflammation, and to uncover the role of inflammation in AD, mimetics of infections such as: LPS (bacteria), zymosan (yeast) or poly I.C. (virus) have been used in rodent models. These mimetics work by activating the PRRs, such as toll-like receptor 4 (TLR4), driving the systemic production of pro-inflammatory cytokines. Dosing mice with LPS leads to increased brain immune-receptor expression and cytokine levels, which are accompanied with behavioural changes (Dantzer and Kelley, 2007). Peripheral inflammation has also been shown to increase the levels of AD related neuropathology. Repeated dosing of LPS can also cause the accumulation of Aβ in both wild type and transgenic APP mice due to increased β-secretase activity (Lee et al., 2008; Sheng et al., 2003b), and LPS treatment of mice transgenic for

human tau results in the increased phosphorylation and accumulation of tau in neurons (Kitazawa et al., 2005). Pre-natal challenge of wild type mice with the viral mimetic poly I.C. also causes increased: cytokine level, Aβ deposition and tau phosphorylation in adult life (Krstic et al., 2012). These studies demonstrate that peripheral inflammation can increase the accumulation of the two neuro-pathological hallmarks of AD, strengthening the hypothesis that inflammation is involved in the underlying pathology. Whilst LPS is a useful tool for measuring the acute responses to an immune stimulus, it does not accurately model a real infection. Our lab have previously shown that infection with the attenuated bacterium *Salmonella typhimurium* SL3261 (*S. typhimurium*) leads to a completely different neuro-inflammatory and behavioural response compared to repeated injection of LPS (Puentener et al., 2012). There is limited published work investigating the effect of real life infections on AD pathology in the brain of mice, but infection of wild type mice with the bacterium *Chlamydia pneumoniae* leads to the deposition of Aβ in plaques similar to those found in AD patients or APP mice (Little et al., 2004). Infection of APP/PS1 mice with the respiratory pathogen *Bordetella pertussis*, causes increased numbers of Aβ plaques and activation of glial cells (McManus et al., 2014).

Microglia have been hypothesised to be involved in the pathogenesis of AD, either by responding to altered microenvironment in the ageing brain and early stages of the disease (i.e. Aβ accumulation or synapse loss) or in response to low grade chronic systemic immune activation, however their precise role in AD is far from clear. Microglia are the CNS macrophages, which under normal conditions patrol the brain and react to potential threats. This is supported by observations that they surround Aβ plaques in AD brains, however they are unable to clear these deposits away (Rogers et al., 1988) and this may contribute to their activated phenotype in AD. The presence of activated microglia in the brains of AD patients has been measured by positron emission topography (PET) imaging, and negatively correlates with cognitive function, and *in-vitro* stimulation of these cells with Aβ or pro-inflammatory molecules can cause damage to co cultured neurons (Edison et al., 2008). This does not prove a detrimental role for microglia in disease, as the activation of microglia is likely to occur in areas with extensive damage and therefore this would negatively correlate with cognitive function.

1.3.2.1 Systemic infection with *Salmonella typhimurium*

The effect of peripheral inflammation on the brain has been researched using bacterial or viral mimetics, however this is not comparable to a real life infection, our lab models the effect of real life infections on the brain. The species of bacteria *Salmonella enterica* are gram negative bacteria, able to infect the small intestine of humans and other mammals. Most bacteria in this family infect the small intestine causing gastro-enteritis, however a few serotypes can cause systemic infection and enteric fever. One of these is *Salmonella typhii* which causes human typhoid fever, a serious condition affecting 20 million people and causing 200,000 deaths per year (Crump et al., 2004). Typhoid fever is spread by the ingestion of food or water with infected human faeces. The related serotype *S. typhimurium*, does not cause serious disease in humans, however it causes enteric fever in mice which is similar to typhoid fever in humans. For this reason *S. typhimurium*, and attenuated strains of this bacterium, have been used extensively to model human typhoid fever in mice (Mittrücker and Kaufmann, 2000). Attenuated strains of *S. typhimurium*, such as SL3261, cause more mild pathology than the wild type bacterium, and in this case were produced by knocking out the AroA gene. The AroA gene allows the biosynthesis of an intermediate in the production of folate, this means that the bacteria have to rely on the host folate levels to grow which significantly reduces virulence (Hoiseth and Stocker, 1981). *S. typhimurium* first colonises the gut of mice, by transcytosis through M cells located at Peyer's patches (Carter and Collins, 1974). The bacterium is then taken up by macrophages or dendritic cells, where it proliferates inside phagosomes, and is transported to mesenteric lymph nodes (Mittrücker and Kaufmann, 2000). From the lymphatic system, *S. typhimurium* infects the circulation but it is quickly removed by phagocytic cells in the spleen and liver (Broz et al., 2012; Dunlap et al., 1992). The spleen and liver then become colonised by the bacteria, and splenomegaly can be observed in infected mice. The bacterial infection is eventually cleared around six weeks after initial infection (Hess et al., 1996).

1.3.2.2 Innate immune response

Cells of the innate immune system, such as neutrophils and macrophages, are able to quickly respond to invading pathogens. They are able to recognise invading bacteria via the expression of receptors that bind to molecules that are associated with pathogens –PAMPs. For example toll-like

receptors (TLRs) recognise a wide variety of molecules including LPS found on the coats of gram negative bacteria. This enables innate immune cells to: phagocytose and destroy bacteria, recruit other immune cells and activate adaptive immunity by the presentation of bacterial antigens. During the initial stages of *S. typhimurium* infection macrophages and neutrophils are recruited to the sites of infection, and are essential in controlling the levels of bacteria by phagocytosis (Friedman and Moon, 1977; Vassiloyanakopoulos et al., 1998). High levels of the cytokines IFNγ and TNFα are essential in switching macrophages into a phagocytic phenotype more capable of killing *S. typhimurium* (Mittrücker and Kaufmann, 2000). In response to activation of PAMPs by *S. typhimurium*, cells of the innate immune system produce many cytokines and chemokines such as: TNFα, IL-6, IL-1β and IL-12 or KC. The production of these cytokines and chemokines mediate: tissue inflammation and recruitment of immune cells and stimulate differentiation of CD4 T-cells to a Th1 phenotype. The innate immune system is essential in controlling the levels of bacteria in the early stages of disease, however it is unable to fully clear the infection. To clear intracellular infection with *S. typhimurium*, activation of the adaptive immune system is required.

1.3.2.3 The adaptive response

The adaptive immune system is comprised of B and T cells, which can be further subdivided into many categories depending on phenotype, function and maturation stage. Both B cells and T cells can recognise specific antigens from an invading pathogen, and therefore adaptive immunity allows a specific response against an infection. *S. typhimurium* is an intra-cellular bacteria, and therefore CD4+ T-cells are essential in clearing the infection. Macrophages and dendritic cells produce the cytokine IL-12, which promotes the differentiation of CD4+ T-cells into a Th1 phenotype which in turn stimulates the anti-microbial activity of macrophages allowing the destruction of intracellular bacteria (Hess et al., 1996). CD4+ T-cells also provide help to antigen specific B-cells, to produce antibodies against *S. typhimurium*. Although not as important as CD4+ cells, CD8+ T-cells also have a role in the clearance of *S. typhimurium* infection, they recognise and lyse cells infected with *S. typhimurium* through antigen presentation on MHCI (Mittrücker and Kaufmann, 2000). Activated B-cells produce antibodies against *S. typhimurium*, and although it is an intracellular bacteria they still play a role in clearance. Immunoglobulin G (IgG) antibodies can bind extracellular bacteria and promote phagocytosis through Fc gamma receptors (FcγRs), and IgA antibodies can prevent entry of *S. typhimurium* through the gut mucosa.

In summary, *S. typhimurium* initially infects the gut and quickly colonises the spleen and liver of mice. The initial response is characterised by high cytokine levels, in particular IFNγ, which enable phagocytic cells to control the infection. The adaptive immune response is mainly characterised by CD4+ T-cells, which enable the clearance of intracellular *S. typhimurium*, however CD8+ T-cells, NK cells and B-cells also play a role.

1.4 Fc gamma receptors

IgG is the most prevalent isotype found in serum. FcγRs bind to the constant region of IgG and are expressed on the surface of a wide range of immune effector cells. The following section will describe the biology of FcγRs and their ligand-IgG, their expression in the CNS and their potential involvement in the underlying pathology of neurodegenerative disease.

1.4.1 FcγR biology

FcγRs are a family of receptors with the ability to bind to the Fc region of IgG. Human FcγRs can be functionally divided into three classes: activating (FcγRI, FcγRIIa, FcγRIIc and FcγRIIIa), inhibitory (FcγRIIb) or gpi linked decoy (FcγRIIIb). There are a number of subclasses of human IgG (IgG1, IgG2, IgG3 and IgG4), each with varying affinity for the different FcγRs (Bruhns et al., 2009). There are four known murine FcγRs: three activating (FcγRI, FcγRIII, and FcγRIV) and one inhibitory (FcγRIIb) (Nimmerjahn and Ravetch, 2008). Mice have four IgG subclasses (IgG1, IgG2a, IgG2b and IgG3), but it should be noted that the nomenclature is different between species and therefore human IgG1 is not homologous to murine IgG1. Figure 1.4 shows murine (A) and human (B) FcγRs, and their relative affinity for different IgG subclasses.

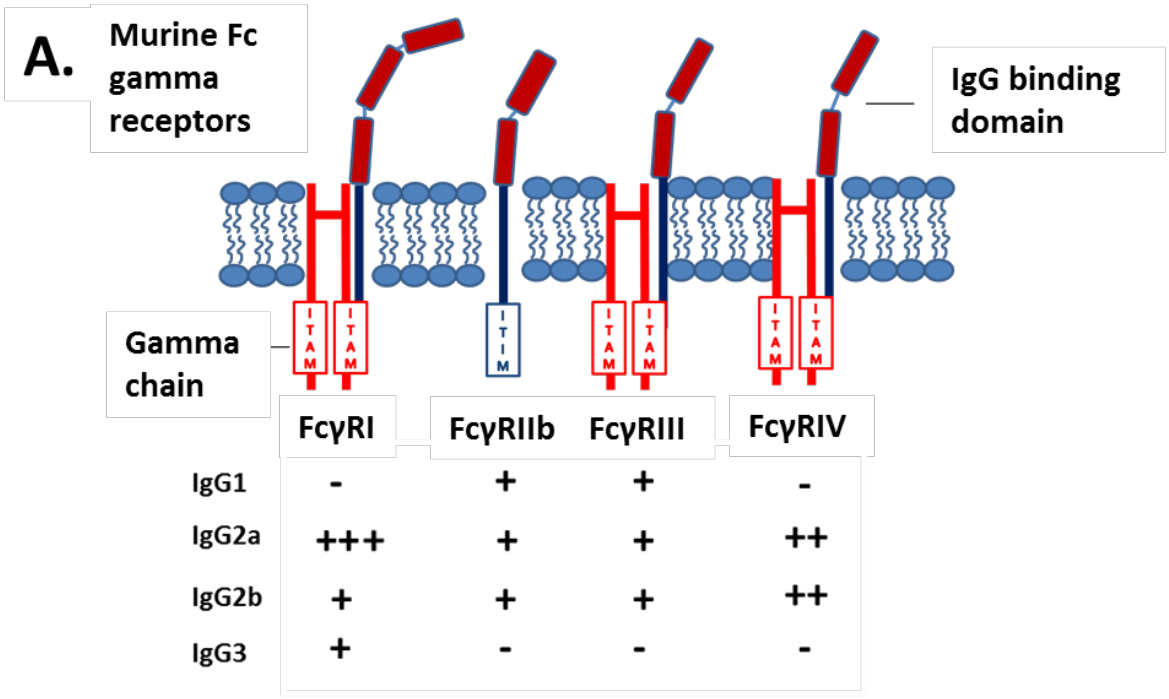

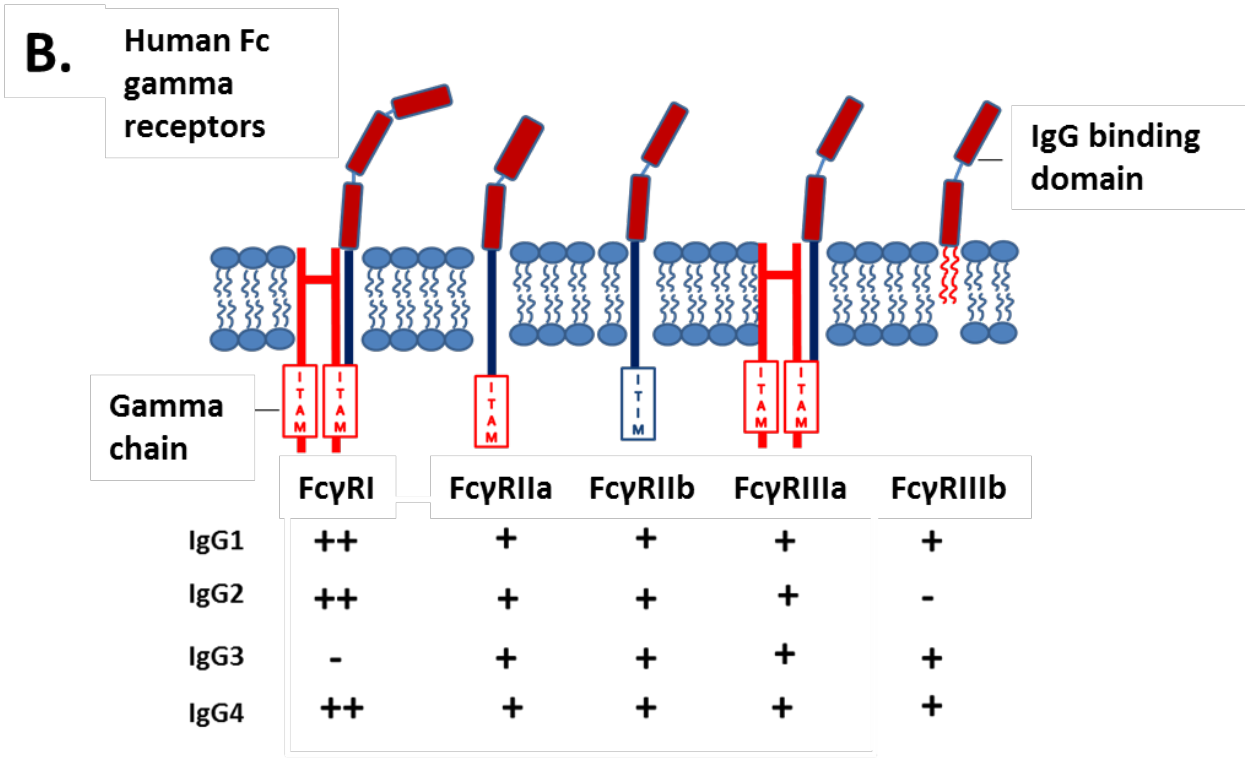

Figure 1. 4 Mouse and human FcγRs and their relative affinity for different IgG Isotypes

Activating Fc receptors (with the exception of human FcγRIIa and IIc) are associated with and signal through a separate cytoplasmic gamma chain (Fcγ chain). The Fcγ chain contains immune-tyrosine activation motifs (ITAMs), which mediate the cellular signalling in response to FcγR ligation. A common model used to study the roles of activating FcγRs *in vivo* are mice deficient for the Fcγ chain, these mice do not express functional activating FcγRs. This results in: decreased antibody mediated phagocytosis, abnormal platelet activation and an attenuated immune response to immune complexes (Takai et al., 1994). Unlike other activating receptors, human FcγRIIa and FcγRIIc have an intrinsic ITAM in their cytoplasmic domain which mediates the cellular signalling in response to IgG ligation.

Ligation of IgG-immune complexes by activating FcγRs results in the crosslinking of the cytoplasmic chains and the phosphorylation of ITAMs. This forms a binding site for splenic tyrosine kinase (SYK), which then activates downstream signalling cascades such as the phosphoinositol-3 kinase (PI3K) and RAS/RAF pathways. Activation of the PI3K pathway leads to the activation of phospholipase C, which in turn causes an increase in cellular calcium. Activation of these pathways and the increased calcium activate the cell, this results in a pro-inflammatory response which can include: proliferation, cytokine/chemokine release, antibody dependent cellular cytotoxicity (ADCC), phagocytosis and antigen presentation (Nimmerjahn and Ravetch, 2008). The inhibitory FcγRIIb signals through an intrinsic cytoplasmic immuno tyrosine inhibitory motif (ITIM), cross-linking with an activating receptor results in ITIM phosphorylation and the recruitment of proteins to the plasma membrane (Nimmerjahn and Ravetch, 2008). The phosphatase SHIP1 is recruited to the membrane, and it de-phosphorylates PIP_{345} preventing downstream activation of the PI3K pathways. Other adaptor proteins are recruited to inhibit the activation of other important pathways such as RAS/RAF. The process of FcγR mediated activation or inhibition of an effector cell is outlined in figure 1.5. The inhibitory receptor is usually expressed by the same cells as activating receptors, therefore the functional consequences of FcγR ligation depends on the ratio of activating to inhibitory FcγRs expressed on the effector cell. Cells that have a high ratio of activating to inhibitory FcγRs are more prone to an uncontrolled immune response; this is demonstrated by FcγRIIb$^{-/-}$ mice which have an exacerbated response to autoantibodies inducing more tissue damage (Clynes et al., 1999; Yuasa et al., 1999). The response is also determined by the subclass of antibody; for example human IgG1 has higher affinity for activating FcγRs as compared to human IgG4, and will induce a more pro-inflammatory response (Bruhns et al., 2009).

FcγRII and FcγRIII in both humans and mice are classified as low affinity receptors and are unable to bind monomeric IgG, and instead bind to immune complexes or antibody opsonised cells. Immune complexes are multivalent and therefore have higher avidity, enabling binding of lower affinity receptors (Ravetch and Bolland, 2001).The importance of avidity in the binding interactions of the low affinity receptors is demonstrated by increased binding for immune complexes of increasing size, and that the disruption of FcγRIIa localisation in lipid rafts reduces the binding to immune complexes (Bournazos et al., 2009a; Lux et al., 2013).

FcγRI is different to other FcγRs as it possesses an extra immunoglobulin like domain, and has much higher affinity for certain subclasses of IgG (Allen and Seed, 1989; Bruhns et al., 2009). This enables the ligation of monomeric IgG, causing FcγRI to be occupied by monomeric IgG in areas such as the serum, where IgG concentration is high (Allen and Seed, 1989; van der Poel et al., 2011). Binding of monomeric IgG does not activate the cytoplasmic gamma chain, as it does not cross link the receptor. However, it has been shown that FcγRI can mediate functions such as antigen presentation in the absence of gamma chain activation (van Vugt et al., 1999). The occupation of FcγRI by monomeric IgG prevents FcγRI from binding to immune complexes, however it has been shown that FcγRI is important for a number of responses to infection and to therapeutic antibodies where binding to immune complexes is essential (Barnes et al., 2002; Bevaart et al., 2006; Mancardi et al., 2013). Upon cytokine stimulation it is thought that the cellular localisation of FcγRI changes, and expression is increased, leading to increased capacity to bind immune complexes compared to monomeric IgG. This allows FcγRI to take part in the immune response in the presence of saturating levels of IgG (van der Poel et al., 2010). FcγRIV is unique to mice, and seems to be functionally similar to human FcγRIIIa. FcγRIV has intermediate affinity for IgG2a and IgG2b when compared to FcγRI (Nimmerjahn et al., 2005b).

The neonatal Fc receptor (FcRn) is another receptor able to ligate the constant region of IgG (apart from IgG3), however it is not related to the FcγRs. FcRn is expressed in the gut of new born mammals, and enables the transfer of maternal IgG into the bloodstream, granting passive immunity. FcRn is also expressed by adult endothelial cells and it is responsible for the long serum half-life of IgG (about three weeks in human and 1 week in mouse). FcRn is only able to bind to IgG under acidic conditions (pH6-6.5), not at neutral pH (7.0) (Raghavan et al., 1995). This enables FcRn to bind to IgG in acidic conditions such as in endosomes or in the gut of a new born, to prevent degradation by releasing IgG into circulation. In the CNS, the expression (Ober et al., 2004) of FcRn on endothelial cells facilitates the removal of IgG from the brain (Cooper et al., 2013).

FcRn is also expressed by haematopoetic cells which also are involved in the increased half life of IgG (Montoyo et al., 2009).

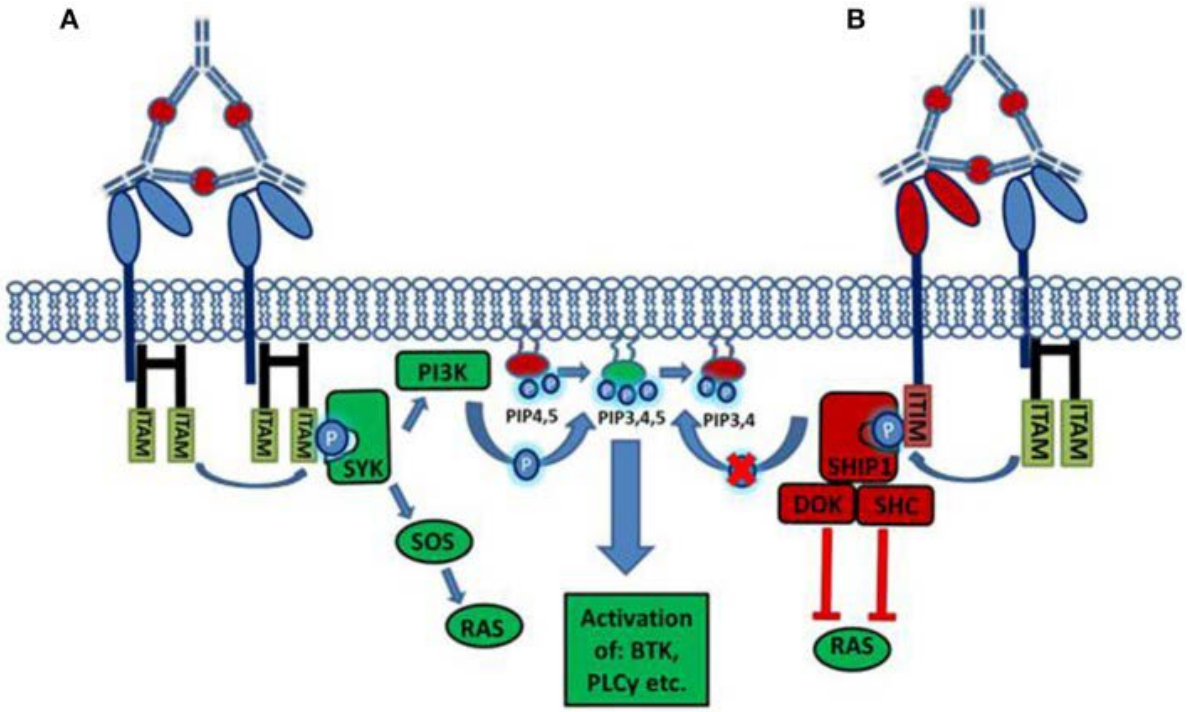

Figure 1. 5 Activation or inhibition of a cell by Fc receptor ligation of IgG immune complexes

A. Cross linking of activating FcγRs by IgG immune complexes results in the phosphorylation of cytoplasmic ITAM motifs. This allows the recruitment of SH2 domain containing kinases of the SYK family. These kinases activate pathways such as the RAS and PI3K pathways resulting in increased cellular calcium and activation of the cell. **B.** The cross linking of an inhibitory receptor to an activating receptor results in the phosphorylation of an ITIM, leading to the recruitment of the phosphatase SHIP1. SHIP1 removes the 5'phosphate from PiP_{345} inhibiting downstream PI3K signalling, and also interacts with other adaptor proteins to inhibit other pathways.

1.4.2 IgG Antibody structure and Function

IgG antibodies are the ligands of FcγRs, and are the most common isotype found in serum. IgG antibodies are composed of four polypeptide chains: two heavy chains and two light chains. The heavy chains are linked by two disulphide bonds and are each linked to a light chain by a further disulphide bond, figure 1.6 shows the structure of an IgG1 antibody. The antibody molecule can be split into 2 functionally distinct domains: the variable region which is responsible for antigen binding and the constant region which controls antibody effector function. IgG Immune complexes can activate the classical complement pathway through interactions with the C1q complex or activate effector cells through interactions with FcγRs (Arlaud et al., 2002; Ravetch and Bolland, 2001). In mice and humans there are four subclasses of IgG each with varying effector functions. The ability of IgG to bind specifically to a target, activate immune cells, its long serum half-life and its low off target toxicity makes IgG an ideal drug candidate. Treatment with monoclonal antibodies (passive immunisation) has been successful in management of numerous cancers and inflammatory diseases, and can work by a number of mechanisms (Chan and Carter, 2010). For example, antibodies are able to treat B-cell lymphoma by binding and depleting malignant B-cells, this is mediated by antibody dependent cellular cytotoxicity (ADCC) (Chan and Carter, 2010). Increased knowledge of the IgG structure and its interactions with receptors, now allow the optimisation of therapeutic antibodies. This section will describe the structure of IgG, and the progress that has been made in the optimisation of therapeutic antibodies.

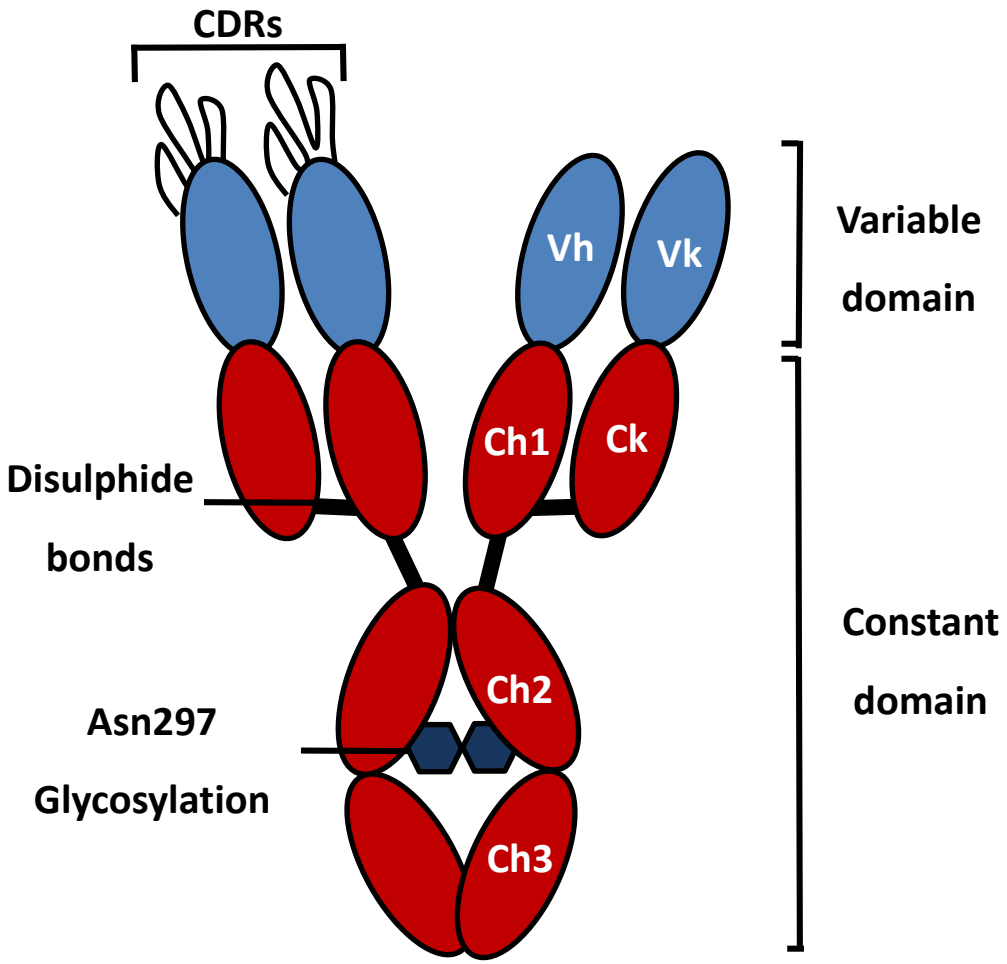

Figure 1. 6 The structure of an IgG Antibody

The most common type antibody in circulation is the IgG isotype; it is made up of two variable regions which bind antigens and one constant domain which is responsible for effector function. Each IgG is made up of four polypeptide chains; two heavy chains with four immunoglobulin domains each and two light chains with two immunoglobulin domains. The variable regions of IgG which bind to a specific antigen are each composed from one immunoglobulin domain from a heavy chain and one from a light chain. Within the variable domains there are regions of hyper variability called complementary determining regions (CDRs), these correspond to loops which make contacts with an antigen. The effector function of an antibody is defined by the structure of the CH2 and CH3 domains of the heavy chains, different IgG subtypes have different amino acid sequences. The difference in sequence between isotypes modifies Fc receptor and complement interactions. The two heavy chains are held in an open conformation by a sugar structure linked to ASN297, this is essential for FcγR binding. Residues with the CH2 domain and the sugar structure are important for interactions with FcγRs and complement factor C1q.

1.4.2.1 The Variable Domain and Antigen Specificity

An IgG antibody has two identical variable domains which are composed of an immunoglobulin domain from a heavy chain and one from a light chain. It is the combined structure of heavy and light variable domains which define the antigen specificity of an antibody. Each antibody has a unique specificity that is determined by the amino acid sequence of the variable domains. In particular there are three regions in each variable domain which demonstrate hyper variability; these hyper variable regions (complementary differentiation regions or CDRs) correspond to three loops that make contacts with the antigen. Surrounding the CDRs there are four regions which have lower variability, these are known as framework regions one-four (Chothia and Lesk, 1987; Chothia et al., 1989). The first therapeutic antibodies developed, were produced from rodent hybridomas, however they suffered from low serum half-life and were highly immunogenic. To reduce the immunogenicity of these antibodies and allow effective interaction with human FcγRs and FcRn, the variable domain of the rodent antibody was cloned onto the constant domain of human IgG (Boulianne et al., 1984). These antibodies were named chimeric antibodies, however the rodent variable domain still generated an immune response in patients and the subsequent antibody response rendered them less effective. To further reduce the rodent sequence content of therapeutic antibodies, humanised antibodies were produced. The CDRs were cloned from rodent antibodies onto human framework regions, minimising the rodent amino acid sequence used (Jones et al., 1986). It is now possible to produce fully human antibodies from phage display libraries (McCafferty et al., 1990), or from transgenic mice (Lonberg et al., 1994).

1.4.2.2 The Constant domain and effector function

The effector function of an antibody is determined by the constant domains of the IgG heavy chain. The constant domain of IgG is able to interact with: FcγRs on effector cells, FcRn expressed by endothelial cells and complement factor C1q. The ligation of different proteins is carried out by different sections of the heavy chain, and small amino acid changes can have a large effect on binding affinity (Chan and Carter, 2010). The crystal structures of human IgG1 in complex with FcγRIIIa and FcRn have been solved, and alongside mutational analyses have highlighted residues that are important for binding to these receptors (Burmeister et al., 1994; Shields et al., 2001; Sondermann et al., 2000). Binding to FcγRs is mediated by residues in the CH2 domain proximal to the hinge region, and the different binding affinities of different IgG subclasses is caused by small

amino acid differences in the constant regions. Binding to C1q is mediated by residues in the hinge and CH2 regions, whilst binding to FcRn is mediated by residues in the CH2 and CH3 domains (Shields et al., 2001). The pH dependence of FcRn binding to IgG is mediated by histidine residues in both the CH2 and CH3 domains (Kim et al., 1994; Kim et al., 1999). Under acidic conditions, the histidine residues are protonated allowing binding to FcRn, but at neutral pH the histidines are not protonated and IgG does not bind to FcRn as strongly (Raghavan et al., 1995; Shields et al., 2001).

Mature IgG antibodies are glycosylated on Asn297 found in the constant heavy domain 2 (CH2), the complex sugar structure has proven essential for interactions with FcγRs and complement (Jefferis and Lund, 2002) (see figure 1.7). Removal of the sugar complex reduces the binding of FcγRs and C1q to the Fc portion of IgG; this is because the sugar residues hold the two heavy chains in an open conformation allowing these interactions (Huber et al., 1976; Shields et al., 2001). Serum IgG contains a huge variation in the sugar moiety attached to Asn297and B-cells can modify the sugar structure during class switching. These subtle changes in Fc region structure can have profound effects on FcγR interactions. Individuals with auto immune conditions such as arthritis display a different population of glycosylated serum IgG, which are thought to be more pro-inflammatory (Parekh et al., 1985). Recently it has been found that modifications to the sugar moiety have an effect on the binding of FcγRs. The absence of fucose from this sugar chain greatly enhances the binding of IgG1 to FcγRIIIa (Shields et al., 2002; Shinkawa et al., 2003). Figure 1.7 shows an example of the oligosaccharide attached to Asn297.

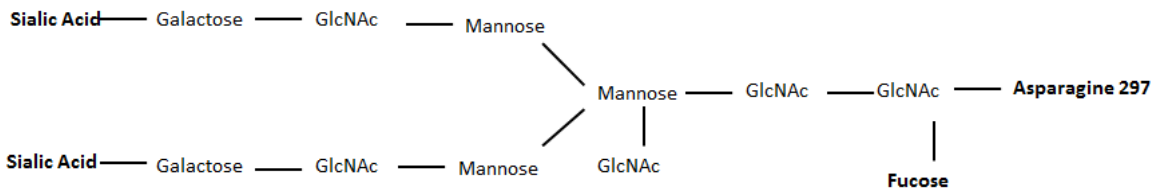

Figure 1. 7 The sugar moiety attached to asparagine 297 of IgG heavy chain

Nb. GlcNAc is N-acetylglucosamine

1.4.2.3 Antibody engineering to alter effector function

Wild type immunoglobulins already display high heterogeneity in their effector function, due to different subclasses and variation in glycosylation pattern. When designing therapeutic antibodies, it is possible to select an appropriate subclass for the application. For example, a neutralising antibody that does not require FcγR activation to function might be produced with an IgG4 constant region as it naturally has lower affinity for FcγRs than other subclasses. Conversely, an antibody which is required to kill a target cell will require a stronger effector function to allow ADCC, and therefore would be produced with an IgG1 constant region. Understanding how the constant domain interacts with FcγRs allows modification of the amino acid sequence and glycan structure, to optimise the effector function of therapeutic antibodies.

To produce antibodies with reduced effector function, there are a number of modifications that can be made. Production of a human IgG2/IgG4 chimeric antibody has low affinity for FcγRs and better stability than an IgG4 antibody alone (Rother et al., 2007). The FES mutation (L234F, L235E, P331S) in human IgG1 reduces antibody effector function without significantly changing the structure of the Fc domain (Oganesyan et al., 2008). Fucosylation of IgG1 lowers affinity for FcγRIIIa, as the extra sugar sterically hinders binding to the receptor (Shields et al., 2002). Reducing the effector function of antibodies can also be achieved by augmenting the binding to the inhibitory receptor, the mutant selectively (S267E, L328F) increases the affinity of human IgG1 for FcγRIIb by 400 fold (Horton et al., 2011). Modifications to the Fc region of IgG can also be used to selectively increase the affinity for activating FcγRs. Mutation such as S298A/E333A/K334A increases the binding of human IgG1 (human) to FcγRIIIa, and improve *in vivo* tumour killing (Bowles et al., 2006; Lazar et al., 2006), The affinity to the FcγRIIa can also be selectively increased with the mutation G236A, this causes a 70 fold increase in FcγRIIa binding relative to FcγRIIIb and enhances phagocytosis of immune complexes (Richards et al., 2008). Aglycosylated IgG has very low affinity for FcγRs, however mutation (E382V, M428) leads to selective high affinity binding of FcγRI (Jung et al., 2010). IgG already has a long serum half-life, and this is due to the binding of FcRn which is expressed by endothelial cells. Random mutation of residues surrounding FcRn binding sites, found Fc mutants that had higher affinity for FcRn, and increased serum persistence (Ghetie et al., 1997).

1.4.3 Humoral Immunity in the CNS

1.4.3.1 FcγR Expression on CNS cells

The role of FcγRs in peripheral organs have been well characterised, but expression levels and function in the CNS are less well described. Multiple cell types within the CNS express FcγRs, and changes in expression patterns occur in response to different stimuli. Table 1.1 and 1.2 summarise the expression pattern and function of FcγRs on CNS cells in humans and mice respectively, under healthy and diseased conditions.

Human microglia express: FcγRI, FcγRIIa, FcγRIIb and FcγRIIIa albeit at very low levels under normal conditions. The expression is increased on microglia in the CNS of patients with MS (Ulvestad et al., 1994), and a number of neurodegenerative conditions(Fuller et al., 2014). In AD ramified microglia in the parenchyma, but especially those associated with plaques express higher levels of: FcγRI, FcγRII and FcγRIII compared to age matched controls (Peress et al., 1993). Interestingly the expression of FcγRI and FcγRIIb are decreased on microglia of AD patients whose plaques were cleared by active immunotherapy (Zotova et al., 2013). Age related macular degeneration is associated with an increased number of CD45+ leukocytes expressing activating FcγRIIa (and to a lesser extent inhibitory FcγRIIb) at the choroid-retinal epithelial cell interface (Murinello et al., 2014). Finally increased FcγRI microglial expression is found in the CNS of patients with PD (Orr et al., 2005). Murine microglia express all known FcγRs: FcγRI, FcγRIIb, FcγRIII and FcγRIV. The expression of these receptors is increased in response to a number of different insults to the CNS. All four FcγRs are up regulated on microglia in response to prion disease and further up-regulated by systemic inflammation, whilst the up regulation of FcγRII/III has been observed in TG2576 APP mice (Lunnon et al., 2011; Wilcock et al., 2004b). FcγR expression can also be altered under experimental conditions, Type III hypersensitivity (or Arthus reaction) in the CNS (brain and retina) induces robust expression of FcγRI, FcγRIIb, FcγRIII and FcγRIV followed by a neuro-inflammatory response (Murinello et al., 2014; Teeling et al., 2012). Normal ageing is also associated with increased FcγR immuno-reactivity, and microglia especially those in white matter regions of the CNS, show elevated expression of FcγRI but not other FcγRs (Hart et al., 2012).

The expression of FcγRs on neurons was once controversial, however a number of studies have now documented their expression on neurons both *in vitro* and *in vivo*. Human sensory and motor neurons express the high affinity FcγRI which enable the cells to take up IgG from the surroundings (Andoh and Kuraishi, 2004; Mohamed et al., 2002). The inhibitory FcγRIIb has been detected on healthy neurons in the hippocampus of both mice and humans. The expression of FcγRIIb is increased on neurons in the AD brain, and also in response to treatment with Aβ (Kam et al., 2013; Nakamura et al., 2007). Murine neurons have been found to express FcγRII/III which mediate the uptake of therapeutic anti-tau antibodies into neurons (Congdon et al., 2013). Finally neurons in the hippocampus of $APOE^{-/-}$ mice express FcγRIV and signal in response to the higher levels of IgG in the CNS (Fernandez-Vizarra et al., 2012).

There are a limited number of studies investigating FcγR expression on other CNS cell types. FcγRI has been detected on astrocytes cultured in vitro, and also on rat astrocytes in vivo in response to BBB permeability changes (Li et al., 2008). There is also evidence that the Fcγ chain is required for differentiation of oligodendrocytes, however with the other immune-receptors that also signal through the Fcγ chain it is not possible to conclude that FcγRs are required (Nakahara et al., 2003). Finally, Murine CNS endothelial cells express FcRn and FcγRIIb. FcRn has been found to mediate the transport of therapeutic anti-Aβ antibodies from the CNS into the periphery (Deane et al., 2005).

1.4.3.2 Immunoglobulin G entry into the CNS

Despite tight control by the BBB, it is apparent that small amounts of IgG enter the healthy brain and it has been estimated that 0.1% of circulating IgG enters the CNS via passive diffusion (Poduslo et al., 1994). However, this may be altered during ageing and/or disease, and associated changes in BBB integrity and interaction with FcRn. For example, under healthy conditions, IgG is removed from the CNS by an efficient process of reverse transcytosis across the BBB (Zhang and Pardridge, 2001), mediated by FcRn (Deane et al., 2005; Schlachetzki et al., 2002).This transport of IgG is saturated at high levels of IgG, reducing the rate of IgG efflux. It is widely recognised that a functional BBB limits passage of macromolecules and cells from the periphery and that disruption of the BBB by insults such as, ageing, stress and systemic inflammation, obesity, all risk factors for earlier onset of clinical symptoms in AD patients, are associated with an influx of serum proteins including IgG (Diamond et al., 2006; Lu et al., 2001).Under these conditions the net influx of IgG

would be increased, resulting in accumulation of IgG in the parenchyma, and around cerebral vessels.

Cell Type	FcγRs Expressed	Conditions for expression	References
Microglia	FcγRI, FcγRIIb, FcγRIII and FcγRIV	**All↑**: Neurodegeneration +/- systemic LPS, immune complex formation in retina **FcγRII/III↑**: Aβ immunotherapy or arthus reaction in the brain **FcγRI↑**: ageing, especially in white matter regions	(Hart et al., 2012; Lunnon et al., 2011; Murinello et al., 2014; Teeling et al., 2012; Wilcock et al., 2004b)
Neurons	FcγRIIb, FcγRIV FcγRII/III	**FcγRIIb↑:** Aβ treatment **FcγRIV↑:** $APOE^{-/-}$ genetic background	(Kam et al., 2013) (Fernandez-Vizarra et al., 2012)
Astrocytes	FcγRI	**FcγRI↑:** increased CNS IgG	(Li et al., 2008)
Oligodendrocytes	Fcγ chain	**Fcγ chain** is expressed by oligodendrocyte precursor cells	(Nakahara et al., 2003)
Endothelial cells	FcRN	**FcRN** constitutively expressed on CNS endothelium	(Deane et al., 2005)

Table 1. 1 Expression of FcγRs on murine CNS cells

This table shows the expression patterns of FcγRs on different murine CNS cell types. The conditions in which up or down regulation of specific FcγRs has been observed have been recorded.

Cell Type	FcγRs Expressed	Conditions for expression	References
Microglia	FcγRI, FcγRIIa, FcγRIIb, FcγRIIIa	**All**↑ Alzheimer's Disease, Multiple Sclerosis **FcγRI**↑ Parkinson's Disease **FcγRI &FcγRIIb**↓ Alzheimer's Disease after plaque clearance **FcγRIIa &FcγRIIb**↑ Age related macular degeneration	(Murinello et al., 2014; Orr et al., 2005; Peress et al., 1993; Ulvestad et al., 1994; Zotova et al., 2013)
Neurons	FcγRI, FcγRIIb	**FcRI** Expressed constitutively on sensory and motor neurons **FcRIIb**↑ Alzheimer's disease	(Andoh and Kuraishi, 2004; Mohamed et al., 2002) (Kam et al., 2013)

Table 1. 2 Expression of FcγRs on human CNS cells

This table shows the expression patterns of FcγRs on different human CNS cell types. The conditions in which up or down regulation of specific FcγRs has been observed have been recorded. There are a limited number of studies examining FcγR expression for most human CNS cell types.

1.4.4 New roles for FcγRs in neurodegeneration

There are emerging roles for different FcγRs in the underlying pathology of neurodegenerative disorders. As outlined in the previous section, increased expression of all FcγRs is consistently reported in human brain tissue of neuro-inflammatory and degenerative diseases including: PD, AD, and Multiple sclerosis (Cribbs et al., 2012; Nyland et al., 1984; Orr et al., 2005; Peress et al., 1993; Ulvestad et al., 1994). There is evidence that ligation of specific FcγRs in the CNS by IgG and alternate ligands can promote neuroinflammation and/or enhance neurodegeneration.

1.4.4.1 Auto antibodies

Apart from elevated FcγR, increased levels of total IgG in the CNS has also been reported in various neurodegenerative diseases, possibly as a result of an age-related increase in BBB permeability (Bouras et al., 2005). Serum from AD and PD patients are known to contain auto-antibodies against glutamatergic and dopaminergic neurons, which are selectively affected in AD and PD patients respectively. Furthermore, neurons of the substantia nigra (SN) from patients with idiopathic cases of PD have been found to be immuno-reactive for IgG (Orr et al., 2005). IgG isolated from the sera of PD patients, injected into the brains of mice, specifically binds neurons in the SN. This binding induces neuroinflammation as measured by increased expression of CD11b, and loss of SN neurons (He et al., 2002). The use of Fcγ chain deficient mice, which lack all activating FcγRs or $F(ab')_2$ fragments of PD IgG prevented these responses (He et al., 2002), demonstrating that an FcγR mediated mechanism could drive neurodegeneration in PD. A similar role for FcγRs in the pathology of AD is described. Increased expression of FcγRs (FcγRI, FcγRII, and FcγRIIIa) in disease affected areas of AD patients has been observed on both glial cells and neurons (Bouras et al., 2005; Peress et al., 1993). Application of serum-derived IgG from AD patients, containing neuron specific antibodies, into the forebrain of rats results in the selective reduction of cholinergic neurons, supporting the concept that in AD auto-reactive antibodies could in part drive neuronal loss (Engelhardt et al., 2000). The histological examination of brain tissue from AD patients provides further evidence for a detrimental role of these antibodies, as cholinergic neurons that stain positive for IgG also express markers of degeneration such as caspase 3 (D'Andrea, 2003).

1.4.4.2 Neuronal FcγRs

Evidence for a detrimental role of increased influx of serum derived IgG into the CNS was recently shown in ApoE deficient mice. This model is of interest to AD researchers because the ApoE4 allele is the largest genetic risk factor for sporadic AD (Strittmatter and Roses, 1995). ApoE deficient mice develop many neuropathological changes in common with AD including: increased BBB permeability, accumulation of intra-neuronal Aβ, hyper-phosphorylation of tau and cognitive impairment (Fernandez-Vizarra et al., 2012). A critical role for FcγR was elegantly shown in this experimental model. When crossed with an Fcγ chain deficient mice, the double knock out animals have similar increased BBB permeability. However they are protected from other neuropathological changes including: microgliosis, neuronal damage and cognitive impairment. Fcγ chain deficient mice also do not express other immune receptors, so this should be taken into account when analysing this data. However specific knock down of FcγRIV with siRNA prevents similar effects of IgG on primary neurons in vitro. These results imply that it is the interaction between IgG in the brain and FcγR expressing neurons that drive AD-like pathology in these mice. Neurons of AD patients and APP transgenic mice also express the inhibitory receptor/FcγRIIb (Kam et al., 2013). FcγRIIb has a low affinity for monomeric IgG1 ($K_D = 9.43 \times 10^{-6}$ M), but binds with high affinity to Aβ ($K_D = 5.67 \times 10^{-8}$ M). Aβ is a potent inducer of neuronal apoptosis, and this effect is ameliorated in FcγRIIb deficient neurons (Kam et al., 2013). It is not currently known if Aβ signals through FcγRIIb using the same signalling pathway as immune complexes. It will be important to understand if cross-linking of neuronal FcγRIIb by immune complexes can induce the same effect.

1.4.4.3 Protection from neurodegeneration in Fcγ chain $^{-/-}$ mice

Our own studies have provided evidence that the Fcγ chain also contributes to IgG-mediated inflammation and neuronal function. Formation of IgG immune complexes in the mouse brain (Teeling et al., 2012) or the retina results in a transient, but robust neuroinflammatory response, that depends on activating FcγRs (Murinello et al., 2014). Further, using an experimental model of neurodegeneration we show that FcγRs are expressed on microglia and up-regulated following systemic inflammation. The latter is associated with increased production of pro-inflammatory cytokines, which is attenuated in Fcγ chain deficient mice (Lunnon et al., 2011). The Fcγ chain deficient background is also neuroprotective in other experimental models of neurodegenerative

disease, including ischemic stroke (Komine-Kobayashi et al., 2004) and synuclein-induced neurodegeneration following AAV transfer (Cao et al., 2012; Cao et al., 2010).

1.4.4.4 The effects of soluble inflammatory mediators

The ligation of auto antibody coated neurons, or plaques coated in antibody, by activating FcγRs will lead to the polarisation macrophages to an m2b phenotype and the production of a number of cytokines and inflammatory mediators (Mosser and Edwards, 2008). Receptors for a number of cytokines are expressed on neurons and other cells in the brain.

Neuronal function is tightly regulated and a small change in homeostasis can be detrimental depending on the levels of cytokines produced. At physiological levels TNFα has important roles in regulating normal brain activity including regulation of synaptic scaling (Stellwagen and Malenka, 2006). Low levels of monomeric IgG in the brain (0.2-20ug/ml) are observed under healthy conditions and induce these levels of TNFα via tonic signalling of FcγRI expressed on microglia. Under these condition TNFα is neuroprotective against excitotoxicity, but increasing levels of monomeric IgG abrogates this effect eventually becoming neurotoxic (Hulse et al., 2008). At higher levels, TNFα, at least *in vitro* is neurotoxic causing loss of cells by signalling through TNFR1 (Yang et al., 2002). Therefore increased TNFα production as a result of excessive FcγR ligation could be twofold: high levels could induce apoptosis of susceptible neurons or it could interfere with TNFα's regulation of synaptic plasticity. IL-1β is also important for the function of neurons under physiological conditions. Normal concentrations of IL-1β are essential for hippocampal long term potentiation (LTP), however higher pathological levels (10ng/ml) result in the inhibition of LTP (Bellinger et al., 1993; Katsuki et al., 1990; Ross et al., 2003). *In vivo* studies are sparse, but *in vitro* studies have provided further evidence of a critical role of FcγR in neuronal damage. Microglia co-cultured with dopaminergic neurons coated with IgG from the sera of PD patients, results in increased levels of pro-inflammatory cytokines (TNFα), reactive oxygen species synthesis, and the initiation of cell death in co-cultured neurons. The damage to neurons was shown to be dependent on nitric oxide (NO) production, as inducible NO synthase inhibitors but not cytokine blocking antibodies could inhibit neuronal death. This effect was shown to be Fcγ chain-dependent as microglia from Fcγ chain deficient mice fail to induce cytokine/ROS production or neuronal damage (Le et al., 2001).Recently it was shown that microglial activation in response to LPS or Aβ

could epigenetically regulate the expression of synaptic proteins, silencing neuroligin gene expression, causing synapse loss (Bie, 2014). The mediators produced by microglia which cause these effects are yet unknown, but it is possible that antibody mediated inflammation could also cause silencing neuroligin gene expression resulting in synapse loss. Therefore the increased production of: TNFα, IL-1β, NO or other inflammatory mediators by m2b polarised microglia could lead to impairment of neuronal function or exacerbation of neuronal/synapse loss in AD patients.

FcγRs may contribute to the pathology of neurodegenerative diseases through a number of mechanisms and thus it is important to consider this when developing immunotherapies targeting CNS antigens. Targeting Aβ leads to changes in FcγR expression on CNS effector cells, if this increases the ratio of activating to inhibitory FcγR it could exacerbate existing pathology. Furthermore immune complexes formed in the CNS may interact with other FcγR expressing cells such as neurons. The function of FcγRs expressed by neurons is unclear, but it seems that their ligation can induce neuron loss.

1.5 Immunotherapy for Alzheimer's disease

The amyloid cascade hypothesis has driven the majority of AD research and drug development in the past twenty years. One approach to clear Aβ from the brain is to immunise against Aβ, either by active or passive immunotherapy. Immunisation against Aβ reduces parenchymal deposits in transgenic mouse models and to a certain extent in humans (Morgan et al., 2000; Nicoll et al., 2006; Ostrowitzki et al., 2012; Rinne et al., 2010; Schenk et al., 1999). In the next section I will outline preclinical work demonstrating efficacy in transgenic APP mice, summarise previous and current clinical trials for Aβ immunotherapy and outline evidence that FcγRs are involved in Aβ clearance and the side effects associated with immunisation.

1.5.1 Active Immunotherapy

Mice transgenic for human APP are frequently used to model AD pathology. These mice develop deposits of Aβ in the brain parenchyma and around cerebral blood vessels, with associated neuro-inflammation and cognitive deficits (Games et al., 1995; Holcomb et al., 1998; Hsiao et al., 1996). Dale Schenk et al first showed that immunisation of PDAPP mice with a synthetic Aβ peptide and Complete Freund's Adjuvant (CFA) could promote the production of anti-Aβ antibodies, which prevent the deposition of Aβ when given to young mice (6 weeks), and stimulate the clearance of plaques from disease-affected older mice (11months) reversing cognitive deficits (Morgan et al., 2000; Schenk et al., 1999). In 2000 Elan pharmaceuticals began clinical trials of an Aβ vaccine (AN1792) which was well tolerated in phase I, with some patients developing a high titre (over 1 in 1000) of anti-Aβ antibodies (Schenk, 2002). However the subsequent phase IIa trial was halted due to a subset (6%) of patients developing meningocephalitis (Orgogozo et al., 2003). This seemed to be due to the generation of auto reactive, Aβ specific T-cells, due to the adjuvant or the peptide used to immunise (Kathryn, 2002). Post mortem analysis of patients enrolled in these trials has revealed that immunisation with AN1792 induced the removal of parenchymal Aβ deposits, with increased efficacy associated with higher Aβ antibody titres (Holmes et al., 2008; Nicoll et al., 2006; Nicoll et al., 2003). Whilst parenchymal Aβ was removed from actively immunised AD patients; a concurrent deposition of Aβ around blood vessels and increased incidence of micro haemorrhage was observed (Boche et al., 2008). The immunised patients showed no improvement in cognition (Holmes et al., 2008), however this trial was underpowered to detect such an effect. Next generation active immunotherapy now employs shortened peptides from the N-terminal region, avoiding the

T-cells activation through T-cells specific epitopes (Maier et al., 2006). A summary of past and present active vaccines is shown in table 1.3.The company Affiris developed the AD02 vaccine for AD, which instead of vaccinating with full length Aβ or a peptide fragment thereof, a synthetic peptide which mimics Aβ was used. The idea behind this was to stimulate the production of antibodies against the synthetic peptide that would cross react to Aβ but not to full length APP. After a good safety profile in phase I, AD02 failed to improve cognition in patients in phase II trials. It was later claimed that the placebo group, patients receiving adjuvant alone, were actually protected from cognitive decline. The adjuvant has now been renamed AD04, and an open label phase II study is continuing. The drawback of active immunisation is that clinicians have little control over the antibody titre and it is hard to reverse treatment in the face of serious adverse effects.

Active immunisation

Vaccine	Company	Peptide	Adjuvant	Meningo-cephalitis	ARIA	Developmental stage	Ref.
AN1972	Elan	Aβ 1-42	QS-21	Yes	?	Phase II abandoned due to side effects	(Boche et al., 2008; Nicoll et al., 2003; Orgogozo et al., 2003; Schenk et al., 1999)
CAD106	Novartis	Aβ 1-5 + Qβ linker	?	No	Yes	Phase IIb	
AAC O1	Elan/Janssen / Pfizer	Aβ 1-6	QS- 21	No	?	Phase IIb	
AD02	Affiris	Aβ 1-5 (mimitope peptide)	Alum	No	?	Phase II	

Table 1. 3 Anti-Aβ Vaccines that have reached Clinical Trials

This table shows a summary of and monoclonal antibodies which have been tested in clinical trials for AD.

1.5.2 Passive Immunotherapy

To circumvent problems with active immunisation, monoclonal antibodies were raised against Aβ for use as passive immunotherapy. Monoclonal Aβ antibodies are also able to clear Aβ deposition and reverse cognitive deficiencies in APP transgenic mice (Bard et al., 2000; DeMattos et al., 2001; Wilcock et al., 2004b). Antibodies that are able to reduce parenchymal Aβ (such as 3D6 which recognise the N-terminus of Aβ) are associated with an increased deposition of Aβ around the vasculature, and an increased incidence of micro haemorrhage (Wilcock et al., 2004c; Zago et al.).

A number of monoclonal antibodies have been tested in clinical trials, which are summarised in table 1.4. Bapineuzumab (Elan, IgG1- N-terminus) and Solanezumab (Eli Lilly, IgG1, mid terminal epitope) were the first antibodies to be tested in humans. Bapineuzumab (IgG1 humanised 3D6) binds to the N-terminus of Aβ and is able to bind and breakdown plaques, activating microglia and promoting phagocytosis through FcγRs (Bard et al., 2000). Solanezumab (IgG1 humanised m266) binds to a mid-terminal epitope and is unable to bind plaques, causing clearance by binding of circulating and CNS soluble forms (e.g. oligomeric species) of Aβ (DeMattos et al., 2001). During phase II clinical trials both antibodies showed promising changes to cerebro-spinal fluid (CSF) biomarkers such as Aβ, indicating that these therapies could be effective in humans (Imbimbo et al., 2012; Salloway et al., 2010). However only Bapineuzumab was shown to reduce Aβ load in the brains of AD patients measured by PET scan (Rinne et al., 2010). Patients in phase II trials were monitored using magnetic resonance imaging (MRI) scans and side effects were detected in the Bapineuzumab trial, designated Amyloid Related Imaging Abnormalities (ARIAs) (Salloway et al., 2010). Vasogenic edema (ARIA-E) was detected in 9.7% of patients treated with Bapineuzumab and 0% in the placebo group, a higher frequency of micro-haemorrhages (ARIA-H) were detected in Bapineuzumab treated patients compared to controls (Salloway et al., 2010). Vasogenic edema is the leakage of fluid from cerebral blood vessels due to a leaky blood brain barrier, and the incidence of ARIA-E was higher in ApoE4 carriers (Salloway et al., 2010). Due to these side effects experienced by the patients, the top dose of Bapineuzumab given in phase III was abandoned, potentially contributing to the lack of efficacy in the trial (Salloway et al., 2014). ARIA-E was not observed in Solanezumab treated patients, indicating that it was likely that the clearance of plaques and concomitant microglial activation are responsible for the initiation of the vascular problems (Imbimbo et al., 2012). Both antibodies reached phase III trials, but failed to meet primary end points, which was to improve overall cognition of patients (Doody et al., 2014; Salloway et al.,

2014). Post hoc analysis found that Solanezumab caused a modest improvement in the cognition of patients in the earlier stages of disease. As a result a new phase III trial was carried out in patients in the earlier stages of AD, the data from this trial was presented at the Alzheimer's association international conference (2015), and showed that Solanezumab significantly improved cognition.

Passive immunisation

Antibody	Company	Epitope	Species	Subclass	ARIA	Developmental stage	Ref.
Bapineuzumab	Janssen/ Pfizer	N-terminus AA 1-5	Aggregated and soluble Aβ	Humanised IgG1	Yes	Failed to meet primary endpoints in Phase III	(Rinne et al., 2010; Salloway et al., 2014; Salloway et al., 2010)
Solanezumab	Eli Lily	Mid terminus AA 13-26	Soluble Aβ	Humanised IgG1	No	Repeat phase III in mild AD showed modest cognitive benefit + A4 trial in MCI patients and DIAN trial (familial AD)	(DeMattos et al., 2001; Doody et al., 2014; Imbimbo et al., 2012)
Gantenerumab	Roche	N-terminus and mid terminus AA 1-5 +?	Conformational epitope of fibrillar Aβ	Fully human IgG1	Yes	Phase III in MCI failed but DIAN trial (familial AD) continuing	(Bohrmann et al., 2012; Koenigsknecht-Talboo et al., 2008; Ostrowitzki et al., 2012)
Ponezumab	Pfizer	C terminus of Aβ40	Aβ1-40	Humanised IgG2 (Fc mutant)	No	Discontinued after Phase II for AD; but reactivated for CAA	(Burstein et al., 2013; Freeman et al., 2012; Landen et al., 2013)

Crenezumab	Genentech	Mid terminus AA 12-23	All forms of Aβ	Humanised IgG4	No	Phase III + API trial	(Adolfsson et al., 2012)
Ban2401	Bioarctic/ EISAI	?	Aβ protofibrils	Humanised IgG1	Yes	Phase IIb	
Aducanumab	Biogen	N-terminus AA3-6	Conformational epitope of fibrilar Aβ	Fully Human IgG1	Yes	Phase III	
GSK933776	GSK	N-terminus AA1-5	All forms of Aβ	Fully human IgG1 Effector reduced (alanine 235 and 237)	No	Phase I	(Andreasen et al., 2015)

Table 1. 4 Anti-Aβ Antibodies that have been tested in Clinical Trials

This table shows a summary of and monoclonal antibodies which have been tested in clinical trials for AD.

There are a number of new antibodies and vaccines entering clinical trials which are also summarised in table 1.4. Roche has continued its development of Gantenerumab-a fully human IgG1 antibody, which binds to a conformational epitope of Aβ with higher affinity for fibrillar than soluble Aβ (Bohrmann et al., 2012). Gantenerumab has entered phase III trials; like Bapineuzumab it is able to clear Aβ from the brain but also causes ARIA-E and ARIA-H (Ostrowitzki et al., 2012). Solanezumab showed that the therapeutic window for treating AD patients is likely earlier in the course of disease. As a result a number of clinical trials have aimed to treat before the onset of AD. Gantenerumab was used in the SCarlet RoAD trial, which enrolled patients in the pro-dromal stages of AD (MCI) to test if immunotherapy could prevent progression to AD. Unfortunately, this trial was abandoned due to a futility analysis earlier in 2015. Gantenerumab and Solanezumab are both being used in the Dominantly Inherited Alzheimer's Network trials (DIAN), where patients who carry mutations in the APP gene and will develop AD in mid-life, are treated prophylactically.

To address the problem of vascular damage associated with immunotherapy, Crenezumab has been developed by Genentech. Crenezumab is able to bind to all forms of Aβ and previous studies would predict that it would induce vascular damage (Salloway et al., 2010; Wilcock et al., 2004c), but it is built on a human IgG4 backbone which has lower affinity for activating FcγRs (Bruhns et al., 2009). This reduces microglial activation in comparison to its IgG1 form *in vitro*, but still allows phagocytosis of opsonised oligomers of Aβ. During a phase I trial during patients received 10-fold higher doses of Crenezumab than were given in the Bapineuzumab trial, with no detectable vascular side effects (Adolfsson et al., 2012). Crenezumab was then tested in the phase II ABBY trial with a dose of 15 mg/kg, overall there were no changes in cognition, like Solanezumab when stratified for mild cases only Crenezumab had a positive effect, the phase II trial is being extended in an open label study until 2016, and a familial AD prevention trial using Crenezumab is underway. Patients from Colombia, who possess a mutation in the PS1 gene who will develop AD during mid-life, have been recruited to the Alzheimer's prevention initiative (API) trial and treated with Crenezumab.

A separate problem may arise with the strategy of targeting all forms of Aβ, where soluble forms in the brain saturate the available antibodies, preventing efficient plaque clearance. This has been demonstrated in extensively aged (22 month) PDAPP mice, where 3D6 (Bapineuzumab) is unable to clear plaques after systemic administration due to the high levels of Aβ in the brain (DeMattos et al., 2012). These observations may explain the clinical findings that Bapineuzumab does not clear all of the deposits from the brains of AD patients. A number of companies have developed

antibodies specifically targeting the aggregated forms of Aβ. Biogen have developed a fully human anti-Aβ antibody Aducanumab (human IgG1, N-terminus conformational epitope) that was derived from healthy aged patients and specifically recognises aggregated rather than soluble forms of Aβ. Data from phase I presented at the AD/PD conference in 2015 has given a boost to the field of AD immunotherapy. Aducanumab significantly lowered Aβ levels in the brain and this clearance was far more robust than clearance of plaques in Bapineuzumab or Gantenerumab trials. Alongside reduction in Aβ, Aducanumab caused a significant improvement in cognition compared to the placebo group. Like Gantenerumab and Bapineuzumab, Aducanumab caused increased ARIA-E in patients, in a dose dependent manner. Eli Lily has developed an antibody which binds to a form of Aβ (pyroglutamate Aβ) located almost exclusively in plaques. Preclinical studies have shown that this antibody is able to clear plaques from the brains of the extensively aged mice without inducing micro-haemorrhage, probably because it cannot bind to vascular Aβ (DeMattos et al., 2012). A potential problem with this strategy is that breaking up plaques could increase the levels of toxic species such as oligomers and cause an increase in vascular Aβ, which this antibody would be unable to remove.

In spite of a number of clinical failures of anti-Aβ antibodies, there have been a couple of success stories that justify continuing to develop immunotherapy for AD. There are many reasons that the first generation of antibodies failed to improve the clinical outcome of patients including: treating too late in the disease, inflammatory side effects and poor target engagement. New study design, modification of therapeutic antibodies and the targeting of specific species of Aβ have helped to overcome these issues. Perhaps the most exciting prospect is Aducanumab, which has already shown promising signs in early clinical trials. However, Aducanumab like other antibodies able to bind to aggregated Aβ, causes damage to the cerebral vasculature which could prove a stumbling block in the future. Importantly, the trials for Solanezumab and Aducanumab have demonstrated that clearance of Aβ from the brain of AD patients can slow the rate of cognitive decline, supporting the important role of Aβ in the pathology of AD.

1.5.3 Mechanisms of antibody mediated plaque clearance

There are a number of putative mechanisms explaining the action of anti Aβ immunotherapy; importantly they are not mutually exclusive and may be epitope and IgG subtype dependant. Mechanisms of Aβ clearance are summarised in figure 1.7.

1.5.3.1 Evidence for Fc gamma receptor mediated phagocytosis of Aβ

A possible role for FcγRs in the mechanism of antibody mediated Aβ clearance has been investigated. Antibodies, such as 3D6 cross the BBB and bind to fibrillar Aβ, this leads to clearance of plaques by FcγR mediated phagocytosis and mechanisms independent of FcγRs (Bard et al., 2000; Wilcock et al., 2006; Wilcock et al., 2004b). Intracranial injection of plaque-binding Aβ antibodies (2H6) into APP mice (TG2576) results in the rapid break down and removal of plaques. The response is bi-phasic: 24 hours after injection diffuse Aβ is removed, followed by the clearance of dense thioflavin S positive plaques after 72 hours-coinciding with activation of microglia (Wilcock et al., 2003). These initial observations indicated that microglial activation may be required to clear dense deposits, this was confirmed when inhibition of microglial activation by dexamethasone prevented the clearance of deposits (Wilcock et al., 2004a). Intracranial injection of antibodies lacking the Fc region ($F(ab)_2$), also prevent microglial activation and impaired the clearance of the same dense deposits (Wilcock et al., 2004a), supporting the hypothesis that microglia clear Aβ through FcγRs. Systemic administration of plaque binding antibodies also results in microglial activation, while mAbs targeting the soluble species, for example m266 do not (Koenigsknecht-Talboo et al., 2008; Wilcock et al., 2004b). This activation of microglia is characterized by increased expression of CD45, MHCII and FcγRII/III (Wilcock et al., 2004b). Further evidence for a role of FcγR in microglial activation comes from studies using Crenezumab (IgG4), which show reduced microglial activation as measured by cytokine production and p38 signalling in comparison to IgG1(Adolfsson et al., 2012). In addition, reduction of FcγR affinity by de-glycosylation results in reduced microglial activation and reduced clearance of Aβ compared to intact IgG after systemic treatment (Koenigsknecht-Talboo et al., 2008; Wilcock et al., 2006). There is limited evidence of the role of FcγRs in the clearance of Aβ from the brains of human AD patients, although monoclonal antibodies can stimulate the uptake of Aβ by microglia in human *ex vivo* brain tissue (Ostrowitzki et al., 2012).

1.5.3.2 Catalytic Dissociation/ inhibition of fibrilisation

In vitro application of anti-Aβ antibodies can inhibit the formation of fibrillar Aβ in the absence of other molecules (Solomon et al., 1996). This suggests that binding of an antibody to Aβ can cause a conformational change in the protein or sterically hinder fibrillisation (Morgan, 2009). Therefore treatment of patients with anti-Aβ antibodies may lead to a reduction in the amount of plaques by either binding to and changing the conformation of plaque associated Aβ or by binding to smaller species and preventing further aggregation. This is supported by studies showing that single chain variable domains (scFvs) can bind to Aβ and inhibit plaque formation *in vitro* and in vivo (Frenkel et al., 2000; Fukuchi et al., 2006; Liu et al., 2004).

1.5.3.3 Peripheral Sink

Soluble Aβ can also be found in the plasma of AD patients and healthy individuals. Therefore treatment with an anti-Aβ antibody which can bind soluble forms, will lead to target engagement in the periphery as well as the CNS. It has been suggested that an alternative route of Aβ clearance from the CNS is through antibody mediated Aβ clearance from the plasma, which creates a concentration gradient causing increased efflux of Aβ from the CNS (DeMattos et al., 2001). Formation of small immune complexes between Aβ and antibody in the periphery would allow clearance by complement receptor 1 (CR1) expressing cells (Arlaud et al., 2002). This putative mechanism is difficult experimentally to separate from other mechanisms of clearance.

1.5.3.4 Neonatal Fc receptor mediated clearance

FcRn can facilitate the removal of IgG from immune privileged areas such as the brain, where it is expressed by brain endothelial cells (Roopenian and Akilesh, 2007). In the context of immunotherapy, it has been shown that Aβ clearance from the brain of APP mice is partially dependant of FcRn mediated efflux. Knocking out FcRn in TG2576 significantly reduces the antibody mediated clearance of Aβ from the brain (Deane et al., 2005). This can be explained by the uptake of antibody bound to Aβ by brain endothelial cells, leading to binding of IgG by FcRn in an endosome, and the efflux of IgG and Aβ into the circulation.

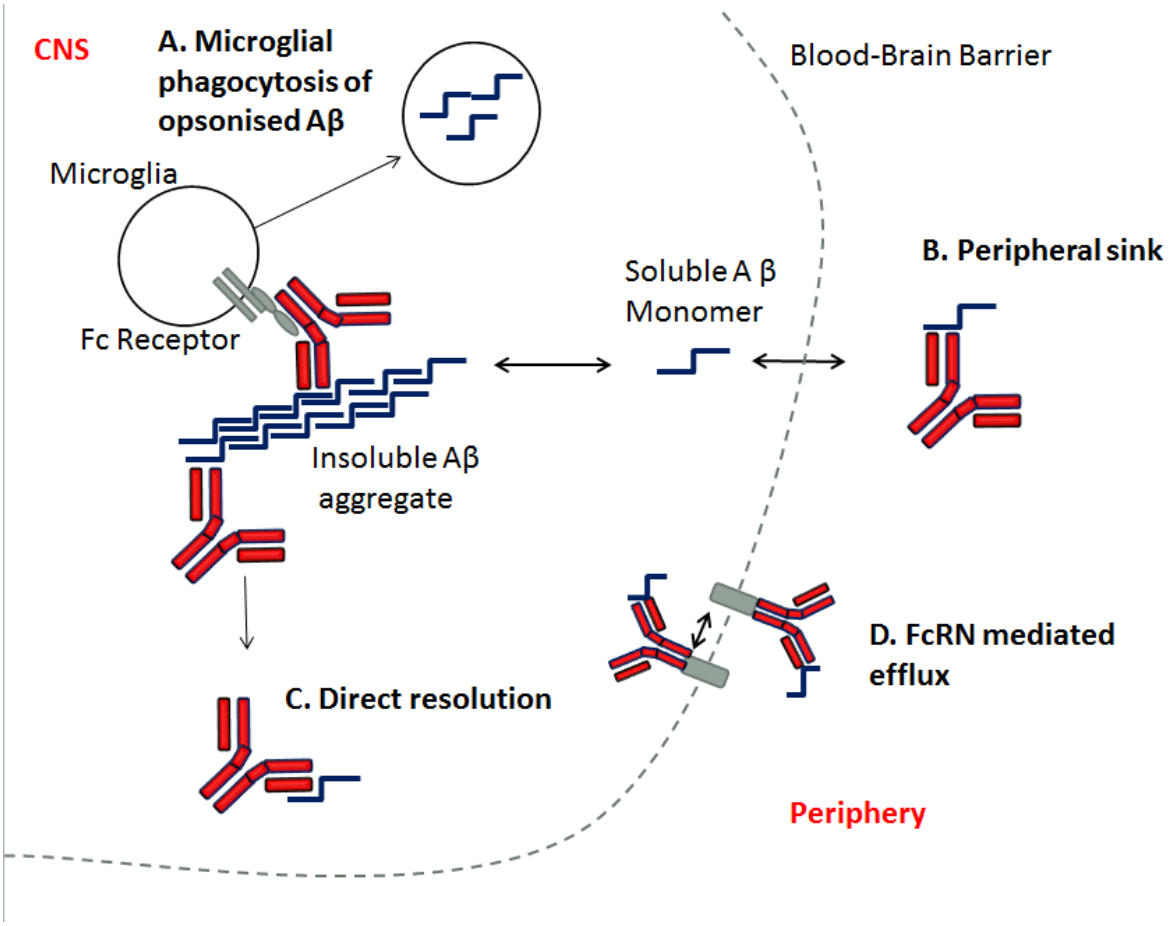

Figure 1. 8 Different mechanisms of antibody mediated clearance of Aβ from the CNS

A. Antibodies enter the CNS and bind to Aβ, activating microglia, stimulating phagocytosis

B. Antibodies do not need to enter the CNS but bind Aβ in the periphery creating a concentration gradient which causes efflux of Aβ from the CNS.

C. Antibodies directly disaggregate plaques by changing the conformation of monomers, preventing fibrilisation.

D. The neonatal Fc receptor expressed by brain endothelial cells, shuttles antibody bound to Aβ across the BBB

1.5.4 Evidence for Fc receptor involvement in side effects

Passive immunotherapy is able to clear plaques from the brains of both APP mice and humans, but this intervention is associated with ARIA-E and ARIA-H (Ostrowitzki et al., 2012; Salloway et al., 2010; Wilcock et al., 2004c). Antibodies such as the plaque binding 3D6 or 2H6, promote FcγR-mediated phagocytosis and microglial activation and cause increased incidence of micro-haemorrhage in APP mice. M266 which does not induce microglial activation, does not increase micro haemorrhage .These observations suggest that induction of side effects appears to depend on antibody specificity and FcγR interaction on microglia. These findings are translated into humans as recent clinical trials, with patients receiving plaque-binding antibodies: Bapineuzumab, Gantenerumab and Aducanumab developing vascular side effects, but no detectable vascular damage occurs in patients receiving soluble Aβ specific Solanezumab (Imbimbo et al., 2012; Ostrowitzki et al., 2012; Salloway et al., 2010). In APP mice reduction of FcγR affinity by de-glycosylation of Aβ specific antibodies results in the reduction of vascular Aβ deposition and micro haemorrhage in comparison to treatment with the fully glycosylated, whole IgG (Wilcock et al., 2006). The inhibition of microglial activation via ablation of the CD40-CD40L pathway using an anti CD40L antibody, also reduces vascular side effects associated with immunotherapy, further supporting the role of microglia in side effects, (Obregon et al., 2008). These findings have also been replicated in the clinic during the development of Genentech's new antibody Crenezumab. Because Crenezumab has lower affinity for FcγR, it causes less microglial activation as measured by cytokine production and reduced p38 signalling in comparison to IgG1(Adolfsson et al., 2012). The reduced FcγR affinity results in the prevention of vascular damage in Crenezumab treated patients (Adolfsson et al., 2012). This evidence suggests that side effects are at least in part, linked to activation of CNS FcγRs.

In vivo studies have shown that anti-Aβ immunotherapy causes increased activity of matrix metalloproteinases (MMPs) 2 and 9, providing a potential mechanism for the side effects associated with immunotherapy (Wilcock et al., 2011a). Research into the effect of inflammation on stroke has shown that central or peripheral inflammation can increase brain IL-1β, and this in turn increases MMP-9 expression in the brain. MMP-9 cleaves the tight junction protein claudin-5 expressed by brain endothelial cells, disrupting tight junctions and increasing vascular permeability (McColl et al., 2008; Thornton et al., 2008). This reduction in the integrity of tight junctions could explain the

incidence of ARIA-E after immunotherapy, as FcγR mediated inflammation could cause increase IL-1β, inducing MMP-9 cleavage of claudin-5.

It is well established that inflammation is a key neuropathological feature of AD, and there is a growing body of evidence implicating FcγRs themselves in the pathology of numerous neurodegenerative conditions (Fuller et al., 2014). Thus, it is important to consider the consequences of increasing FcγR expression and activation through immunotherapy and/or other factors, such as systemic infections. Soluble inflammatory mediators such as TNFα and IL-1β have divergent roles within the CNS and regulate the function of neurons. Intracranial administration of these mediators causes changes in neuronal function, and therefore increased CNS levels of these cytokines as a result of immunotherapy could further disrupt synaptic function in AD patients.

1.6 Summary and aims of this thesis

The development of new therapies for AD is one of our most urgent unmet clinical needs. The exact causes of AD are currently unknown, however there is significant evidence that the accumulation of the protein Aβ is an important part of its pathology, and the majority of new drugs are focussed on Aβ clearance. One approach is to immunise patients against Aβ either by passive or active immunotherapy (Doody et al., 2014; Salloway et al., 2014; Schenk et al., 1999). Antibodies against Aβ have been able to clear deposits from the brains of patients, and there is some evidence that this helps to slow down the cognitive decline associated with the disease (Doody et al., 2014). However, patients treated with these antibodies also experience side effects, caused by damage to the cerebral vasculature. It is thought that this vascular damage is caused by a pro-inflammatory response to the therapeutic antibodies, mediated by activation of microglia or macrophages, via binding to FcγRs (Wilcock et al., 2006). These side effects have limited the safe dose given in clinical trials-potentially reducing the efficacy of treatment, but it may be possible to reduce these side effects by modifying the Fc region of therapeutic antibodies (Adolfsson et al., 2012). Although new clinical candidate antibodies have been produced on different Fc regions in an attempt to reduce the side effects associated with therapies, there is limited published work describing the importance of antibody effector function in the brain. The main aim of this thesis is to characterise the importance of the Fc region in the *in vivo* clearance of plaques and the neuro-inflammatory response to anti-Aβ immunotherapy, enabling the selection of safer and/or more efficacious Fc regions for the treatment of AD.

1.6.1 Hypothesis and aims

1.6.1.1 Hypothesis

The vascular damage to the brains of AD patients that occurs during anti-Aβ immunotherapy is caused by the activation of CNS FcγRs, leading to a pro-inflammatory response and changes to the cerebral vasculature. We hypothesise that engineering of the Fc region of therapeutic antibodies could ameliorate these side effects by altering the affinity for FcγRs.

1.6.1.2 Aims

1. To recombinantly produce and characterise well described anti-Aβ antibodies with mouse IgG1 or IgG2a constant domains *in vitro*.
2. To characterise the TG2576 model for the expression of FcγRs.
3. To characterise the role of IgG subclass in the clearance of plaques and neuro-inflammatory response to an anti-Aβ antibody *in vivo*.
4. To directly compare mouse IgG2a versions of clinical candidate antibodies for their ability to clear plaques and mediate neuro-inflammation *in vitro* and vivo.
5. To characterise the response of TG2576 mice to peripheral infection with Salmonella typhimurium; and to investigate whether this will prime the CNS to respond in an exacerbated fashion to immunotherapy.

Chapter 2: Materials and Methods

2.1 *In vivo* experiments

2.1.1 Animals

Animals used in experiments were obtained from our in-house animal research facility, or directly from Taconic (USA). All animals were housed under 12 hour light dark cycles and given access to food and water *ad libitum*. All procedures were ethically approved and performed in concurrence with UK home office guidelines, or the equivalent Danish laws.

2.1.2 Breeding of TG2576

Hemizygous male transgenic mice were purchased from Taconic (USA) and shipped to the Southampton biomedical research facility (BRF). The mice were re-derived into a clean animal facility for breeding, and male offspring bearing the APP transgene were selected. Transgenic male mice were bred with wild type SJL females (in house) producing offspring with a 50% chance of possessing the transgene. All breeding was carried out by BRF staff.

2.1.3 Genotyping

TG2576 mice were genotyped by measuring the expression of the human APP transgene. DNA was extracted from tail tips of mice using an Illustra DNA isolation kit (GE healthcare, Amersham, UK) according to the manufacturer's guidelines. 1µl of purified DNA was added to a mastermix containing: Taq polymerase and buffer (Sigma, Dorset, UK), 25mM $MgCL_2$, forward and reverse primers for both huAPP and β-actin and 0.5mM dNTPs (Sigma, Dorset, UK). The mastermix was per sample as follows:

1.2µl 10x buffer

2.4µl MgCl2 (25mM)

0.24µl 10mM dNTPs

0.6µl 20µM APP forward primer

0.6µl 20µM APP reverse primer

0.3µl 20µM Control forward primer

0.3µl 20µM Control reverse primer

0.06µl Taq DNA polymerse

5.3µl water

The primer sequences for hAPP and β-actin can be found in table 2.1. Samples were cycled as follows in a PCR machine:

1. **94^{0}C -3 mins**
2. **94^{0}C -30 seconds**
3. **55^{0}C -1 minute**
4. **72^{0}C -1 minute**
5. **Cycle 2-4 35 times**
6. **72^{0}C 2 minutes**
7. **10^{0}C forever**

The PCR products were separated on a 3% agarose gel containing ethidium bromide. The agarose gels were prepared by the addition of 3% W/V agarose into TAE buffer (appendix), this solution was heated in a microwave until the agarose was dissolved. Once the temperature of the solution had cooled down to 60^{0}C, 5µl of ethidium bromide (Fisher, Loughborough, UK) was added per 100µl and the solution was poured into a gel mould and allowed to set. The gel was placed into an electrophoresis tank containing TAE buffer, and 10µl of PCR product or 100bp DNA ladder (Fisher, Loughborough, UK) were loaded. Samples were run at 140V and 400mA for 1 hour 30 minutes. The DNA bands were visualised using ultraviolet light, and photographed. The product from the β-actin primers is 320 base pairs long and the product of the human APP primers is 371 base pairs. As shown in figure 2.1 transgenic mice have two bands and wild type mice have only one.

Primer	Sequence 5'>3'
APP forward primer	AGGACTGACCACTCGACCAG
APP reverse primer	CGGGGGTCTAGTTCTGCAT
β-Actin forward primer	CTAGGCCACAGAATTGAAAGATCT
β-Actin reverse primer	GTAGGTGGAAATTCTAGCATCATCC

Table 2. 1 Primer sequences for genotyping PCR

The primer sequences that were ordered from Sigma as 100μM stocks, which were diluted to 20μM working stocks.

377bp

324bp

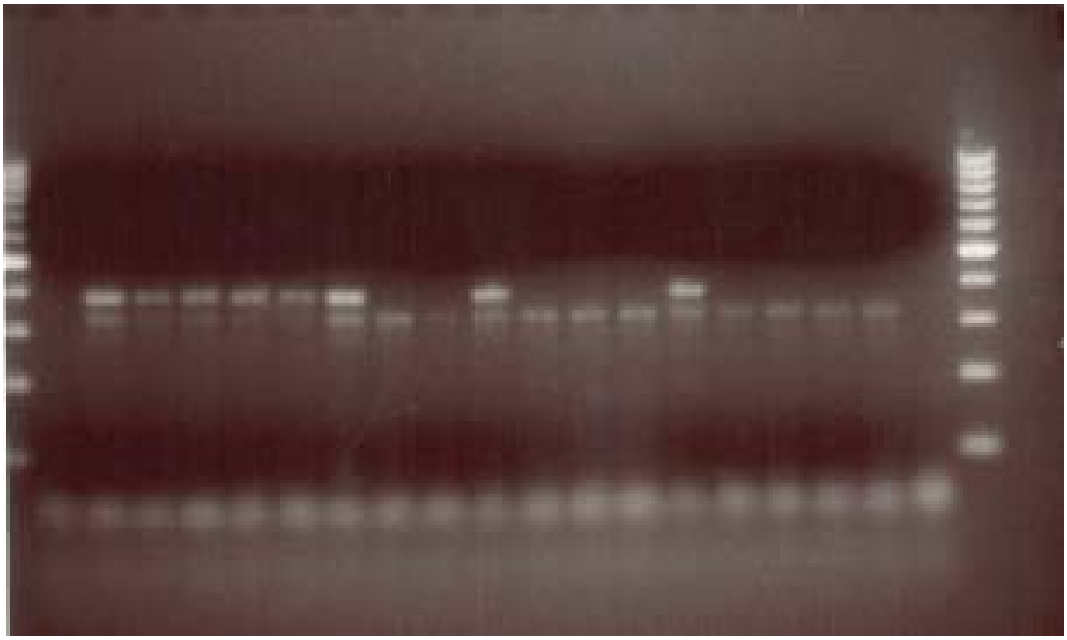

Figure 2. 1 Example Agarose gel for genotyping of TG2576 mice

PCR products run on a gel, mice possessing the APP transgene have two DNA bands, wild type mice have one

2.1.4 Stereotaxic surgery

Antibodies were directly injected into the hippocampus of mice using stereotaxic surgery. The animals were anaesthetised with Isofluorane or Sevofluorane inhalation anaesthetics, and the incision area was shaved and sterilised with iodine. The mouse was fitted to a stereotactic frame using ear bars, and a mask supplying anaesthetic was secured over the nose piece. Throughout the procedure the temperature of the mouse was regulated by a temperature probe and heat mat. A sagittal incision was made exposing the skull, allowing the location of bregma, the point at which the sagittal and coronal sutures meet, the location of injection was marked by measuring distance from bregma. A burr hole/holes were drilled into the skull using a dentist's drill. A fire pulled capillary was inserted into the brain, and 2µl of antibody was slowly injected. The capillary was slowly withdrawn, and the incision sutured before allowing the mice to recover in a heated chamber. Mice were given Buprenorphine (RB pharmaceuticals, Slough, UK) for analgesia.

2.1.5 Salmonella infection

TG2576 mice were infected with the attenuated bacterial strain *Salmonella Typhirmurium* SL3261. High concentration stocks of the bacteria were kept at -80^{0}C until use. Mice were moved into a containment level 2 facility 48 hours before injection to acclimatise to the room. To prevent cross infection, mice were house in filter topped cages and kept in a negative pressure environment. Mice were injected into the peritoneum with 1x10^6 CFU of *S. typhimurium* or saline. To monitor the health of mice, body weight was measured every day for a week following infection and then once a week until the end of the experiemnt. Project licence regulations state that the mice cannot drop more than 15% body weight, and if they do they should be culled. All procedures involving *S. typhimurium* or *S. typhimurium* infected animals were carried out in a containment level 2 hood to prevent spreading of the bacteria to other mice in the facility.

2.1.6 Behavioural assays

2.1.6.1 Contextual fear conditioning

The contextual fear conditioning paradigm is a well characterised behavioural test that measured short term memory. Mice were brought to the room 24 hours before the start of the test to habituate to the environment. The test chamber contained a wire mesh floor, and a video camera mounted in the top to record. Between each test run the chamber was thoroughly cleaned using 10% ethanol. Figure 2.2 summarises the protocol. In the training phase a single mouse was placed into the testing chamber and observed for 90 seconds, then over a period of two minutes the mice were subjected to four random electric shocks which were each accompanied by white noise. The mice were placed back into their home cage for one hour, before their return to the testing chamber for the acquisition phase for three minutes. Three hours after the acquisition phase, mice were placed in a novel environment for the cued test. After 60 seconds in the new environment, the white noise that accompanied the electrical shocks was played continuously for two minutes. After the test, the video recordings were reviewed and the amount of time the mice spent freezing in the: training, acquisition and cued phases was measured. The time spent freezing relates to the anxiety levels of the mouse, and the data collected from the first 90 seconds of the training phase was used to find any mice that were highly anxious before the test and would therefore need to be excluded. In this experiment no mice were abnormally anxious before at the start of training, so no mice were excluded. The amount of time spent freezing in the acquisition and cued phases was expressed as percentage of total time. The mice were randomly assigned numbers and the videos were analysed blind to avoid bias. To verify accurate measurement of time spent freezing, 10 mice were measured by an independent scientist (Kate Pedersen) and the scores correlated well.

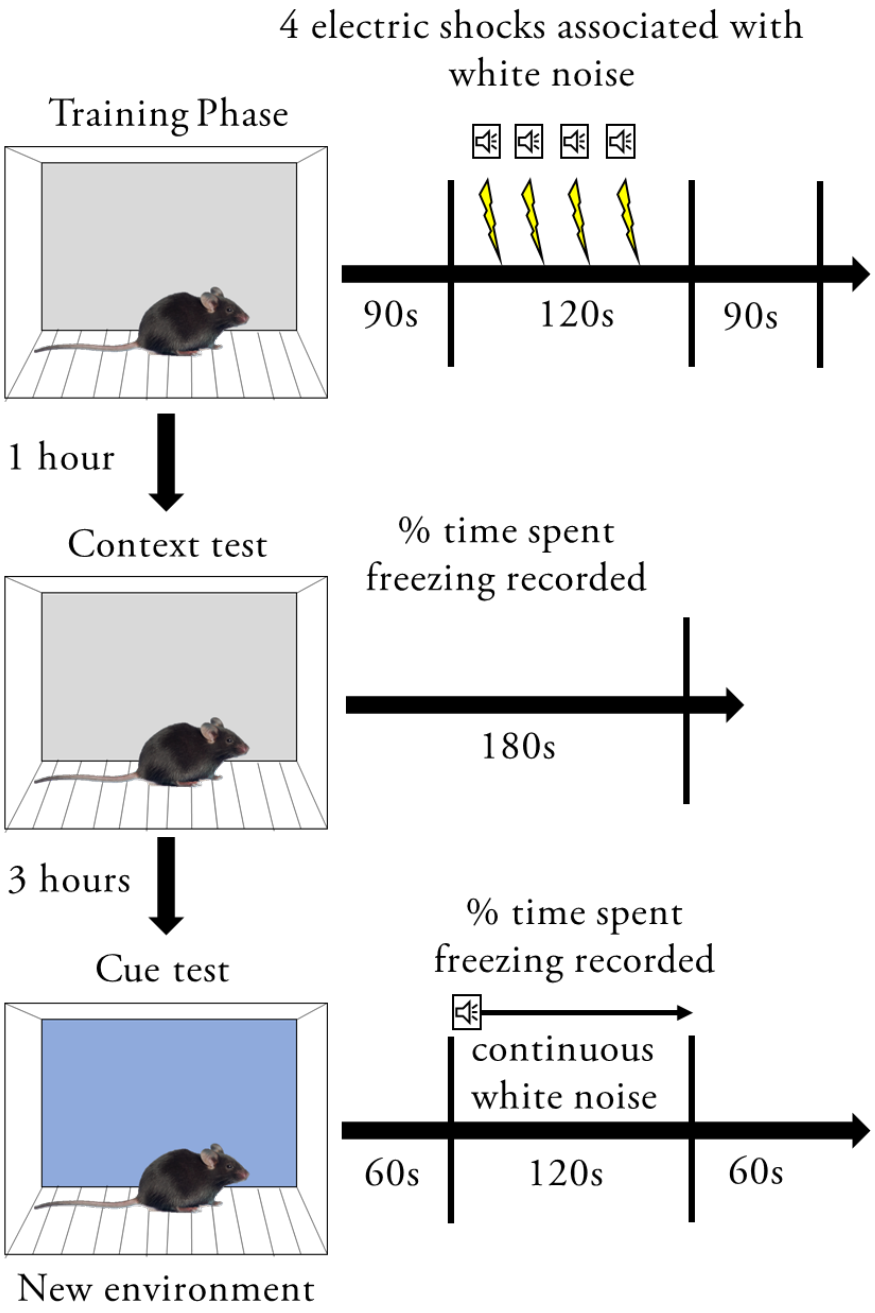

Figure 2. 2 Fear conditioning behaviour method

The fear conditioning behaviour was performed in two phases. The mice were placed into the chamber, and left to acclimatise for 90 seconds. Over the following 120 seconds, the mice were subjected to a series of four electric shocks accompanied by white noise. The mice were then left in the chamber for 90 seconds before being returned to their home cage. One hour later the mice were returned to the cage for 180 seconds, and the percentage of the time spent freezing was measured. Three hours following the acquisition test, mice were placed into a new environment and the white noise was played continuously for two minutes, recording the amount of time spent freezing.

2.1.6.2 Nesting behaviour

Nest building is a natural behaviour of mice, and is important for reproduction and thermoregulation. The behaviour to build a nest has been shown to be sensitive to hippocampal lesions or genetic/pharmaceutical changes. Mice are moved into the nesting cage one hour before the beginning of the dark cycle. The nesting cage contains a 0.5cm covering of sawdust and a 5cmx5cm square of cotton wadding (nestlet, LBS Biotech, Horley, UK) placed in the middle with no other environmental enrichment, the mice still have free access to food and water. The mice will then tear up the nestlet and use the cotton to make a nest. The morning after the quality of nests that the mice have built are scored using the following five point scale adapted from RM Deacon (Deacon, 2006b).

1. Nestlet more than 90% intact
2. Nestlet partially torn (50-90% intact) no nest site
3. Nestlet mostly torn (greater than 50%) but no defined nest site. i.e. torn nestlet is not gathered in one quarter of the cage
4. Nestlet is mostly shredded, and there is a defined nest site in one quarter of the cage, walls are lower than a mouse laying on its side for more than 50% of its circumference
5. A near perfect nest using >90% of the nestlet, the nest is positioned in one corner and the nest walls are as tall as a mouse laying on its side for greater than 50% of its circumference

If the nest has qualities of two of the scores above, it is possible to award scores of .5. All assessment of nests were completed by Mr Alex Collcutt who was blinded to the treatment groups.

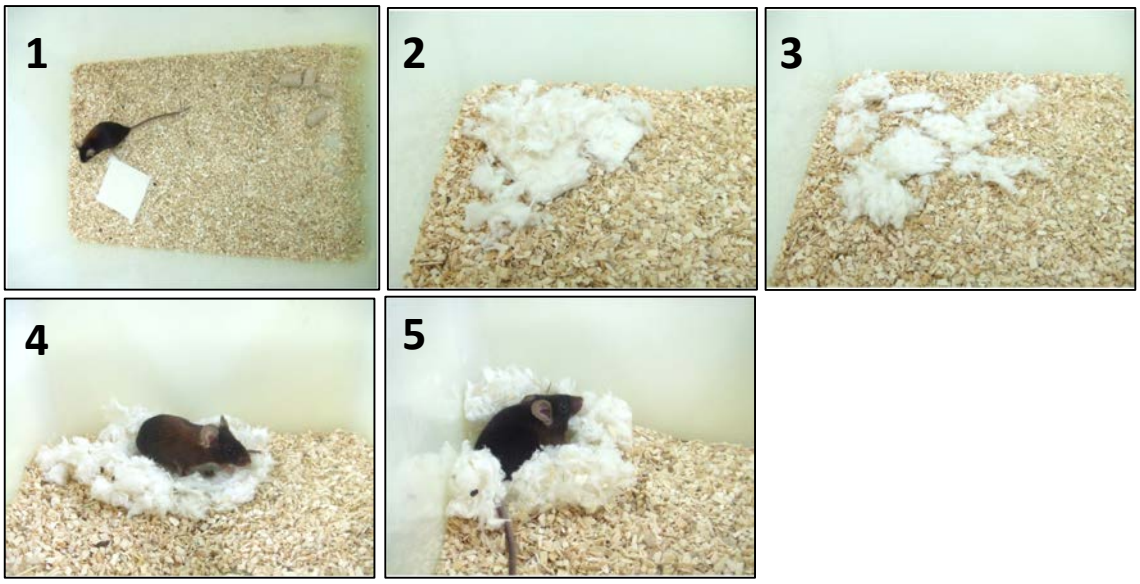

Figure 2. 3 Example nest scores

Example nests, and their respective scores in the top left corner. Images sourced from:(Deacon, 2006b)

2.2 Collection of tissue and protein measurement

2.2.1 Immunohistochemistry

2.2.2 Collection and processing of tissue for histology

Mice were terminally anaesthetised by an overdose with avertin (appendix), followed by transcardial perfusion using heparinised saline. For immunohistochemistry the whole brain or a hemi brain was embedded in optimum cutting temperature (OCT, Sakura Finetek, Thatcham, UK) and stored at -80°C before cutting. Coronal sections of 10µm were cut using a cryostat and collected onto APS coated slide (see appendix), sections stored at -20°C until use.

2.2.3 Mouse Immunohistochemistry

Fresh frozen sections were dried for 30 minutes at 37 ^{0}C, before fixation in 4^{0}C ethanol for 15 minutes. Sections were then placed in PBS (see appendix), outlined with a wax pen (Vector, Burlingame, CA) and blocked with 60µl of PBS with 10 % serum from the same species as the secondary antibody (Sigma, Dorset, UK) + 2% BSA (Fisher, Loughborough, UK) for one hour. For fluorescent immunohistochemistry sections were incubated with primary antibody (for concentrations see table 3.1) in a 1:5 dilution of the blocking buffer overnight at 4^{0}C. The sections were washed three times for ten minutes in PBS before incubation for one hour with a secondary fluorescent antibody (see table 2.6). Slides were washed three times in PBS and cover slipped using Prolong gold anti-fade reagent™ with DAPI (Invitrogen, Paisley, UK). For DAB immunohistochemistry sections endogenous peroxidase activity was quenched in 1% hydrogen peroxide (Sigma, Dorset, UK) for ten minutes before three short washes in PBS. Sections were then incubated overnight with primary antibody in a 1:5 dilution of the blocking buffer at 4^{0}C. Sections were washed three times in PBS and incubated with a biotinylated secondary antibody (Vector, Burlingame, CA) for 1 hour before a further three washes and incubation with Vector ABC system for 45 minutes (Vector, Burlingame, CA). After three washes sections were developed in a DAB solution (appendix), counterstained in haematoxylin and dehydrated in graded alcohols and xylene before cover-slipping using the mounting medium DPX (Fisher Scientific, Loughborough, UK). See table 2.5 for a full list of antibodies and conditions used.

Primary Antibody Target	Antibody Type	Clone/catalogue number	Source	Primary dilution
CD68	mAb Rat α mouse	FA11	AbD Serotec	1:500
CD11B	mAb Rat α mouse	5C6	AbD Serotec	1:500
MHCII	mAb Rat α mouse	M5/114.15.2	eBioscience	1:500
CD45	mAb Rat α mouse	IBL-3/16	AbD Serotec	1:1000
CD64	mAb Rat α mouse	AT152-9	In House	1:500
CD16/32	mAb Rat α mouse	MCA2305F	AbD Serotec	1:500
CD32B	mAb Rat α mouse	AT128	In house	1:250
CD16	mAb Rat α mouse	AT154-2	In House	1:250
FcγRIV	mAb Rat α mouse	AT137	In house	1:500
CD3	mAb Rat α mouse	KT3	AbD Serotec	1:500
Laminin	pAb Rabbit α mouse	L9393	Sigma	1:500
Claudin-5	pAb Rabbit α mouse	341600	Invitrogen (Novex)	1:200
Aβ	pAb Rabbit α human	Ab2359	Abcam	1:500
Aβ (N-terminus)	mAb Mouse α human	3D6	In house	1:1000
Aβ (mid- domain)	mAb Mouse α human	4G8	Covance	1:2000
CD206	mAb Rat α mouse	MR5D3	AbD Serotec	1:500
CD31	mAb Rat α mouse	390	eBiocience	1:500
NG2	pAb Rabbit α mouse	Ab5320	Millipore	1:500

Table 2. 2 Primary antibodies and conditions used for murine immunohistochemistry

Secondary antibody target (label)	Antibody type	Catalogue number	Source	Dilution
Rabbit IgG (546nm)	mAb Goat α Rabbit	A-11011	Invitrogen	1:500
Rat IgG (488nm)	mAb Donkey α rat	A-21208	Invitrogen	1:500
Mouse IgG (FITC)	pAb Sheep $F(ab)_2$ α mouse	F2266	Sigma	1:500
Mouse IgG (biotin)	pAb Horse α mouse	BA-2001	Vector	1:100
Rat IgG (biotin)	pAb Rabbit α Rat	BA-4001	Vector	1:100
Rabbit IgG(biotin	pAb Goat α Rabbit	BA-1000	Vector	1:200

Table 2. 3 Secondary antibodies used in murine immunohistochemistry

2.2.4 Congo red stain

To stain brain sections for congophilic plaques, brain tissue was processed in the same way as for mouse immunohistochemistry. Ten micron sections were fixed to APS coated slides by incubating in 4^0C 100% ethanol (Fisher, Loughborough, UK) for 15 minutes. Sections were treated with a 0.3% Congo red solution (Sigma, see appendix for recipe) for 20 minutes before 5 dips in the de-staining solution (appendix). Sections were counterstained using haematoxylin and then cover-slipped using dpx mounting medium, or with pro-long-gold anti-fade reagent containing dapi.

2.2.5 Human tissue

The post-mortem tissue of the AD cases was provided by BRAIN UK under the ethics approval obtained from the National Research Ethics Committee South Central Hampshire B (REC reference 14/SC/0098). Brain sections were used from three AD patients, two MS patients and one patient with severe peripheral inflammation. Tissue was formalin fixed and embedded in paraffin wax, and cut into 5μm sections on a wax microtome.

2.2.6 Human immunohistochemistry

Formalin fixed paraffin embedded human brain and tonsil tissue was used to characterise FcγR expression and binding of antibodies. Cut sections were de-waxed in clearene (Surgipath Europe, Peterborough) and rehydrated. Endogenous peroxidase activity was quenched using 3% H2O2 (Sigma, Dorset, UK) in methanol (Fisher, Loughborough, UK). Tissue was subjected to different antigen retrievals dependent on the antigen stained for (see table 3.7 for methods for each antibody). Sections were then blocked using a different solution depending on the species of secondary antibody (See table 3.8). Primary antibodies were added an optimised concentration for an optimised length of time (Table.3.7) Secondary antibodies were incubated for 30 mins followed by a 30 minute incubation with ABC detection system (Vector). Slides were developed using DAB (Vector) for an optimised length of time.

Primary Antibody Target	Species	Clone/catalogue number	Source	Antigen retrieval	Primary dilution
CD32	mAb Rabbit	EP888Y	Abcam	EDTA, pressure cooker, 2mins	1:2000
CD32A	mAb Rabbit	EPR6658	Abcam	EDTA, pressure cooker, 2mins	1:1000
CD16	mAb Mouse	2H7	AbD Serotec	EDTA, pressure cooker, 2mins	1:40
Aβ 16-24	mAb Mouse	4G8	Covance	80% Formic acid, 30 mins	1:4000

Table 2. 4 Anti-human primary antibodies

Secondary antibody target	Species	Catalogue number	Block	Source	Dilution
Mouse IgG	Rabbit	ab97044	DMEM, FCS, BSA	Abcam	1:600
Rabbit IgG	Swine	ZO19602-2	DMEM, FCS, BSA	Dako	1:400

Table 2. 5 Secondary antibodies for use in human immunohistochemistry

2.2.7 Microscopy and quantification of staining

Light microscopy (DAB) and fluorescent images were taken on a Leica DM5000 microscope using QWIN or LAS software. The quantification of DAB images was performed using the freeware-ImageJ. For the quantification of staining within the hippocampus, sections from -2.0mm from bregma were used. Three separate images were taken with a 20x objective spanning the hippocampus. All images were de-convoluted using HDAB RGB values, which splits images into haematoxylin and DAB channels. The DAB staining was turned into a binary image, and the percentage area above a marker specific threshold was set. The threshold was selected by taking random images and finding a threshold at which the binary staining represented actual cellular staining. Quantifications were automated using a macro, and were expressed as percentage area above threshold. The exception to this is quantification of staining surrounding the pial membrane, which was quantified in the same way however a region 150 pixels either side of the membrane was selected in image J. The number of T-cells present in the brain was quantified by staining for CD3 and then counting the number of T-cells in the hippocampus, this number was normalised to the hippocampal area, expressing results in cells per mm^2. To quantify the number of T-cells that were in the brain parenchyma rather than blood vessels, co-staining of CD3 and Laminin was used. The number of T-cells that were not associated with blood vessels were counted. To ensure impartiality during quantification, it was performed blinded to experimental groups and mouse genotype.

2.2.8 Mesoscale Cytokine and Aβ measurements

2.2.9 Homogenisation of tissue for cytokine and amyloid beta measurement

Protein was extracted from tissue in two stages. Firstly hippocampal tissue was placed in a buffer containing: 150mM NaCl, 25mM TRIS 1% triton x-100 and complete mini protease inhibitors (Roche, UK). The tissue was mechanically homogenized and the homogenate was centrifuged at 20,000g at 4^0C for 1 hour to remove insoluble material. The supernatant from this fraction was used to measure pro-inflammatory cytokine levels and the triton soluble Aβ fraction using multiplex MSD technology. The pellet was re-suspended in 70% formic acid and incubated for 15 minutes to solubilise aggregated forms of Aβ, this solution was neutralised in 20 volumes of pH8 TRIS, and centrifuged at 20,000g for 1 hour and the supernatant used to measure the formic acid soluble Aβ fraction. Total protein levels were measured by BCA protein assay (Pierce, Belvedere, IL), following manufacturer's instructions.

2.2.10 Mesoscale Discovery cytokine and Abeta measurement

Multispot ELISAs (Mesoscale Discovery, Rockville, MD) were used to determine the concentration of cytokines and Aβ peptide in brain homogenate. Briefly, 96 well Mesoscale plates were blocked with supplied diluent for half an hour, before addition of sample or supplied calibrator in duplicate and incubated for two hours on a shaking plate. The plates were washed three times before addition of secondary Sulfotag linked antibodies, and incubated for a further two hours. The plates were washed a further three times, and filled with 150µl read buffer per well and plates were measured on a Sector PR400 reader. Values for cytokine levels were normalised to the total protein concentration measured in each sample.

Cytokine	Expressed by	Effects
IFN-γ	T-cells, NK cells	Polarises macrophages to a more phagocytic and anti-microbial phenotype, inhibits th2 polarisation.
IL-1β	Macrophages, epithelial cells, keratinocytes, T cells, dendritic cells, fibroblasts	Activation of macrophages and t cells, activates local endothelium, drives sickness behaviours, induces fever
IL-2	T cells	Induces T cell proliferation
IL-4	T cells and mast cells	Activates B cells, induces class switching to IgE
IL-5	T cells	Activates eosinophils
IL-6	Macrophages, T cells, endothelium	Stimulates the release of acute phase proteins by hepatocytes, causes proliferation of T and B cells, also induces fever response
IL-10	Monocytes	Anti-inflammatory cytokine, inhibits the activation of macrophages
IL-12 (p70)	Macrophages, dendritic cells	Activation of NK cells, polarisation of T-cells to th1 phenotype
KC (mouse CXCL1)	Macrophages, mast cells	Neutrophil chemoattractant
TNFα	Macrophages, neutrophils, NK cells, T cells	Stimulates t-cell polarisation to th1, causes localised inflammation and vascular changes, induces fever

Table 2.6 Cytokines measured by MSD assay

References for this table can be found in (Janeway 2010)

2.3 Recombinant production and purification of antibodies

2.3.1 Sequences of antibody variable domains

To recombinantly generate anti-Aβ antibodies for use *in vitro* and *in vivo,* the sequences of antibody variable regions were obtained from the public domain. Table 2.6 shows the amino acid sequence of the heavy and light chain variable domains from antibodies used in this thesis, and the source of the sequences.

2.3.2 Designing constructs for 3D6 expression

To produce recombinant antibodies the unique sequence of the variable region of both the heavy and light chains is required. This information was found in the patents for Bapineuzumab (3D6) as the amino acid sequence shown in figure 2.1. The amino acid sequence was converted to DNA codons using internet based software (http://bioinformatics.picr.man.ac.uk/research/software/tools/sequenceconverter.htm) and edited to allow vector cloning. Onto all constructs a leader sequence and a HinDIII restriction site sequence was added to the 5' end. To allow cloning of the kappa variable region into puc18, a 3' BSiWI restriction site was added to 3D6 kappa constructs. The sequence for a SpeI site was added into the framework region four of the heavy chain to allow cloning into the TOPO vectors for mouse heavy chain. The edited sequences can be seen in figure 2.1, black bases correspond to original DNA, red bases show the 5' leader sequences and restriction enzyme sites are denoted in different colours. Sequences were optimised for expression in *cricetulus griseus* (Chinese Hamster) using Geneart software. Following optimisation constructs were checked for changes to existing restriction sites or for the addition of restriction sites needed downstream using (NEBcutter v.02). The optimised sequence was then ordered from geneart and delivered in a plasmid containing ampicillin resistance.

Antibody	Heavy chain variable domain sequence	Light chain variable domain sequence	Ref.
3D6	EVKLVESGGGLVKPGASLKLS CAASGFTFSNYGMSWVRQNS DKRLEWVASIRSGGGRTYYSD NVKGRFTISRENAKNTLYLQM SSLKSEDTALYYCVRYDHYSGS SDYWGQGTTVTVSS	YVVMTQTPLTLSVTIGQPASIS CKSSQSLLDSDGKTYLNWLLQ RPGQSPKRLIYLVSKLDSGVPD RFTGSGSGTDFTLKISRIEAEDL GLYYCWQGTHFPRTFGGGTK LEIK	US Patent No. 7,790,856B2
Gantenerumab	MWTLVSWVALTAGLVAGQV ELVESGGGLVQPGGSLRLSCA ASGFTFSSYAMSWVRQAPGK GLEWVSAINASGTRTYYADSV KGRFTISRDNSKNTLYLQMNS LRAEDTAVYYCARGKGNTHK PYGYVRYFDVWGQGTLVTVS S	MWTLVSWVALTAGLVAGDIV LTQSPATLSLSPGERATLSCRAS QSVSSSYLAWYQQKPGQAPRL LIYGASSRATGVPARFSGSGSG TDFTLTISSLEPEDFATYYCLQI YNMPITFGQGTKVEIK	EMBL database ID: CHEMBL1743025
mC2	EVQLVESGGGLVQPGGSLKLS CAASGFTFSSYGMSWVRQTPD KRLELVASINSNGGSTYYPDSV KGRFTISRDNAKNTLYLQMSS LKSEDTAMYYCASGDYWGQG STLTVSS	DVVMTQTPLSLPVSLGDQASI SCRSSQSLVYSNGDTYLHWYL QKPGQSPKLLIYKVSNRFSGVP DRFSGSGSGTDFTLKISRVEAE DLGVYFCSQSTHVPWTFGGG TKLEIK	WO 2008011348 A2 WO 2007068412 A2

Table 2. 6 Sequences of the variable regions of recombinant antibodies used in study

Amino acid sequences of variable regions for antibodies: 3D6, Gantenerumab and mC2. All sequences were obtained from the public domain.

Protein	Amino acid sequence
Mouse IgG1 Heavy chain constant region	AKTTPPSVYPLAPGSAAQTNSMVTLGCLVKGYFPEPVTVTWNSGSLSSGV HTFPAVLQSDLYTLSSSVTVPSSPRPSETVTCNVAHPASSTKVDKKIVPRD CGCKPCICTVPEVSSVFIFPPKPKDVLTITLTPKVTCVVVDISKDDPEVQFS WFVDDVEVHTAQTQPREEQFNSTFRSVSELPIMHQDWLNGKEFKCRVN SAAFPAPIEKTISKTKGRPKAPQVYTIPPPKEQMAKDKVSLTCMITDFFPE DITVEWQWNGQPAENYKNTQPIMNTNGSYFVYSKLNVQKSNWEAGNT FTCSVLHEGLHNHHTEKSLSHSPGK
Mouse IgG2a Heavy chain constant region	AKTTAPSVYPLAPVCGDTTGSSVTLGCLVKGYFPEPVTLTWNSGSLSSGV HTFPAVLQSDLYTLSSSVTVTSSTWPSQSITCNVAHPASSTKVDKKIEPRG PTIKPCPPCKCPAPNLLGGPSVFIFPPKIKDVLMISLSPIVTCVVVDVSEDD PDVQISWFVNNVEVHTAQTQTHREDYNSTLRVVSALPIQHQDWMSGK EFKCKVNNKDLPAPIERTISKPKGSVRAPQVYVLPPPEEEMTKKQVTLTC MVTDFMPEDIYVEWTNNGKTELNYKNTEPVLDSDGSYFMYSKLRVEKK NWVERNSYSCSVVHEGLHNHHTTKSFSRTPGK
Mouse Kappa chain constant region	RADAAPTVSIFPPSSEQLTSGGASVVCFLNNFYPKDINVKWKIDGSERQN GVLNSWTDQDSKDSTYSMSSTLTLTKDEYERHNSYTCEATHKTSTSPIVK SFNRNEC

Table 2. 7 Sequences of the constant regions of recombinant antibodies used in study

Table 3.10 shows the amino acid sequences for the constant heavy(cH) regions of mouse IgG1 and IgG2a, and also the sequence for the constant domain of the mouse kappa chain (cK)

2.3.3 Transformation of plasmids into *E. coli*

All plasmids were transformed into *Escherichia coli* JM109 competent cells (Promega, Southampton, UK) using the following protocol. JM109 cells were defrosted on ice, and 100µl of cell suspension transferred to a clean tube containing 30µl of the plasmid and 200µl of 0.1M $CaCl_2$. The transformation reaction was left on ice for 30 minutes before heat shock at 42 ^{0}C for exactly 45 seconds. The cells were then placed back on ice before addition of 0.5ml super optimal broth (Invitrogen, Paisley, UK) and incubation at 37 ^{0}C with shaking for 1 hour. Transformed cells were then plated out onto an LB agar plate impregnated with 100µg/ml ampicillin or kanamycin (depending on plasmid resistance) to select for successfully transformed colonies. The plates were left at 37 ^{0}C overnight, and individual colonies picked into 5ml LB broth containing the same antibiotic resistance (5 colonies per transformant).

2.3.4 Purification of plasmids from E.coli

Plasmids were purified from overnight 5ml cultures of E.coli using a QIAGEN mini-prep kit according manufacturer's instructions (QIAGEN, Crawley, UK). Briefly, 5ml *E. coli* cultures were spun at 4000rpm for 3 minutes, and the pellet was re-suspended in 250µl buffer P1. Re-suspended cells were transferred to a micro centrifuge tube and 250µl of the lysis buffer P2 was added. After 5 minutes the lysis reaction was stopped with buffer N3 and tubes were spun at 13,000rpm for 10 minutes. The supernatant was transferred into a DNA binding column and spun at 13,000rpm for 1 minute, followed with consecutive washes using 500µl buffer PB and 750µl buffer PE. A final spin at 13,000rpm was used to remove the residual wash buffer and the column was transferred to a clean collection tube. To elute DNA, 50µl of buffer EB was applied to the column membrane and was left to stand on the bench for 1 minute, followed by 1 minute at 13,000rpm.

2.3.5 Restriction digest of Plasmids

To check that plasmids contained the correct sized inserts or to isolate the inserts for ligation into vectors, restriction digests were performed on the DNA mini preps. Conditions of reactions were dependent on restriction enzymes used, and whether inserts were being isolated afterwards. Details of restriction enzymes and buffers used can be found in table 3.11. In general if two restriction

enzymes could operate under the same conditions to check for inserts a 10µl reaction was set up using: 0.5µl of each enzyme, 1µl of appropriate 10x buffer, 5µl of DNA and 3µl of water. To digest DNA and vectors for ligation a 20 µl reaction was set up: 1µl of each enzyme, 10µl of mini-prep DNA or 1ug of vector (up to 10µl), 2µl of appropriate 10x buffer and 6µl water. Following restriction digest, products were separated by size agarose gel electrophoresis using a 0.9% agarose (Ultrapure Invitrogen, Paisley, UK) in TAE buffer with 5µl GelRed (Cambridge Bioscience, Cambridge, UK) per 100ml to visualise DNA. If enzymes could not perform under the same conditions consecutive digests were performed on the DNA.

Restriction Enzyme	Target Sequence	Optimal Temperature	Optimal Buffer	Source
HinDIII	A|AGCT T	37^{0}C	Buffer E	Promega, Southampton, UK
SpeI	A|CTAGT	37^{0}C	Buffer E	Promega, Southampton, UK
BSiWI	C|GTACG	50^{0}C	Buffer 3	Promega, Southampton, UK
EcoRI	G|AATTC	37^{0}C	Buffer E	Promega, Southampton, UK
BamHI	G|GATCC	37^{0}C	Buffer E	Promega, Southampton, UK
NotI	GC|GGCCGC	37^{0}C	Buffer D	Promega, Southampton, UK

Table 2. 8 Restriction Enzymes and optimal temperatures for digest

This table shows all restriction enzymes used for vector cloning along with conditions used for restriction digests.

2.3.6 Sequencing of plasmids

To ensure that plasmids carried the correct insert, plasmids were sequenced at each cloning stage. Each plasmid was sequenced using the BigDye direct cycle sequencing kit™ (Applied Biosytems, Paisley, UK), 3µl of DNA was added to 2µl BigDye™, 2µl buffer, 2µl water and 1µl plasmid primer (see table 2.2). The DNA was amplified using the following cycle: 95 ^{0}C for 10 seconds, 50 ^{0}C for 5 seconds for 25 cycles. DNA was then precipitated by the addition of 25µl 100% ethanol and 1µl 3M NaAc leaving on ice for 10 minutes. Samples were then centrifuged for 30 minutes at 4^{0}C and 13,000rpm, the supernatant aspirated. The pellet was then washed with 125µl 70% ethanol and spun for a further 5 minutes at 13,000rpm. The supernatant was aspirated and 10µl Formaide added, the samples were then sequenced In house.

Vector	Sequence of Primer
pEE6.4	GCAGTGTAGTCTGAGCAGTAC
pEE12.4	GGCAGTGTAGTCTGAGCAGTA

Table 2. 9 Primers used for sequencing plasmids

2.3.7 Extraction of DNA from agarose gel

Inserts and vectors were extracted from agarose gel ready for ligation using the QIAEX II gel extraction kit (QIAGEN, CRAWLEY, UK). DNA was visualised with UV light, and bands containing inserts were cut out using a sharp blade. The gel containing DNA was added to 1ml of

buffer QX1 in a micro centrifuge tube, and to it 10µl of QIAEX beads were added. The tubes were heated to 50^0C for 10 minutes with occasional shaking to dissolve the agarose. Samples were then spun at 13,000rpm for 30 seconds, the supernatant discarded and the pellet washed with 500µl QX1 to remove residual agarose. The pellet was then washed twice with 500µl of PE buffer, aspirating PE and leaving the tube open to air-dry. The pellet was re-suspended in 20µl TE buffer, centrifuged for 30 seconds at 13,000rpm, and the supernatant containing extracted DNA collected.

2.3.8 Ligation of inserts in vectors

To ligate inserts into new vectors, both the inserts and vectors were digested by restriction enzymes and extracted from a gel as described above. The extracted inserts and vectors were ligated by the addition of 12µl of insert and 12µl of vector to 3µl T4 DNA ligase (Promega, Southampton, UK) and 3µl Ligation buffer (Promega, Southampton, UK). The ligation reaction was then left at 4^0C overnight. The ligated vector was then transformed into JM109 cells.

2.3.9 Transfection into 293 F cells

To generate enough plasmid for a transient transfection, plasmids were initially transformed into JM109 cells as described previously. 5ml of LB containing transformed cells were used to spike 1.5L of LB and this was incubated at 37^0C on a shaker for three days. After three days a mega-kit (Qiagen, Crawley, UK) was used to isolate plasmid DNA following the manufacturer's instructions. To transfect 293 F cells with 3D6 IgG1 or IgG2a, 500µg of each plasmid was made up in 10ml of sterile 150mM NaCl. For each transfection 1.5mg of Linear PEI (Sigma, Dorset, UK) was made up in 7.5ml 150mM NaCl. Plasmid solutions were mixed with Linear PEI and incubated at room temperature for 10 minutes. $50x10^7$ of 293 F cells were re-suspended in 25ml of freestyle media (Invitrogen, Paisley, UK) for each transfection. Cells were mixed with linear PEI and plasmid solution and incubated for four hours at 37°C, before the addition of valproic acid (Sigma, Dorset, UK) to a final concentration of 3.75mM.

2.3.10 Concentration and purification of Antibodies

7 days after transfection, media containing transfected cells was spun at 4000rpm for 10 minutes and the supernatant passed through a 0.2 μm filter (Millipore, Watford, UK). Monoclonal antibodies were purified from concentrated supernatant using a protein A column. First the protein A column was equilibrated with 2.5M glycine buffer (Appendix) to remove any bound protein, followed by a wash through with pH8 TRIS buffer (Appendix) to remove glycine buffer. The filtered supernatant was then loaded onto the column and after a peak at 280nm was observed, the run off was collected. Once the sample was added to the protein A column, TRIS buffer was added. When the 280nm peak had returned to baseline the column was eluted with 2.5M glycine buffer. When a second peak at 280nm was observed the run off was collected in a fresh beaker until the peak returned to baseline, this fraction contained the monoclonal antibody. The elution was repeated after inverting the column. Gel electrophoresis was used to determine if all antibody had been purified from the supernatant.

2.3.11 Isotype control Antibodies

Throughout this thesis isotype control antibodies have been used *in vitro* and *in vivo*. These antibodies were selected based on their subclass and lack of cross reactivity to mouse proteins. The exact isotype control antibodies used vary depending on the availability in the laboratory the experiment was performed in. These antibodies were produced and purified in the same manner as the anti-Aβ antibodies generated.

2.4 *In vitro* analysis of antibodies

2.4.1 Quality control of antibodies

2.4.1.1 Nanodrop measurement of protein concentration

A280nm absorbance was used to calculate the concentration of antibodies after purification using a nanodrop (Thermo Scientific). The A280nm of purified antibodies was measured, and the concentration of IgG was calculated using the molar extinction coefficient.

2.4.1.2 Endotoxin

Purified antibody was tested for levels of endotoxin using the endosafe LAL test (Charles River), following the manufacturers protocol. Briefly, antibodies were diluted 1:20 in endotoxin low PBS in a 6ml Bijous. Just before testing the sample was vortexed for 30 seconds and loaded into the cassette. Endotoxin concentration was calculated in endotoxin units (EU) per milligram of protein. All antibodies produced contained less than 3EU/mg.

2.4.1.3 HPLC

The levels of aggregate in antibody preparations was measured using HPLC. The time taken for aggregate or monomeric IgG to pass through had been measured previously. 20 µl of antibody was loaded onto a HPLC column, and the A280nm readings were measured in the run off from the column.

2.4.2 ELISA to determine antibody binding to Aβ peptide

To measure the binding of recombinant antibodies to Aβ peptide a binding assay was developed. 96 well flat Nunc Maxisorp plates (Nunc, Denmark) were coated with 0.1ug/ml $A\beta_{1-40}$ peptide (America Peptide, Sunnyvale, CA) in ELISA coating buffer (appendix) overnight at room temperature. The plates were aspirated and washed five times with ELISA wash buffer. Each well was blocked with 150µl PBS 1% BSA (Fisher, Loughborough, UK) for one hour at room temperature. The plates were aspirated and 200 µl of 0.2µg/ml 3D6 IgG1 or IgG2a was added to the

first column of wells in triplicate and twofold serially dilutions across the plate. Plates were shaken for a one hour incubation at RT, followed by five washes with wash buffer. 100µl of biotinylated horse-anti-mouse (Vector, Burlingame, CA) diluted 1:500 in PBS 1% BSA was added to each well and incubated on a shaking plate for one hour. The plate was washed five times with wash buffer and 100µl Streptavidin poly-HRP (Sanquin, Netherlands) diluted 1:10,000 in PBS 1% BSA was added to each well and incubated on a shaking plate for 30 minutes. The plates were washed for a final time before addition of 100µl of substrate solution 1 (appendix) per well. The reaction was left in a dark place and 50µl stop solution (1M H_2SO_4) was added before background colour change got too high. The OD of each well was read at 450nm.

2.4.3 Cell culture and *In vitro* Fc gamma receptor cross linking

For *in vitro* macrophage activation assays, the mouse macrophage cell line RAW264 was used. The cells were grown in DMEM media (Invitrogen, Paisley, UK) containing 10% FCS (Sigma, Dorset, UK) and Glutamax media supplement (Invitrogen, Paisley, UK) and split 1:10 before becoming confluent. Cells were grown in a sterile incubator at 37^0C with 95% O_2 and 5%CO_2.

To test the ability of antibodies to activate macrophages through Fc receptors, a simple Fc receptor cross linking assay was used. A sterile 96 well ELISA plate (Nunc, Denmark) was coated with 5ug/ml of either mouse IgG1 or IgG2a isotypes overnight in sterile coating buffer (appendix). Plates were washed three times in sterile PBS before being blocked for one hour in PBS 1% Fetal calf serum (Sigma, Dorset, UK). $4x10^4$ RAW 264.7 cells were added per well in 200µl normal media. To prime macrophages, a proportion of the cells were stimulated with 100U/well of IFN-y (Peprotech, London, UK), and incubated overnight at 37^0C. After 24 hours the supernatant was collected and assessed for the levels of TNFα and nitric oxide. To measure the cytokine TNFα in the supernatant of RAW cells a TNFα mouse duo-set ELISA (RnD systems) was used. All manufacturers' instruction were followed, except standard HRP was replaced for poly HRP (Sanquin, Netherlands) to increase sensitivity. The optical density was measured at 450nM. The Griess assay was used to measure the levels of nitric oxide in the supernatant of RAW cells stimulated with IgG1 or IgG2a.

To produce a standard curve, 1μM of sodium nitrite was made up in media, and then 100μl was added to the first 2 wells of a 96 well plate before serial 1:2 dilution across the plate. 50μl of supernatant from each well of the stimulated cells was transferred into the new plate, before addition of 50μl of 1% sulfanamide (Sigma, Dorset, UK) in 2.5% phosphoric acid (Sigma, Dorset, UK) to each well. The plate was left in the dark for 5 minutes and 50μl of 0.1% NED (Sigma, Dorset, UK) in 2.5% phosphoric acid was added. The colour was allowed to develop for five minutes before reading the optical density at 544nM.

2.5 Graphs and Statistical analysis

The data in this thesis were statistically analysed using Graph-pad prism, with the exception of three way analysis of variance (ANOVA) and three way repeated measures ANOVA which were performed using SPSS. Initially, data sets were tested for Gaussian distribution using the D 'Agostino-Pearson omnibus test. In experiments where the group sizes were too small, the residuals were calculated and combined before measurement of normality. If the data sets were normally distributed, depending on the experimental design appropriate parametric statistics were used. For experiments with a single independent variable and two groups, two tailed *t*-tests were used. To reduce the likelihood of type I statistical errors, experiments with three or more groups were initially tested using ANOVA and then post hoc using TUKEY, which is corrected for multiple comparisons. Depending on the number of independent variables in the experiment: one, two or three way ANOVA was used. Three-way repeated measurements ANOVA was used to analyse repeated measurements of weight. If data sets were not normally distributed, the data were transformed using the functions: Y=logY or Y=log(Y+1). Normality tests were repeated for transformed data sets, if the transformed data were normally distributed, they were analysed using the parametric tests that were previously described. If the transformed data sets were not normally distributed, the original data sets were analysed using appropriate non-parametric tests (i.e. Mann Whitney U test and Kruskal Wallis test). All graphs presented in this thesis were constructed using Graphpad prism, and display mean and standard deviation.

Chapter 3: Production and characterisation of anti amyoid beta antibodies

3.1 Introduction

The aim of this thesis is to test the hypothesis that the effector function of therapeutic anti-Aβ antibodies is important for the clearance of Aβ and the associated neuro-inflammatory response. I generated murine versions anti-Aβ antibodies which have been tested in clinical trials for Alzheimer's disease, with different Fc regions to allow testing of this hypothesis *in vivo*.

IgG antibodies are composed of four chains: two identical heavy chains consisting of four immunoglobulin domains and two identical light chains each consisting of two immunoglobulin domains. Each heavy or light chain contains a variable domain and a constant domain. The combined variable domains form the antigen binding site and the sequence of these domains defines the specificity of an antibody. The Fc region of IgG defines the effector function of an antibody, containing binding sites for: FcγR and complement components (C1q) and FcRn. Different subclasses of IgG have different heavy chain constant region sequences giving different binding affinities for FcγR and complement (Bruhns, 2012). It is possible to generate recombinant antibodies by synthesising the DNA sequence for the variable domains and cloning this sequence into a plasmid containing standard constant domain sequences for the subclass of IgG required. Well characterised anti-Aβ antibodies were generated with either a mouse IgG1 or IgG2a constant regions due to their differing FcγR affinities. Antibodies with an IgG2a constant region are more pro-inflammatory than IgG1, due to their higher affinity for activating FcγRs (Bruhns, 2012). The production of antibodies with the same binding characteristics for Aβ but different Fc regions, will allow the testing of the importance of antibody effector function *in vivo*. Also the production of three different clinical antibodies allowed the direct comparison of antibody binding *in vitro*.

3.2 Methods

The antibodies were generated using two different methods. To generate 3D6 IgG1 and 3D6 IgG2a in Southampton, the sequence of the variable domain for each antibody was taken from the patent and synthesised by a contract research organisation (Geneart^{tm}). The variable domains were then cloned into vectors containing the appropriate mouse IgG constant domain and expressed by transient transfection. Antibodies generated at Lundbeck A/S were produced by ordering two separate plasmids for the heavy and light chains of each antibody from Geneart^{tm}, and these plasmids were co-transfected. Each antibody produced was subject to standard quality control tests: endotoxin, HPLC, Mass spectrometry and electrophoresis. The panel of antibodies was tested by *in vitro* assays to characterise the binding to Aβ plaques or recombinant peptide, and ability to activate effector cells through FcγRs.

3.3 Results

3.3.1 Production of 3D6 IgG1 and IgG2a

The antibody 3D6 was produced as both IgG1 and IgG2a subclasses for *in vitro* and *in vivo* experiments. The sequences of the 3D6 variable regions were obtained from the Bapineuzumab patent (US Patent No. 7,790,856B2). DNA sequences for the variable regions from both the heavy and light chains were ordered in separate plasmids from Geneart^{tm}, with restriction enzyme sites to allow cloning into our in house vectors. Vectors containing the variable domains of 3D6 were taken through a series of cloning steps. The purpose of these steps was to ligate the variable regions of 3D6 into vectors containing sequences for the constant regions of IgG1 and IgG2a. A summary of cloning steps is depicted in figure 3.1. The final product of this cloning were two vectors: one containing both heavy and light chains for 3D6 IgG1, and one containing heavy and light chains for 3D6 IgG2a.

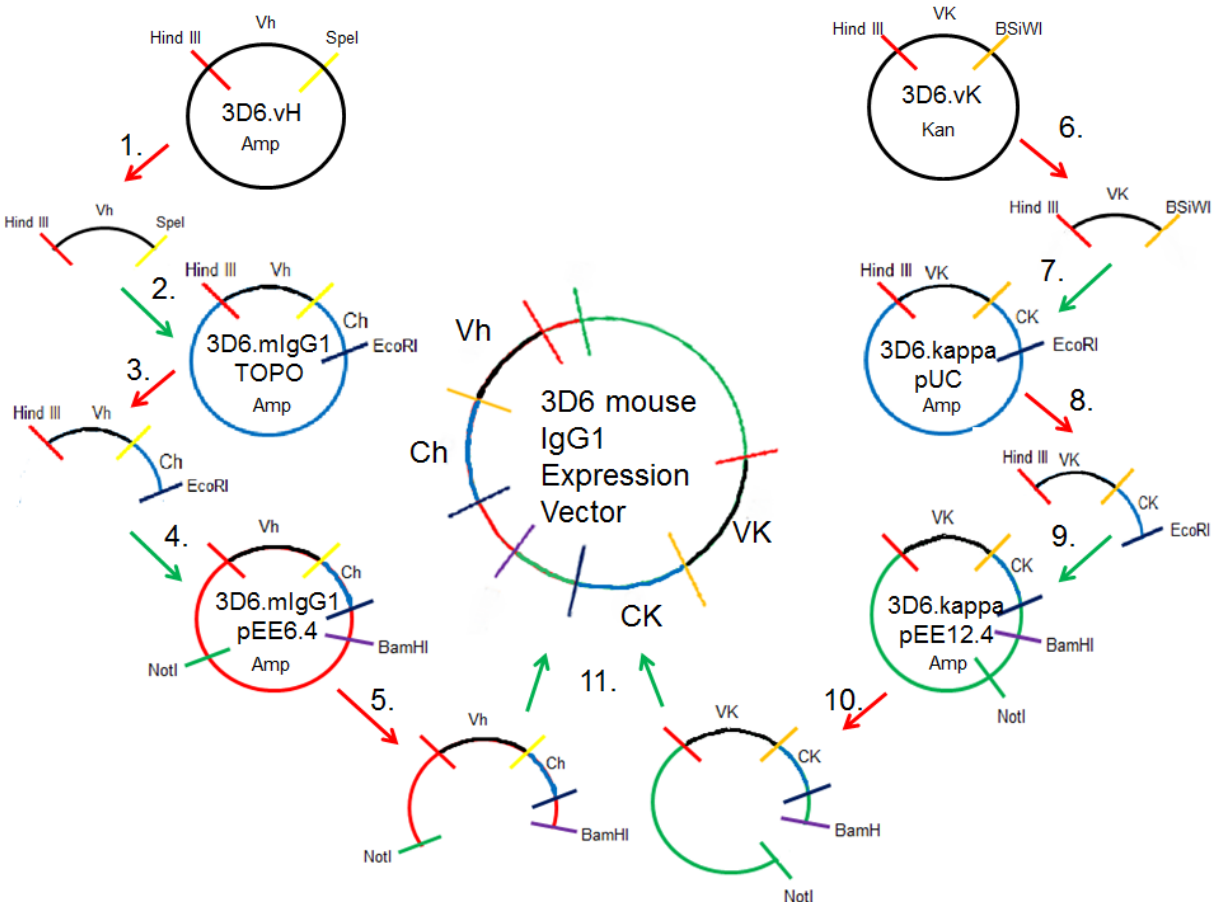

Figure 3. 1 Vector Cloning Diagram for the production of recombinant antibodies

Figure 3.1 shows the step taken to produce the expression vector for 3D6 IgG1 recombinant antibody. Constructs of the variable heavy (vH) and variable kappa (vK) domains of 3D6 were ordered from Geneart[tm] (Regensburg, Germany), and were ligated into a plasmid containing ampicillin and kanamycin resistance respectively. The vH sequence was excised from the plasmid with a Hind III and SpeI digest (**1**.) and ligated into the vector TOPO mouse γ1 (**2**.) which contains the sequence for the three heavy constant domains (cH). The vH region was excised from this vector along with CH domains by HindIII EcoRI digest (**3**.) and ligated into vector pee6.4 (**4**.). The vK domain sequence was excised using a HindIII+BSiWI digest (**6**.), and ligated into vector puc18 mouse kappa (**7**.) containing the sequence for the mouse kappa constant domain. The vK and cK sequences were cut out by HindIII and EcoR1 digest (**8**.) and ligated into the pee12.4 vector (**9**.). Both vectors pEE6.4 and pEE12.4 were digested by NotI and BamHI

The DNA sequence of 3D6 heavy chain variable region (vH) was cut out of the plasmid ordered from Geneart[tm] using a HinDIII and SpeI double digest. At the same time two new plasmids were digested using the same enzymes: TOPO IgG1 plasmid containing the constant region for mouse IgG1, and TOPO IgG2a plasmid, containing constant regions for mouse IgG2a (step 1 in fig. 3.1). The 3D6vH sequence was ligated into both TOPO IgG1 and TOPO IgG2a vectors (step 2 in fig 3.1). The DNA sequence of 3D6 light chain variable region (vK) was cut out of the plasmid ordered from Geneart[tm] using a HinDIII and BSiWI double digest. At the same time a new plasmid was digested using the same enzymes- puc18 mouse kappa vector, which contains the sequence for the mouse constant light chain domain (step 6 in fig 3.1). The digest products were ligated together (step 7 in fig 3.1). Figure 3.2A shows agarose gels from this vector cloning step. The 400bp bands in Lanes 1 + 2 correspond to the 3D6 heavy variable domain, this was ligated into vectors TOPO my1 (Lane 5) and TOPO my2a (Lane 6). The variable region of 3D6 Kappa chain (400bp lane 9) was ligated into the puc18 mouse kappa vector (lane 11).

The ligation products were separately transformed into chemically competent JM109 cells, successfully transformed cells were then selected on ampicillin impregnated agar plates. Successful transformants were selected and plasmids purified by overnight miniprep. Figure 3.2B shows this digest, all vectors except for lane 2 contain an insert at 400bp and therefore the variable domains have been successfully ligated into the new vector. To ensure plasmids contained the correct inserts, vectors were digested and sequenced.

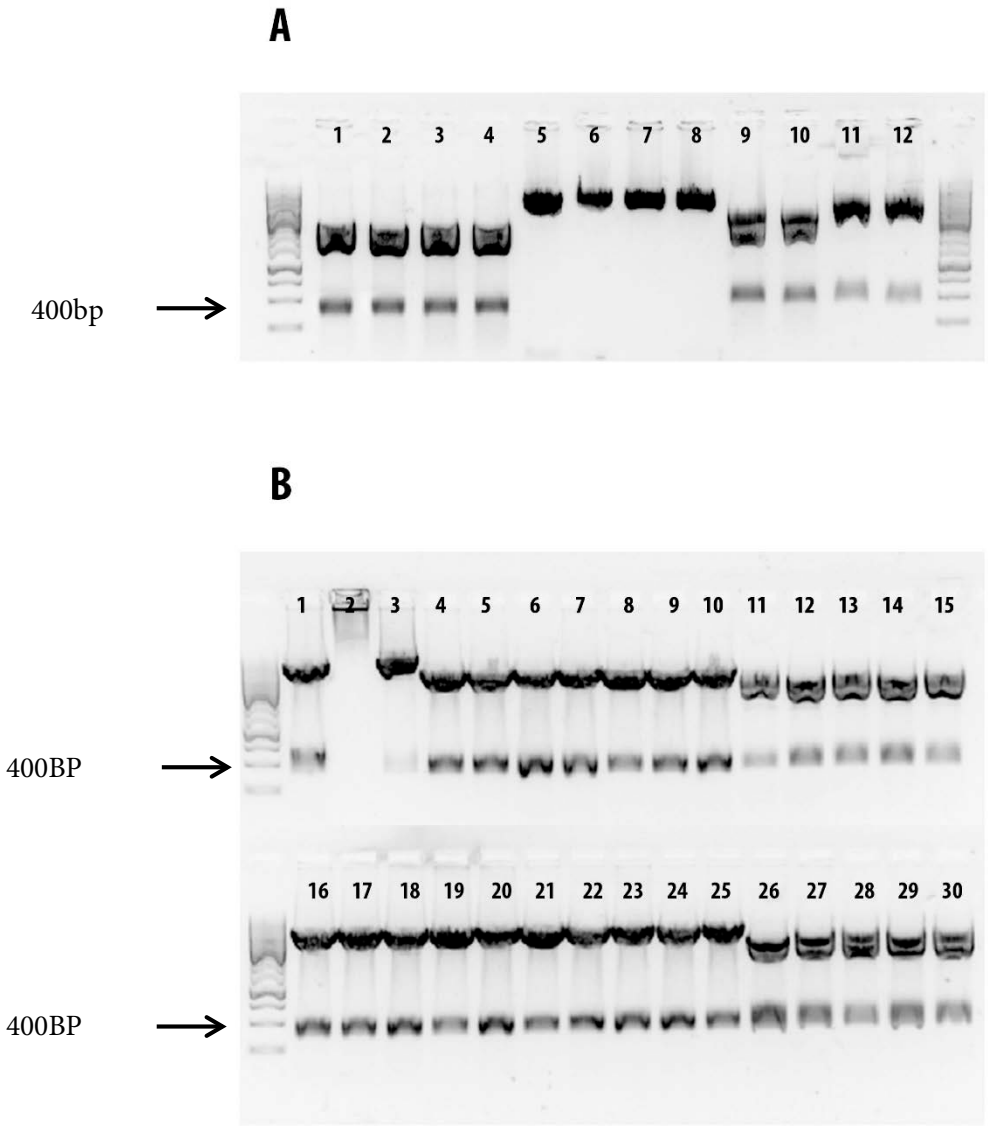

Figure 3. 2 HindIII + SpeI Digest of vH domain and HindII + BSiWI digest of vK domain

A. Constructs: 3D6 vH (1, 2), vector TOPO mγ1 (5, 6) and vector TOPO mγ2a (7, 8) were digested by HinDIII and SpeI. Constructs: vK 3D6 (9), All bands ran at the correct size (400bp).

B. Restriction digests of vectors: 3D6 mγ1 (1-5), 3D6 mγ2a (6-10), 3D6 K puc18 (11-15). All plasmids have inserts at around 400bp (except lane 2) indicating that the ligation was successful.

One of the five samples with an insert at 400bp and a confirmed correct sequence was selected for each vector. The full length heavy or kappa chain (3D6 variable domains+ constant domains) was excised from each vector by a HindIII and EcoRI digest. Two new vectors were also digested in the same way: pEE6.4 for heavy chains and pEE12.4 for kappa chain (steps 3 and 8 fig 3.1). The full heavy or light chains were then ligated into their appropriate vector. Figure 3.3A shows the products of the restriction digest: 3D6TOPOIgG1 (lane 1) and 3D6 TOPOIgG2a (lane 2) both contain 1.8Kb inserts which are the complete heavy chain. These 1.8 Kb inserts were ligated into pEE6.4 (Lanes 7 and 8). 3D6kappa.pUC18 was digested to obtain a 0.8Kb band which corresponds to the full light chain (lane 3), which was ligated into pEE12.4 (lane 11). The three new vectors were transformed into JM109 cells, successful transformants were selected on an ampicillin impregnated agar plate. Five colonies from each plate were picked and grown up overnight in LB broth with ampicillin before purification of plasmids by mini prep. To test if new vectors contained inserts, they were digested again by HinDIII and EcoRI and sequenced. The products of this restriction digest are shown in Fig 3.3B: 3D6kappa.pEE12.4 (1-5), 3D6IgG1.pEE6.4 (6-10) and 3D6IgG2a.pEE6.4 (10-15). For each vector there is at least one lane that has the correct insert size and sequence.

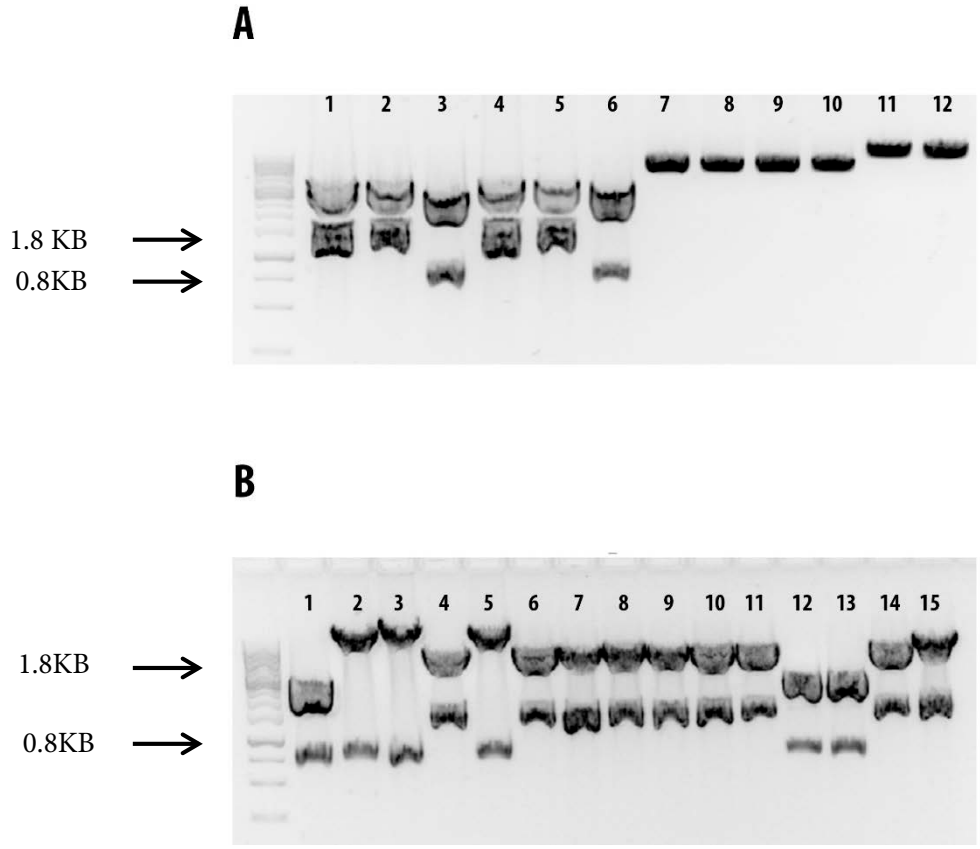

Figure 3. 3 HindIII an EcoRI restriction digest of constructs from TOPO and puc18 vectors

A. Plasmids: TOPO.mg1.3D6 (1), TOPO.mg2a.3D6 (2), puc18.mk.3D6 (3), pEE12.4 (7-10) and pEE6.4 (11, 12) were digested by HinDIII and EcoRI and run on an agarose gel. Bands corresponding to: complete heavy chains (1.8Kb), complete kappa chains (0.8Kb) are seen in the correct lanes.

B. Plasmids were purified from overnight culture and all were digested to check for inserts at the correct length (heavy chain=1.8Kb, kappa chain=0.8Kb). Restriction products were run in the following lanes: 3D6.Kappa.pEE12.4 (1-5), 3D6.mIgG1.pEE6.4 (6-10), 3D6.mIgG2a.pEE6.4 (11-15)

To produce the final expression vectors, pEE6.4 and pEE12.4 vectors containing complete heavy or light chains needed to be ligated together, so each vector would contain the complete antibody sequence. pEE6.4 and pEE12.4 were digested by Not1 and BamHI enzymes. Products from this digest were run on a gel and fragments of 4Kb from pEE6.4 were ligated to fragments of 10.5Kb from pEE6.4 (step 11.Fig 3.1). Agarose gels from the digest are shown in figure 3.4A. Lanes 1 and 2 are digest products from 3D6kappa.pEE12.4, the 4KB bands were excised and ligated into the 10.5Kb bands from lane 3 (3D6IgG1.pEE6.4) and lane 4 (3D6IgG2a.pEE6.4). Finally the two expression vectors were transformed into JM109 cells, and successful transformants selected on an ampicillin impregnated agar plate. Eight colonies from each plate were picked and grown up overnight in LB broth with ampicillin before purification of plasmids by mini prep. The mini preps were digested by Not1 and BamHI to check for the correct sized fragments, this is shown in fig. 3.4B. Lanes 1-8 correspond to 3D6 IgG1 and lanes 9-16 correspond to 3D6 IgG2a. Vectors in lanes1, 4, 8, 11, 13, 14 and 16 all contained fragments that could be the correct size, however it is not a clear digest. To ensure the expression vectors contained both heavy and kappa chains of 3D6, they were digested with HinDIII and EcoRI. Vectors containing both regions should be cut into four fragments, this was seen in lanes: 8, 11, 13, 14 and 16 (figure 3.4C) Vector cloning has been successful and at least one vector for 3D6 IgG1 and 3D6 IgG2a contain both the heavy and light chains. The expression vector in lane 8 was selected for 3D6 IgG1, and the expression vector in lane 11 was selected for 3D6 IgG2a. The selected expression vectors were amplified and transfected into 293F cells, to express the final antibody. All batches of antibody produced were tested for endotoxin and aggregate levels, all antibodies used for *in vivo* experiments contained <2 Endotoxin units per mg of antibody and had low levels of aggregate.

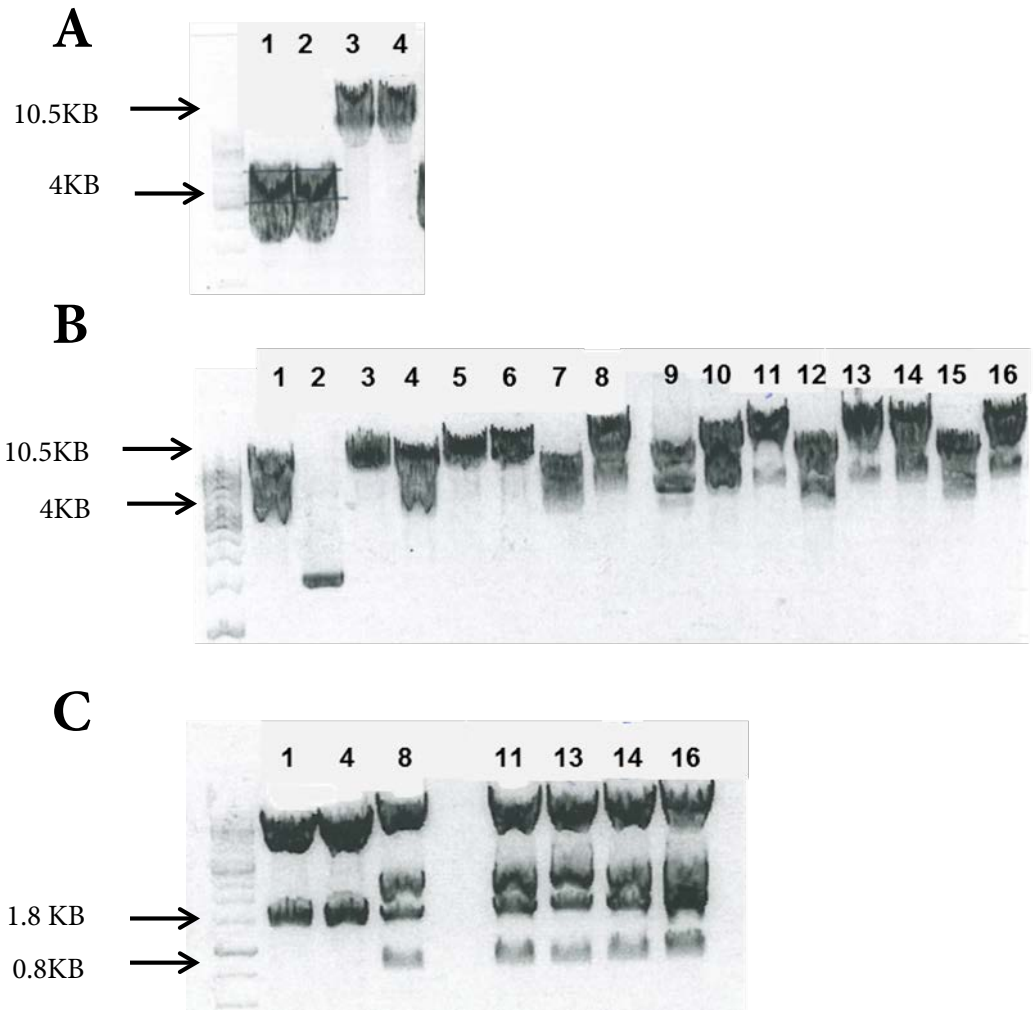

Figure 3. 4 BamH1 and Not1 digest of pEE6.4 and 12.4 and ligation to produce final expression vectors for 3D6 IgG1 and IgG2a

A. Plasmids: 3D6mIgG1 pEE6.4 (1), 3D6mIgG2apEE6.4 (2), 3D6kappa.pEE12.4 (3), 3D6kappa.pEE12.4 (4), were digested by BamH1 and NotI and run on a gel. Bands corresponding to: complete heavy chains and complete kappa chains were excised and ligated.

B. Plasmids were purified from overnight culture and all were digested to check for correct length of fragments, lanes 1-8 correspond to 3D6 mIgG1 and lanes 9-16 correspond to 3D6 mIgG2a. Lanes: 1, 4, 8, 11, 13, 14 and 16 have the correct sized fragments.

C. To check if expression vectors contained both the heavy and kappa chain of 3D6, vectors: 1, 4, 8, 11, 13, 14 and 16 were digested by HinDIII and EcoRI. Vectors in lanes: 8, 11, 13, 14 and 16 were cut into four fragments of the correct size and therefore expression vectors for both 3D6 IgG1 and IgG2a have been produced

3.3.2 Characterisation of 3D6 IgG1 and 3D6 IgG2a

To generate sufficient antibody *in vitro* and *in vivo* experiments, the final vectors for 3D6 mIgG1 and 3D6 mIgG2a were transfected into 293F cells for transient expression. After seven days the supernatant was collected and sterile filtered before purification by protein A chromatography. The purified antibodies were concentrated and dialysed into sterile endotoxin free PBS. All batches of antibody used *in vivo* had less than 3EU/mg of antibody. Expression of 3D6 antibody was very low, yielding 0.5-1mg per litre, in experiments conducted both in Southampton and Denmark. Figure 3.5A shows HPLC traces (a280nm) for 3D6 IgG1 and 3D6 IgG2a and endotoxin units per mg of antibody measured by LAL assay. Both antibodies have low levels of aggregate and low levels of endotoxin.

The antibody 3D6 is the original IgG2b murine version of the clinical candidate Bapineuzumab, which is able to bind and clear plaques from the brains of both mice and humans (Bard et al., 2000; Rinne et al., 2010; Zago et al., 2013). I generated 3D6 as both IgG1 and IgG2a subclasses. Both subclasses have the same variable domains and therefore the same ability to engage plaques, but the constant regions are different and therefore different effector functions. To characterise the binding and effector function of 3D6 before *in vivo* experiments, a number of *in vitro* assays were used.

The ability of the two different subclasses of 3D6 to bind to Aβ plaques was tested using immunofluorescence using coronal section of the cortex and hippocampus of 18 month old TG2576 mice. Antigenic retrieval using formic acid is often required to visualize antibody binding to plaques, but to better mimic *in vivo* plaque engagement no antigenic retrieval was used. Figure 3.5B shows that both 3D6 IgG1 and 3D6 IgG2a are able to label plaques in brain sections without antigenic retrieval, and appear to bind in an equivalent manner. They do not bind to structures in the brain of wild type mice, and irrelevant isotype control antibodies do not bind to plaques in TG2576 brain sections. The binding to recombinant Aβ peptide was tested by immobilizing Aβ peptide (Aβ40) Fig. 3.5C shows that both 3D6 IgG1 and 3D6 IgG2a bind to immobilised Aβ in a concentration dependent manner. Both subclasses bind to Aβ with the same affinity in this assay, while isotype control antibodies do not bind the immobilized peptide.

The ability of each antibody to activate effector cells was tested using an FcγR cross linking assay. 3D6 IgG1 or 3D6 IgG2a were immobilised onto 96 well plates, before the addition of the mouse macrophage cell line RAW 2.64. The cells were incubated with the immobilised antibody for 24

hours before measurement of TNFα in the supernatant. Immobilisation of the antibody onto plastic plate enables the cross-linking of FcγRs expressed on the cell surface of RAW 264 cells, and promote cell activation and cytokine release. Figure 3.5D shows that 3D6 IgG2a causes the production of 3-fold higher levels of TNFα compared to 3D6 IgG1.

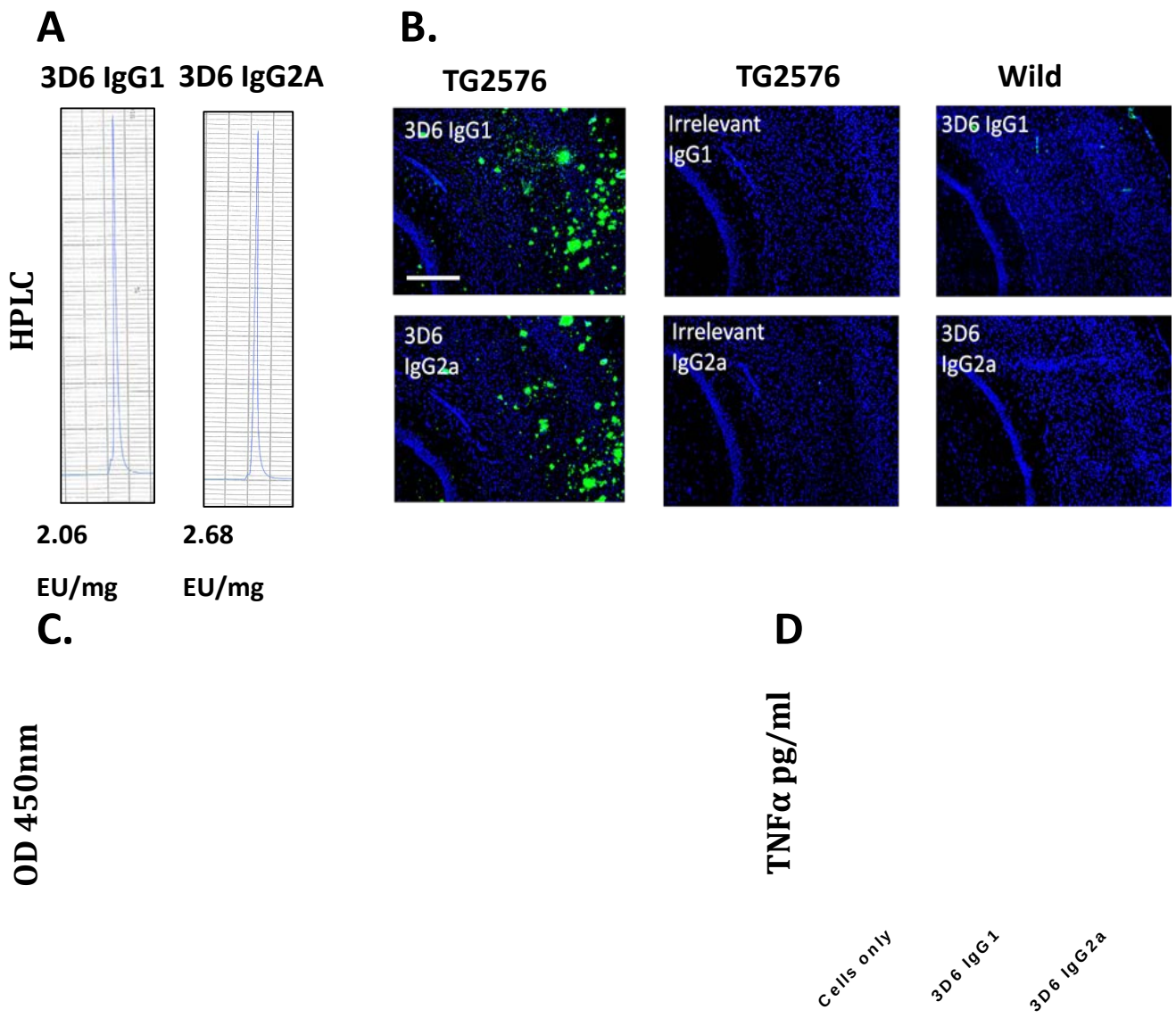

Figure 3. 5 Comparison the binding and effector function of 3D6 IgG1 and IgG2a

A. HPLC traces (a280nm) of 3D6 IgG1 and IgG2a, both antibodies have low levels of aggregate present. Endotoxin levels measured by LAL assay (3D6 IgG1, 2.06EU/mg) (3D6 IgG2a, 2.68 EU/mg). **B.** Binding of 3D6 IgG1 and IgG2a to TG2576 and wild type brain sections. Both subclasses of 3D6 binds strongly to plaques in tissue sections of TG2576 mice and does not bind to tissue from WT mice, irrelevant isotype controls do not bind to plaques. **C.** I*n vitro* binding of both subclasses of 3D6 to immobilised $A\beta_{1-40}$ peptide. Both subclasses of 3D6 bind to immobilised peptide with the same affinity, irrelevant isotype controls do not bind. **D.** shows TNFα levels produced by RAW2.64 cells in response to immobilised 3D6 IgG1 and IgG2a. 3D6 IgG2a stimulates 3-fold higher TNFα levels as compared to cells only or cells stimulated with immobilized 3D6 IgG1.

3.3.3 Production of 3D6 Gantenerumab and mC2

Due to the low expression levels of 3D6, systemic treatment was not possible as this treatment requires 2.5mg antibody per mouse, as compared to 4µg antibody per mouse for intracranial injections. I produced two additional anti-Aβ antibodies: a human/murine chimeric version of the Gantenerumab (chGantenerumab), originally developed by Roche (Bohrmann et al., 2012) and a murine version Crenezumab (mC2), originally developed by AC Immune (Adolfsson et al., 2012). I generated IgG1 and IgG2a versions of these antibodies, as well as 3D6. The full antibody sequence was ordered in a plasmid from Geneart^{tm}. These plasmids were then transiently transfected into HEK cells, and purified in the same manner as described previously.

3.3.4 Characterisation of 3D6 Gantenerumab and mC2

Figure 3.6A shows HPLC traces (a280nm) and endotoxin levels of the three antibodies produced. All antibodies have low levels of aggregate and undetectable endotoxin by the LAL assay. The three anti-Aβ antibodies were characterised for binding to Aβ as described previously. First, the specificity and relative affinity to Aβ was tested by measuring binding to immobilised Aβ 1-40 peptide. Figure 3.6C shows that both 3D6 and *ch*Gantenerumab bind to recombinant peptide with relative high affinity (EC50 3D6 = 0.17pM; EC50 *ch*Gantenerumab = 0.34pM) however 100 fold higher levels of mC2 were required to reach half maximal binding (EC50 mC2 =17.4pM), suggesting significantly lower affinity to immobilized Aβ peptide. Antibodies were then tested for binding to Aβ plaques in brain sections from TG2576 mice, and to better mimic *in vivo* binding conditions, tissue sections were not subjected to any antigen retrieval before immuno-staining. 3D6 bound plaques in tissue obtained from TG2576, while no binding was observed in wild type mice. The antibody mC2 also bound but fewer plaques were labelled (Figure 3.6B). *Ch*Gantenerumab labelled plaques, however it also appeared to bind to neurons in both TG2576 and wild type mice. We then tested the ability of these antibodies to bind to plaques in TG2576 tissue sections with and without formic acid antigenic retrieval (Figure 3.7). Formic acid antigenic retrieval is a commonly used method for the immunohistochemical detection of Aβ. Formic acid solubilises the aggregated Aβ found in plaques, exposing epitopes for the antibodies to bind. Fresh frozen tissue sections were formalin fixed, followed by formic acid treatment, to further characterise the binding. 3D6 bound plaques with and without formic acid treatment; however, incubation of tissue with formic acid increased the intensity of staining. mC2 bound poorly to plaques in fresh frozen, unfixed tissue,

but after formic acid treatment mC2 strongly labelled plaques. *ch*Gantenerumab showed a high neuronal background staining, however plaque staining is visible in formic acid treated sections. The plaques and Aβ found in TG2576 mouse brains might differ in conformation from those found in the brain of AD patients, and therefore the binding characteristics of the antibodies to tissue obtained from AD patients was also assessed. Figure 3.8 shows staining from the cingulate gyrus of an AD patient. The results found in AD brain sections were comparable to those in mouse tissue. 3D6 binds Aβ without antigen retrieval, but binds to plaques better after formic acid treatment. mC2 labels plaques without formic acid but to a lower degree than 3D6, while mC2 labels plaques well after formic acid treatment. chGantenerumab shows a high degree of neuronal background staining, but plaques are visible after formic acid treatment.

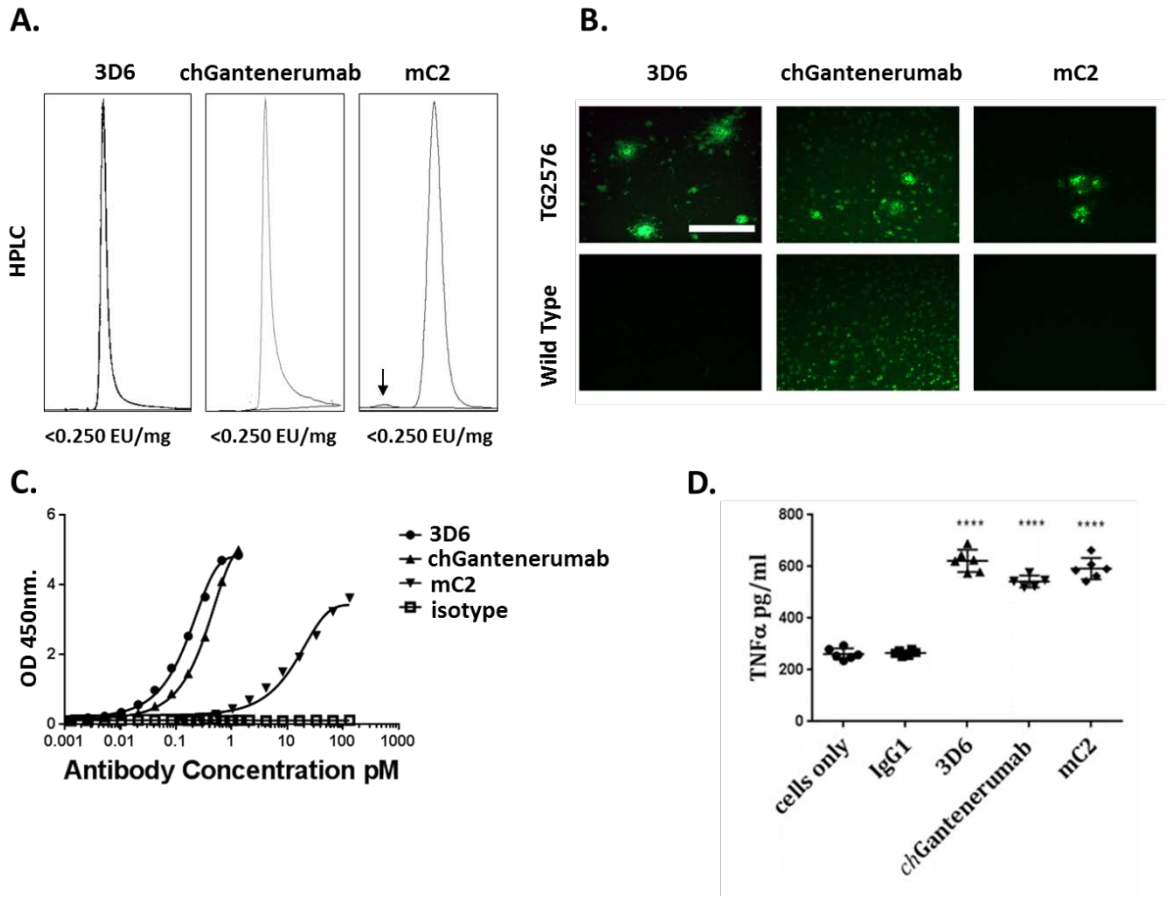

Figure 3. 6 *In vitro* binding and effector function of 3D6 chGantenerumab and mC2

A. HPLC traces (a280nm) of 3D6, chGantenerumab and mC2. All antibodies have low aggregate, there is a small proportion in mC2 which is indicated by a black arrow. **B.** Binding of 3D6, chGantenerumab and mC2 to TG2576 and wild type (WT) brain sections. 3D6 binds strongly to plaques in tissue sections of TG2576 mice and does not bind to tissue obtained from WT mice. *chGantenerumab* binds to plaques but also appears to bind to neurons in both TG2576 and WT mice. mC2 binds to plaques, but labels them less strongly than 3D6. **C.** *In vitro* binding of anti Aβ antibodies to immobilised $A\beta_{1\text{-}40}$. 3D6 and chGantenerumab both bind with relatively high affinity (EC50 3D6 = 0.17pM; EC50 chGantenerumab = 0.34pM) mC2 bound with lower relative affinity (EC50 MC2 =17.4pM) **D.** TNFα levels produced by RAW 2.64 cell line in response to immobilised Aβ antibodies against an IgG1 control. All three IgG2a anti Aβ antibodies cause increased production of TNFα in comparison to IgG1 and cell only controls.

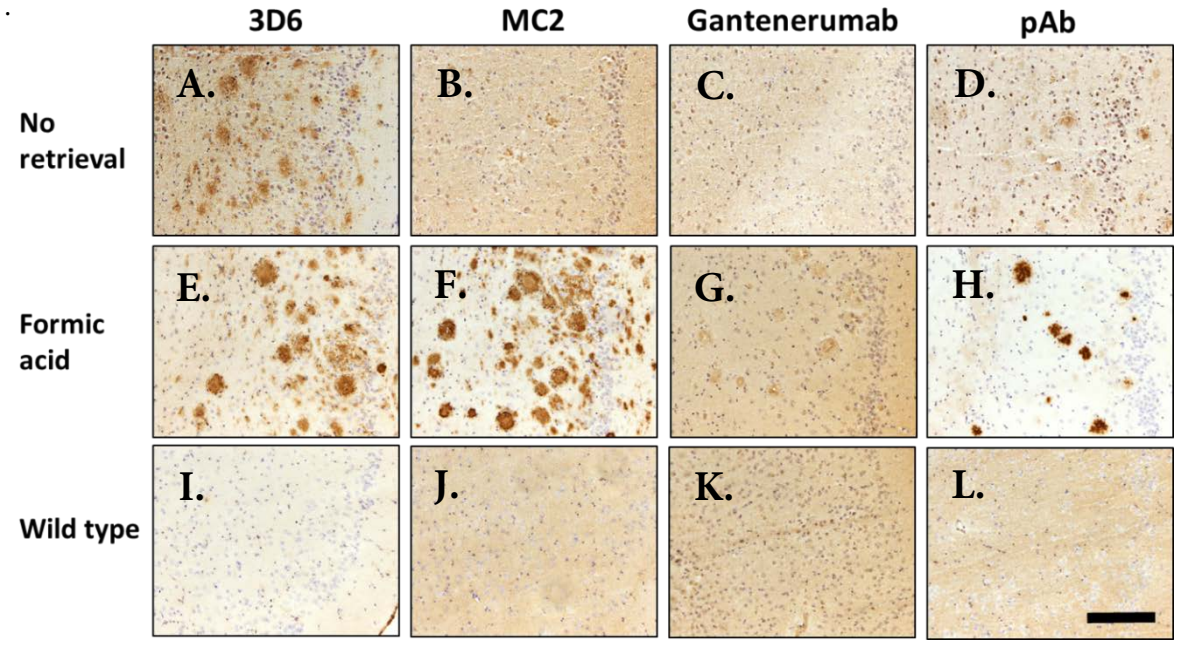

Figure 3. 7 Binding of Aβ antibodies to formalin fixed TG2576 brain sections with and without formic acid antigen retrieval.

The antibodies 3D6, mC2 and chGantenerumab and a commercial polyclonal antibody were compared for their ability to bind plaques in TG2576 tissue sections treated with and without formic acid antigen retrieval. 3D6 binds to plaques in TG2576 brain without formic acid (A), formic acid treatment increases the strength of staining (E) and it does not bind to wild type brain sections (I). mC2 stains plaques faintly without formic acid treatment (B), treatment greatly improves staining of plaques (F). chGantenerumab does not stain plaques without formic acid treatment (C), there is faint plaque staining after formic acid treatment (G) although there is higher background than the other antibodies. The polyclonal antibody (pAb- clone number?) faintly stains plaques without formic acid (D), with formic acid the staining becomes much stronger (H).Images were taken with a 10x objective, (scale bar=400μm).

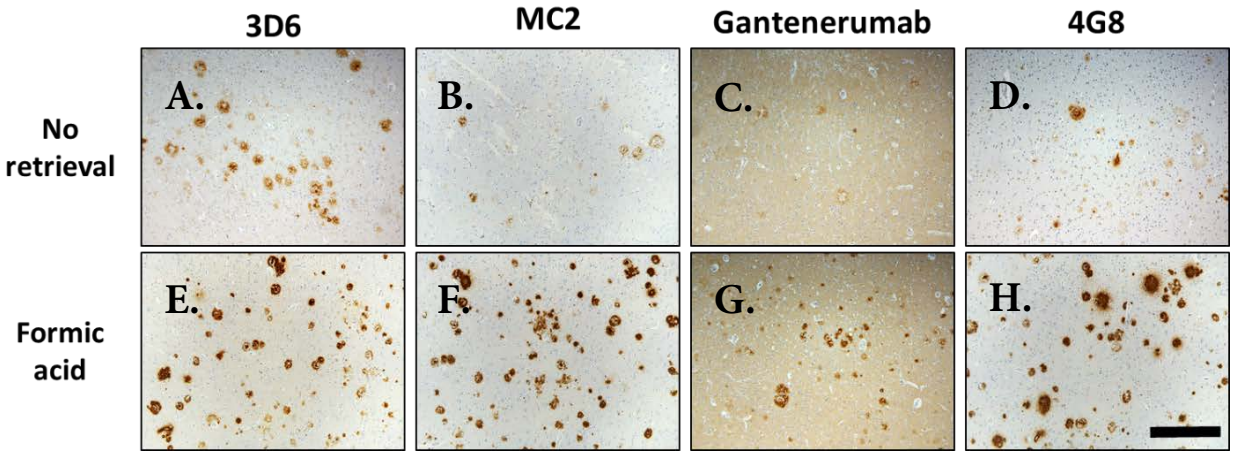

Figure 3. 8 Binding of Aβ antibodies to formalin fixed human brain sections with and without formic acid antigen retrieval

The antibodies 3D6, mC2 and chGantenerumab and the antibody 4G8 were compared for their ability to bind to plaques in human brain tissue sections with and without formic acid antigen retrieval. 3D6 binds to plaques in human brain tissue (cingulate gyrus) without formic acid (A), formic acid treatment increases immunoreactivity (B) mC2 stains plaques faintly without formic acid treatment (B), treatment greatly improves staining of plaques (F). chGantenerumab very weakly stain plaques without formic acid treatment (C), there is faint plaque staining after formic acid treatment (G) although there is higher background than the other antibodies. The polyclonal antibody (pAb) faintly stains plaques without formic acid (D), with formic acid the staining becomes much stronger (H).Image were captured with a 10x objective, (scale bar=400µm).

3.4 Discussion

Bapineuzumab is an anti-Aβ antibody (N-terminus AA1-5, hIgG1) developed for the treatment of AD. In phase II clinical trials Bapineuzumab was able to reduce the deposition of Aβ in the brains of AD patients (Rinne et al., 2010), however it also causes damage to the cerebral vasculature (Salloway et al., 2010). It is thought that these vascular side effects are caused by an inflammatory response to Bapineuzumab in the brain, and as a result the dose was reduced in phase III trials. This reduced dose is a potential reason for the failure of Bapineuzumab to meet its primary endpoint of improvement in cognition (Salloway et al., 2014). This thesis is focussed on the role of FcγRs in the neuro-inflammatory response to anti-Aβ immunotherapy, and to test if engineering the constant region of these antibodies could be an approach to improve safety. We generated the antibody 3D6 (original murine version of Bapineuzumab) as both IgG1 and IgG2a subclasses, to allow comparison of the two subclasses *in vivo*. Both 3D6 IgG1 and IgG2a possess the same variable regions and therefore have the same ability to bind to Aβ. Both antibodies were equally good at binding to both recombinant Aβ immobilised on an ELISA plate, and to plaques in brain sections of TG2576 mice. Murine IgG1 and IgG2a versions were also produced for two other well characterised anti-Aβ antibodies: mC2 (Crenezumab) and Gantenerumab. IgG1 and IgG2a versions of mC2 or chGantenerumab behaved in the same manner in binding assays. The rationale for choosing the two subclasses is their contrasting affinity for FcγRs. Mouse IgG2a has stronger relative affinity for activating FcγRs in comparison to IgG1, associated with a stronger pro-inflammatory response (Bruhns, 2012; Nimmerjahn and Ravetch, 2005). This was shown by our FcγR cross-linking assay, where 3D6 IgG2a activated RAW 264.7 cells and caused more TNFα to be produced than 3D6 IgG1. These antibodies have the same ability to bind to their target but differing effector functions, and are therefore suitable to test the role of antibody effector function on the clearance of plaques and the induction of neuro-inflammation in an *in vivo* model of AD.

The yield of both 3D6 IgG1 and IgG2a antibodies after transfection was exceptionally poor. This was not due to the expression system used, as this was found in three independent laboratories. It would be interesting to find the reason for this low yield to improve production, however it goes beyond the scope of this PhD. Each transfection in 293F cells produced an average of 0.5mg of antibody, and this put limitations on the type and duration of experiment could be performed. Stereotaxic surgery allows the precise delivery of substances into a specific brain region. This method has already been used to characterise the response of transgenic APP mice to anti-Aβ

immunotherapy, and provides a rapid model of plaque clearance and neuro-inflammation (Carty et al., 2006; Wilcock et al., 2004a). Importantly this method only requires a single injection of 2μg of antibody to clear plaques and therefore all three antibodies can be tested using this approach. Intracranial injection of antibody is a useful model to provide insight into the underlying mechanisms of plaque clearance and associated inflammation, while systemic administration is more clinically relevant. To perform a two month systemic trial, at least 60mg of each antibody is required at a dose of 10 mg/kg. The low yield of 3D6 made this unfeasible, and therefore we were unable to dose mice with this antibody systemically and instead used mC2

The production of three antibodies used in clinical trials gave us the opportunity to directly compare the characteristics of these antibodies *in vitro*. All three antibodies were able to bind to plaques in brain sections of hAPP transgenic (TG2576) mice and human AD patients. The antibody 3D6 is bound to plaques without antigenic retrieval, which could predict better plaque engagement in vivo. chGantenerumab is able to bind to plaques, however it also labels neurons in both transgenic and wild type mice, which could indicate binding to neuronal APP, however further investigation is needed. mC2 is also able to bind to plaques without antigenic retrieval, albeit weaker compared to 3D6. This disparity in plaque binding can be explained by the different epitopes of Aβ that the antibodies bind to. 3D6 binds to the N-terminus (AA 1-5) and many antibodies targeting this site are able to bind to plaques-probably because this epitope is exposed (Serpell, 2000). mC2 binds to the central domain of Aβ (AA 12-23), and antibodies such as m266 which binds to the same region (AA 13-26) and has an almost identical CDR sequence to mC2, is unable to bind to plaques because the epitope is not available to bind when Aβ is aggregated. This is supported by staining of mouse and human tissue where solubilisation of plaques with formic acid allows mC2 to bind. The Aβ ELISA allowed ranking of the antibodies by relative affinity for the recombinant peptide; 3D6>chGantenerumab>>>mC2, but there are limitations to this approach which should considered when interpreting this data. Due to Aβ's propensity to aggregate, when the plates are coated with peptide, it is not possible to predict whether monomers, oligomers or larger structures are present on the plate and in what proportion. Therefore when analysing the relative affinities, we do not know which species the antibodies are binding to. Based on immunohistochemistry, mC2 appears to be better at binding to soluble Aβ species (as solubilisation with formic acid allows binding). The disparity in binding to recombinant peptide between mC2 and 3D6 may be due to aggregation of Aβ, forming fibrils that mC2 cannot bind and not representative of the antibody's ability to bind to soluble Aβ.

In conclusion, we generated three antibodies which have been in clinical trials for AD, each with IgG1 or IgG2a constant regions. Using these antibodies we can test the role that both effector function and target binding play in the clearance of Aβ and induction of neuro-inflammation.

Chapter 4: Characterisation of Fc gamma receptor expression in TG2576 mice and human AD patients

4.1 Introduction

Familial AD is caused by mutations in the APP gene or the enzymes responsible for the cleavage of APP to Aβ (Citron et al., 1992; Cruts and Van Broeckhoven, 1998; Goate et al., 1991; Nilsberth et al., 2001). The mutations increase the total amount of Aβ produced, or increase the Aβ42: Aβ40 ratio. The most commonly used models of AD are mice which overexpress human APP containing one or more of these mutations. These mice develop a number of pathologies in common with human disease characteristics such as: deposition of Aβ as plaques, cognitive deficits and neuroinflammation as measured by increased immune receptor expression on microglia. One of the most frequently used mouse strain is the TG2576 model, with the Swedish double mutation (KM670/671NL) under the control of the hamster prion promoter (Hsiao et al., 1996). These mice develop plaques between 9-12 months and have neuro-inflammation and cognitive deficits (Benzing et al., 1999; Hsiao et al., 1996; Kawarabayashi et al., 2001; Westerman et al., 2002). TG2576 mice have already been used extensively in the development of anti-Aβ immunotherapy (Arendash et al., 2001; Freeman et al., 2012; Obregon et al., 2008; Shoji et al., 2003; Wilcock et al., 2003), therefore we have chosen to use this to investigate the role of FcγR effector function in plaque clearance and inflammation.

FcγRs bind to the constant domain of IgG, and are expressed on a wide variety of cell types including the CNS macrophages- microglia (Fuller et al., 2014). There are two distinct types of FcγR- activating and inhibitory; activating receptors contain or are associated with a cytoplasmic ITAM motif whilst the inhibitory receptor contains an ITIM motif. Ligation of IgG-immune complexes by activating FcγRs results in the crosslinking of cytoplasmic chains causing phosphorylation of ITAMs, resulting in the activation of downstream signalling cascades such as the PI3K pathway. This results in increased cellular calcium and activation of the cell which can induce: proliferation, cytokine/chemokine release, phagocytosis or antigen presentation (Nimmerjahn and Ravetch, 2008). When the Inhibitory receptor, FcγRIIb, ligates an immune complex the cytoplasmic ITIM inhibits activation of these pathways (Nimmerjahn and Ravetch, 2008).To increase the complexity, there are also a number of IgG subclasses each of which has a distinct binding pattern to different FcγRs (Bruhns, 2012). Therefore the response to immunotherapy will be dependent on the subclass of the antibody used, but also the balance of activating and inhibitory FcγR expression on effector cells. This is demonstrated by models of

immune complex disease and/or autoimmune disease, where mice lacking the inhibitory FcγR have exacerbated pathology whereas those lacking activating receptors are protected (Yuasa et al., 1999).

Microglia in the brains of AD patients and in mouse models express increased levels of FcγRs (Bouras et al., 2005; Peress et al., 1993; Wilcock et al., 2004b). This chapter describes a full characterisation of the basal expression of FcγRs and other immune receptors in the TG2576 model, as well as the basal levels of cytokines expressed in the brain. These results are validated using human brain tissue of AD patients. Understanding the expression levels of the different FcγRs will allow us to interpret the response of these mice to immunotherapy. To our knowledge, this is the first time the protein levels of all mouse FcγRs have been examined in this model.

4.2 Methods

4.2.1 Study design

TG2576 mice and wild type littermates were aged until 18 months old (n=5), before sacrifice and perfusion with heparinised saline. One hemi-brain was embedded for immunohistochemistry and the other was snap frozen for measurement of cytokine protein levels.

4.2.2 Quantification of staining in the brain

To measure immune phenotype, brains were cut on a cryostat at 10μm and stained for different immune markers. The area above threshold of staining was quantified using imageJ. The staining was quantified in four different brain regions based on Aβ load. The regions are shown in fig. 4.1 and are: the hippocampus (HC), the primary somatosensory cortex (SC), the posterior parietal association cortex (PPTA) and the piriform cortex (PC).

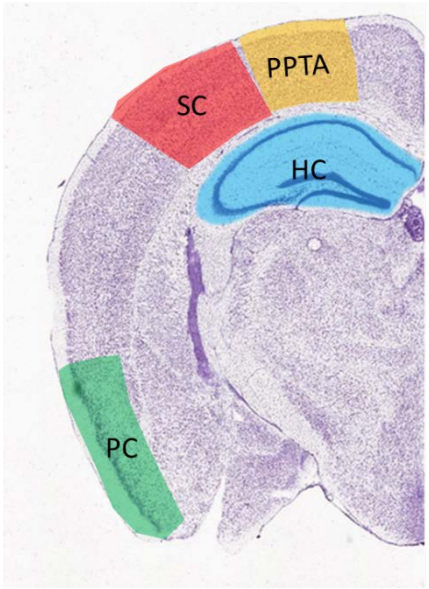

Figure 4. 1 Areas of the brain quantified for immune receptor expression

This figure shows the areas of brain that were quantified for staining of immune receptors. The following areas were used: the hippocampus (blue), the primary somatosensory cortex (red), the posterior parietal association cortex (yellow) and the posterior piriform cortex (green)

4.3 Results

4.3.1 Expression of immune receptors in the TG2576 mice

Reagents have been generated in house for the detection of the different mouse FcγRs and were validated for their use in immunohistochemistry by staining spleen sections from wild type mice and Fc gamma deficient mice lacking activating FcγRs. This validation included a commercially available antibody which binds to both FcγRIIb and FcγRIII. All antibodies show positive staining the wild type spleen sections (Appendix B), and staining for the activating receptors (FcγRI, FcγRIII, and FcγRIV) is lost in gamma chain deficient mice. The staining of the inhibitory receptor (FcγRIIb) is unaffected. The expression levels of FcγRs and other immune receptors in 18 month old TG2576 were quantified in four different brain regions: the hippocampus (HC), piriform cortex (PC) primary somatosensory cortex (SC) and posterior parietal association area (PPtA). Figures 4.2 and 4.3 show representative images comparing wild type and TG2576 mice and the quantification of this staining is shown in figure 4.4. Higher magnification images showing the morphology of cells expressing FcγRs are shown in figure 4.6.

4.3.1.1 FcγRI

FcγRI is expressed by microglia of both TG2576 and WT mice. The expression of FcγRI is particularly high in focal regions which appear to be on cells associated with plaques, but can also be detected on ramified microglial cells throughout the parenchyma (figure 4.6C). Quantification of FcγRI staining (Figure 4.4) shows a clear trend towards increased expression in APP mice than in WT mice, there is at least a 2-fold increase in staining in all four brain regions. However, the only significant change is in the piriform cortex where there is a 6-fold increase in FcγRI expression compared to controls ($p=0.022$).

4.3.1.2 FcγRIIb

FcγRIIb expression can be detected on cells associated with the vasculature in the hippocampal fissure, and their morphology suggests perivascular macrophages (Figure 4.6E). The expression of FcγRIIb on microglia is not widespread, however some examples of ramified microglia can be

detected (figure 4.6F). There is a trend towards increased FcγRIIb expression in the hippocampus of TG2576 mice compared to WT (figures 4.2 and 4.4).

4.3.1.3 FcγRIII

FcγRIII is expressed in the same regions as FcγRI, particularly on cells associated with plaques. Higher magnification images (Figure 4.6 I&J) show that FcγRIII is expressed by cells with the morphology of perivascular macrophages and ramified microglia. There is a 5-fold increase in FcγRIII in TG2576 mice compared to WT in the piriform cortex (p=0.027). Using a commercial antibody which recognises both FcγRIIb and FcγRIII yields higher staining than either specific antibody. The staining pattern is similar to FcγRI, with the highest levels on cells associated with plaques. Similar to the FcγRIII antibody, there was staining of both perivascular cells and ramified microglia (Figure 4.6 M&N). Increased expression of FcγRII/III was found in all brain regions of TG2576 mice (Figure 4.2 and 4.4). There is a 20-fold increase in expression in TG2576 the piriform cortex (p=0.0045) and a 12-fold increase in the primary somatosensory cortex (P=0.020) compared to WT. The cell type associated with the vasculature expressing FcγRII/III could be: endothelial cells, perivascular macrophages or pericytes. To find out which cell type express FcγRII/III, brain sections were double stained for FcγRII/III and markers of the different cells. Figure 4.5 shows double staining of FcγRII/II and markers of: endothelial cells (CD31), pericytes (NG2) and perivascular macrophages (CD206). FcγRII/III positive cells associate with, but do not co-localise with endothelial cells (CD31 positive) or pericytes (NG2 positive cells). Co-localisation was detected between FcγRII/III and CD206, indicating expression of FcγRs on perivascular macrophages.

4.3.1.4 FcγRIV

FcγRIV expression is low in all brain regions, with no significant difference between TG2576 and WT. There is faint staining of cells associated with the vasculature (figure 4.6Q).

4.3.1.5 Aβ and other immune receptors

There is no detectable human Aβ in WT mice as they do not possess the APP transgene. In 18 month old TG2576 mice many plaques can be identified in all brain regions studied, with particularly high numbers in the hippocampus and piriform cortex (figure 4.3). CD11B is expressed

at higher levels in TG2576 mice than in WT mice and in particular on cells associated with plaques. There are trends towards higher expression levels in TG2576 mice compared to WT in all brain regions, and a 10 fold increase in the piriform cortex ($p=0.0013$). CD45 is another marker commonly used for detecting neuro-inflammatory changes in the brain and its expression is much lower than CD11B. A 4-fold increase in the piriform cortex of TG2576 mice compared to WT was found ($p=0.002$). MHCII is a gene expressed by antigen presenting cells, and is responsible for presenting antigens to CD4 T-cells. There are low levels of MHCII expressed in the brains of both TG2576 and WT mice. Unlike the microglial activation markers CD11b and CD45, MHCII is not expressed on cells associated with plaques, positive cells appear to associate with the vasculature. There is a 4-fold increase in MHCII in the hippocampus of TG2576 mice compared to WT ($p=0.03$).

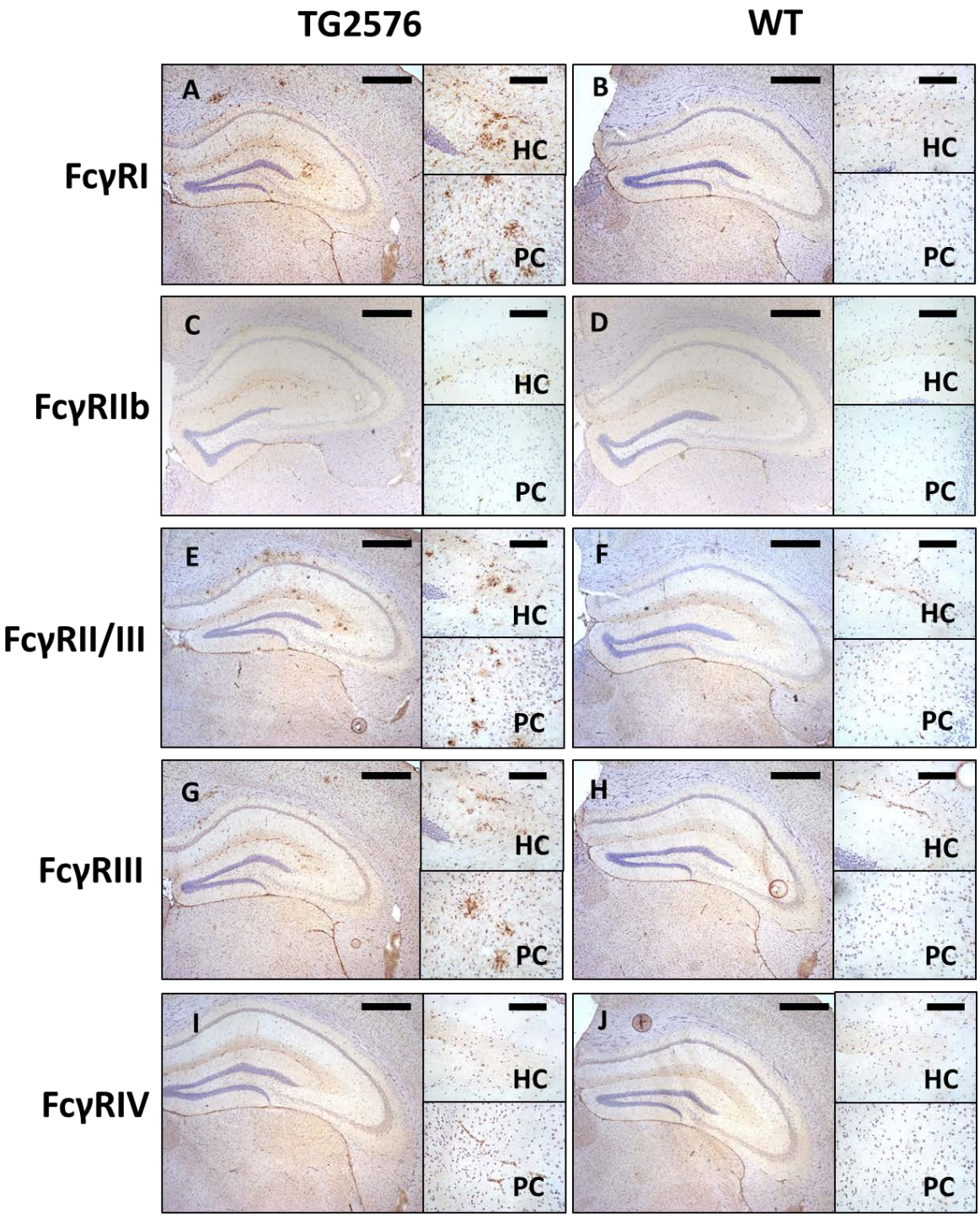

Figure 4. 2 FcγR expression in 18 month TG2576 mice versus wild type littermate controls.

The expression of FcγRs in the brains of TG2576 mice and wild type littermates (n=5, 1 section per mouse), was measured by immunohistochemistry. FcγRI (A, B), FcγRIIb (C, D), FcγRII/III (E, F), FcγRIII (G, H) and FcγRIV (I, J). Larger images were taken with a 5x objective, and inset pictures were taken with a 20x objective (scale bars =500μm and 125μm respectively). HC= hippocampus and PC = piriform cortex. The quantification of staining can be found in figure 4.5.

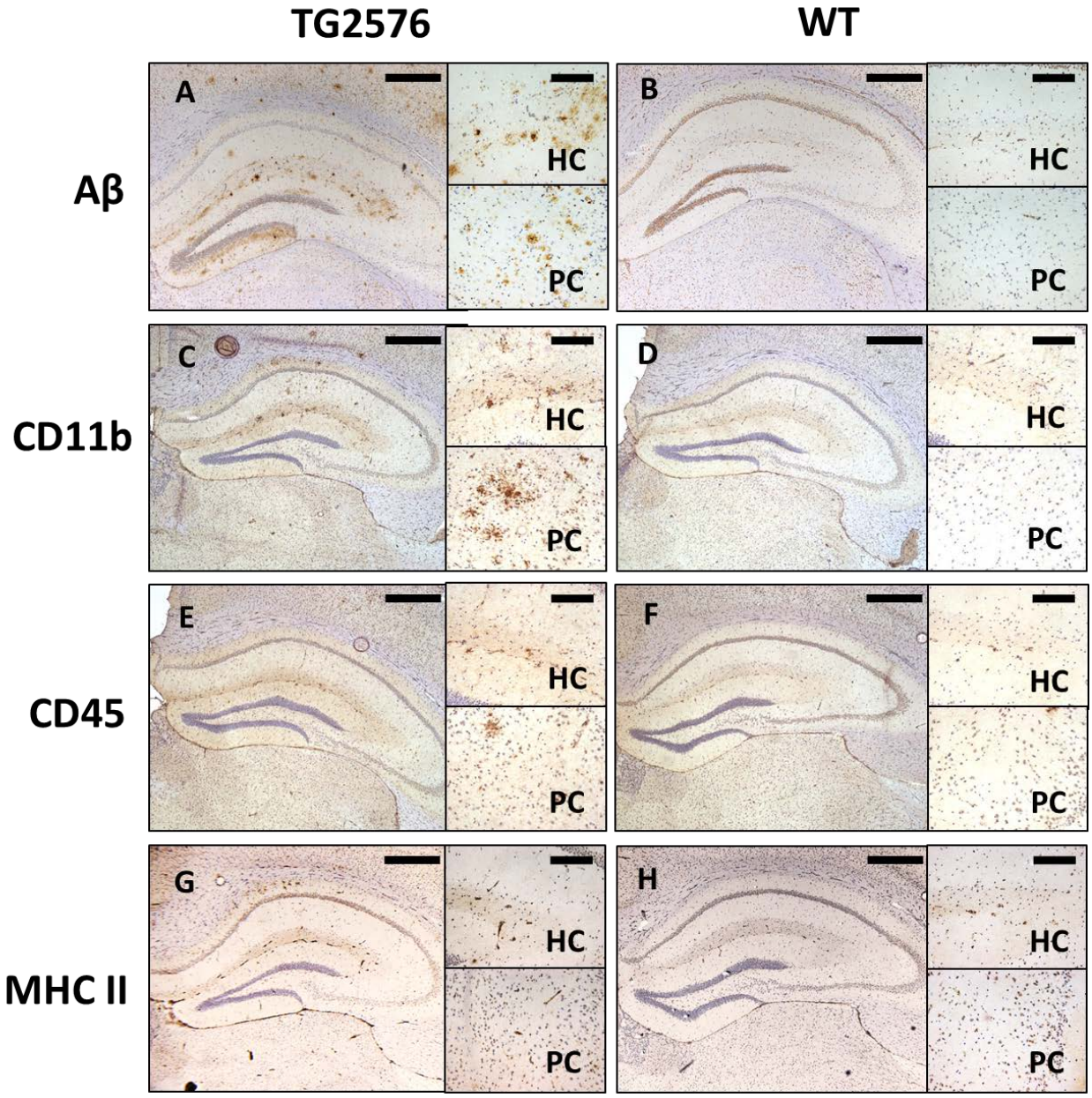

Figure 4. 3 Aβ deposition and immune receptor expression in 18 month TG2576 mice versus wild type littermate controls.

The expression of Aβ and immune receptors in the brains of TG2576 mice and wild type littermates was measured by immunohistochemistry (n=5, 1 section/mouse). Aβ (A, B), CD11b (C, D), CD45 (E, F) and MHCII (G, H). Larger images were taken with a 5x objective, and inset pictures were taken with a 20x objective (scale bars =500μm and 125μm respectively). HC= hippocampus and PC = piriform cortex. The quantification of staining can be found in figure 4.5.

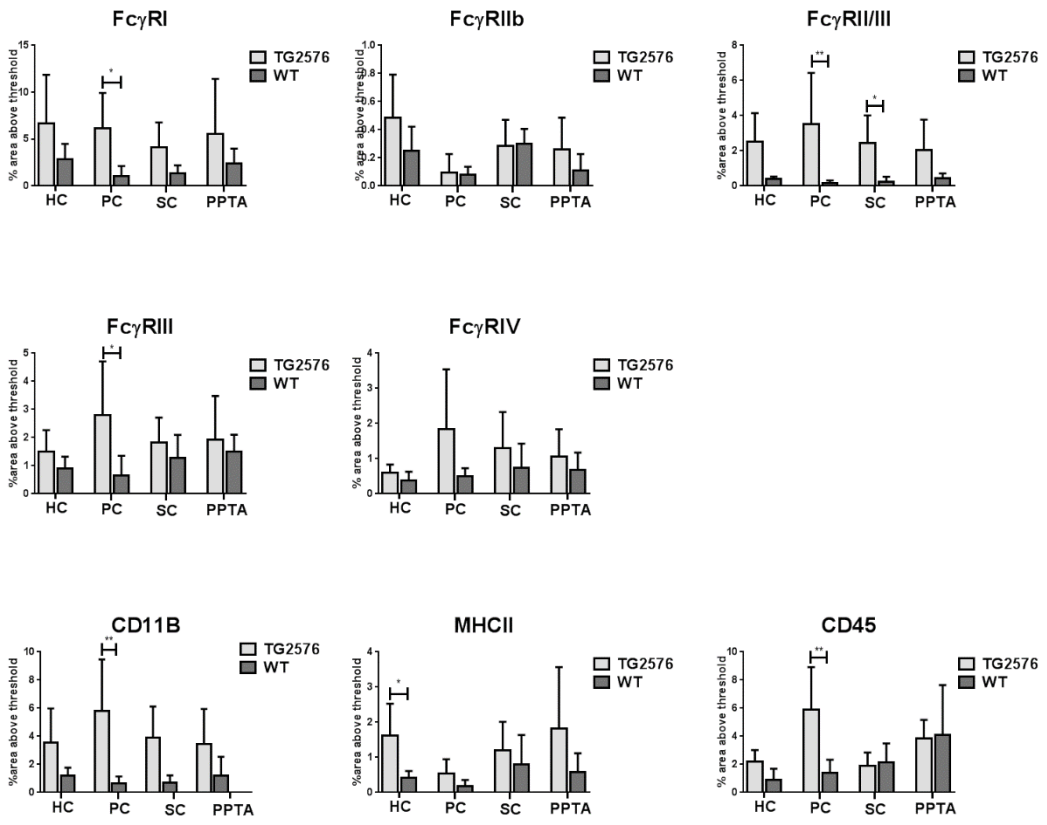

Figure 4. 4 Quantification of immune receptor staining

The levels of immune receptor staining in TG2576 and wild type mice (n=5) were quantified using image J. This figure shows the area above threshold of staining in four brain regions: the hippocampus (HC), the primary somatosensory cortex (SC), the posterior parietal association cortex (PPTA) and the piriform/entorhinal cortex (PC). Locations of these brain regions can be seen in figure 4.1. Data were analysed by one way ANOVA and Bonferroni post hoc test (FcγRI, FcγRIIb, FcγRIV, CD11B and CD45) or Kruskal-Wallis and Dunn's post hoc test (FcγRII/III and FcγRIII), data presented as mean+/- S.D. FcyRI was significantly higher in the PC of TG2576 mice (p=0.022). FcyRIII was significantly higher in the PC of TG2576 mice (p=0.027). FcyRII/III was significantly higher in the PC (p=0.0045) and SC (p=0.04) of TG2576 mice. CD11B was significantly upregulated in the PC (p=0.0013) of TG2576 mice. CD45 was significantly upregulated in the PC (p= 0.002) of TG2576 mice and MHCII was significantly increased in the HC (p=0.03).

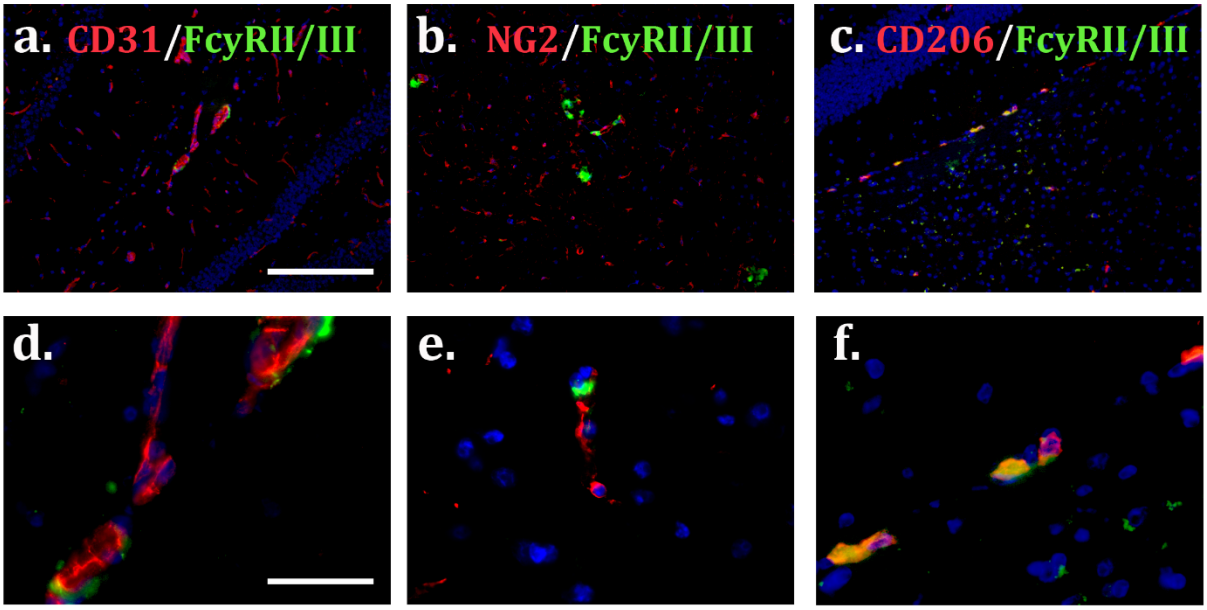

Figure 4. 5 Double fluorescent staining of FcγRII/III with CD31, NG2 and CD206

To elucidate the perivascular cell type expressing FcγRs, sections from TG2576 mice were double stained for FcγRII/III and markers expressed by endothelial cells (CD31), pericytes (NG2) and perivascular macrophages (CD206). Images shown are representative of n=5. **a,d** CD31 (red) FcγRII/III (green). **b,e.** NG2 (red) FcγRII/III (green). **c,f.** CD206 (red) FcγRII/III (green). Ina all images DAPI is blue. Images were taken with a x20 objective (a, b, c scale bar 200μm) or a x100 objective (d, e, f scale bar 40μm). This immunostaining was performed by third year undergraduate student Miss Amanda Hyne.

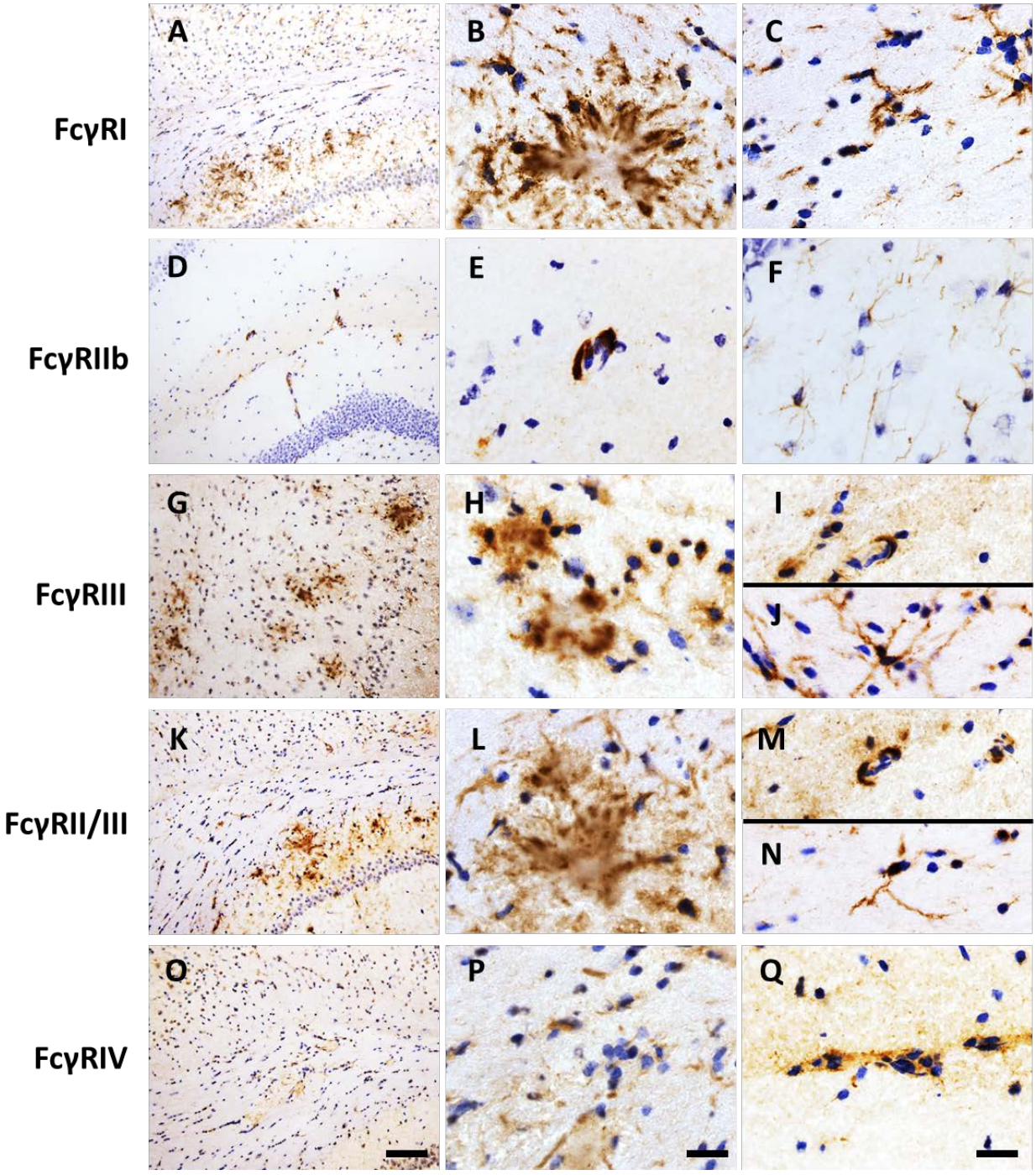

Figure 4. 6 High magnification images of FcγR expression in TG2576 mice

The expression of FcγRs TG2576 mice: FcγRI (A, B and C), FcγRIIb (D, E and F), FcγRIII (G, H, I and J), FcγRII/III (K, L, M and N) and FcγRIV (O, P and Q). Images are represenatative of n=5, and were taken with a 20x objective (A, D, G, K and O scale bar=100μm) or a 100x objective (B, C, E, F, H, I, J, L, M, N, P and Q scale bar=20 μm).

4.3.2 Co-localisation of immune receptors with amyloid beta

Microglia in the AD brain express markers of activation, including FcγRs, and surround Aβ deposits (Peress et al., 1993). The staining of cells expressing immune receptors in 18 month old TG2576 mice are largely in clusters, likely surrounding Aβ deposits. To confirm this, double immunofluorescence was used to label Aβ and immune receptors and images were taken with a confocal microscope. Figure 4.7 shows a selection of confocal images demonstrating that microglial cells are associated with Aβ plaques expressing: CD11b, FcγRI and FcγRIII. Individual z stack images show individual microglia expressing FcγRI interacting with a plaque.

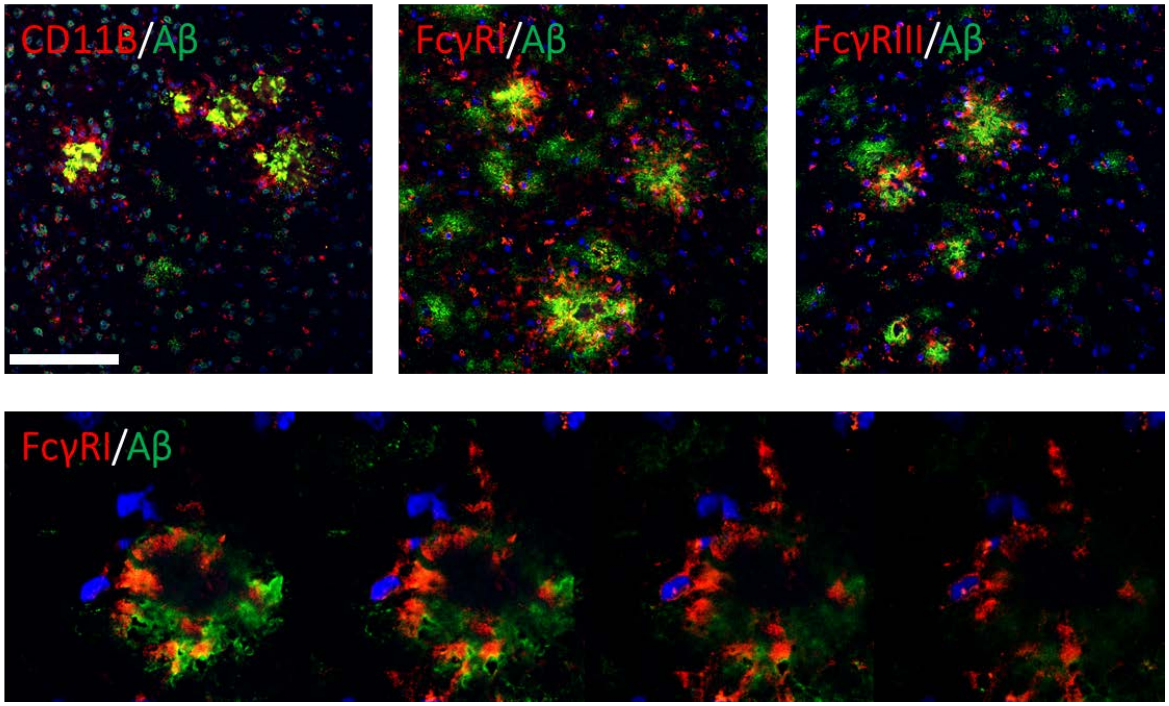

Figure 4. 7 Confocal co-localisation of microglia expressing immune receptors with Ab plaques

Microglia expressing: CD11B (A), FcγRI (B) and FcγRIII (C) surround deposits of Aβ. Z-stack images clearly showing individual microglia expressing FcγRI interacting with Aβ.In all images DAPI is blue. Images were taken on a Leica SP8 confocal microscope with a 40x objective (scale bar=100μm). Individual z-stack images of FcγRI staining are digital zooms of the 40x image.

4.3.3 Cytokine levels in TG2576 brains

The levels of cytokines were measured in brain homogenate from 18 month old TG2576 mice and WT controls (n=5) using a multiplex immune assay (MSD). The levels of cytokines are shown in figure 4.8, there was no detectable IFN-γ or TNFα in any of the samples and therefore they have not been shown in this figure. There are no differences between TG2576 mice and WT mice at 18 months.

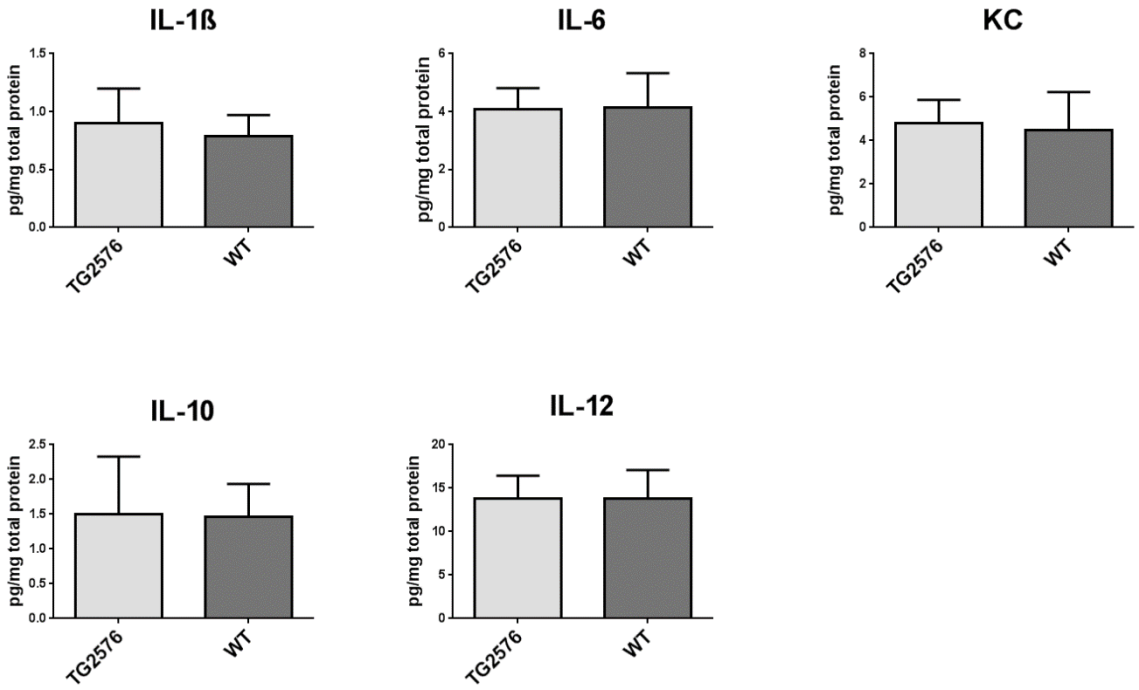

Figure 4. 8 Cytokine concentration in brain homogenate of 18 month old TG2576 mice are the same as in wild type controls

Cytokine levels in brain homogenate from TG2576 and wild type littermates was measured by a multiplex immune assay (MSD). TNFα and IFNγ assays were not included as levels of these cytokines were undetectable. Data were analysed by two-tailed T test (n=5), no significant differences were found between wild type and transgenic, data presented as mean+/- S.D.

4.3.4 Human FcγR expression in the brain

The expression of FcγRs was also investigated in three human AD cases, figure 4.9 shows representative images taken of the cingulate gyrus of an AD patient with high levels of Aβ accumulation. The monoclonal antibodies were optimised first in paraffin embedded tonsil tissue (Appendix B). FcγRI was detected on microglial cells clustering around plaques (Figure 4.9B), the receptor is also expressed by ramified microglia throughout the brain parenchyma (Figure 4.9C). The expression of FcγRIIa is less widespread than FcγRI, but appears on more rounded and less ramified cells and expression can be detected on perivascular cells (Figure 4.9F). FcγRIIb was not detected on microglial cells in any of the patients studied, FcγRIIb expression was only detected on neurons and small amoeboid cells associated with blood vessels (Figure 4.9H&I). FcγRIIIa expression could be detected on microglial cells clustering around plaques (Figure 4.9K), and more ramified cells throughout the parenchyma (4.9L).

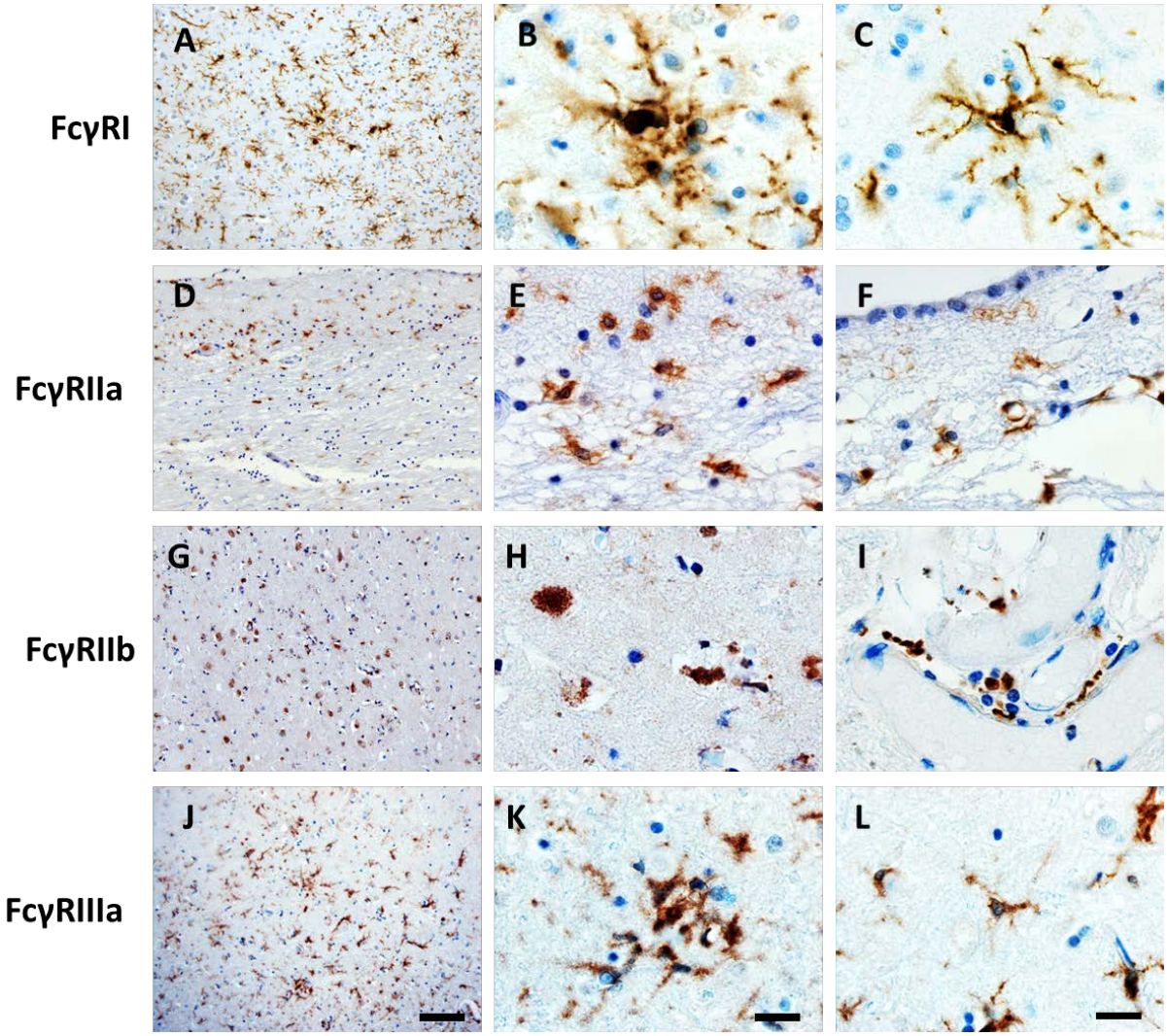

Figure 4. 9 FcγR Expression in human AD brain

The expression of FcγRs in human AD case in occipital cortex: FcγRI (A, B and C), FcγRIIa (D, E and F), FcγRIIb (G, H and I) and FcγRIIIa (J, K and L). Images were taken with a x20 objective (A,D, G and J scale bar=100μm) or a x100 objective (B,C,E,F,H,I,K and L scale bar=20 μm).

4.4 Discussion

Activation of microglia has previously been reported in the TG2576 mouse model of AD- particularly surrounding deposits of Aβ (Apelt and Schliebs, 2001; Benzing et al., 1999). Here we show that there is substantial deposition of Aβ plaques in the brain of 18 month old TG2576 mice, and that this is associated with the up-regulation of microglial activation markers. The expression of these markers is particularly noticeable in clusters which are similar in shape and location to Aβ deposits, and confocal microscopy confirmed that cells expressing CD11B and the activating FcγRs: FcγRI and FcγRIII directly in contact with plaques. This reflects previous work which shows that microglial cells are able to respond to the deposition of Aβ and surround plaques, but lack the ability to clear them away (DiCarlo et al., 2001). Microglial activation in TG2576 mice is reported to be associated with increased cytokine mRNA and protein compared to wild type (Abbas et al., 2002; Apelt and Schliebs, 2001; Mehlhorn et al., 2000; Sly et al., 2001), but other studies did not find differences in the protein levels of cytokines (Farr et al., 2014). In this study there were no differences in any of the seven measured cytokines (IFNγ, TNFα, IL-1β, IL-6, KC, IL-10, and IL-12) between 18 month old TG2576 mice and wild type littermates., despite clear evidence for morphological and phenotype changes to microglia This disparity with previously published work can be explained the differences in the techniques used to detect cytokine levels. Previous studies measured the cytokine mRNA levels, whereas we measured the protein levels of cytokine using a multiplex ELISA, and mRNA levels of cytokines may not be reflective of the actual protein levels. Other explanations include the microbial load of mice or stress levels of the mice, which induce low grade systemic inflammation, which may result in neuroinflammation, and in particular under conditions with altered CNS microenvironment that can 'prime' microglia.

FcγRs are thought to be important for the clearance of Aβ by therapeutic antibodies, but at the same time could be involved in the underlying mechanisms of the inflammatory side effects associated with immunotherapy (Fuller et al., 2014). The cellular response to IgG immune complexes, and therefore the ability of effector cells to clear plaques and induce inflammation, is defined by the pattern of FcγR expression and the subclass of antibody used (Nimmerjahn and Ravetch, 2008). Here we showed that the activating receptors: FcγRI and FcγRIII are significantly up-regulated by microglia when compared to wild type littermates, and in particular on cells

directly in contact with Aβ. Due to the increased expression of FcγRI and FcγRIII by microglial cells, and the relatively low levels of FcγRIIb and FcγRIV it is likely that the effector function of anti-Aβ antibodies will be mediated by one or both of these receptors. In the previous chapter the generation and characterisation of anti-Aβ antibodies with murine IgG1 and IgG2a constant domains was described. IgG2a is able to ligate both FcγRI and FcγRIV, while murine IgG1 has higher relative affinity for the inhibitory FcγRIIb. Thus the altered FcR expression patterns in TG2576 may have consequences for immunotherapy and choice of subclass used. Increased microglial FcγRI expression has been shown in numerous human diseases and mouse models of disease(Fuller et al., 2014). The broad expression of FcγRI on microglia, the high affinity of FcγRI for IgG and the low levels of IgG in the brain suggest that FcγRI could play an important role in the effector function of anti-Aβ antibodies. FcγRs were also detected on perivascular macrophages, confirmed by double staining with a directly FITC labelled FcγRII/III antibody and CD206-a specific marker for perivascular macrophages. Cells of similar morphology also express: FcγRI, FcγRIIb and FcγRIII, indicating that perivascular cells could also be involved in the response to therapeutic anti-Aβ antibodies. This could have particular importance for the vascular side effects associated with immunotherapy, as they are thought to be caused by CNS inflammation around blood vessels (Wilcock et al., 2011a). The expression of FcγRs by different cell types within the CNS will make it difficult to tease apart the cell type/types involved in the neuro-inflammatory response to anti-Aβ immunotherapy.

The FcγR expression pattern in human AD patients is comparable to TG2576 mice, and is similar to previously published work (Peress et al., 1993), although the addition of specific antibodies against FcγRIIa and FcγRIIb are novel. There is widespread expression of FcγRI by microglia surrounding deposits of Aβ, and also on microglial cells with a ramified morphology throughout the parenchyma. The expression of FcγRIII in mouse and FcγRIIIa in humans is also similar, with expression on cells surrounding plaques and on ramified microglia. The inhibitory receptor FcγRIIb is not widely expressed by microglia in either TG2576 mice or human AD. Neurons in the AD brain express FcγRIIb as previously reported (Kam et al., 2013) the expression of FcγRIIb by neurons was not observed in TG2576 mice. Mice do not possess FcγRIIa and humans do not possess FcγRIV, but the expression of both of these receptors is low in the brain. As the expression of FcγRs in the brain is comparable to human AD, the response of brain effector cells to therapeutic antibodies is likely to be translatable.

The regions of the brain that were quantified for the expression of immune receptors were chosen based on incidence of pathology. The hippocampus is an interesting brain region for AD researchers because of role in early stages of the disease and is essential for memory formation. In TG2576 mice there is substantial plaque pathology in the hippocampus. Significant increased expression of MHCII was detected and strong trends for increased expression of FcγRI, CD11B and FcγRII/III. The lack of significant increase in FcγRI is likely due to the higher baseline expression in WT mice compared with other regions. The hippocampus is a useful area to use when carrying out passive immunisation studies as it is easily accessible by stereotaxic injection. Because it has high Aβ load and expression of FcγRs, it is a suitable area to directly administer anti-Aβ antibodies to characterise the clearance of plaques and inflammatory response.

The piriform cortex is a region that processes inputs from the olfactory bulbs and has efferent connections to the entorhinal cortex. It is a crucial region for the processing of odours, which is a very important sense for rodents. In this region there are a large number of plaques, and associated with these plaques is an up-regulation of many immune markers. In this study I found that five of the markers studied were significantly higher. The high levels of pathology and FcγR expression make this a suitable area for immunisation studies. Due to its location it is not practical to inject directly, and therefore its use will be limited to systemic treatment studies. Due to the high levels of pathology in this region, it would be interesting to use a behaviour based on association of a specific odour with a negative or positive stimulus as this may be significantly altered in these mice.

In conclusion, by 18 months old, TG2576 mice have extensive plaque deposition in a number of brain areas, which is accompanied by the increased expression FcγRs on cells in direct contact with plaques, but also wider expression in the brain parenchyma, especially FcγRI. Administration of antibodies to this altered microenvironment may result in higher inflammatory potential when compared to a control healthy brain, but maybe dependent on the IgG subclass used for immunotherapy. I will test this hypothesis in the next chapter.

Chapter 5: The role of antibody effector function in the neuro-inflammatory response to intracranial 3D6 injection

5.1 Introduction

Passive immunisation with anti-Aβ antibodies has proven successful at removing plaques from the brains of APP transgenic mice and AD patients (Rinne et al., 2010; Wilcock et al., 2004b). One mechanism proposed for antibody mediated clearance of Aβ is by activation of microglia through FcγRs, inducing the phagocytic clearance of plaques (Morgan et al., 2005). Previous studies have shown that intracranial injection of anti Aβ antibody 2H6 (murine IgG2b) is able to clear plaques within 72 hours with a concomitant activation of microglia, as measured by increased expression of CD45, FcRII/III and MHCII (Wilcock et al., 2003). The same antibody was also able to clear plaques and activate microglia when given systemically, however this occurs with increased deposition of Aβ around the cerebral vasculature and increased incidence of micro-haemorrhage (Wilcock et al., 2004c). This vascular damage was prevented by de-glycosylation of 2H6, which reduces FcγR and binding, indicating that the vascular side effects could be FcγR mediated (Carty et al., 2006; Wilcock et al., 2006).

A number of monoclonal antibodies have reached clinical trials for the treatment of AD, however none have significantly improved cognition in patients with AD. One key issue with immunotherapy is that like mice, the patients treated with anti-Aβ antibodies experience damage to their cerebral vasculature (Salloway et al., 2010). These side effects have strictly limited the effective dose that can be given to patients, which in turn could explain the lack of efficacy in clinical trials. There is also indirect evidence that the vascular side effects observed in patients may be mediated through FcγR engagement. Bapineuzumab and Gantenerumab are both human IgG1 antibodies, which have high affinity for activating FcγRs. Both of these antibodies have been associated with micro-haemorrhage and edema of cerebral blood vessels in patients (Bohrmann et al., 2012; Rinne et al., 2010). Crenezumab is a human IgG4 antibody which has reduced FcγR affinity compared to IgG1. No vascular damage has been observed in Crenezumab treated patients, even at a dose 10 times higher than Bapineuzumab (Adolfsson et al., 2012). There have not been any studies directly comparing these antibodies *in vivo* to understand the differences between these antibodies.

The aim of this study was to understand the role of antibody effector function in the clearance of plaques and the associated inflammatory response, with the aim to provide rationale for antibody engineering to optimize clinical candidate antibodies. The antibody 3D6 (murine version of Bapineuzumab) was produced as both mouse IgG1 and mouse IgG2a subclasses-due to their

contrasting FcγR affinities (Bruhns, 2012). 3D6 IgG1 and IgG2a or irrelevant isotype controls were injected intra-cranially into 14 month APP transgenic (TG2576) mice. The ability of each antibody to clear plaques and the subsequent neuro-inflammatory response was measured by immunohistochemistry and multiplex immune assays.

5.2 Methods

5.2.1 Study design

5.2.1.1 Intracranial injections into 14 month old mice

Fourteen month old female TG2576 mice were split randomly into four groups (n=10, all females): 3D6 IgG1, 3D6 IgG2a, Irrelevant IgG1 and irrelevant IgG2a. Mice were anaesthetised using sevofluorane, the skull exposed and a small hole drilled in the skull and injected with 2µl of appropriate antibody into the right hippocampus at stereotaxic coordinates: -2.0, +1.7, and -1.6 from bregma. At seven days post injection, mice were transcardially perfused with heparinised saline and the brains were dissected. Six of the brains from each group were embedded for immunohistochemistry, and four prepared so a punch of tissue could be collected from the antibody injected area. Hippocampal punches were homogenised, and the levels of cytokines measured using a multiplex immune assay (MSD), and normalised to total protein concentration. The experiment was repeated usingTG2576 mice (n= 6 per group all females) collecting brain tissue as described above at three days post injection, and cytokine levels were measured in the same manner.

5.2.1.2 Intracranial injections into 18 month old mice

The procedure was repeated in 18 month old TG2576 mice using a modified protocol. Instead of a unilateral injection into the right hippocampus, TG2576 (n=5, 4 males, 1 female) and wild type littermates were injected bilaterally at coordinates: -2.0, +/- 1.7, -1.4. Reducing the depth of the injection prevents the capillary from reaching the hippocampal fissure, and therefore reduces the likelihood of damaging this blood vessel. Seven days after injection, mice were transcardially perfused and the brains were removed. The right hemibrain was embedded for immunohistochemistry, while the left hemibrain was prepared and a hippocampal punch taken. The hippocampal punch was homogenised, and two fractions of proteins were obtained: triton soluble and formic acid soluble. Multiplex immune assays were used to determine the concentration of Aβ in both brain fractions, and the levels of pro-inflammatory cytokines in the triton soluble fraction.

5.2.2 Quantification

The quantification of immunohistochemistry was performed using the free to access software imageJ. For the hippocampus, three x20 objective images were taken per mouse per cell marker, and the average percentage area above threshold for the three images was determined using imageJ. To quantify staining around the pial membrane, four images were taken spanning the length of the membrane. The images were blinded, and the area above threshold was determined 150 pixels either side of the membrane. To quantify the number of congo red positive plaques, the slides were blinded and the number of plaques were counted in the injected side of the brain, normalising to the un-injected side.

5.2.3 Statistical analysis

To test whether the data sets were normally distributed, the residuals were calculated before using the D'Agnostino-Pearson omnibus test. Non-parametric data sets were transformed using the function Y=logY, before re-calculation of residuals and normality testing. All data sets, or the transformed data, were normally distributed. Data from these experiments were analysed using two-way ANOVA, with the independent variables: antibody specificity (3D6 vs. irrelevant control antibody) and antibody effector function (IgG1 vs. IgG2a). If the two way ANOVA found significant differences due to each variable, or an interaction between the two variables, the data was analysed using the Tukey post hoc test, which is corrected for multiple comparisons.

5.3 Results

5.3.1 Intracranial injection of 3D6 into 14 month old TG2576 mice

Fourteen month TG2576 mice were injected into the hippocampus (-2.0mm, +1.7mm,-1.6mm) with: 3D6 IgG1, IgG2a or irrelevant isotype controls (n=10). Seven days later mice were perfused and brain tissue collected. Changes in the phenotype of microglia and clearance of plaques was measured by immunohistochemistry (n=6), whilst pro-inflammatory cytokine levels were measured by Mesoscale Discovery 7-plex assay (n=4).

5.3.1.1 Identification of the injection site

Large proteins, and in particular IgG, do not diffuse well through the brain parenchyma (Wolak et al., 2015). To allow measurement of the neuro-inflammatory response to injected antibodies, and the clearance of plaques by immunohistochemistry it is therefore important to use brain sections proximal to the injection site. Although all mice were injected at the same stereotaxic coordinates, there is always some variation in the exact site of injection. To determine the exact site of injection, sections 150 µm apart (every 16th section) of 10 µm were collected onto a separate slide, and stained for expression of CD11b. Figure 5.1 shows a series of sections through the hippocampus of one animal, stained for the microglial marker CD11b. The injection site is clearly visible in sections 4 and 5 and faintly in section 6, with increased microglial CD11b expression due to mechanical trauma of injection. Based on this information any slide collected between sections 4 and 6 are close to the injection site, would be suitable to use for immunohistochemistry. This process was successfully repeated for all animals.

Injecting into the hippocampus always carries a risk of hitting the large vessels located in the hippocampal fissure. When these vessels are damaged, severe neuron loss can be observed in the detate gyrus and CA3 areas of the hippocampus, however this is usually a very rare occurrence. Unfortunately TG2576 animals appear to be exquisitely sensitive to vascular damage, and 10 out of 24 animals exhibited neuron loss and inflammation following intracranial injection. Figure 5.1A shows an example of such an animal stained with CD11b. Complete loss of one blade of the dentate

gyrus can be observed, with high levels of CD11b expression in the area of neuronal death. Due to the high levels of immune activation in these mice, it was not possible to measure the microglial response to antibody effector function. All mice exhibiting this neuronal damage were excluded from measurement of immune markers and IgG by immunohistochemistry, reducing the n number to 3-4 per group.

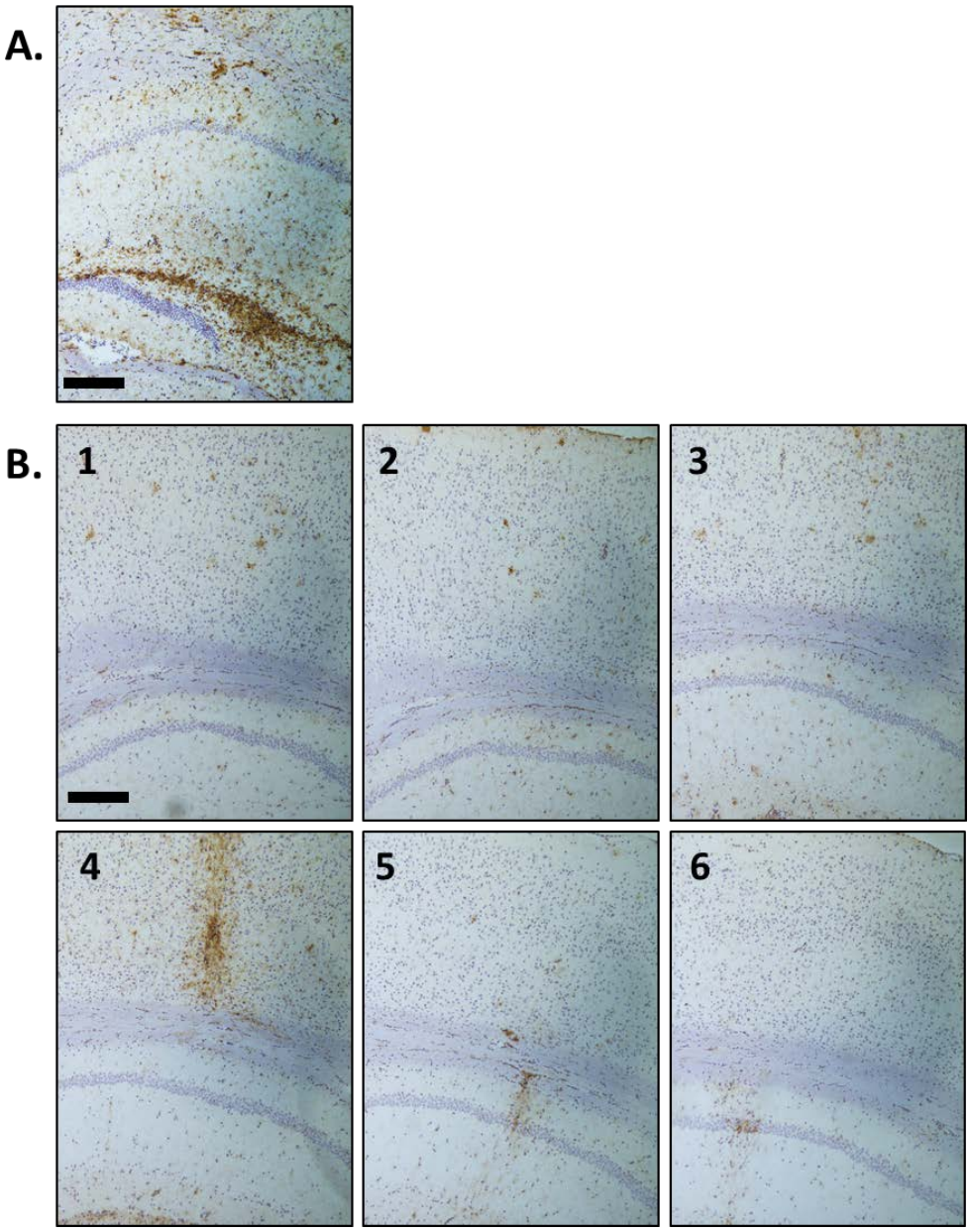

Figure 5. 1 Location of injection site and damage caused by intracranial injection

A. Injection into the hippocampus can induce severe neuroinflammation and neurodegeneration due to damage of blood vessels in the hippocampal fissure. This figure shows CD11b expression levels of one representative animal. Total loss of one blade of the dentate gyrus and intense CD11b staining can be observed. 10 out of 24 animals exhibited this damage, and were excluded from the study. **B.** To locate the site of injection in each mouse every 16th section cut on the cryostat was collected separately and stained for CD11b. This figure shows coronal sections through the brain of a mouse, the injection site is detectable in sections 4, 5 and 6. The images were taken with a 10x objective (scale bars =200µM).

5.3.1.2 Antibody binding and clearance of plaques

To detect the target engagement and the clearance of plaques by 3D6 or irrelevant antibodies, brain sections were stained for the presence of mouse IgG. Semi-quantitative measurement of IgG staining shows that there are significantly higher levels of IgG in the brains of mice injected with both 3D6 subclasses compared to irrelevant controls (Fig. 5.2, $p<0.001$). This indicates that 3D6 is retained in the brain, whereas the irrelevant antibodies are cleared away. Although the levels of IgG are higher in both subclasses of 3D6, the actual staining pattern is very different. Tissue obtained from mice injected with 3D6 IgG1, shows clear IgG binding to structures resembling Aβ plaques found in the cortex and hippocampus, as well as diffuse staining of IgG. Mice injected with 3D6 IgG2a show strong diffuse staining, but no Aβ plaques positive for IgG. These data suggest that both IgG subclasses are able to engage Aβ *in vivo* while irrelevant control antibodies do not. The difference in plaque-associated IgG may be due to effector function, with 3D6 IgG2a able to clear plaques bound, whereas the reduced effector function of 3D6 IgG1 is unable to clear the plaques. To test the clearance of plaques a number of techniques were applied. The method that gave best results in fresh frozen tissue was the use of histological dye-congo red, which stains congophilic plaques, but not diffuse plaques. Fig 5.3A shows quantification of congophilic plaque number, normalised to the number of plaques in the unaffected, contralateral side of the brain. There was a non-statistically significant decrease in congophilic plaque number in mice treated with 3D6 IgG2a compared to other treatments.

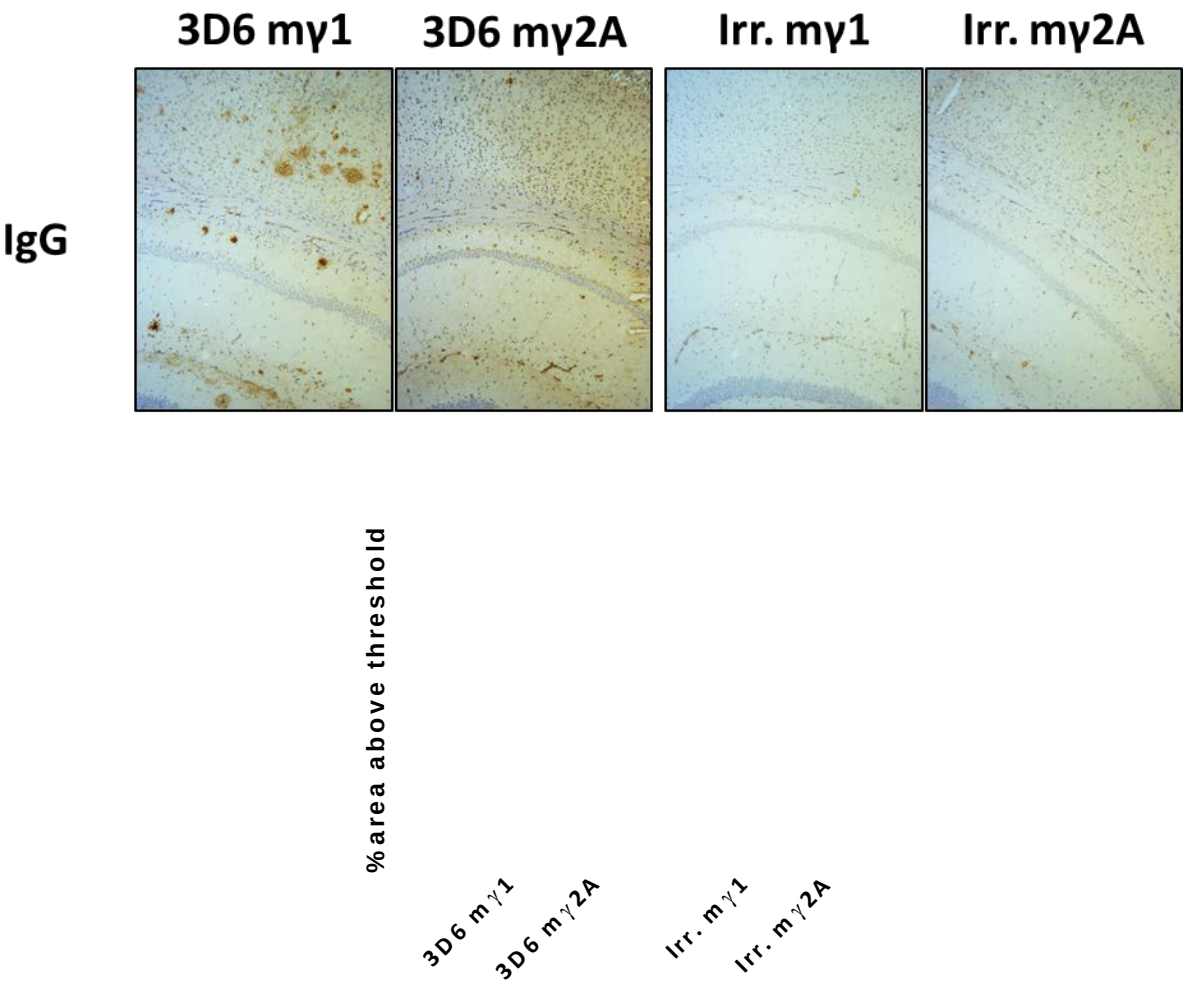

Figure 5. 2 Mouse IgG stain shows retention of anti-Aβ antibodies at 7days, but not irrelevant controls

Brain sections from TG2576 mice injected with antibodies were stained for IgG. Low levels of staining were detected in the tissue obtained from mice receiving isotype control antibodies, indicating clearance of the irrelevant antibodies by seven days. Animals injected with 3D6 IgG1 or IgG2a, had higher diffuse staining than irrelevant controls, and animals injected with 3D6 IgG1 had plaque like structures in the hippocampus and cortex positive for IgG but those injected with 3D6 IgG2a did not. Quantification of IgG levels in brain sections revealed significantly more IgG compared to irrelevant controls ($p<0.001$), however there was no significant effect of subclass on the total IgG levels. Data was analysed by two-way ANOVA and Tukey post hoc test, data represented as mean plus S.D (n=3/4).

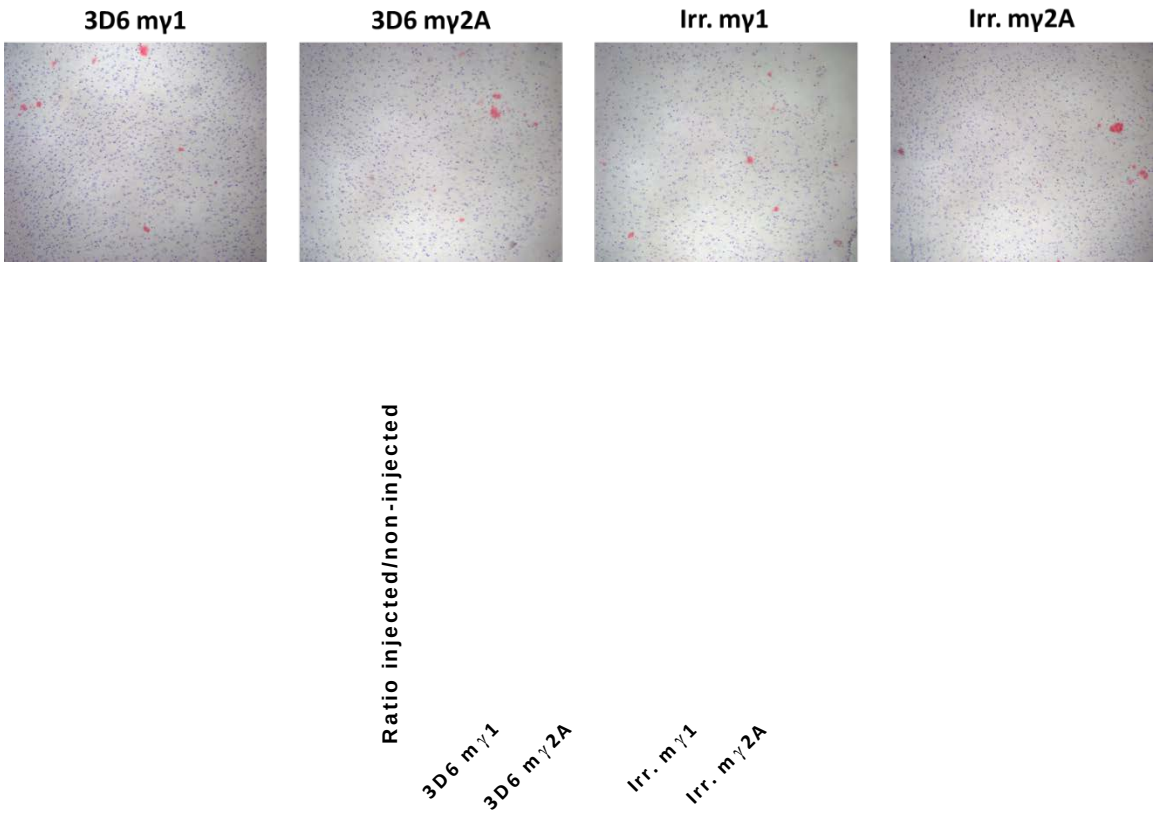

Figure 5. 3 Intracranial injection with 3D6 IgG2a causes a non-significant reduction in the numbers of congo red positive plaques

Seven days after intracranial administration of antibodies, the number of congophilic plaques were counted in the injected hemisphere and this was normalised to the number in the un-injected side. Injection of 3D6 IgG2a causes a non-statistically significant reduction in the number of congophilic plaques. Data analysed by Kruskal-wallis and Dunn's post hoc test., data represented as mean and S.D (n=3/4, 4 sections used per mouse).

5.3.1.3 The neuro-inflammatory response to injection of 3D6

The neuro-inflammatory response to the antibodies was measured seven days after intracerebral injection by assessing phenotype changes to microglia using immunohistochemistry. Fig 5.4 shows representative examples for the staining patterns for the surface markers: CD68, FcγRI and FcγRIV and fig 5.5 shows the quantification in two brain regions-the hippocampus and the area surrounding the pial membrane. In the hippocampus, the expression levels of: FcγRI, CD68 or FcγRIV were not significantly different in any group. In the hippocampus the expression of these markers was similar to that shown in chapter 4, with microglia in the parenchyma and surrounding plaques both positive for these markers. The expression of FcγRIV was more variable, but staining could be seen around the area of injection and on a small number of Aβ deposits.

After injection with antibodies into the hippocampus, there were a number of changes to microglia in a particular regions of the brain, associated with the pial membrane. Injection of 3D6 IgG2a resulted in a significant increase in the expression levels of the marker CD68 compared to 3D6 IgG1 ($p=0.002$). Injection of 3D6 IgG2a or irrelevant IgG2a resulted an increase in the levels of FcγRI staining surrounding the pial membrane while either IgG1 subclasses did not ($p=0.01$), post hoc analysis showed that there was significantly higher expression of FcγRI in 3D6 IgG2a compared to 3D6 IgG1 ($p=0.002$). Injection of 3D6 IgG2a also induced a significant increase in the expression of FcγRIV compared to either 3D6 IgG1 ($p=0.005$) or irrelevant IgG2a ($p=0.032$) antibodies. To study if injection of anti-Aβ antibodies induces a functional change of immune cells in the CNS, I next measured the levels of pro-inflammatory cytokines in the brain, seven days after intracranial injection of antibodies (Figure 5.6, n=4). Injection with 3D6 IgG2a led a 3-fold increase in the levels of the pro-inflammatory cytokine IL-1β compared to 3D6 IgG1 ($p=0.011$) and irrelevant IgG2a ($p=0.009$). There was also a significant increase in the levels of KC in the brains of mice injected with 3D6 compared to irrelevant antibodies ($p=0.013$), but there was no effect of the subclass of 3D6. There was also a trend towards increased IL-6 in the brains of mice injected with 3D6 IgG2a, however the response was highly variable. Previous studies of the microglial response to anti-Aβ immunotherapy did not include cytokine levels, and were restricted to microglial phenotype changes which occurred at three days post injection (Wilcock et al., 2003). To investigate if our anti-Aβ antibodies induce a differential cytokine response at this earlier time point, the experiment was repeated using a three day time point. Unlike the seven day time point, at three days post injection there were no changes in the levels of any cytokine measured (fig. 5.7).

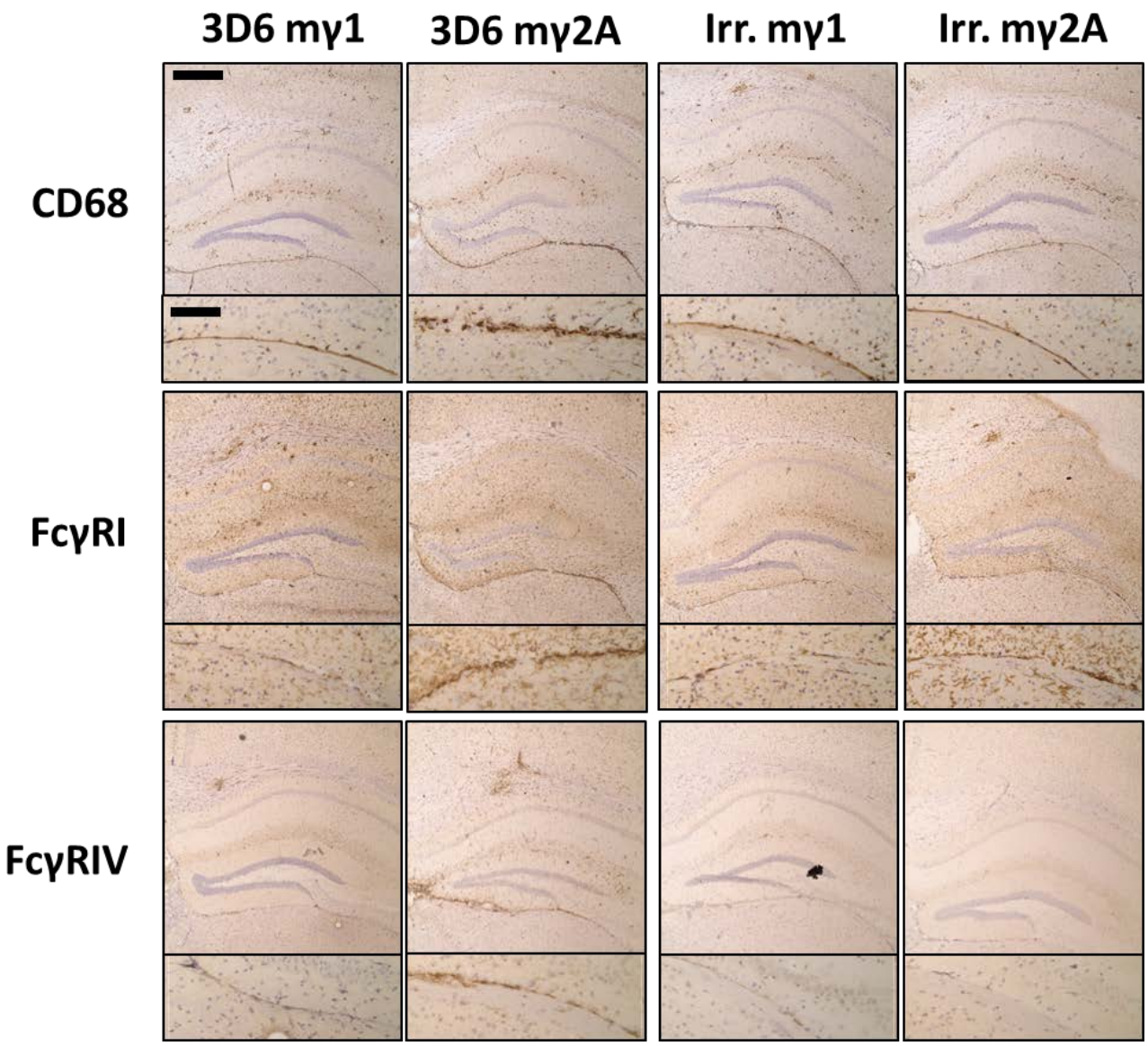

Figure 5. 4 Microglial phenotype changes measured at seven days after intracranial injection with 3D6 or irrelevant control antibodies

Seven days after injection with 3D6 IgG1 IgG2a and irrelevant controls, 10μm fresh frozen brain sections were stained for the expression levels of the microglial activation markers, CD68, FcγRI and FcγRIV. Representative images of n=3/4 (1 section per mouse) are shown Images of the hippocampus and pial membrane were taken with a 5x objective and smaller images were taken with a 20x, scale bars are 100μm, 400μm respectively.

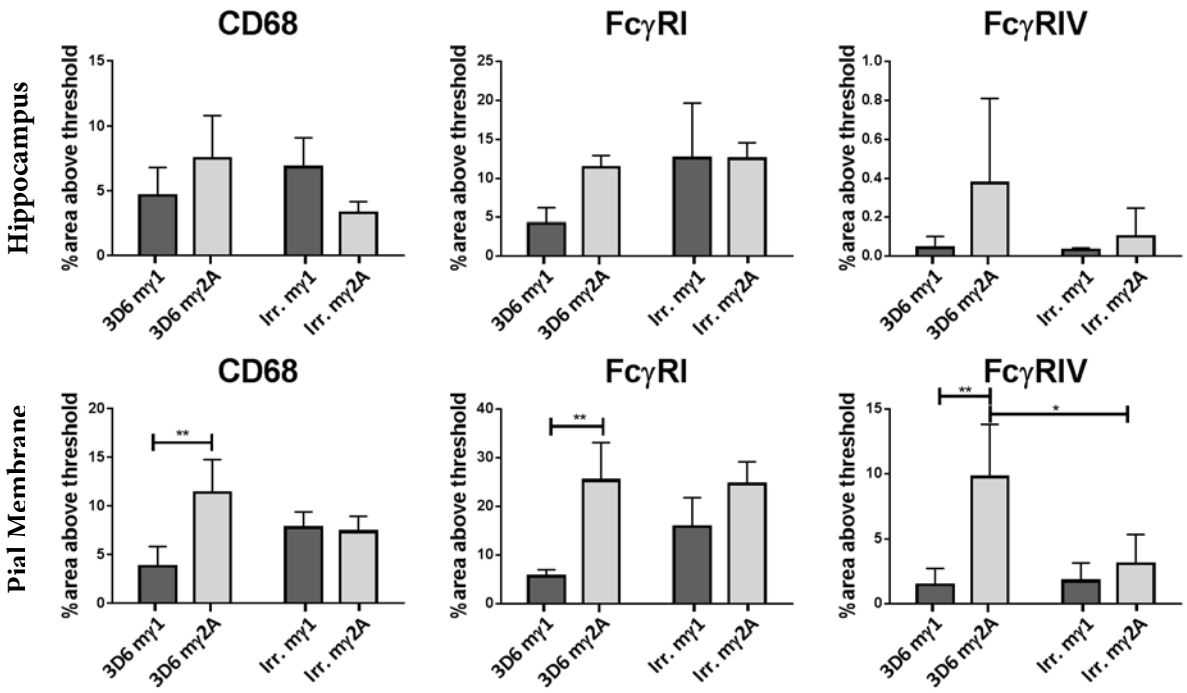

Figure 5. 5 Quantification of immune receptor expression

The expression of: CD68, FcγRI and FcγRIV were quantified in the hippocampus and the pial membrane after intracerebral injection of antibodies. The expression levels were quantified as percentage area above threshold. After injection of 3D6 IgG2a, CD68 is significantly up-regulated around the pial membrane compared to injection of 3D6 IgG1 (p=0.002). FcγRI is significantly up-regulated surrounding the pial membrane after injection of an IgG2a antibody irrespective of antibody specificity (p=0.01), 3D6 IgG2a injection causes significant up-regulation of FcγRI compared to 3D6 IgG1 (p=0.002). FcγRIV is significantly up-regulated after injection with 3D6 IgG2a compared to 3D6 IgG1 (p=0.005) and Irr. IgG2a (p=0.032). Data was analysed by two way ANOVA and Tukey post hoc test. Data presented as mean and S.D. (n=3/4)

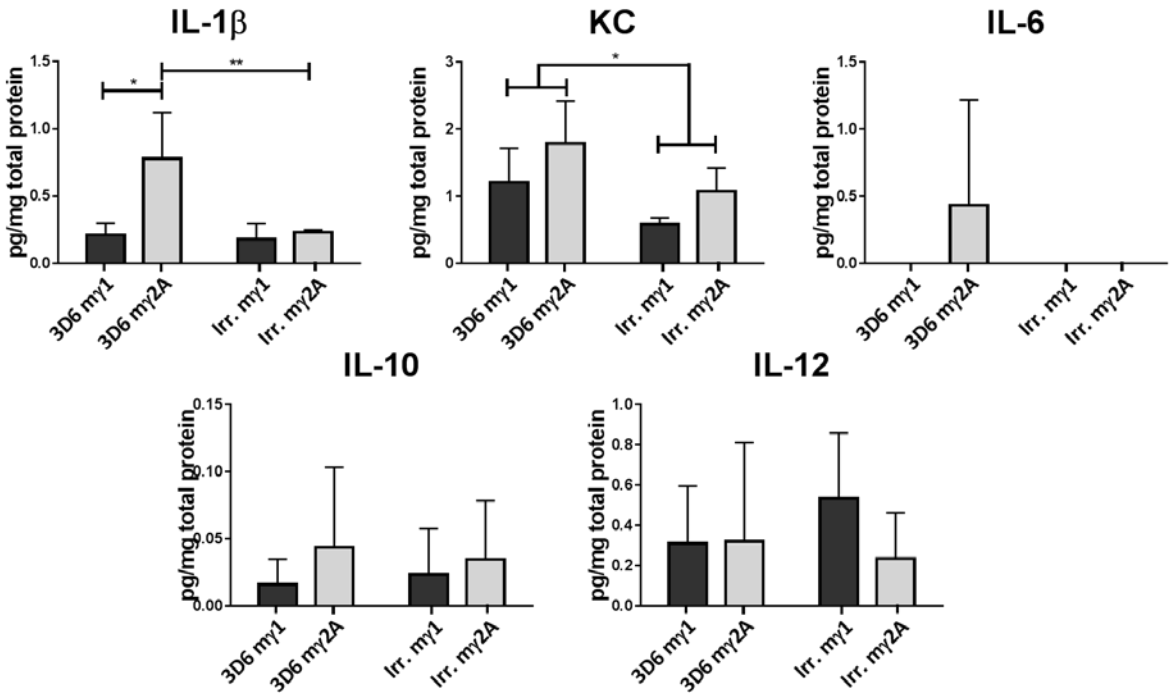

Figure 5. 6 Brain cytokine levels after intracranial injection of 3D6 IgG1 and IgG2a

The levels of cytokines were measured in the brain homogenate (enriched for the site of injection) of 14 month old TG2576 mice, seven days after intracranial injection of antibody. Cytokine levels were measured using a multiplex immune assay, and normalised to total protein concentration, expressed as pg/mg. Intracranial injection of 3D6 IgG2a caused a 3-fold increase in the levels of IL-1β compared to injections of 3D6 IgG1 ($p=0.011$) and irrelevant IgG2a ($p=0.009$). Injection of 3D6 led to increased levels of KC ($p=0.013$), however there was no significant difference between 3D6 subclasses. Data sets were analysed by 2-way ANOVA and Bonferroni post hoc test, and presented as mean and standard deviation (n=4).

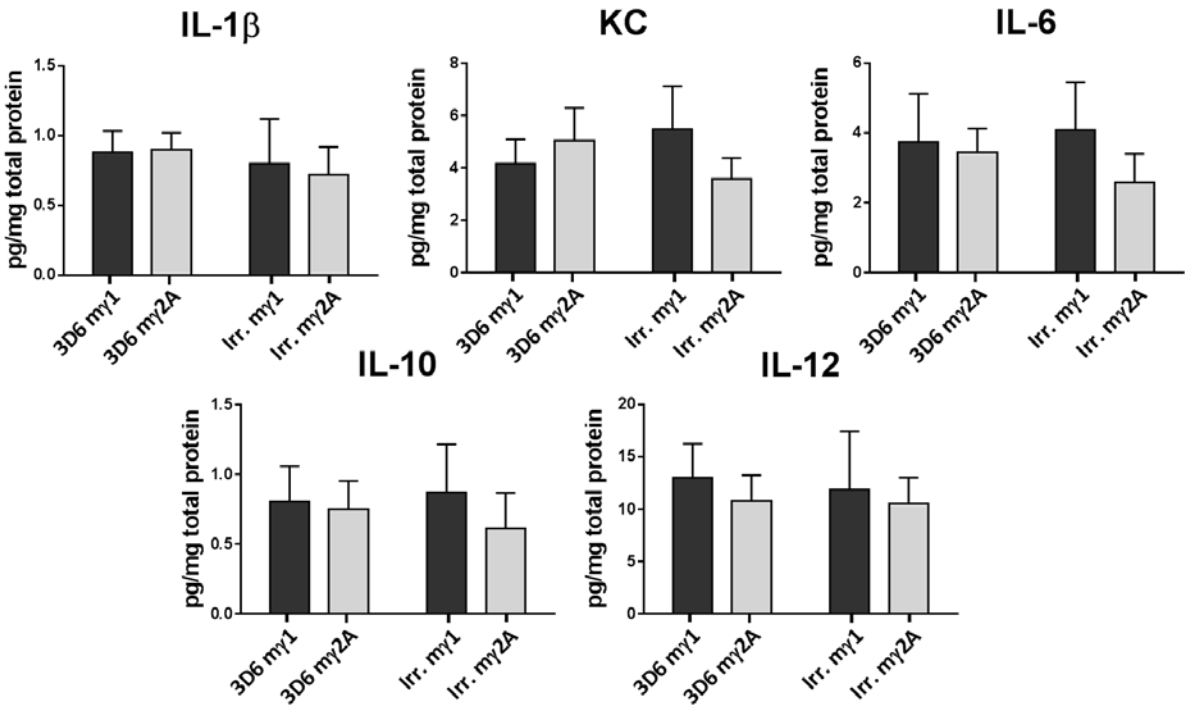

Figure 5. 7 Brain cytokine levels 3 days post injection of 3D6 IgG1 and IgG2a

The levels of cytokines were measured in the brain homogenate (enriched for the site of injection) of 14 month old TG2576 mice, seven days after intracranial injection of antibody. Cytokine levels were measured using a multiplex immune assay, and normalised to total protein concentration, expressed as pg/mg. There were no changes in cytokines three days after injection of antibody. Data sets were analysed by 2-way ANOVA and Tukey post hoc test, and presented as mean and standard deviation (n=6).

5.3.2 Injection of 3D6 into 18 month old TG2576 mice.

A number of limitations were identified following injection of 3D6 into the hippocampus of 14 month old TG2576 mice. The injection itself caused significant vascular damage in a number of mice, causing a loss of power due to the exclusion of 2-3 mice per group. At 14 months the pathology in TG2576 mice is variable, and immunohistochemical analysis did not allow to accurate measurement of Aβ clearance from the brain. To address these limitations, the experiment was repeated in 18 month old mice. The coordinates of injection were altered to reduce the risk of damaging blood vessels in the hippocampal fissure (-2.0, +/- 1.7,-1.4). Each mouse received a bi-lateral injection of 2μg antibody to allow one hemibrain for immunohistochemistry and the other to measure Aβ clearance from the brain, using a multiplex immune assay to quantify the protein levels of Aβ in brain homogenate. As TG2576 mice are prone to both seizures and have a very high risk of developing tumours as they age (unpublished observation), the number of mice available in our ageing colony declined leaving sufficient mice to inject five mice per treatment group.

5.3.3 Amyloid beta peptide levels

A multiplex immune assay was used to measure the concentration of three different peptides: Aβ38, Aβ40 and Aβ42. Aβ exists as a wide range of different sized species, ranging from: monomers to fibrils. To enable the measurement of these different species of Aβ, two different fractions were obtained from brain homogenate: triton soluble-containing mostly soluble Aβ species and formic acid soluble, containing mostly aggregated species of Aβ. Seven days after intra-cranial-injection of 3D6 showed a trend towards reduced Aβ42 in the soluble (triton soluble fraction), but no significant changes in the levels of triton soluble or formic acid soluble Aβ were found (Fig. 5.8). However, there were non-statistically significant reductions of every Aβ peptide in animals injected with 3D6 IgG2a in comparison with 3D6 IgG1, but there was high variability. The mean levels of triton soluble Aβ after 3D6 IgG1 injection were: Aβ38= 226pg/mg (S.D=152) Aβ40=1147pg/mg (S.D=1360) Aβ42=38.6pg/mg (S.D=31.3), compared to the mean levels of triton soluble Aβ after 3D6 IgG2a injection Aβ38= 142.7pg/mg (S.D=77.1) Aβ40=490pg/mg (S.D=232) Aβ42=22.3pg/mg (S.D= 8.2). Similar trends were seen with formic acid soluble Aβ, 3D6 IgG1: Aβ38=22236pg/mg (S.D=11806) Aβ40=42158pg/mg (S.D=28643) Aβ42=3765pg/mg (S.D=3398), compared to the mean levels of formic acid soluble Aβ after 3D6 IgG2a injection Aβ38= 13636pg/mg (S.D=11209) Aβ40=24147pg/mg (S.D=22926) Aβ42=2033pg/mg (S.D=1826).

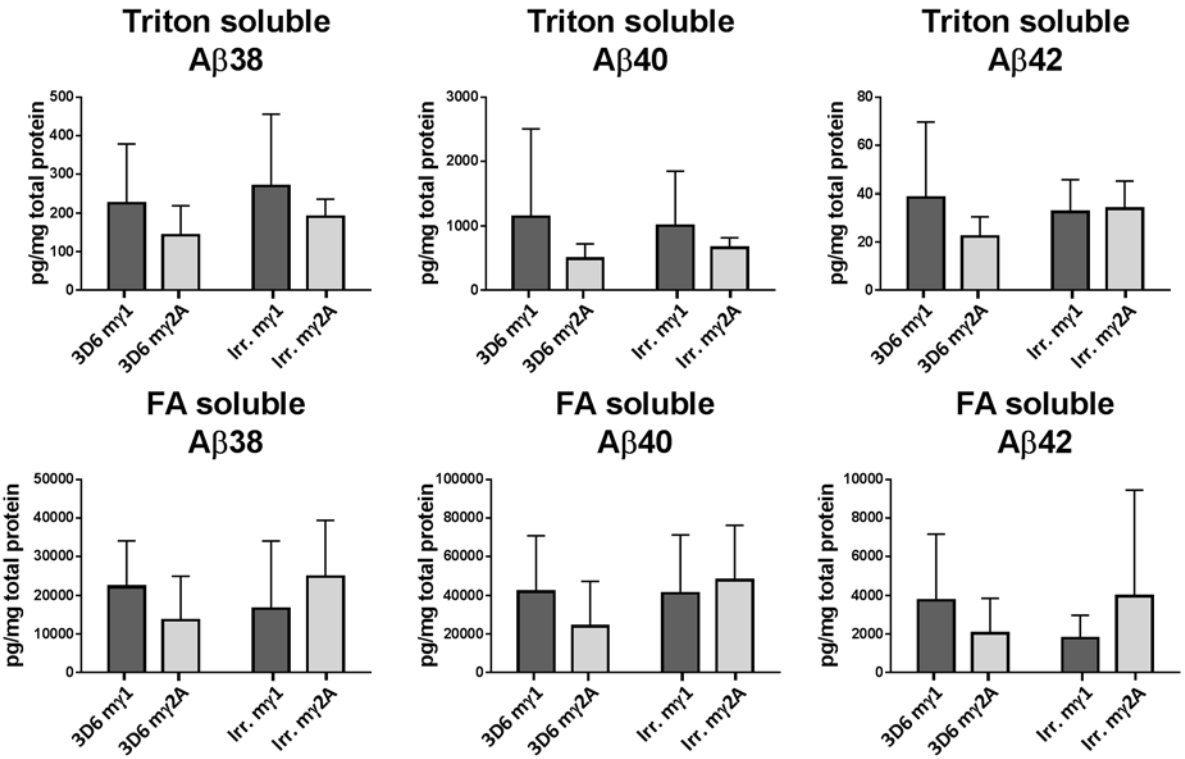

Figure 5. 8 Aβ peptide levels after intracranial injection

The levels of three Aβ peptides were measured in brain homogenates, seven days after injection with 3D6 and irrelevant controls into the hippocampus of 18 month old transgenic mice. The levels were measured in two fractions of protein: triton soluble and formic acid soluble. There were no significant changes in the concentration of Aβ in brains of any group. However there were lower levels of Aβ in mice injected with 3D6 IgG2a in both formic acid and triton soluble fractions compared to 3D6IgG1. Cytokine levels were measured using a multiplex immune assay (MSD), and data presented as pg/mg total protein (n=5, mean +/- S.D.)

5.3.3.1 Cytokine levels

The levels of cytokines in brain homogenate were measured by multiplex assay. Injection of 18 month old TG2576 mice with 3D6 IgG2a leads to a significant increase in the levels of IL-1β compared to 3D6 IgG1 ($p=0.006$) and Irrelevant IgG2a ($p=0.022$), and a non-statistically significant, increase in TNFα concentration in the brains of mice injected with 3D6 m2γA ($p=0.06$). Unlike the 14 month old mice, there was no change in the expression levels of KC following injection of 3D6.To test whether the increased IL-1β levels after intracranial injection of 3D6 IgG2a is due to specific binding of the antibodies to Aβ in the brain, wild type mice lacking human APP were used as a control. Injection of 3D6 IgG2a did not increase the levels of IL-1β in the brains of mice lacking human Aβ (fig.5.10). Therefore the changes in IL-1β in TG2576 mice are due to target engagement of 3D6 IgG2a to Aβ.

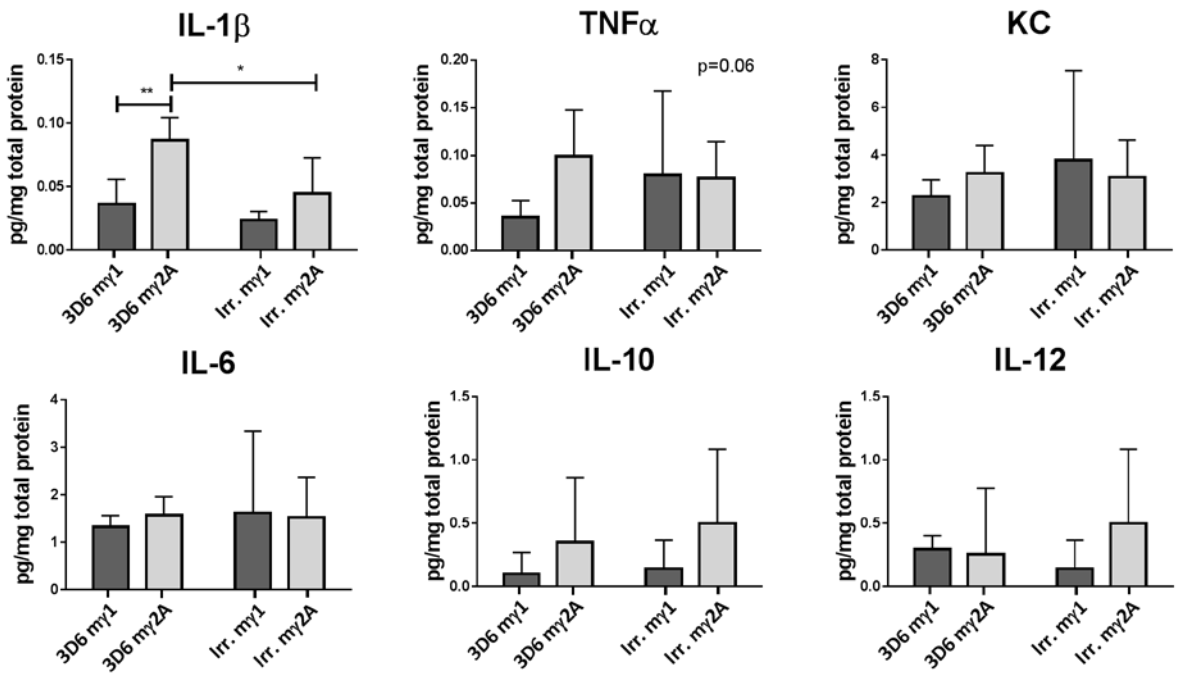

Figure 5. 9 Cytokine levels 7 days after intracranial injection of 3D6 into 18 month old TG2576 mice

The levels of cytokines were measured in the brains of 18 month old TG2576 mice, seven days after intracranial injection of antibody into the hippocampus. Cytokine levels were measured using a multiplex immune assay(MSD), and normalised to total protein concentration, expressed as pg/mg. Intracranial injection of 3D6 IgG2a caused a 3-fold increase in the levels of IL-1β compared to injections of 3D6 IgG1 (p=0.006) and irrelevant IgG2a (p=0.022). There was a non-significant increase in TNFα in 3D6 IgG2a injected animals (p=0.06). Data sets were analysed by 2-way ANOVA and Tukey post hoc test, and presented as mean and standard deviation (n=5).

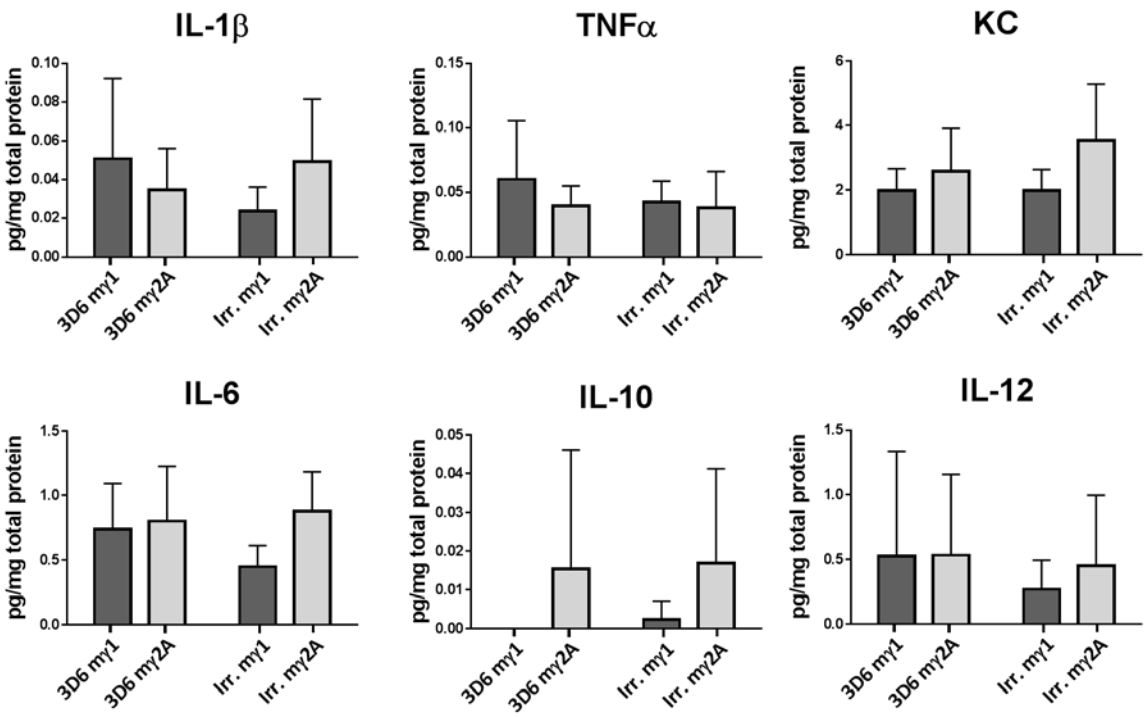

Figure 5. 10 Intracranial injection of 3D6 and irrelevant control antibodies into 18 month old wild type mice

The levels of cytokines were measured in the brains of 18 month old wild type mice, seven days after intracranial injection of 3D6 IgG1 and IgG2a or irrelevant IgG1 or IgG2a. The levels of cytokines were measured in the brains of 18 month old TG2576 mice, seven days after intracranial injection of antibody into the hippocampus. Cytokine levels were measured using a multiplex immune assay, and normalised to total protein concentration, expressed as pg/mg. There were no significant differences between any groups measured. Data sets were analysed by 2-way ANOVA and Tukey post hoc test, and presented as mean and standard deviation (n=5).

5.4 Discussion

Passive immunisation with anti-Aβ antibodies is able to clear Aβ deposits from the brains of both mice and AD patients (DeMattos et al., 2001; Rinne et al., 2010; Wilcock et al., 2003), in transgenic mouse models of AD this reverses cognitive deficits associated with these models (Wilcock et al., 2004c). However, in both mice and humans the clearance of Aβ plaques is associated with damage to the cerebral vasculature; a side effect which has limited the top dose given in clinical trials (Bohrmann et al., 2012; Pfeifer et al., 2002; Salloway et al., 2010; Wilcock et al., 2004c). There is evidence from both mouse and human studies that the activation of FcγRs plays a key role in the underlying mechanisms that are responsible for the vascular damage, ARIA-E, seen after immunotherapy (Adolfsson et al., 2012; Freeman et al., 2012; Wilcock et al., 2006). It may be possible to improve immunotherapy for AD by engineering the Fc region of therapeutic antibodies, to improve the efficacy and/or reduce the risk of causing vascular damage. To study the role of antibody effector function in the clearance of plaques and the neuro-inflammatory response in more detail, we generated the antibody 3D6 with two different constant regions, IgG1 and IgG2a to allow direct comparison *in vivo*. Using our IgG1 and IgG2a 3D6, I provide experimental evidence that the effector function of anti-Aβ antibodies is important for both the clearance of plaques and the neuro-inflammatory response.

5.4.1 Role of antibody effector function in neuroinflammation

For the first time we have shown that IgG2a, a subclass able to ligate the high/medium affinity receptors FcγRI and FcγRIV, induces a significant increase in IL-1β protein levels, while an IgG1 antibody, unable to bind these FcγR, does not. The increased levels of IL-1β following 3D6 IgG2a were associated with reduced level of Aβ plaques and a strong microglial phenotype change, especially around the pial membrane in 14 month old TG2576 mice. The finding that 3D6 IgG2a induces increased IL-1β concentration relative to 3D6 IgG1 and control antibodies was reproducible in two independent experiments, performed in two different laboratories, University of Southampton and Lundbeck. The increase in IL-1β levels occurs at seven days after injection, not at three days, suggesting different kinetics to microglial phenotype changes shown in previous studies, however these studies did not measure cytokine production (Wilcock et al., 2003). IL-1β is expressed as pro-IL-1β, which is functionally inactive and requires activation of the inflammasome allowing proteolytic cleavage of pro-IL-1β by caspase 1 to produce mature IL-1β. The MSD assay

detects the levels of IL-1β, however it cannot distinguish pro IL-1β from mature IL-1β. To understand whether the IL-1β produced in response to 3D6 IgG2a is functionally active, it would be necessary to use western blotting to determine its size.

The difference in pro-inflammatory cytokine levels (IL-1β, KC) produced by injection of 3D6 IgG1 and 3D6 IgG2a can be explained by the different effector functions of the antibodies. Mouse IgG2a is more pro-inflammatory than mouse IgG1 due to its higher affinity for activating FcγRs, FcγRI and FcγRIV and its ability to fix complement. In contrast, mouse IgG1 has higher affinity for the inhibitory receptor FcγRIIb and does not fix complement (Bruhns, 2012; Nimmerjahn and Ravetch, 2008). This was illustrated in chapter 3, where I showed that *in vitro* that an IgG2a constant region stimulates production of 3-fold higher levels of TNFα than an IgG1 antibody. No other published studies have compared the cytokine response to different subclasses of anti-Aβ antibodies *in vivo*, so this is a novel finding.

It is thought that damage to the vasculature after passive immunisation is initiated by FcγR mediated neuro-inflammation. Ligation of FcγRs by immune complexes results in the cross-linking of cytoplasmic gamma chains and release of pro-inflammatory cytokines and reactive oxygen species (Mosser and Edwards, 2008). Here, injection of the anti-Aβ antibody 3D6 IgG2a results in the increased production of IL-1β, although the cellular source remains to be identified. Wilcock et al previously showed that passive immunisation with the anti-Aβ antibody 2H6 results in the activation of matrix metalloproteinases (MMPs). The authors hypothesised that the increased production of pro-inflammatory mediators causes the activation of MMPs, and remodelling of the cerebral vasculature leading to increased permeability and micro-haemorrhage incidence (Wilcock et al., 2011a).

Pro-inflammatory cytokines have divergent roles within the CNS and have been described to modulate neuronal activity. Therefore, increased IL-1β in response to anti-Aβ immunotherapy could have an impact on the function of neurons. Long term potentiation (LTP) is a measure of a synapse's ability to change and adapt to a strong signal, and is essential for learning and memory (Purves 2008). Low levels of IL-1β increase LTP, hippocampal neurons, whereas high concentrations can inhibit LTP (Bellinger et al., 1993; Katsuki et al., 1990; Ross et al., 2003). Therefore increased IL-1β production in response to treatment with 3D6 IgG2a could impair the function of neurons in the hippocampus- and influence cognitive assessment of patients during

clinical trials. The function of neurons after immunotherapy could be tested in mice by direct measurement of neuronal activity using electrophysiology, or indirectly using behavioural assays.

There were no significant changes in the expression of CD68, FcγRI and FcγRIV in the hippocampus of 14 month old TG2576 mice injected with 3D6 IgG2a, however this experiment was underpowered to detect an effect. As shown in the chapter 4, the hippocampus of TG2576 mice has high basal expression of FcγRs and other microglial activation markers, making it difficult detect subtle changes after injection of antibodies. The lepto-meninges is the membrane that envelops the outside of the brain and is formed of three layers: the arachnoid, the dura and pia. The pial membrane is the innermost meningeal layer, and forms the boundary with the brain parenchyma, separating it from large pial arteries and the Virchow-Robin space-through which CSF travels (Zlokovic, 2008). Microglial phenotype changes were mostly found in the area surrounding this pial membrane. The microglial marker CD68 (macrosialin) is a member of the scavenger receptor family, and is expressed on lysosomal membranes and at a lower level on the cell surface. Microglial cells express CD68, and upregulation is indicative of increased phagocytic activity. Mice injected with 3D6 IgG2a showed increased expression of CD68 surrounding the pial membrane compared to 3D6 IgG1. The increased expression of CD68 on cells surrounding the pial membrane could be explained by increased phagocytosis of Aβ/3D6 immune complexes. There were also increases in the expression of FcγRI and FcγRIV on cells surrounding the pial membrane. The expression of FcγRI was significantly up-regulated in mice injected with either 3D6 IgG2a or the irrelevant IgG2a control. FcγRI is a high affinity receptor, which is up-regulated following activation and unlike FcγRI in the periphery able to ligate free monomeric IgG. The increase in the expression of FcγRI could therefore be explained by the ligation of FcγRI by the presence of aggregated or monomeric IgG2a antibodies, driving increased receptor expression. FcγRIV was specifically up-regulated in mice injected with 3D6 IgG2a but not with irrelevant IgG2a. This up-regulation could be explained by the formation or accumulation of Aβ/3D6 IgG2a immune complexes, and crosslinking of FcγRIV causing receptor up-regulation.

5.4.2 Role of effector function in amyloid beta clearance

The experiments described in this chapter show evidence that effector function plays a key role in driving microglial phenotype changes and IL-1β production, but effector function is also critical for plaque clearance. The measurement of plaque load was technically challenging due to the methods

available. The brains collected for immunohistochemistry were fresh frozen to allow the detection of phenotype changes to microglia. This type of tissue is less useful for immunohistochemical detection of aggregated Aβ and plaques, which requires treatment with formic acid to expose epitopes for antibody binding. Treatment of fresh frozen tissue with formic acid can cause damage to tissue, even with post fixing in formalin, making it less suitable for the quantification of plaque clearance. As shown in chapter 3, antibodies that bind to the N-terminus are the best at binding to plaques without antigenic retrieval, because epitopes in the N-terminus of Aβ are exposed (Serpell, 2000). Because we injected 3D6, which binds to the N-terminus we could not use another N-terminus binding antibody to detect Aβ due to antigenic masking. To quantify plaque removal after 3D6 injection, histological dye congo red was used. Congo red binds to and stains congophillic plaques, and at 14 months the number of congophilic plaques in the brains of TG2576 is highly variable. This variability was partially compensated by normalisation to the number of plaques in the un-injected side of the brain. 3D6 IgG2a reduced the numbers of congophilic plaques after injection, however this result was not significant-partly due to the low number of mice in each treatment group. To allow quantification of Aβ peptide concentration, a multiplex immune assay measuring: Aβ38, 40 and 42 was used following injection of 3D6 in 18 month old TG2576 mice. These peptides were measured in two different fractions of protein: triton soluble and formic acid soluble. There were no significant changes to the levels of Aβ after treatment with 3D6, however in both fractions there was less Aβ in animals injected with 3D6 IgG2a compared to 3D6 IgG1. Although there was not a significant reduction in Aβ, in both experiments there were strong trends, indicating that the effector function of 3D6 is important for the clearance of plaques. Although 3D6 IgG1 did not reduce plaque or Aβ peptide level, it was bound to plaques in the brain of TG2576 mice at seven days. It would therefore be interesting to investigate the kinetics of clearance with 3D6 IgG1. The weaker effector function of IgG1 compared to IgG2a, may be able to clear plaques, but over a longer period of time. This could enable plaque clearance with reduced cytokine levels, and reduced vascular damage.

5.4.3 Limitations of the intracranial injection model

Stereotaxic injections into the brain always risk causing damage to cerebral blood vessels, and injections into this hippocampus can occasionally cause the breakage of a large vessels inducing severe degeneration in the dentate gyrus and CA3 regions of the hippocampus. It appears that TG2576 mice are exquisitely sensitive to vascular damage in the hippocampus, as 42% of mice injected lost a significant portion of the dentate gyrus. Fourteen month old TG2576 mice were injected into the stratum radiatum which is located directly above the hippocampal fissure, a region that is rich in large blood vessels. In this brain region there is substantial deposition of Aβ as plaques, but also as CAA surrounding blood vessels .The accumulation of Aβ around the vasculature in both AD patients and transgenic mice, causes changes to vascular integrity, which could explain the sensitivity of mice to intracranial injection (Nicolakakis and Hamel, 2011). This damage caused a strong glial response measured by increased expression of CD68 and CD11b and neuronal loss, and was also observed following injection of irrelevant control antibodies. It was therefore not possible to measure the neuro-inflammatory response to intracerebral Aβ specific antibodies in these mice. As a result, 42% of the mice were excluded from this study severely reducing the power of the experiment. To reduce the risk of damage occurring the injection coordinates were altered for injections into 18 month old animals. Instead of injecting 1.6mm into the brain, the capillary was only inserted 1.4mm. When injecting antibodies into the brain, finely pulled glass capillaries are used to minimise injection mediated damage. Other researchers have injected Aβ antibodies using Hamilton syringes to TG2576 mice, using stereotaxic coordinates that pass directly through the hippocampal fissure. One of these studies shows that injection of 2H6 into the hippocampus of TG2576 mice results in the up-regulation of CD45 and MHCII in the hippocampus (Wilcock et al., 2004a). Expression of these markers appears to coincide with areas of neurodegeneration, possibly caused by injection damage.

It should be noted that injection mediated vascular damage may also have occurred in the tissue used for cytokine analysis. However, injection mediated inflammation occurred in all treatment groups, and therefore does not explain the difference in IL-1β levels. However, injection damage could alter the phenotype and function of microglial cells, priming them to respond in an exacerbated fashion to 3D6.

In conclusion , the results in this chapter provides proof of principle that antibody effector function plays a role in the clearance of Aβ but this is associated with an increased neuroinflammatory response Engineering of the Fc region, could be explored to modify the neuro-inflammatory response to anti-Aβ antibodies.

Chapter 6: Systemic treatment of TG2576 mice with mC2 IgG1 and IgG2a

6.1 Introduction

One neuropathological hallmark of Alzheimer's disease is the accumulation of the protein Aβ as deposits called plaques. Aβ is produced by the cleavage of APP; and mutations in the APP gene or its processing machinery are sufficient to drive early onset AD (Hardy and Selkoe, 2002). This led to the idea that Aβ is the central factor in the pathology of sporadic AD, and as a result there has been significant effort to develop therapies to clear Aβ or to prevent its deposition (Nitsch and Hock, 2008). Passive immunisation with monoclonal antibodies against Aβ have proven effective at removing Aβ plaques and reversing cognitive deficits in mice transgenic for human APP (Bacskai et al., 2002; Dodart et al., 2002; Wilcock et al., 2004c). These results have not yet convincingly translated into benefits for patients, with a number of antibodies failing to meet their endpoints (e.g. improve cognition) in clinical trials (Doody et al., 2014; Salloway et al., 2014). One of the key issues in these trials has been the development of inflammatory side effects in the brains of patients after treatment with antibody. There is evidence that these side effects are due to the activation of microglia through FcγRs, as reducing the affinity for FcγRs is able to reduce the damage caused to the vasculature (Carty et al., 2006; Freeman et al., 2012; Wilcock et al., 2006).

In the previous chapters I investigated the effect of FcγR affinity of the anti-Aβ antibody 3D6, on its ability to clear plaques and to cause neuroinflammation in transgenic APP mice (TG2576) following intracerebral injection. I found that the IgG2a subclass of 3D6 allowed better clearance of Aβ but also induced more inflammation, and therefore carries a greater risk of causing side effects. Direct injection of antibodies into the hippocampus allows relatively rapid characterisation of plaque clearance and inflammation, but there are limitations with this approach. Humans receive treatment via systemic administration, therefore this method of administration is less clinically relevant. A second limitation of intracerebral injection is the risk of mechanically damaging the vasculature, as I showed in the previous chapter, which allows neurotoxic plasma proteins and circulating immune cells into the brain. To better model anti-Aβ immunotherapy, and to characterise a more physiological neuro-inflammatory response as well as functional behavioural assessment it is necessary to inject antibodies systemically.

Due to the low yield of 3D6 by transient transfection, it was injected directly into the brain and it was not possible to carry out a systemic treatment trial. Another antibody, mC2, the murine version of Crenezumab was produced as both IgG1and IgG2a subclasses. Crenezumab was developed by

Genentech and AC immune, and was selected for its ability to bind to all forms of Aβ (Adolfsson et al., 2012). We therefore thought that Crenezumab was a suitable candidate for testing the role of FcγR activation on inflammation and plaque clearance in the TG2576 model after systemic administration.

Eighteen month old TG2576 mice were injected I.P. with 10mg/kg mC2 IgG1, mC2 IgG2a or isotype control antibodies weekly for a period of eight weeks. This time point was selected as it has previously been shown that plaque clearance and microglial activation occur after systemic antibody treatment (Wilcock et al., 2004b). The mice were assessed for clearance of plaques and neuroinflammation as well as cognitive improvement using the fear conditioning behaviour test after eight weeks of antibody treatment. The hypothesis of this experiment is that mC2 IgG2a will be more efficient at clearing plaques and cause more inflammation than mC2 IgG1 due to its higher affinity for activating FcγRs.

6.2 Methods

6.2.1 Animals used and experimental design

Female TG2576 mice and littermate controls were obtained from Taconic and aged until 18 months old. Mice were house under 12 hour light dark cycles, with free access to food and water. The mice were randomly assigned into four experimental groups: mC2 IgG1, mC2 IgG2a, Irrelevant IgG1 and irrelevant IgG2a (n=8-10 TG2576 and n=8-10 littermate controls per group). The mice received 10mg/kg of the relevant antibody for a period of eight weeks, delivered via intraperitoneal injection. Twenty four hours after the final injection cognitive function of the mice was tested using the contextual fear conditioning paradigm. Seven days after the final injection, mice were terminally anaesthetised with avertin and transcardially perfused with heparinised saline. One hemi brain was removed and frozen in OCT for immunohistochemistry, the other hemi brain was snap frozen for analysis load and cytokine levels.

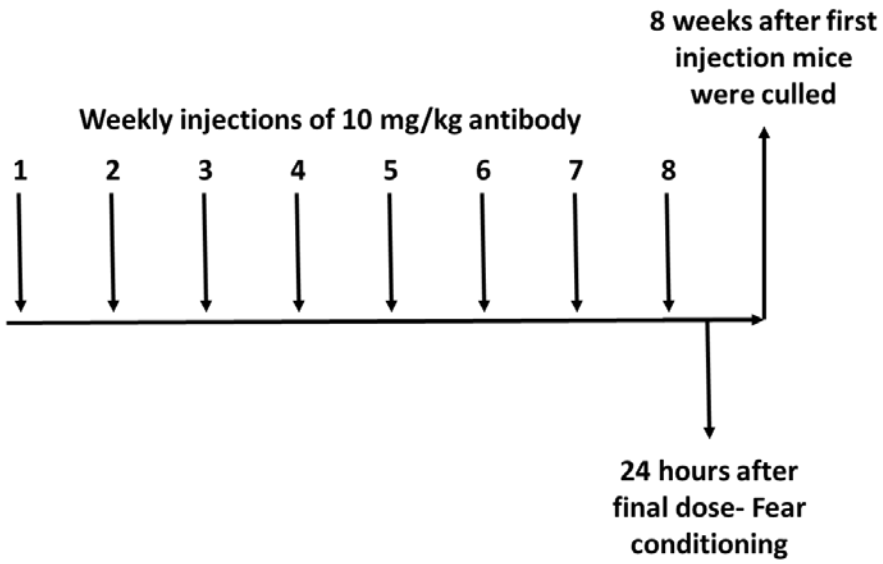

Figure 6. 1 Study Design

Female TG2576 mice (N=8-10) and wild littermates (N=8-10) were given weekly 10mg/kg I.P. injections of: mC2 IgG1, mC2 IgG2a or isotype controls. Twenty-four hours after the final dose, mice were assessed by fear conditioning, and eight weeks after the first injection mice were culled and tissue collected for analysis.

6.2.2 Statistical analysis

Immunohistochemistry and mesoscale data were analysed using 2-way ANOVA and Tukey post hoc test. The independent variables were: antibody specificity (Aβ/Irrelevant) and antibody subclass (IgG1/IgG2a). The analysis was performed and graphs made using Graphpad prism. The data from fear conditioning was analysed by 3-way ANOVA with the independent variables: Genotype (WT/TG), antibody specificity (Aβ/Irrelevant) and antibody subclass (IgG1/IgG2a). This analysis was performed using SPSS. The graphs were made in Graphpad prism and are presented with error bars showing SD.

6.3 Results

To investigate the role that FcγRs play in the clearance of Aβ and neuroinflammation associated with immunotherapy, we produced the anti-Aβ antibody mC2 on two different mouse IgG constant regions-IgG1 and IgG2a. IgG2a is more pro-inflammatory because it can bind to the activating receptors FcγRI and FcγRIV whilst IgG1 cannot (Bruhns, 2012). Mice were received 10mg/kg of each antibody or isotype controls for a period of eight weeks. Twenty-four hours after the final dose the memory of the mice was assessed in the fear conditioning paradigm. If neuroinflammation and plaque clearance are reliant on FcγR engagement you would expect the mC2 Ig2a antibody to induce more inflammation and clear more plaques than mC2 IgG1.

6.3.1 Behaviour

One of the first clinical features of Alzheimer's disease is episodic memory loss followed by progressive cognitive decline, and prevention of this decline is a common primary end point of clinical trials for AD. Mice transgenic for human APP also exhibit a reduction in cognition and memory, which can be reversed by treatment with anti-Aβ antibodies (Arendash et al., 2001; Morgan et al., 2000; Shoji et al., 2003). To test if antibody effector function plays a role in reversing cognitive deficits, we used the well characterised behaviour paradigm-contextual and cued fear conditioning. Under stressful conditions when a mouse is highly anxious, its natural behaviour is to freeze in place, an adaptation to reduce the likelihood of being seen by a predator. The fear conditioning assay exploits this behaviour, by associating a noise or a particular environment with an aversive stimulus (i.e. an electric shock). The amount of time that a mouse then spends freezing when exposed to the same environment or noise, is dependent on the ability of the mouse to remember and associate the environment/noise with the stimulus. During contextual fear conditioning, wild type mice on average froze for longer than 50% of the total time, irrespective of the antibody subclass (Figure 6.2A). Transgenic mice treated with irrelevant control antibodies spent less time freezing (IgG1=24% and IgG2a=22%), indicating reduced memory compared to the wild type mice. Transgenic mice treated with mC2 exhibited improved memory with increased freezing time but no differences were found with regard to the subclass (mC2 IgG1=42%, mC2 IgG2a=37%). Data was analysed using 3-way ANOVA with independent variables: genotype, antibody specificity (i.e. Aβ or irrelevant) and antibody subclass (IgG1 or IgG2a). A significant interaction between genotype and antibody specificity ($p=0.015$) was observed indicating that treatment of transgenic mice with mC2

significantly increased the time spent freezing. There was however no additional effect of antibody subclass (p=0.218). This shows that the antibody mC2 is able to reverse memory deficits in TG2576 mice, however the subclass of the antibody and therefore its effector function has no significant effect on this improvement. During the cued fear conditioning test (Figure 6.2B), wild type mice froze for significantly longer than transgenic mice (p=0.01). However, treatment with mC2 had no effect on the length of time spent freezing.

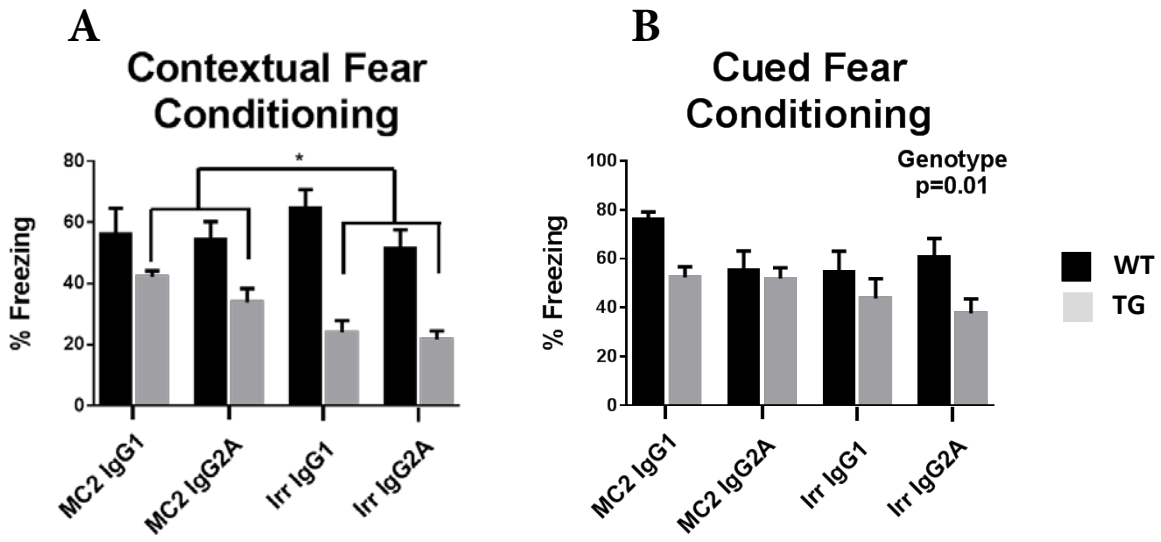

Figure 6. 2 The antibody mC2 is able to reverse cognitive deficits in mice, however there is no effect of antibody subclass

The ability of the antibody mc2 to reverse cognitive deficits in the TG2576 model was investigated using fear conditioning behaviour. 24 hours after the final dose of antibody, mice were assessed by fear conditioning, with higher amounts of time spent freezing indicative of better memory. **A.** Wild type mice in all groups spent on average above 50% of the test time freezing. Transgenic mice treated with isotype control antibodies spent significantly less time freezing (IgG1=24% and IgG2a=22%) indicating a deficit in memory. Treatment with mC2 IgG1 or IgG2a increased the time that transgenic mice spent freezing (mC2 IgG1=42%, mC2 IgG2a=37%), indicating a recovery in memory. The data was analysed by 3-way ANOVA with variables: genotype, isotype and antibody specificity. A significant interaction was found between genotype and specificity (p=0.015) but not between genotype specificity and isotype. This indicates that treatment with mC2 significantly improves cognitive function of transgenic mice, independent of subclass. **B.** During cued fear conditioning, transgenic mice froze significantly less than wild type mice (p=0.01), and this was unaffected by treatment with any antibody.

6.3.2 Target engagement and clearance of Aβ

Antibodies to Aβ have to cross the BBB upon systemic treatment, thus to check for the engagement of plaques by mC2, tissue sections were stained for mouse immunoglobulin to detect if systemically administered antibody bound to plaques (Figure 6.3). Supporting the *in vitro* findings described in chapter 3, mC2 failed to bind to plaques. There was however co-localisation of mouse IgG and Aβ species of smaller size (e.g. oligomers, soluble Aβ) indicating the formation of immune complexes. The clearance of Aβ was measured by two methods: a semi-quantitative immunofluorescence technique detecting plaque load and a quantitative immune assay to detect Aβ peptide levels. One hemi brain was cryo-sectioned at 10μm and stained for Aβ. The other hemi brain from mice was homogenised and two different fractions were isolated : triton soluble derived from smaller less aggregated forms, and formic acid soluble derived from larger more insoluble forms of Aβ (Sudduth et al., 2013).These different fractions were used to detect the levels of three different Aβ peptides: 38, 40 and 42 by a multiplex immune assay (MSD). Figure 6.4 shows the plaque load in the hippocampus and piriform cortex of antibody treated mice. Quantification shows there was no detectable clearance of plaques by either mC2 IgG1 or mC2 IgG2a compared to irrelevant antibody controls. The Aβ peptide level in brain homogenate treatment with mC2 increases the levels of Aβ detected in brain homogenate (figure 6.5). The levels of triton soluble Aβ42 and formic acid soluble Aβ42 were increased after treatment with mC2 irrespective of subclass. Treatment with mC2 IgG2a resulted in significantly higher levels of triton soluble Aβ40.

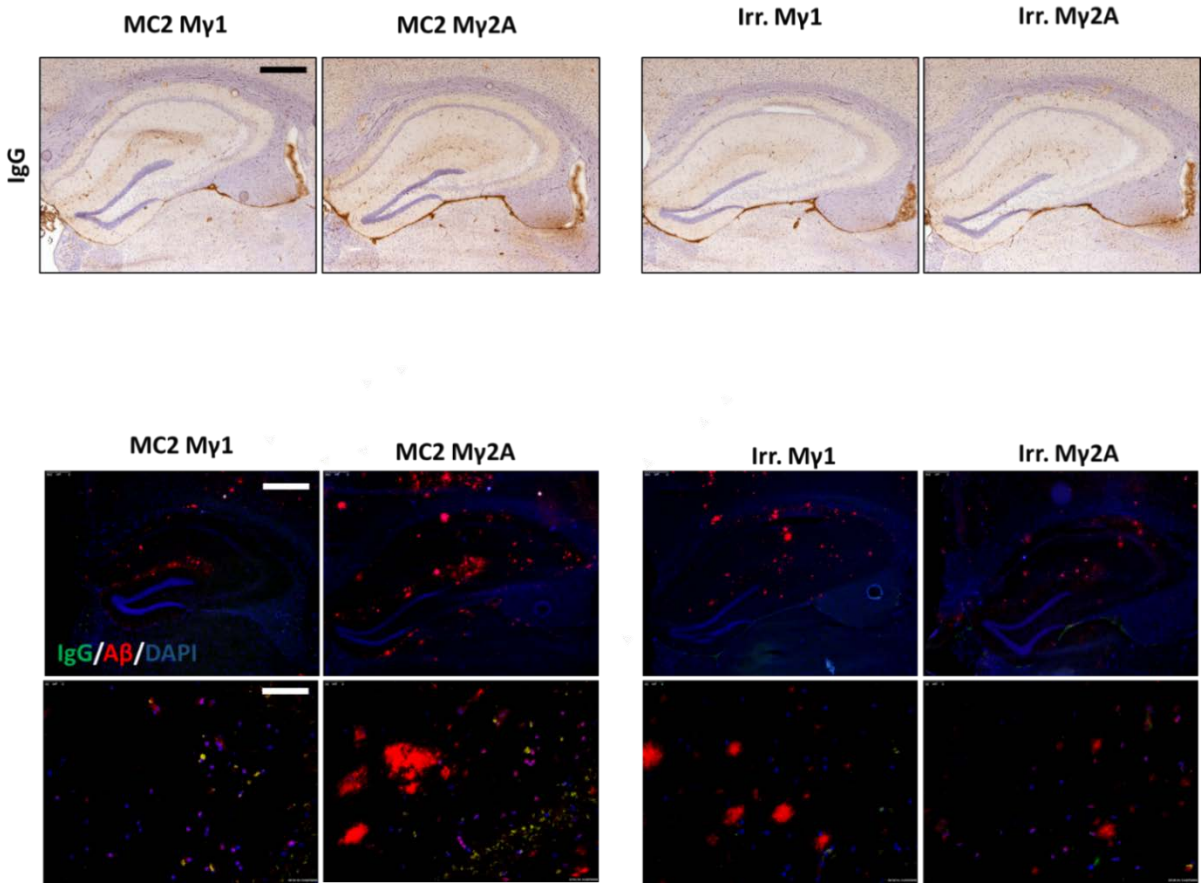

Figure 6. 3 There is no detectable IgG bound to plaques in mC2 treated animals, however there is evidence of immune complex formation with Aβ

To test for target engagement of mC2 IgG1 and IgG2a, sections were stained for mouse IgG to detect mC2 binding to plaques. There was no detectable IgG coating plaques in any group (A), suggesting no plaque engagement. Double staining of mouse IgG with Aβ confirmed that IgG was not binding to plaques, however there was co-localisation of IgG with smaller Aβ deposits in mice injected with mC2 IgG1 or IgG2a- Aβ (red), IgG (green) co-localisation (yellow). Images were taken with a 5x objective and a 40x objective, scale bars are 500μm and 72.5 μm respectively (representative of n=8-10).

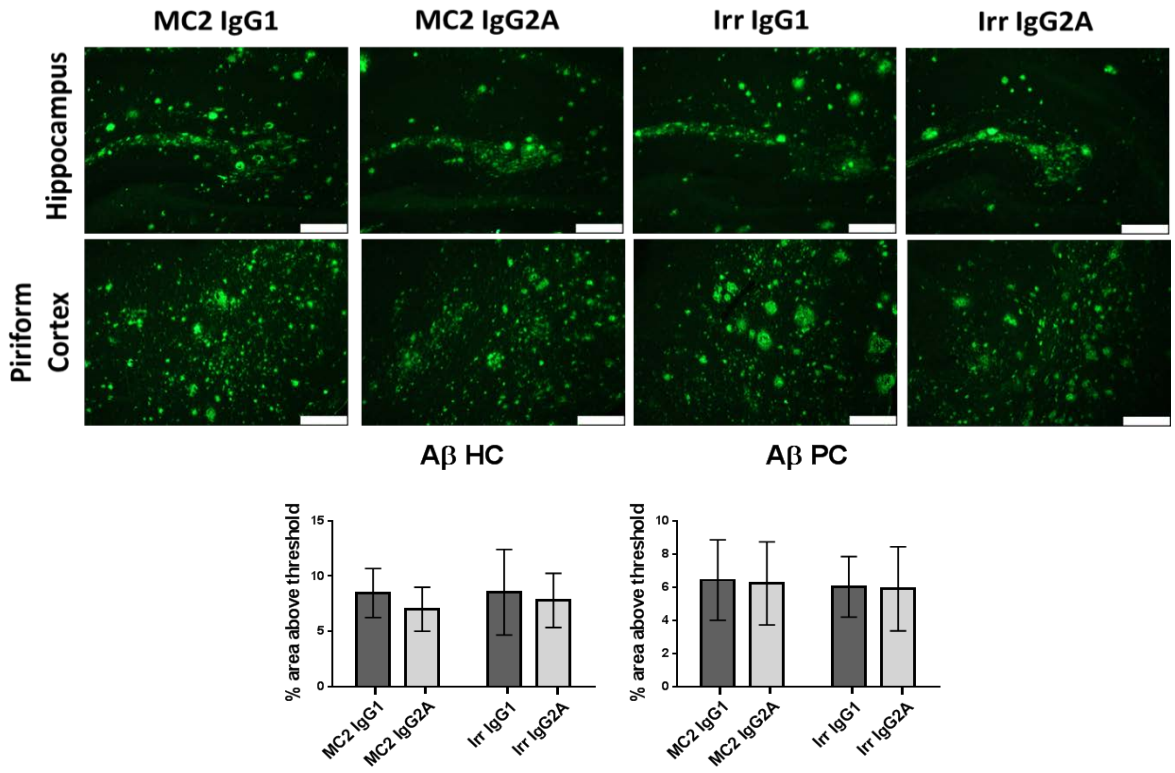

Figure 6. 4 Systemic treatment with mC2 IgG1 or IgGA does not decrease Aβ protein load in TG2576 mice

Plaque clearance was assessed after eight weeks of treatment with 10mg/kg of mC2 IgG1, mC2 IgG2a and isotype controls (n=8-10, 1 section used per mouse) by immunofluorescence. The images are shown from two brain regions: the hippocampus and piriform cortex, images are taken with a 10x objective and scale bars are 250μm (A). The area above threshold of staining was quantified, and no significant difference between treatment groups in either brain region (B).

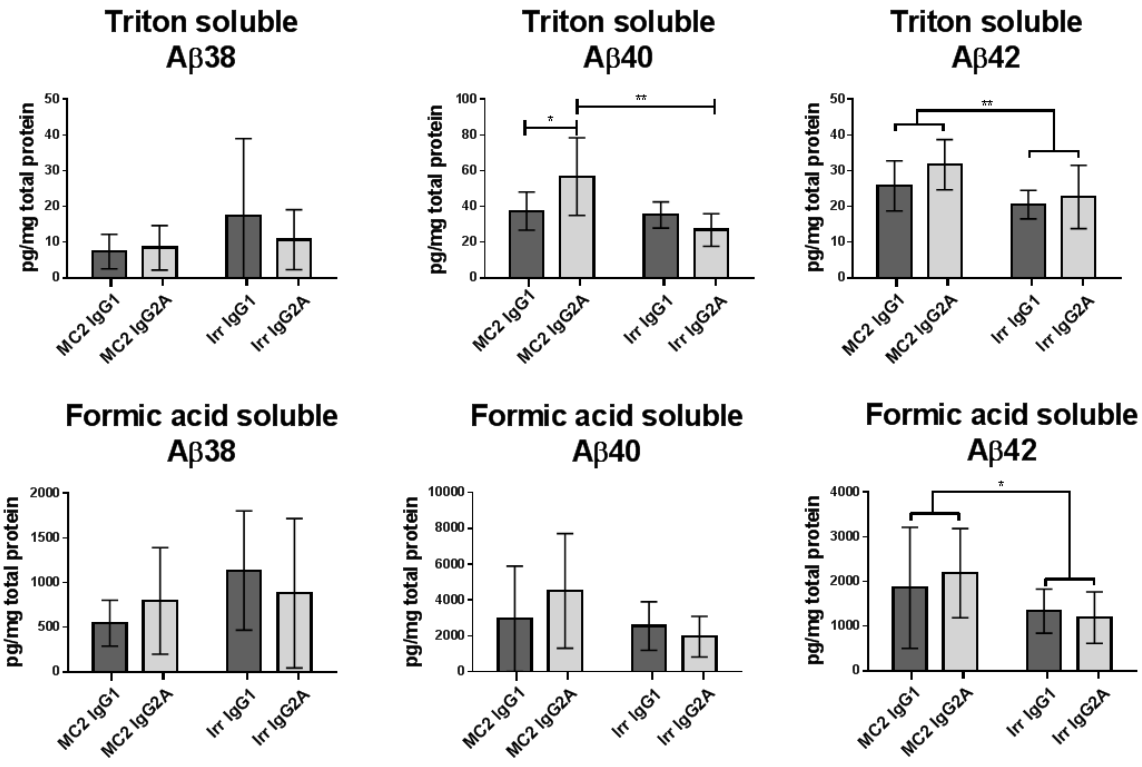

Figure 6. 5 Aβ protein concentration is increased after treatment with mC2 IgG1 or IgG2a

Aβ protein concentration was measured in brain homogenate (containing both the hippocampus and piriform cortex) after eight weeks of treatment with: mC2 IgG1 IgG2a or isotype controls (n=8-10) using a multiplex immune assay (MSD). The levels of three different Aβ peptides were measured in two different fractions obtained from brain homogenate: triton soluble Aβ-derived from more soluble Aβ, and formic acid soluble-derived from more insoluble deposits of Aβ. Treatment with mC2 resulted in the increased levels of triton soluble (p=0.008) and formic acid soluble (p=0.025) Aβ. Treatment with mC2 IgG2a resulted in higher triton soluble Aβ40 compared to mC2 IgG1 (p=0.03) and Irr. IgG2a (p=0.0003).

6.3.3 Neuroinflammation

FcγR mediated inflammation is thought to contribute to damage to the cerebral vasculature following passive immunisation. Therefore, we next investigated the effect of the antibody subclass of mC2 on neuroinflammation after eight weeks of treatment, by assessing microglial phenotype and pro-inflammatory cytokine levels. It has been previously shown that immune complex formation results in increased levels of FcγRs and CD11b on microglia (Teeling et al., 2012; Wilcock et al., 2004b), and that the marker CD68 is up-regulated in response to increased phagocytic activity. Systemic treatment with mC2 significantly increased the expression of CD11b in the hippocampus of TG2576 mice (figure 6.6, p=0.039), but there was no difference between mC2 IgG1 and mC2 IgG2a antibodies (p=0.5). No significant changes in expression of CD11b in the piriform cortex were found, and the expression of CD68 in either the hippocampus or piriform cortex was comparable to irrelevant control antibodies. There was detectable expression of: FcγRI, FcγRII/III and FcγRIII in all groups of mice, but unlike previous studies we did not find an upregulation after systemic treatment with mC2 (Figures 6.7).

A functional way to measure the inflammation, is to measure the concentration of cytokines in the brain. When macrophages are activated through FcγRs they switch to an m2b phenotype, and this has elements of both classically activated and wound healing macrophages, including the production of pro-inflammatory cytokines (Mosser and Edwards, 2008). Figure 6.8 shows the levels of pro-inflammatory cytokines in brain homogenate from TG2576 mice. Significantly higher levels of TNFα (p=0.005), IL-1β (p=0.03), and KC (p=0.001) are observed in the brains of mice injected with mC2 compared to irrelevant control antibodies. There was no interaction between the subclass of the antibody and the levels of cytokines, indicating that the subclass of mC2 had no effect on the levels of cytokines. There was also significantly higher levels of IL-6 in the brains of mice injected with mC2 compared to control antibodies (p=0.026), in this case there was a trend towards an interaction with subclass of mC2 (p=0.10), indicating that mC2 IgG2a induced the expression of more IL-6 than mC2 IgG1. To ensure the increase in cytokines was due to target engagement by mC2, not due to other differences between mC2 and irrelevant antibodies, the levels of cytokines were measured in the brains of wild type mice after immunotherapy. Wild type mice lack human APP, and therefore do not accumulate Aβ in the brain. There were no signifticant changes in the levels of cytokines in the brain of wild type mice treated with mC2 (fig.6.9). However there was a non-statistically significant increase in TNFα in the brains of mice treated with mC2.

In the previous chapter, 3D6 IgG2a induced higher brain IL-1β in TG2576 mice compared to 3D6IgG1 after intracranial injection. In this chapter I show that systemic treatment with mC2 IgG1 or IgG2a causes an increase in the levels of cytokines in the brain at two months, with no effect of antibody subclass. To test whether the difference in cytokine response is due to the method of administration or the antibody itself, 18 month TG2576 mice were intracranially injected with: mC2 IgG1, mC2 IgG2a or irr IgG2a. There were not sufficient numbers of aged mice to include an irrelevant IgG1 group, limiting the conclusions that can be drawn from this data. However, there were no significant differences in brain cytokine levels between mC2 IgG1 and mC2 IgG2a at seven days post injection (fig. 6.11), showing that differences between 3D6 and mC2 were not due to the method of injection.

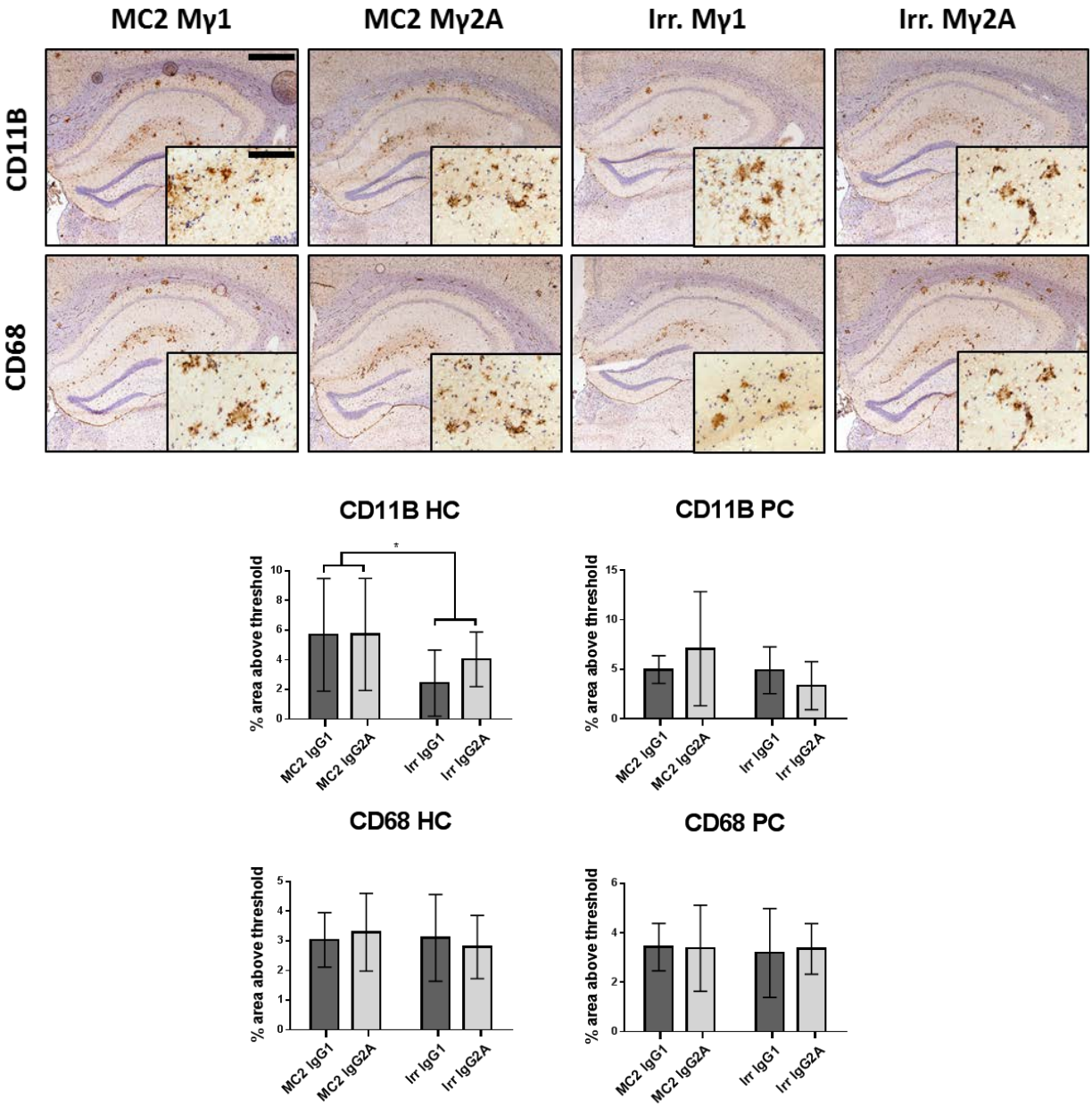

Figure 6. 6 mC2 Treatment significantly increases the expression of CD11b in the hippocampus, but does not alter the expression of CD68

Expression of microglial CD11b and CD68 after injection of anti-Aβ antibodies (n=8-10, 1 section per mouse). Images are taken with a 5x objective and 20x objective, scale bars are 500μm and 125μm respectively. CD11b expression is significantly up-regulated in mice injected with mC2 compared to irrelevant controls (p=0.039). There was no difference between IgG1 and IgG2a. There was no increase in the expression levels of CD68 after mC2 treatment.

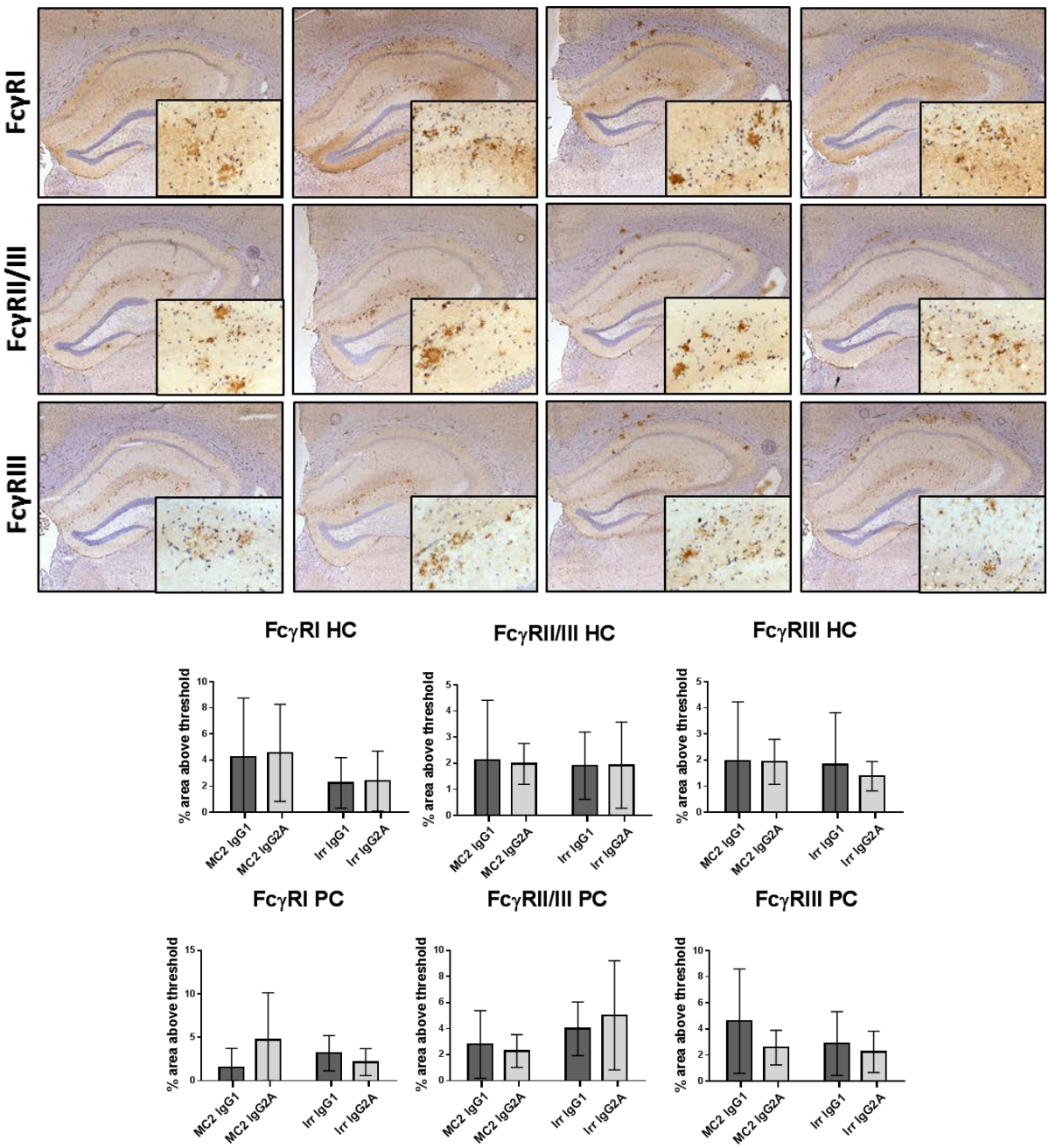

Figure 6. 7 Treatment did not affect the expression of FcγRs in the hippocampus or piriform cortex

Expression of FcγRs after injection of anti-Aβ antibodies (n=8-10, 1 section per mouse). Pictures are taken with a 5x objective and 20x objective, scale bars are 500μm and 125μm respectively. There was no change in the expression of FcγRs after treatment with mC2.

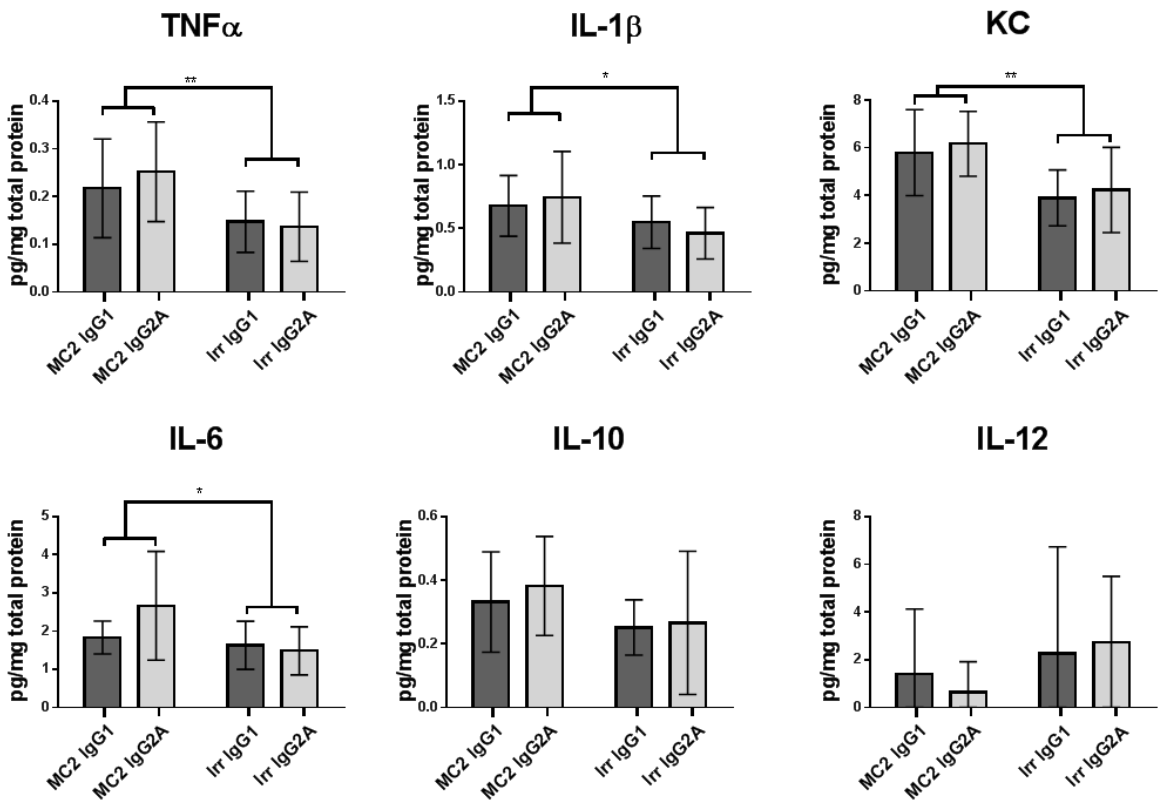

Figure 6. 8 Treatment with mC2 significantly increases the levels of: TNFα, IL-1β, KC and IL-6 in comparison with irrelevant antibodies

Cytokine levels in brain homogenate following systemic treatment with MC2 or controls (n=8-10). Treatment with mC2 leads to a significant increase in the levels of TNFα (p=0.005), IL-1β (p=0.03), mKC/GRO (p=0.001) and IL-6 (p=0.025). There was no effect of mC2 subclass on the levels of TNFα, IL-1β or mKC/GRO, however there was a trend towards increased IL-6 in mC2 IgG2a injected animals in comparison to mC2 IgG1 (p=0.11).

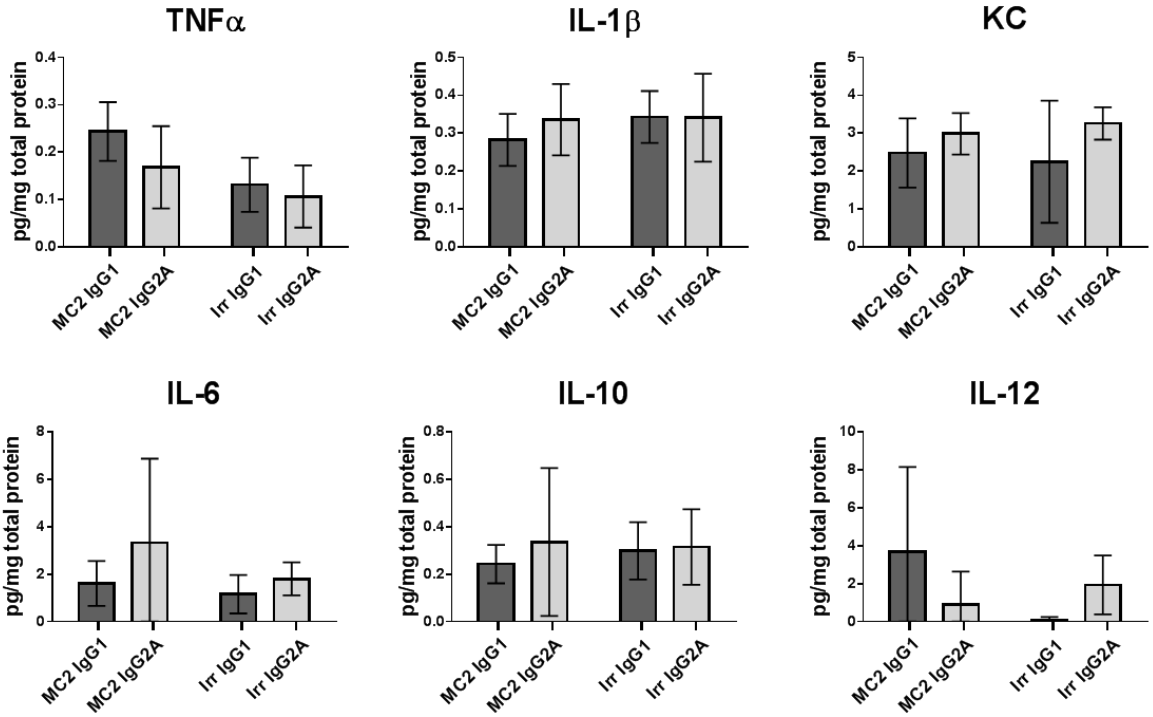

Figure 6. 9 Treatment with mC2 does not significantly increase cytokine levels in the brains of wild type mice

Cytokine levels in brain homogenate of wild type mice were measured using a multiplex immune assay, following systemic treatment with mC2 or controls for eight weeks(n=8-10). There were no significant differences in brain cytokine levels between any groups, however there is a trend towards increased TNFα in mice treated with mC2.

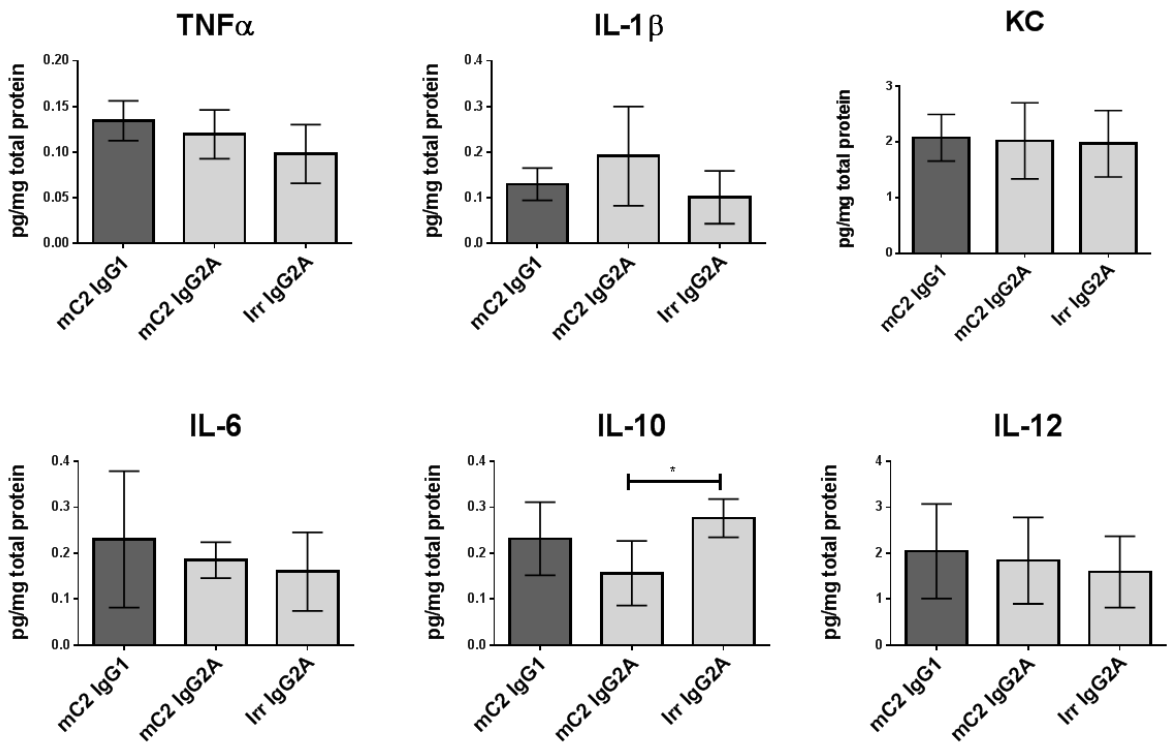

Figure 6. 10 Intracranial injection of mC2 IgG1 and mC2 IgG2a

Eighteen month old TG2576 mice were given intracranial injections of: mC2 IgG1, mC2 IgG2a or an irrelevant IgG2a control (n=6/7). At seven days post injection, the cytokine levels were measured in brain punches from the injected region. There were no significant increases in brain cytokines following mC2 injection, however mC2 IgG2a significantly reduced the levels of IL-10 compared to irrelevant control.

6.4 Discussion

Neuro-inflammation is thought to contribute to the dose limiting vascular damage (ARIA) that is associated with anti-Aβ immunotherapy. It has been shown that reduction in the FcγR binding of antibodies, for example by de-glycosylation can reduce the risk of causing vascular damage in animal models (Carty et al., 2006; Freeman et al., 2012; Wilcock et al., 2006). In the previous chapter 3D6 IgG2a was shown to be better at clearing plaques than 3D6 IgG1, however it also increased the levels of pro-inflammatory cytokine IL-1β. This can be explained by IgG2a's higher affinity for activating FcγRs in comparison to IgG1 (Bruhns, 2012), allowing better phagocytosis and activation of effector cells. The aim of this chapter was to characterise the importance of FcγR binding on the efficacy of an antibody after systemic treatment. To do this we generated the anti-Aβ antibody mC2, the murine version of clinical candidate Crenezumab, with both IgG1 and IgG2a constant regions. 18 month old transgenic mice were treated for eight weeks with 10 mg/kg of either subclass of mC2 or irrelevant control antibodies. The ability of each subclass to clear plaques, induce inflammation and reverse cognitive deficits was tested in the TG2576 mouse model. Here we show that neither subclass of the mC2 antibody was able to reduce plaque load or Aβ peptide levels by this time point. In spite of this, both antibody subclasses were able to reverse cognitive deficits in this model, and increase the levels of pro-inflammatory cytokines in the brain.

These results do not fit with published pre-clinical data for Crenezumab, which shows that systemic treatment with Crenezumab is able to clear plaques from the brains of transgenic mice. However there are a number of important points to consider when comparing these data sets. The most important difference between the studies was the length of time the mice were treated with the antibody. The main objective of this study was to investigate the effect of modifying the FcγR affinity of mC2 on Aβ clearance and neuroinflammation. The eight week treatment regimen was selected as it has been previously shown systemic treatment with 10mg/kg of antibody 2H6 causes microglial activation at two months, which is attenuated at three months (Wilcock et al., 2004b). The lack of plaque clearance could be due to different binding kinetics of mC2 compared to antibodies like 2H6, and therefore if a later time point was chosen, there may have been a reduction in plaque load. However, the most likely explanation for the lack of Aβ clearance by mC2 is the lack of plaque engagement. There was no evidence of mC2 binding to plaques after eight weeks of treatment,

however, there was co-localisation between IgG and Aβ in mice treated with either mC2 IgG1 or IgG2a. This suggests that mC2 is binding to smaller soluble forms of Aβ such as oligomers. In **chapter 3** I showed that mC2 does not bind strongly to aggregated Aβ, and requires formic acid antigenic retrieval to bind to plaques in tissue sections explaining the lack of *in vivo* engagement of plaques. This fits well with data from other antibodies that bind to the mid domain of Aβ such as M266 (the murine version of Solanezumab), which also does not bind to or clear plaques in transgenic APP mice (Dodart et al., 2002). This contradicts published data for Crenezumab, which claim that it binds well to all forms of Aβ.

Interestingly, treatment with mC2 actually increased the levels of Aβ42 in comparison to irrelevant controls. The assay used to measure Aβ levels is a sandwich immune assay, and the presence of immune complexes between mC2 and Aβ could interfere with detection, resulting in an increased signal from unchanged Aβ levels. Furthermore, in the previous chapter, high levels of 3D6 after intracranial injection did not result in increased Aβ detected by this assay. Another explanation for increased levels of Aβ42 is the increased neuro-inflammation after treatment with mC2 IgG1 or IgG2a. It has been shown previously that inflammation can cause increased levels of Aβ production/accumulation (Lee et al., 2008; Sheng et al., 2003b). Therefore the prolonged neuro-inflammation that follows treatment with mC2 could cause increased production and/or accumulation of Aβ in the brains of TG2576 mice.

It is interesting that in the absence of Aβ clearance, an improvement in memory is seen after mC2 treatment. This has previously been reported with antibodies such as Solanezumab, which is unable to clear plaques but can reverse cognitive deficits in mouse models (Dodart et al., 2002). The reason for this is thought to be because solanezumab can bind to soluble forms of Aβ, encouraging clearance from the brain or blocking the toxic effect of these species. Aβ is initially cleaved as a monomer, and aggregates to form oligomers, proto-fibrils and insoluble plaques. Recently it has been suggested that the plaques are actually inert, and that it is smaller oligomeric species which are the most toxic. These oligomeric structures are highly promiscuous and binding to a range of neuronal receptors such as: PrPc, FcγRIIb, and NMDA. Binding to these receptors induces neuronal dysfunction and/or death (Chung et al., 2010; Kam et al., 2013; Lai and McLaurin, 2010). Therefore if an antibody binding to these species could block these interactions, it can protect against neuronal dysfunction (Zago et al., 2012). Due to mC2's inability to bind to aggregated Aβ, and the absence of Aβ peptide clearance, behavioural improvements are likely due to binding of soluble Aβ and blocking synaptotoxicity. This

is supported by evidence of IgG and Aβ co-localisation in mice treated with mC2, indicating the formation of IgG/Aβ immune complexes.

If the reversal of cognitive deficits is due to blocking the interaction of Aβ with neurons, it is likely to occur rapidly after treatment with mC2, and the effects would also reverse once treatment was discontinued. Other studies have shown that the kinetics for clearance of Aβ from the brain occurs over a longer time scale (Bard et al., 2000; DeMattos et al., 2001; Wilcock et al., 2004c; Zago et al., 2013). The hypothesis that mC2 is acting by blocking the synaptotoxic effects of Aβ, could be tested by giving a single bolus dose of mC2 to TG2576 mice, and then changing the length of time before assessing behaviour. If the cognitive changes are due to blocking of this interaction you would expect the cognitive improvement to be short lived and to reverse once the antibody titre in the blood/brain decreases.

Both mC2 IgG1 and mC2 IgG2a significantly increase the levels of pro-inflammatory cytokines in the brain in comparison to isotype control antibodies. This effect was due to target engagement of the antibodies, because injection of the antibodies into wild type mice did not stimulate the same response. This is with the caveat that there was a trend towards increased TNFα in wild type mice injected with mC2, however there was no increase in the other cytokines that were up-regulated after TG2576 mice are treated with mC2. This result could be explained by cross reaction of mC2 to mouse Aβ, forming immune complexes and inducing inflammation in the brains of WT mice. Although mC2 could not bind to plaques in TG2576 mice, there was evidence of immune complex formation in the brain which could activate FcγRs and drive the increased cytokine production. There was a strong trend towards increased IL-6 in mC2 IgG2a treated animals in comparison with mC2 IgG1, however the levels of: TNFα, IL-1β and KC did not differ between subclasses. This is surprising as the IgG2a constant region has higher affinity for activating receptors than IgG1, therefore you would expect IgG2a to produce higher levels of cytokines. When compared to the results of the previous chapter, this can give us some interesting clues to which FcγRs are involved in the induction of inflammation after anti-Aβ immunotherapy. Mouse IgG1 is unable to bind to the high/medium affinity receptors FcγRI and FcγRIV but IgG2a can, also IgG1 is unable to fix complement but IgG2a does. Because the inflammatory response after mC2 was the same irrespective of subclass, it is unlikely that the inflammation was caused by FcγRI, FcγRIV or complement activation (Bruhns, 2012). The only activating receptor which both IgG1 and IgG2a subclasses are able to ligate is FcγRIII, which is expressed by microglia in this model. It stands to reason that the immune complexes formed when mice are treated with mC2, cause an increase in cytokine production by cross-linking of

FcγRIII. From this experiment it is not possible to tell if FcγR mediated removal of immune complexes is required to reverse cognitive deficits of transgenic mice. The blocking of Aβ's interaction with neuronal receptors may be sufficient, and therefore antibody effector function may not be required. To determine the importance of effector function in this model, and therefore inform optimisation of therapeutic antibodies, more experiments are required.

The hypothesis of this experiment was that the ability of an anti-Aβ antibody to clear plaques and to cause a neuro-inflammatory response would be dependent on the ability of the antibody to ligate FcγRs. Because mC2 did not bind to or clear plaques, it is not possible to make any conclusions about the involvement of FcγRs in plaque clearance. However we have shown that mC2 is able to reverse the pathology in these mice without clearing Aβ, and that both subclasses tested caused neuroinflammation.

Chapter 7: The role of antibody binding specificity in clearance of amyloid-β and the neuro-inflammatory response

7.1 Introduction

Due to this success in experimental models, several monoclonal antibodies have reached clinical trials for the treatment of AD, but excitement towards this approach has been tempered by a number of high profile failures to deliver disease modifying effects. Bapineuzumab and Solanezumab both failed in phase III, and a phase III trial for Gantenerumab was abandoned after a futility analysis (Doody et al., 2014; Salloway et al., 2014). With more antibodies for AD entering the clinic, including Aducanumab which has shown promising effects in Phase I, it is imperative to learn from the first generation antibody therapies to inform the development of new and improved clinical candidates. Bapineuzumab, a humanized IgG1, which recognised the N-terminus of Aβ cleared plaques from the brains of patients in a phase II trial however it also caused oedema and micro-haemorrhage of the cerebral vasculature (Rinne et al., 2010; Salloway et al., 2010). These side effects limited the top dose in phase III trials, which potentially contributed to the lack of efficacy (Salloway et al., 2014). These side effects have also been observed with Gantenerumab (hIgG1, N-terminus conformational epitope). Pre-clinical studies have suggested that side effects could be due to inflammation caused by Fc effector function of the therapeutic antibodies, as de-glycosylation can prevent vascular damage *in vivo* (Carty et al., 2006; Freeman et al., 2012; Wilcock et al., 2006). With this in mind, Crenezumab (hIgG4, mid-domain epitope) was generated with a human IgG4 constant region to modify Fc effector function and reduce vascular side effects (Adolfsson et al., 2012). However, the efficacy to clear plaques and the potential to induce side effects is difficult to predict due to inconsistent use of experimental models, epitope specificity (N, mid or C terminus) or antibody subclass.

In this chapter I compared three antibodies which have been in phase III clinical trials for AD: Crenezumab, Bapineuzumab and Gantenerumab. Bapineuzumab is a human IgG1 antibody, which binds to the N-terminus of Aβ (AA 1-5), and can recognise both soluble and insoluble Aβ (Salloway et al., 2014). Gantenerumab is also a human IgG1 antibody which recognises a conformational epitope, making contact with the N-terminus and the mid domain of Aβ, reportedly binding more strongly to more aggregated forms compared to soluble Aβ (Bohrmann et al., 2012). Crenezumab is a human IgG4 antibody which recognises a mid-domain epitope (AA 16-24), and binds to all forms of Aβ (Adolfsson et al., 2012). In **chapter 3** I described the production and characterisation of murine versions of Crenezumab (mC2), Bapineuzumab (3D6) and a mouse/human chimeric version of Gantenerumab (*ch*Gantenerumab) all with an IgG2a constant

regions. These antibodies were directly injected in to the hippocampus ofTG2576 mice, and the ability of each antibody to clear plaques and induce neuro-inflammation were compared.

7.2 Methods

7.2.1 Experimental design

They anti-Aβ antibodies, mC2, 3D6 and chGantenerumab were produced recombinantly and characterised as described in **chapter 3** with a murine IgG2a constant region. Eighteen month old female TG2576 mice (N=6/7) were bilaterally injected into the hippocampus with 2μg of: 3D6, mC2, Gantenerumab or irrelevant control. One week following injection, the mice were culled and the tissue was processed as previously described, taking one hemibrain for IHC and one hemibrain for cytokine/Aβ measurement by mesoscale.

7.3 Results

7.3.1 Clearance of Aβ

We tested the ability of the anti-Aβ antibodies to clear Aβ *in vivo* by injecting 2μg of each antibody into the hippocampus of 18 month old TG2576 mice. Clearance of Aβ after intracerebral injection of antibody into TG2576 mice was quantified by Aβ immuno-staining. Injection of 3D6 significantly reduced Aβ plaque load in comparison to *ch*Gantenerumab and mC2 (Figure 7.1a, p=0.0013 and p=0.026 respectively). Due to the potential of antigenic masking by injected antibodies, congo red staining was used to detect the clearance of congophilic deposits after antibody injection. 3D6 significantly reduced the number of congo red positive plaques in the hippocampus compare to Irrelevant IgG2a and *ch*Gantenerumab injected animals (Figure 7.1b, p=0.0265 and p=0.0178 respectively). The results were confirmed by measuring the levels Aβ38, Aβ40 and Aβ42 in brain homogenate. Diffuse (triton soluble) Aβ levels were not affected seven days post-injection. Supporting the decreased immuno-staining, 3D6 significantly reduced the amount of aggregated (formic acid soluble) Aβ38 compared to Gantenerumab or irrelevant IgG2a injection (figure 7.2d, p=0.0168 and p=0.0073 respectively). 3D6 also significantly lowered the amount of aggregated Aβ42 compared to irrelevant IgG2a (figure 7.2f, p=0.041), and cleared aggregated Aβ40 in 50% of mice treated with this antibody (figure 7.2e). c*h*Gantenerumab and mC2 did not induce significant changes to aggregated Aβ levels.

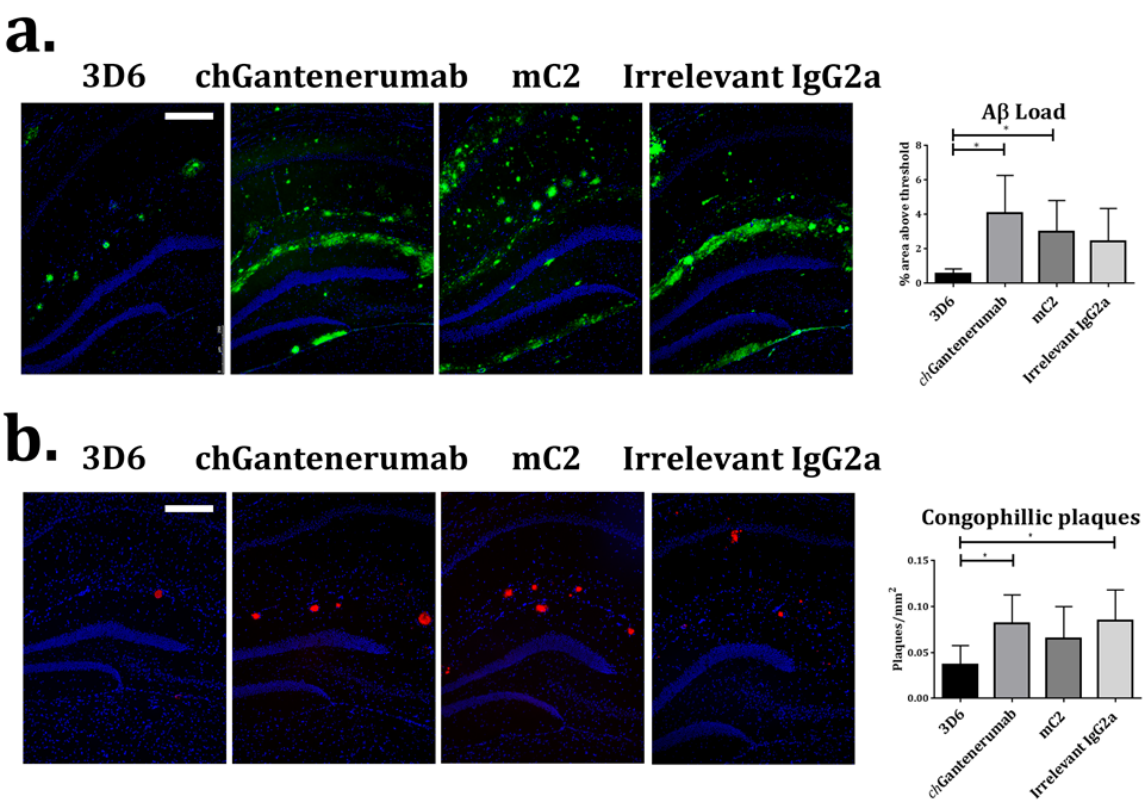

Figure 7. 1 Anti-Aβ immunohistochemistry and congo red stain

a. Tissue sections from TG2576 mice injected with antibodies were immuno-stained for Aβ, and the percentage staining area above threshold was measured. Data were analysed by Kruskal-wallis and Dunn's post hoc test and expressed as mean +/- SD (n=6/7). 3D6 significantly reduced Aβ load compared to mC2 and *ch*Gantenerumab (p=0.0265 and p=0.0013 respectively). Images taken with a x10 objective, scale bar =250μm **b.** To test for clearance of congophilic plaques, brain sections from were stained with congo red. The numbers of congophilic plaques were counted and normalised to hippocampal area and expressed as congophilic plaques/mm^2. Data were analysed by one-way ANOVA and Tukey post hoc test and expressed as mean +/-SD (n=6/7). 3D6 significantly reduced the number of congophilic plaques compared to irrelevant IgG2a and chGantenerumab (p=0.0265 and p=0.0178 respectively). Images taken with a x10 objective, scale bar =250μm

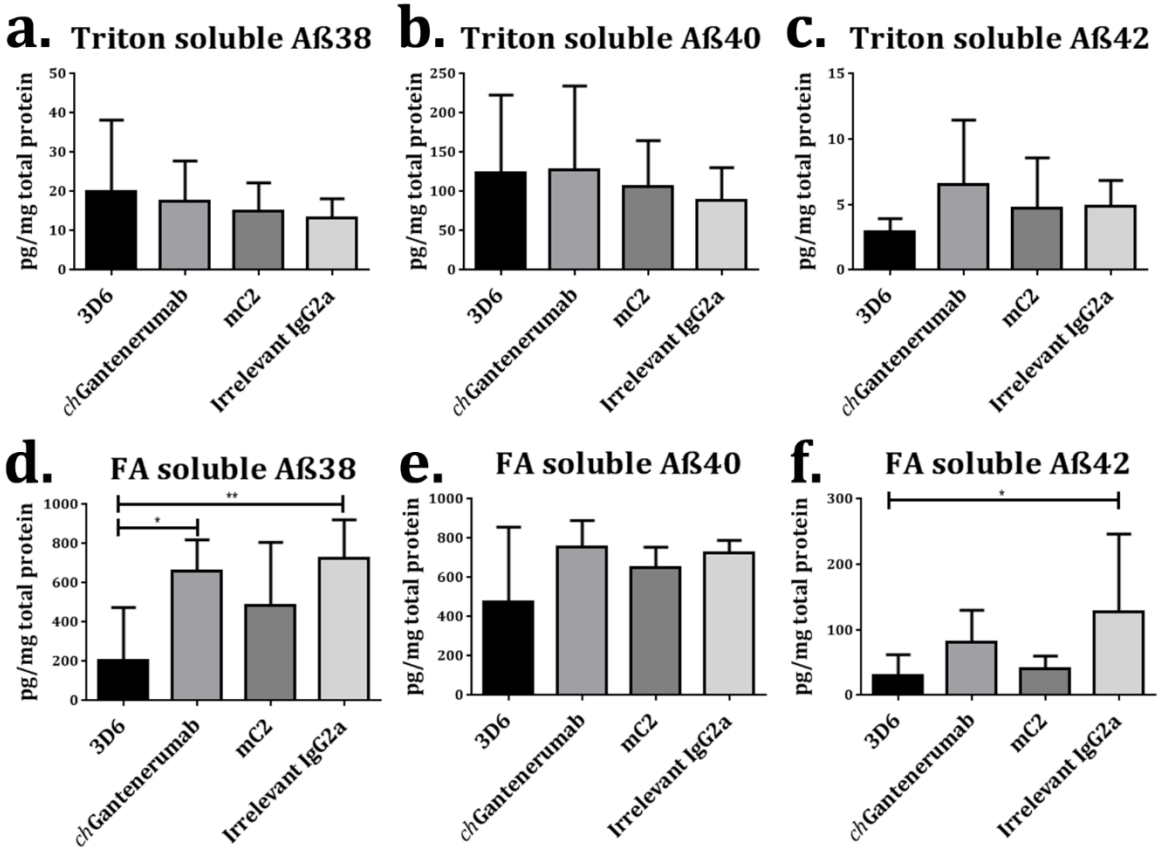

Figure 7. 2 Soluble and insoluble Aβ levels measured by ELISA

A-**C** show levels of triton soluble Aβ38, Aβ40 and Aβ42 respectively. Levels of triton soluble Aβ are not reduced at seven days post injection by any of the antibodies, however there is a trend towards decreased Aβ42 in 3D6 injected animals. **D**-**F** show levels of formic acid soluble Aβ38, Aβ40 and Aβ42 respectively. 3D6 significantly reduced the levels of formic acid soluble Aβ38, and Aβ42 compared to control antibody (** $p<0.01$, *$p<0.05$). MC2 and chGantenerumab do not have a significant effect compared to control.

7.3.2 Inflammatory changes

Neuroinflammation is thought to be a cause of side effects in patients treated with anti-Aβ antibodies, therefore we compared the ability of each of the antibody to induce inflammation after intracerebral injection. We first analysed changes in microglial phenotype by immunohistochemistry. Injection of 3D6 induced a significant increase in the hippocampal expression of microglial marker CD11b, compared to injection with mC2 and irrelevant IgG2a (Figure 4a-h, p=0.0023 and p=0.0017 respectively). *ch*Gantenerumab also induced CD11b upregulation in comparison to mC2 and irrelevant IgG2a (p=0.0093 and p=0.007 respectively). We have previously shown CD11b to be up-regulated after IgG immune complex formation in the brain (Teeling et al., 2012), suggesting that the increase in CD11b may be due to FcγR binding and subsequent activation of microglia. To assess phagocytic activity we analysed expression levels of CD68 and detected increased hippocampal CD68 expression on microglia in 3D6 injected animals, but not in chGantenerumab injected animals, although the increase was not significantly different (Figures 7.5, p=0.08). Sections were also stained for FcγRI expression following injection of antibody (Figure 7.4q-x). Injection of mC2 significantly increases the expression of FcγRI in the hippocampus in comparison to animals injected with chGantenerumab (Figure7.5, p=0.024). Figure 4y-af show staining for mouse IgG, and there is evidence of target engagement by all three anti-Aβ antibodies following intracranial injection, as plaques are positive for IgG. Quantification shows that *ch*Gantenerumab has significantly higher levels of IgG than control injected animals (Figure 7.5 p=0.011). Unlike *in vitro* binding assays, there was no evidence of the *ch*Gantenerumab binding to neurons. Also there were no significant changes in the expression of immune receptors of IgG surrounding the pial membrane.

I showed that *in vitro*, all three Aβ antibodies engage FcγRs resulting in macrophage activation and TNFα secretion. Therefore we next investigated the neuro-inflammatory potential *in vivo*. Injection of 3D6 leads to significantly increased levels of pro-inflammatory cytokines TNFα and IL-1β compared to IgG2a control (Figure 7.6a p=0.0042, 7.6b p=0.0262). Increased levels of KC/GRO in 3D6 injected animals was observed, although this did not reach significance (Figure 7.6d p=0.10). Injection of *ch*Gantenerumab also results in increased neuroinflammation, while mC2 did not affect any cytokine levels measured. These observations suggest that high affinity IgG2a anti-Aβ antibodies reduce Aβ load but this is associated with increased neuroinflammation.

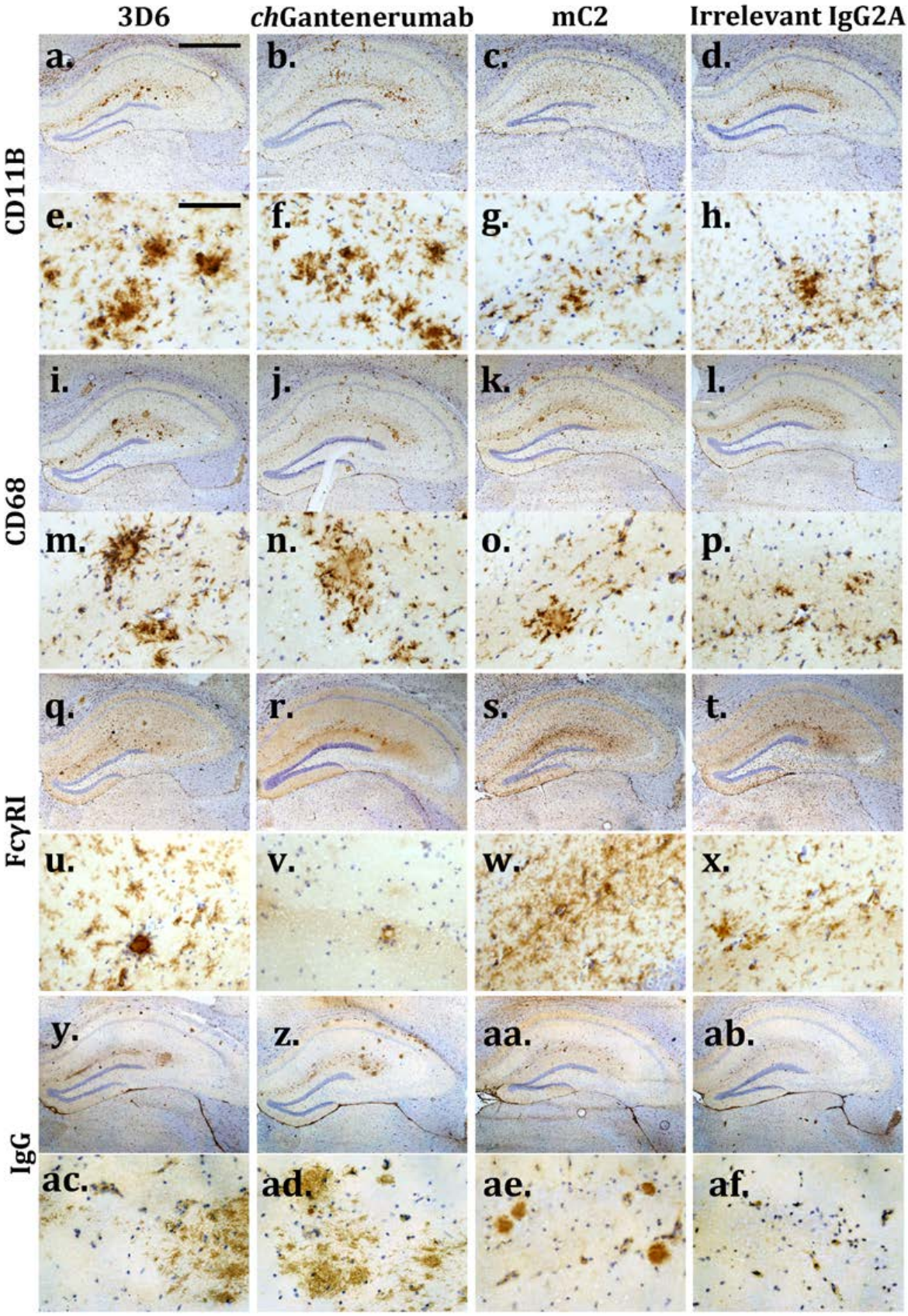
3D6
chGantenerumab
mC2
Irrelevant IgG2A
CD11B
CD68
FcγRI
IgG
a.
b.
c.
d.
e.
f.
g.
h.
i.
j.
k.
l.
m.
n.
o.
p.
q.
r.
s.
t.
u.
v.
w.
x.
y.
z.
aa.
ab.
ac.
ad.
ae.
af.

Figure 7. 3 Expression of microglial activation markers after antibody injection

Expression of microglial markers CD11b and CD68 and IgG distribution in the hippocampus seven days after injection of anti-Aβ antibodies. **a**-**h.** Representative images of CD11b expression. **i**-**p.** Representative images of CD68. **q**-**x** Representative images of FcγRI expression. **y**-**af.** IgG distribution following intracerebral injection of antibody. Pictures are taken with a 5x objective and 40x objective, scale bars are 100μm and 800μm respectively. Quantification of staining is shown in figure 7.5

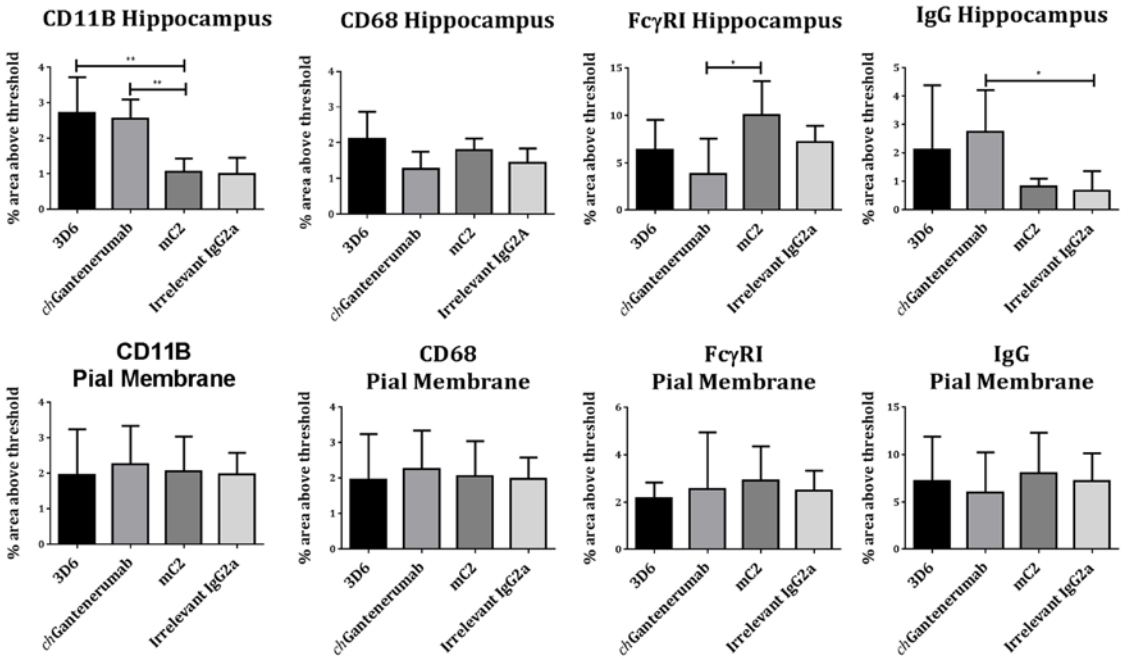

Figure 7. 4 Quantification of Immunohistochemistry

Four markers were quantified (for images see figure 7.4), in two separate brain regions: the hippocampus and pial membrane. Images were taken with a 20x objective and staining was quantified as percentage area above threshold using the freeware imageJ. Staining was quantified as area above threshold of staining and analysed by one way ANOVA and Tukey post hoc test (n=6/7). 3D6 induced a significant increase in the expression of CD11b, compared to injection with mC2 and irrelevant IgG2a (Figure 4a-h, p=0.0023 and p=0.0017 respectively). *ch*Gantenerumab also induced CD11b upregulation in comparison to mC2 and irrelevant IgG2a (p=0.0093 and p=0.007 respectively). *ch*Gantenerumab has significantly higher levels of IgG than control injected animals (p=0.011).

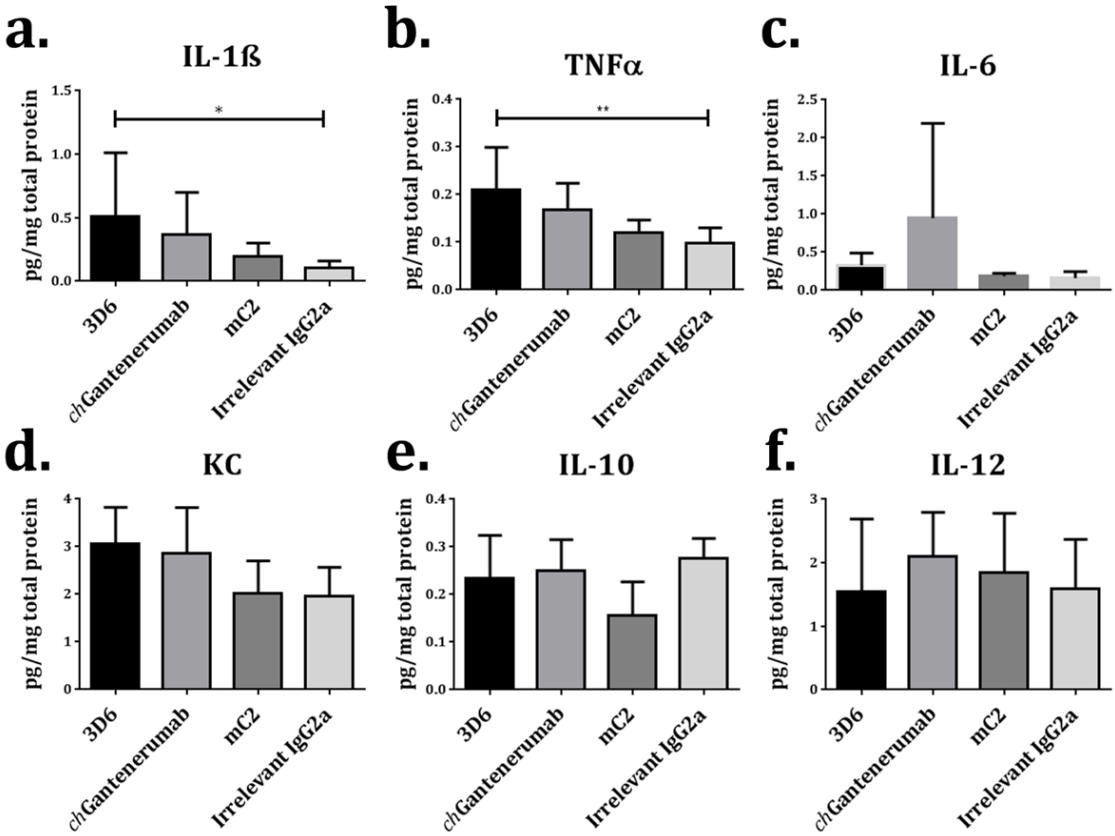

Figure 7. 5 Cytokine levels in hippocampus following intracranial injection of anti- Aβ mAbs

Cytokine levels were measured in homogenate made from hippocampal punches taken from TG2576 mice injected with antibodies. Peptide levels were measured by multiplex ELISA and normalised to total protein concentration. **a-f** show cytokine levels in hippocampal punches expressed as pg/mg total protein. Injection of 3D6 leads to significantly increased levels of pro-inflammatory cytokines TNFα and IL-1β compared to IgG2a control (**a** p=0.0042, **b** p=0.0262). Data were analysed by one-way ANOVA and Tukey post hoc test (n=6/7), and presented as mean +/-SD.

7.4 Discussion

There have been a number of high profile clinical disappointments for anti-Aβ immunotherapy, with Bapineuzumab, Solanezumab, Crenezumab and Gantenerumab all failing to show disease modifying effects in clinical trials. Differences in: epitope and affinities for Aβ, FcγR affinity and the preclinical models used for characterisation make direct comparison difficult. Therefore, to better understand the underlying biological mechanisms, we compared three highly characterised clinical candidates, Bapineuzumab, Gantenerumab and Crenezumab for their ability to clear plaques and induce neuroinflammation in an experimental model of Alzheimer's disease (TG2576). We generated murine, recombinant versions of Bapineuzumab (3D6), Crenezumab, (mC2) and a mouse/human chimeric version of Gantenerumab (*ch*Gantenerumab).These antibodies were produced using the same murine IgG2a constant regions, and were injected intra-cranially into 18 month TG2576 mice. The murine IgG2a constant region is most similar to human IgG1 and has a strong ability to activate human FcγRs and induce inflammation (Bruhns, 2012). We are not aware of previous studies that directly compare murinised versions of Bapineuzumab, Crenezumab and Gantenerumab for their ability to clear plaques and induce inflammation.

In **chapter 3** I showed that all IgG2a antibodies bind to recombinant immobilized peptide and plaques present in the TG2576 brain tissue sections, with 3D6 displaying the highest relative affinity to Aβ. The antibody *ch*Gantenerumab also bound with high affinity to immobilized Aβ peptide, but showed strong binding to neurons in cryo-sections of both transgenic and wild type animals. mC2 was able to bind Aβ peptide *in vitro* and plaques *in vivo*, but the relative affinity was 100-fold weaker than for 3D6. These observations are relevant for biological function, as 3D6, which had the strongest affinity for Aβ plaques in our model, was the only antibody to significantly reduce Aβ levels *in vivo*. 3D6 injection also induced the activation of microglia as measured by their increase in CD11b expression and increased levels of the pro-inflammatory cytokines, IL-1b and TNFα. One of the mechanisms of antibody mediated plaque clearance is through activation of microglia FcγRs and phagocytosis (Wilcock et al., 2003; Wilcock et al., 2004a). Cross linking of FcγRs by immune complexes leads to switching to an "M2b" phenotype (Mosser and Edwards, 2008), characterised by the production of reactive oxygen species and pro-inflammatory cytokines., including IL-1β and TNFα. The antibody subclass we used for this experiment, mouse IgG2a, is a potent inducer of inflammation due to its high affinity for activating receptors (Bruhns et al., 2009). It has previously been shown that the IgG2a version of the anti-pyroglutamate mE8 is better at

clearing plaques than an IgG1 version (with lower FcγR affinity), implying that FcγRs are involved in the clearance of plaques (DeMattos et al., 2012). Gantenerumab did not significantly reduce the levels of Aβ, but detection of mouse IgG bound to plaques provides clear evidence for target engagement. Like 3D6, increased expression of CD11b was observed but minimal change in CD68 expression levels suggest less efficient phagocytosis following injection of *ch*Gantenerumab. As all antibodies were generated as IgG2a isotypes, this lack of phagocytosis and plaque clearance is not due to lack of effector function, but rather dependent on the affinity and/or epitope. 3D6 and *ch*Gantenerumab both bind to residues in the N-terminus of Abeta however *ch*Gantenerumab has a conformational epitope and also binds to residues in the mid domain. *ch*Gantenerumab has a lower EC50 in our Aβ40 binding ELISA, when compared to 3D6 (0.34 pM vs 0.17 pM, respectively) and therefore, clearance of plaques may require more time- this is supported by the changes in microglial phenotype and cytokine production. The antibody mC2 was unable to clear Aβ plaques seven days post injection, but unlike *ch*Gantenerumab, this antibody did not induce any detectable changes in microglial phenotype or cytokine levels, despite having similar effector function. Immunoreactivity for mouse IgG strongly implies that the lack of clearance is due to poor plaque engagement, as IgG levels were not different from control IgG2a antibody. mC2 binds to a mid-domain epitope (AA 16-24) and studies of other antibodies that bind this region such as, m266 (Solanezumab), suggest that this epitope is inaccessible when Aβ is in aggregated forms and this prevents antibodies like m266 from binding to and clearing plaques (Dodart et al., 2002). In fact the CDR sequences of Solanezumab and Crenezumab are very similar, suggesting that their binding to Aβ would be comparable (Watt et al., 2014). This is supported by binding to formic acid treated sections, which shows that mC2 requires the solubilisation of plaques with formic acid to bind. Our results demonstrate that targeting the N-terminus of Aβ is more effective for plaque clearance.

AD patients treated with Bapineuzumab or Gantenerumab have developed dose limiting vascular side effects (ARIAs), but the underlying mechanism are not completely understood. There is evidence that activation of microglia, and/or perivascular macrophages through FcγRs and the subsequent neuro-inflammation may be partly responsible for these side effects. It has been shown that reduced binding to FcγR can decrease the incidence of vascular damage in mice (Carty et al., 2006; Freeman et al., 2012; Wilcock et al., 2006). In this study we provide further experimental evidence that antibody engagement with activating FcγRs generates a pro-inflammatory response in the brain, as IgG2a versions of 3D6 and *ch*Gantenerumab both resulted in microglial activation and elevated cytokine production. The clinical candidate Crenezumab is built on a hIgG4

backbone, which has significantly reduced FcγR affinity compared to hIgG1. This was aimed to reduce the inflammatory response to immunotherapy and therefore reduce the associated side effects, and indeed ARIAs were not reported in patients treated with 10x the maximal dose of Bapineuzumab (Adolfsson et al., 2012). Our study provides an alternative explanation for the lack of side effects: the lack of plaque engagement by the antibody. We show that intracranial injection of an IgG2a murine version of Crenezumab-mC2, failed to clear plaques or induce a pro-inflammatory response. These observations suggest that inflammation related to immunotherapy is not just dependent on the ability of the antibody to engage FcγRs but also on the epitope and ability of the antibody to engage plaques.

The expression of the activating receptor FcγRI was also measured following intracerebral injection of the antibodies. Interestingly the levels of FcγRI expression were significantly higher after mC2 injection than chGantenerumab. The levels of FcγRI were marginally but not significantly higher in mC2 injected compared to irrelevant IgG2a injected animals. Therefore the differential expression of FcγRI could be due to an upregulation following phagocytosis of immune complexes of mC2 and Aβ. However, in most of the mice examined after chGantenerumab injection, the levels of FcγRI expression in the hippocampus were much lower than you would expect based on data from chapter **4.** Therefore the difference in FcγRI detection could be due to reduced expression in the *ch*Gantenerumab injected animals. The antibodies were all produced on an IgG2a constant domain, which ligates FcγRI with high affinity (Bruhns, 2012). The *ch*Gantenerumab animals also had the highest levels of IgG in the brain seven days after intracerebral injection. Therefore the reduced detection of FcγRI after *ch*Gantenerumab injection could be due to the occupancy of FcγRI by antibody bound to plaques, preventing the detection of FcγRI by immunohistochemistry.

3D6 and mC2 are not exactly the same as the final clinical candidates; Bapineuzumab and Crenezumab. This could mean there are slight differences in the binding affinity which could influence the rate of Aβ clearance and inflammation; therefore extrapolating these data should be done with caution. However the clinical antibodies share the same epitope and are incredibly similar in sequence, and therefore the response is likely to be similar. Intra-cranial injection is a useful technique allowing rapid and cost efficient characterisation of the response to an antibody, however there are some limitations to this approach. To limit injection mediated tissue damage, we use pulled glass capillaries to inject into the brain. However, even with caution any injection will cause some tissue damage, which may influence the subsequent immune response. Patients are not injected intra-cranially with these antibodies, and therefore injecting directly into the brain is less

relevant to the clinic than giving a systemic dose of the antibodies. To fully characterise the differences between these antibodies, a systemic trial is needed which would also allow the measurement of cognitive changes.

Treatment with 3D6 is effective at clearing plaques, however part of this response causes increased neuroinflammation. Optimized immunotherapy for AD ideally separates phagocytosis and neuroinflammation, which would allow clearance of Aβ without the induction of detrimental pro-inflammatory cytokine release. In order to achieve this, better understanding of the receptors involved in this processes is essential. We know that a range of different FcγRs are expressed in the brains of AD patients and mouse models (Cribbs et al., 2012; Fuller et al., 2014; Peress et al., 1993), but the physiological role of these receptors in the brain and their relative contribution to neuroinflammation and plaque clearance remains poorly understood. 3D6 has strong target binding and a high risk of causing vascular side effects and inflammation, therefore to minimise toxicity reduction of its effector function will likely be beneficial. In contrast, mC2 with lower target binding, might need stronger FcγR binding to increase efficacy. Based on our results, we conclude that reduction of the effector function of Crenezumab did not have the expected beneficial effects, and the lack of clinical efficacy may be due to its lower plaque engagement, in fact the engagement of Aβ by Crenezumab has been questioned previously (Watt et al., 2014). This is the first time to our knowledge that three clinical candidates have been directly compared *in vivo*, finding that the neuro-inflammatory response and ability to clear plaques are dependent on the specificity of antibody variable regions.

Chapter 8: The effect of systemic infection with *Salmonella Typhimurium* on TG2576 mice.

8.1 Introduction

The concept of immune privilege describes the brain's protection from the peripheral immune system. This is due to the presence of a blood brain barrier (BBB), which tightly regulates the entry of cells and proteins into the brain (Zlokovic, 2008). It was once thought that the brain was completely isolated from peripheral immune responses, however it is now clear that the immune system can communicate with the brain in a number of ways and that the brain plays an integral role in the body's response to infection. This is illustrated by changes in behaviour and physiology that the brain orchestrates when you become ill. For example, after contracting an infection you feel lethargic and anti-social and your core body temperature increases. These changes are collectively termed sickness behaviours, which improve pathogen elimination and prevent the spread of illness to other people (Hart, 1988). Whilst this is beneficial for healthy adults, in a diseased or ageing brain the response to peripheral infection is exacerbated, which may affect the rate of cognitive decline. AD patients with peripheral immune activation exhibit decreased cognition and accelerated cognitive decline (Holmes et al., 2011; Holmes et al., 2009; Holmes et al., 2003). As well as accelerating cognitive decline of AD, there is also a role for the immune system in the development of disease, as a number of immune gene polymorphisms are associated with increased risk of developing AD (Chen et al., 2012; Hollingworth, 2011; Lambert, 2013). It has also been found that certain infections such as: chronic periodontitis or *Chlamydia pneumoniae* are associated with AD (Hammond et al., 2010; Stein et al., 2012).

To understand the brain's response to peripheral inflammation, mimetics of infections such as: LPS (gram negative bacteria), zymosan (yeast) or poly I.C. (virus) have been used in rodent models. Dosing mice with LPS leads to increased brain immune-receptor expression and cytokine levels, which are accompanied with behavioural changes (Dantzer and Kelley, 2007). Our lab have shown that microglia in the brains of mice with a neurodegenerative disease, are primed to respond to LPS, and that this is associated with increased microglial FcγR expression (Lunnon et al., 2011). Repeated dosing of LPS leads to the accumulation of Aβ in both wild type and transgenic APP mice due to increased β-secretase activity (Lee et al., 2008; Sheng et al., 2003b), and LPS treatment of mice transgenic for human tau results in the increased phosphorylation and accumulation of tau in neurons (Kitazawa et al., 2005). Pre-natal challenge of wild type and APP transgenic mice with the viral mimetic poly I.C. results in increased cytokine level, Aβ deposition and tau phosphorylation in adult life upon re-stimulation with the viral mimetic (Krstic et al., 2012). These studies demonstrate

that peripheral inflammation can promote two neuro-pathological hallmarks of AD, strengthening the hypothesis that inflammation is involved in the underlying pathology.

Whilst LPS is a useful tool for measuring the acute responses to an immune stimulus, it does not accurately model a real infection. Our lab have previously shown that infection with the attenuated bacterium *Salmonella typhimurium* SL3261 (*S. typhimurium*) leads to a completely different neuro-inflammatory and behavioural response compared to repeated injection of LPS (Puentener et al., 2012). There is limited published work investigating the effect of real life infections on AD pathology in the brain of mice. (Little et al., 2004; McManus et al., 2014).

In this chapter I have characterised the response of TG2576 mice to infection with an attenuated strain of the bacterium *S. typhimurium (SL3261)*. Twelve month old transgenic mice and wild type littermates, were infected with either $1x10^6$ CFU of *S. typhimurium* or saline, and tissue was collected at one and four weeks post infection. The hypothesis of this experiment is that TG2576 mice with pre-existing neuro-pathology will have an exacerbated neuro-inflammatory response to infection compared to wild type littermates, and that this will worsen the Aβ pathology in the brain. If peripheral infection leads to the activation and/or priming of microglial cells, including the increased expression of activating FcγRs, this could have implications for immunotherapy as this could drive an exacerbated response to anti-Aβ antibody therapy and increase the severity/frequency of side effects.

8.2 Methods

8.2.1 Study design

Twelve month old TG2576 mice and wild type littermates were randomly assigned to one of four groups (n=8, 5 male, 3 female): saline one week, saline four weeks, *S. typhimurium* one week or *S. typhimurium* four weeks. Due to space restrictions in the CL2 facility, the mice were split into two separate cohorts, each with n=4 mice from each group. Each cohort was moved into the CL2 facility 24 hours before infection to acclimatise to the new environment. Mice were then injected I.P. with saline or 1x 10^6 CFU/ml *S. typhimurium*. One day prior to sacrifice, mice were moved into a new individual cage to assess nesting behaviour. On the day of sacrifice, the nesting building was assessed by Mr Alexander Collcutt, who remained blinded to the treatment and genotype throughout. The mice were given an overdose of avertin, the right atrium was pierced and 0.5ml of blood was collected. The mice were then transcardially perfused and the brain, spleen and retinas were harvested for biochemistry cytokine protein levels (mesoscale), Aβ load (mesoscale), and immunohistochemistry.

8.2.2 Quantification of immunohistochemistry

With the exception of the number of CD3+T-cell number in the brain, immunohistochemistry was analysed as described in chapter 2. To quantify T-cell entry into the brain, sections were stained for the T-cell receptor (CD3) and the number of T-cells in the hippocampus were counted which was normalised to hippocampal area. The quantification was performed by a summer student Miss Sophie Thornton, who was blinded for the analysis.

8.2.3 Statistical analysis

For changes in: spleen weight, immune receptor expression, cytokine levels and nesting behaviour, the normality of data sets was tested by calculating residuals and using the D'Agostino Pearson omnibus test. Parametric data was then analysed using 2-way ANOVA and TUKEY post hoc testing (corrected for multiple comparisons). Non parametric data was transformed using the function Y=LogY and residuals were then tested for normality, if normally distributed the log values were analysed in the way described. If the data set was still not normally distributed non

parametric tests; Kruskal-Wallis and Dunn's post hoc test were employed. Weight change data was analysed using 3-way repeated measures ANOVA, using the Greenhouse-Geisser correction for violation of sphericity. Finally, Aβ protein levels was analysed using either a two-tailed t test or Mann Whitney U test depending on the normality of the data. Correlation analysis was performed on pooled data from *S. typhimurium* infected animals from the one week time point. All statistics were performed using Graphpad prism, with the exception of 3-way repeated measures ANOVA which was done using SPSS.

8.3 Results

8.3.1 Weight changes

An important part of our response to infection is to adapt behaviour to reduce the spread of pathogens and enhance the immune system's ability to fight infection. These behavioural changes are termed "sickness behaviours", which include loss of appetite (anorexia) causing weight loss (Hart, 1988). Figure 1A shows the percentage weight change of 12 month old TG2576 mice and wild type littermates after infection with *S. typhimurium* or injection with saline. At one day post infection both TG2576 and wild type mice infected with *S. typhimurium* lose around 5% body weight whereas saline injected controls do not. Body weight of TG2576 mice returns to baseline by seven days post infection. In contrast, wild type mice infected with *S. typhimurium* do not fully re-gain the weight lost over the entire 28 day time course. Statistical analysis demonstrates that infection with *S. typhimurium* results in a significant weight change compared to saline injected animals ($p<0.0001$). This analysis also reveals a significant interaction between *S. typhimurium* and the genotype ($p=0.039$), indicating that TG2576 and wild type mice respond differently to infection. It has been reported that triple transgenic mouse model of AD (APP/PS1/P301L htau), have a greater food intake than wild type littermates and are more metabolically active. This results in higher body weight in young triple transgenic mice compared to wild type, but lower body weight in 18 month old triple transgenic mice (Knight et al., 2012). The differential effect of *S. typhimurium* is not explained by different starting body weight; as figure 1B shows there is no difference in initial weight when wild type and TG2576 mice are compared. We did not measure food intake during this study.

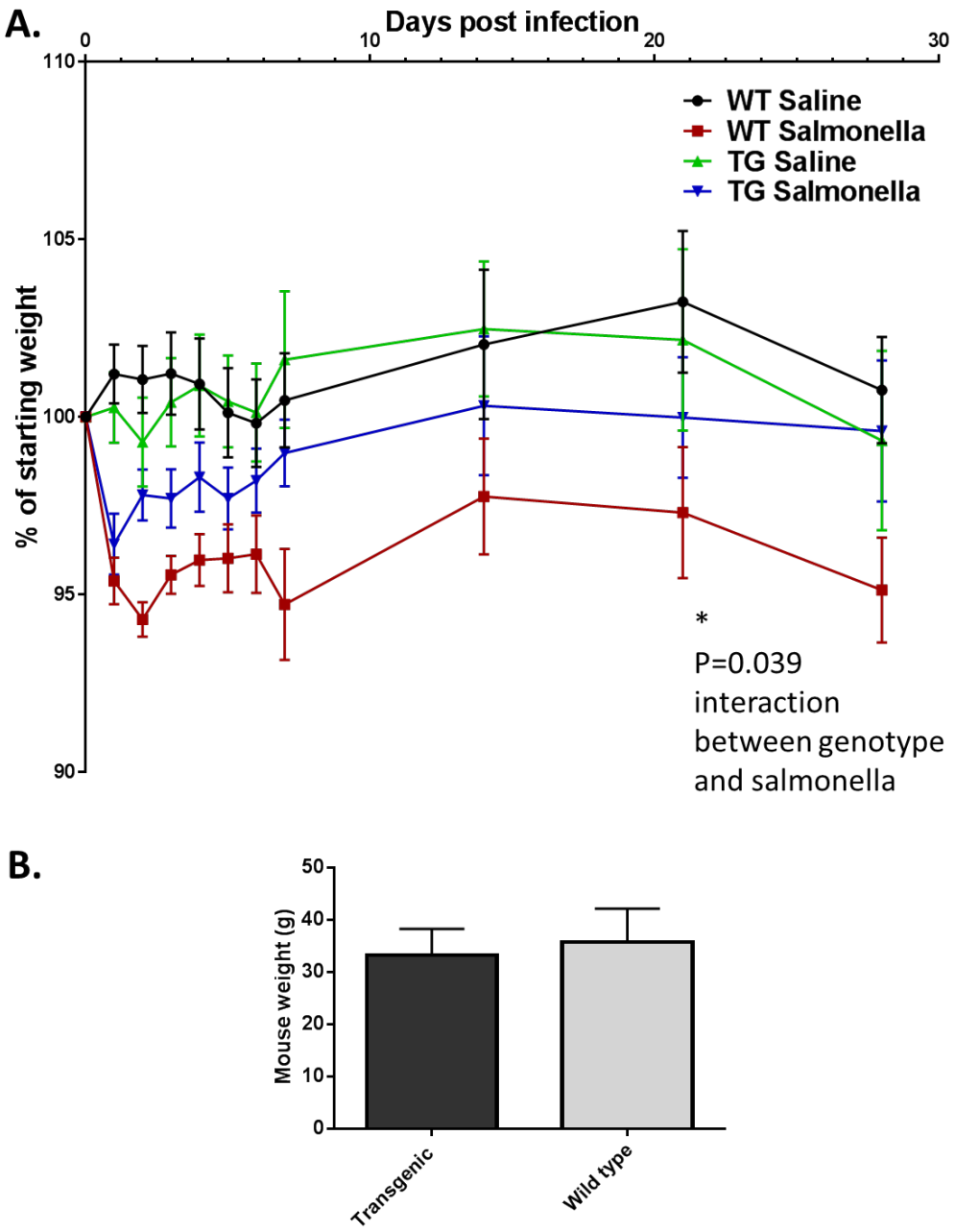

Figure 8. 1 Body weight change of TG2576 and wild type mice after infection with *S. Typhimurium,* and starting body weight.

Mice were weighed daily after infection with *S. typhimurium* for one week, and then once weekly thereafter. **A.** shows the average percentage of starting weight for 30 days after infection with *S. typhimurium* or injection of saline, in wild type or TG2576 mice. The data was analysed using 3-way ANOVA with repeated measures (n=8), and presented as mean and standard deviation. The analysis shows that infection with *S. typhimurium* causes a significant reduction in body weight ($p<0.0001$). There was also a significant interaction with genotype ($p=0.039$). **B.** Average starting weight of TG2576 mice and wild type littermates. Data analysed by two tailed T-test (n=32), and presented as mean and standard deviation.

8.3.2 Peripheral immune response

S. typhimurium is an intracellular bacterium that primarily infects phagocytic cells such as macrophages (Coburn et al., 2006). This infection of immune cells results in the colonisation of immune tissue such as the spleen. The subsequent activation and proliferation of immune cells results in the enlargement of the spleen (splenomegaly), aged TG2576 mice have enlarged spleens compared to littermates, possibly indicating immune activation (unpublished observations). Figure 8.2 shows spleen weight of wild type and TG2576 mice at one and four weeks post infection. *S. typhimurium* infection results in a significant increase in spleen weight at both one ($p<0.0001$) and four weeks ($p<0.0001$) post infection when compared to saline injection, but no difference between wild type and TG2576 mice was observed at either time point.

The peripheral immune response to *S. typhimurium* was also measured by serum cytokine levels at one (figure 8.3) and four (figure 8.4) weeks. At one week post injection, *S. typhimurium* infection increased serum levels of IFNγ, IL-6 and TNFα (300 fold ($p<0.0001$), 400 fold ($p<0.0001$) and 100 fold ($p<0.0001$) respectively). Statistical analysis showed no effect of genotype on the serum cytokine levels, and no statistical interaction with *S.typhimurium*. This demonstrates that the peripheral immune response is similar in transgenic and wild type mice. At four weeks post infection, the levels of most cytokines returned to baseline levels, however, IFNγ, IL-1β, IL-6 and IL-10 remain significantly elevated albeit at lower levels compared to the one week time point. No significant effect of genotype on the serum cytokine levels at four weeks was found (figure 8.4). In conclusion, *S. typhimurium* generates a strong inflammatory response in the periphery, the markers measured were not affected by the genotype of the mouse.

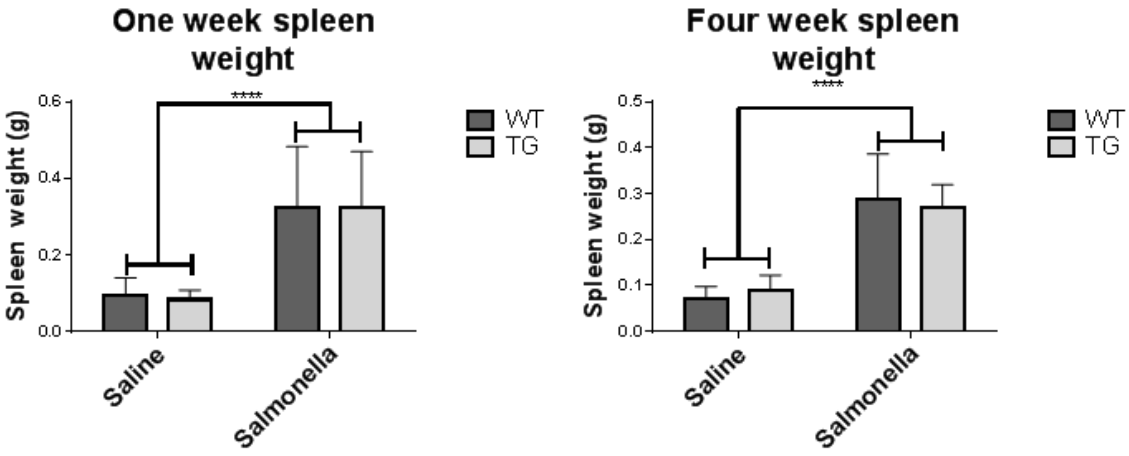

Figure 8. 2 Spleen weight at one and four weeks post infection with *S. typhimurium*

On the day of sacrifice, the spleens of mice infected with *S. typhimurium* or saline injected controls were weighed. *S. typhimurium* infection caused a significant increase in spleen weight at both one ($p<0.0001$) and four weeks ($p<0.0001$) post infection. Data was analysed by 2-way ANOVA and Tukey post hoc test, and is displayed as mean and standard deviation (n=8).

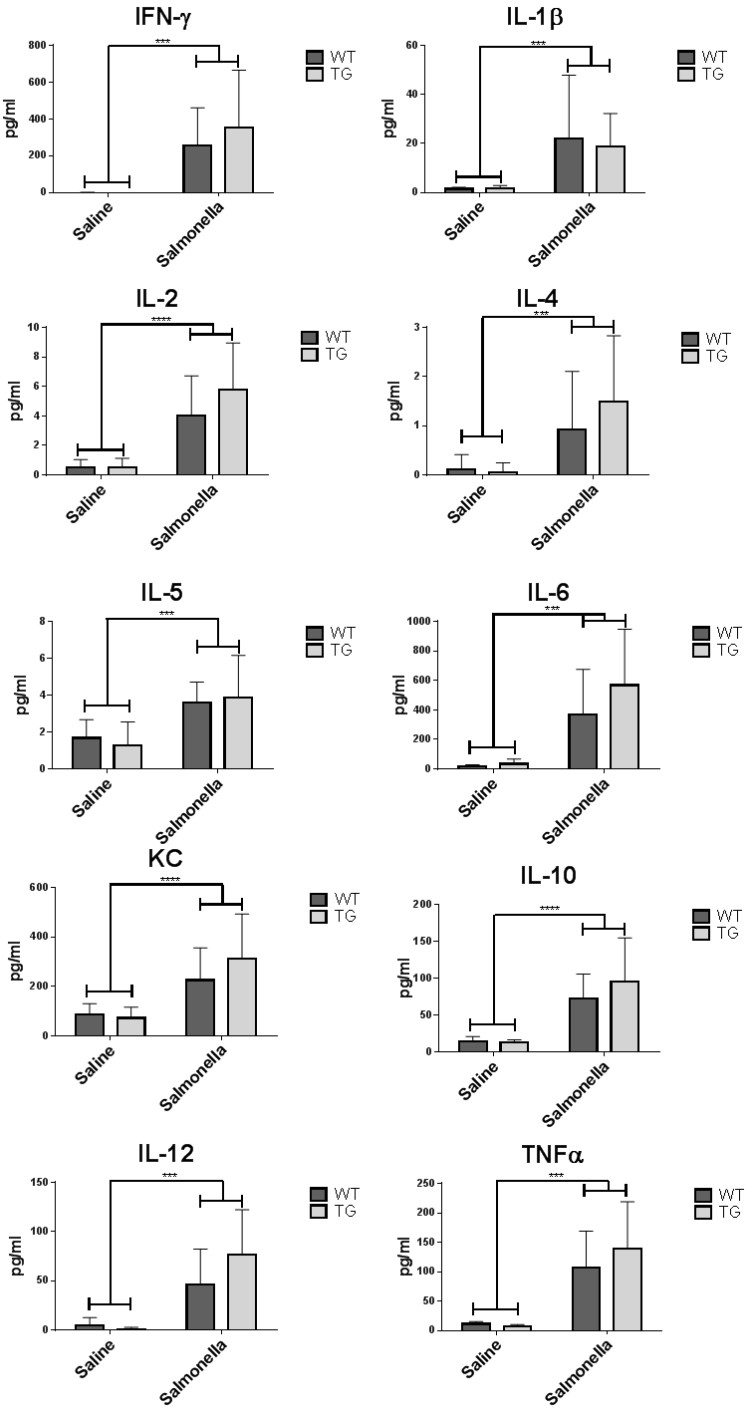

Figure 8. 3 Serum cytokine levels one week after infection with *S. typhimurium*

The levels of 10 cytokines were measured in the serum of TG2576 and wild type mice at one week post infection with *S. typhimurium* or saline, using a multiplex immune assay (MSD). Data is expressed as levels in pg/ml, and was analysed using 2-Way ANOVA, and Tukey post hoc test (n=8). Graphs depict mean and standard deviation.

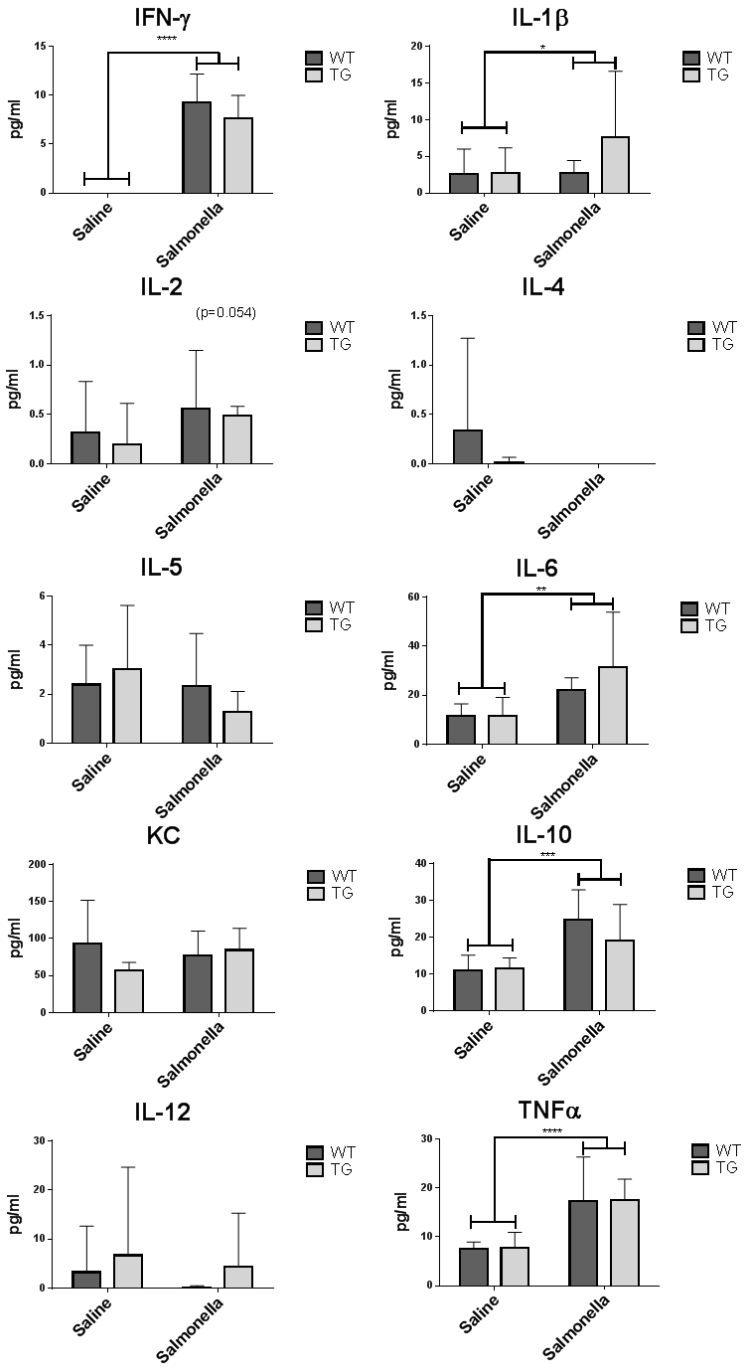

Figure 8. 4 Serum cytokine levels four weeks after infection with *S. typhimurium*

The levels of 10 cytokines were measured in the serum of TG2576 and wild type mice at four weeks post infection with *S. typhimurium* or saline using a multiplex immune assay (MSD), and are expressed in pg/ml. Data sets were analysed using 2-way ANOVA, and Tukey post hoc test (n=8). Graphs depict mean and standard deviation.

8.3.3 The neuro-inflammatory response to *S. typhimurium*

8.3.3.1 Immune phenotype changes

To monitor neuro-inflammatory changes after *S. typhimurium* infection, immunohistochemistry was used to measure changes in the expression of immune receptors in the brain. Infection with S. *typhimurium* results in a significant up regulation of MHCII in the hippocampus on cells associated with the cerebral vasculature, possibly brain endothelial cells, at one week ($p<0.0001$, fig 8.5), this increased expression persists until four weeks post infection ($p<0.0001$, fig.8.6). Higher powered images showing the morphology of cells expressing MHCII can be seen in figure 8.9B. *S. typhimurium* did not significantly affect expression of the myeloid activation markers: CD11b and CD68 at one or four weeks post infection. However, TG2576 mice had significantly higher expression of CD68 than wild type mice ($p=0.0268$, fig.8.6). It has previously been shown that peripheral inflammation can increase the expression of FcγRs in the brains of mice with a neurodegenerative disease, here we also measured the expression levels of FcγRs after *S. typhimurium* infection. At one week post infection *S. typhimurium* caused a significant increase in the expression of FcγRI ($p<0.01$ fig. 8.7). Higher powered images of FcγRI expression can be seen in figure 8.9A. Based on morphology, FcγRI is expressed on ramified microglia and perivascular cells in wild type mice. Ramified microglia and perivascular cells also express FcγRI in TG2576 mice, but cells with a larger soma and that are less ramified are clustered together, likely around plaques. There were also detectable levels of FcγRII/III and FcγRIII but *S. typhimurium* did not affect their expression, and no detectable expression of FcγRIV in the parenchyma of any group. At four weeks, *S. typhimurium* infected mice had non-significant increases in the expression of FcγRI ($p=0.07$, fig. 8.8) and FcγRII/III ($p=0.11$), again there was no effect on FcγRIII expression and no detectable FcγRIV in the parenchyma.

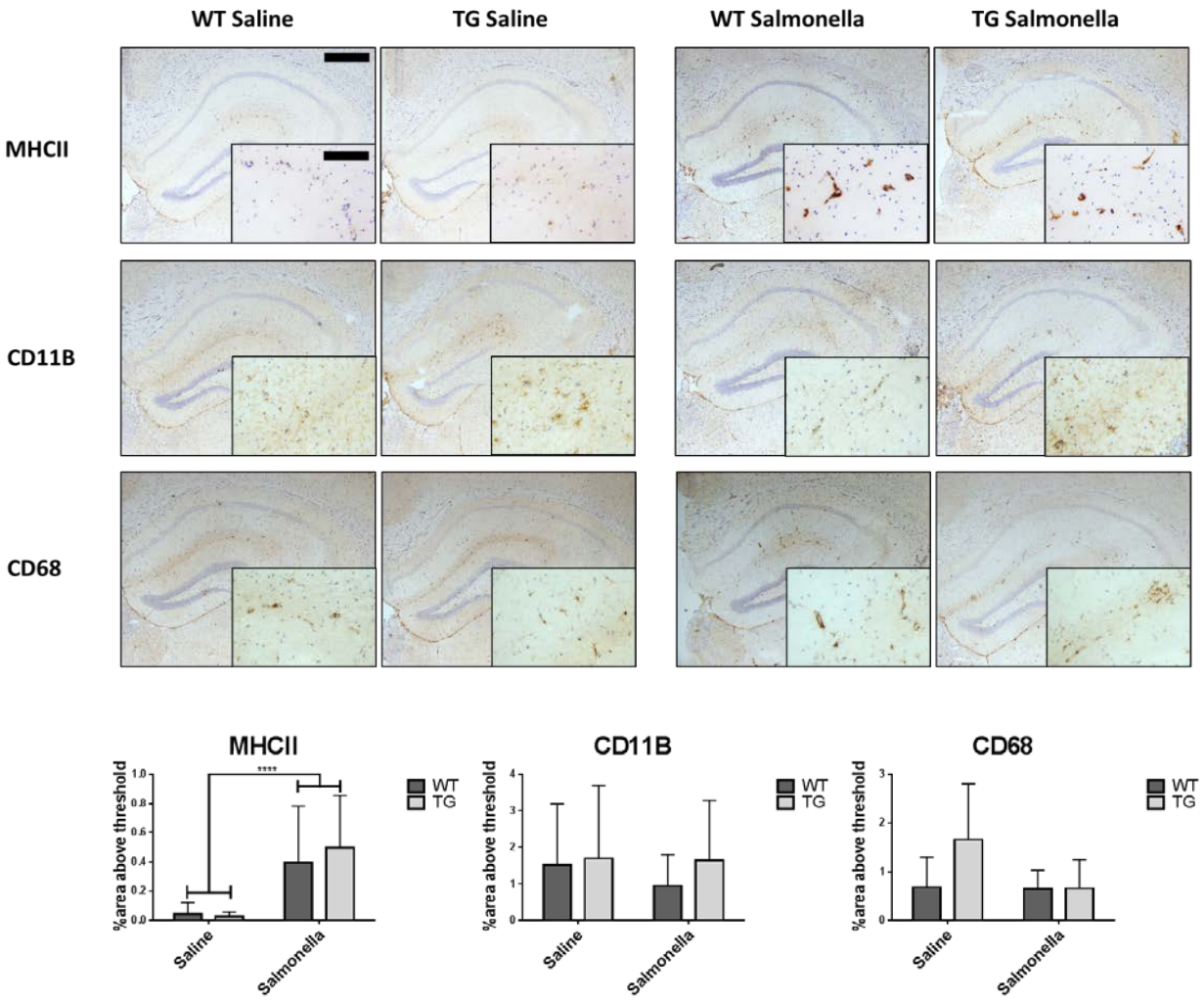

Figure 8. 5 Expression of MHCII, CD11b and CD68 in the hippocampus one week after *S. typhimurium* infection

The expression of: MHCII, CD11b and CD68 at one week post *S. typhimurium* infection(n=8, 1 section per mouse). Images are taken with a 5x objective and 20x objective, scale bars are 500μm and 125μm respectively. *S. typhimurium* infection causes significant up-regulation of MHCII on brain endothelial cells ($p<0.0001$). There were no detectable changes in the expression of microglial markers CD11b or CD68. There were no significant differences between transgenic and wild type mice. Data analysed by 2-way ANOVA and Tukey post hoc test (n=8), graphs depict mean and standard deviation.

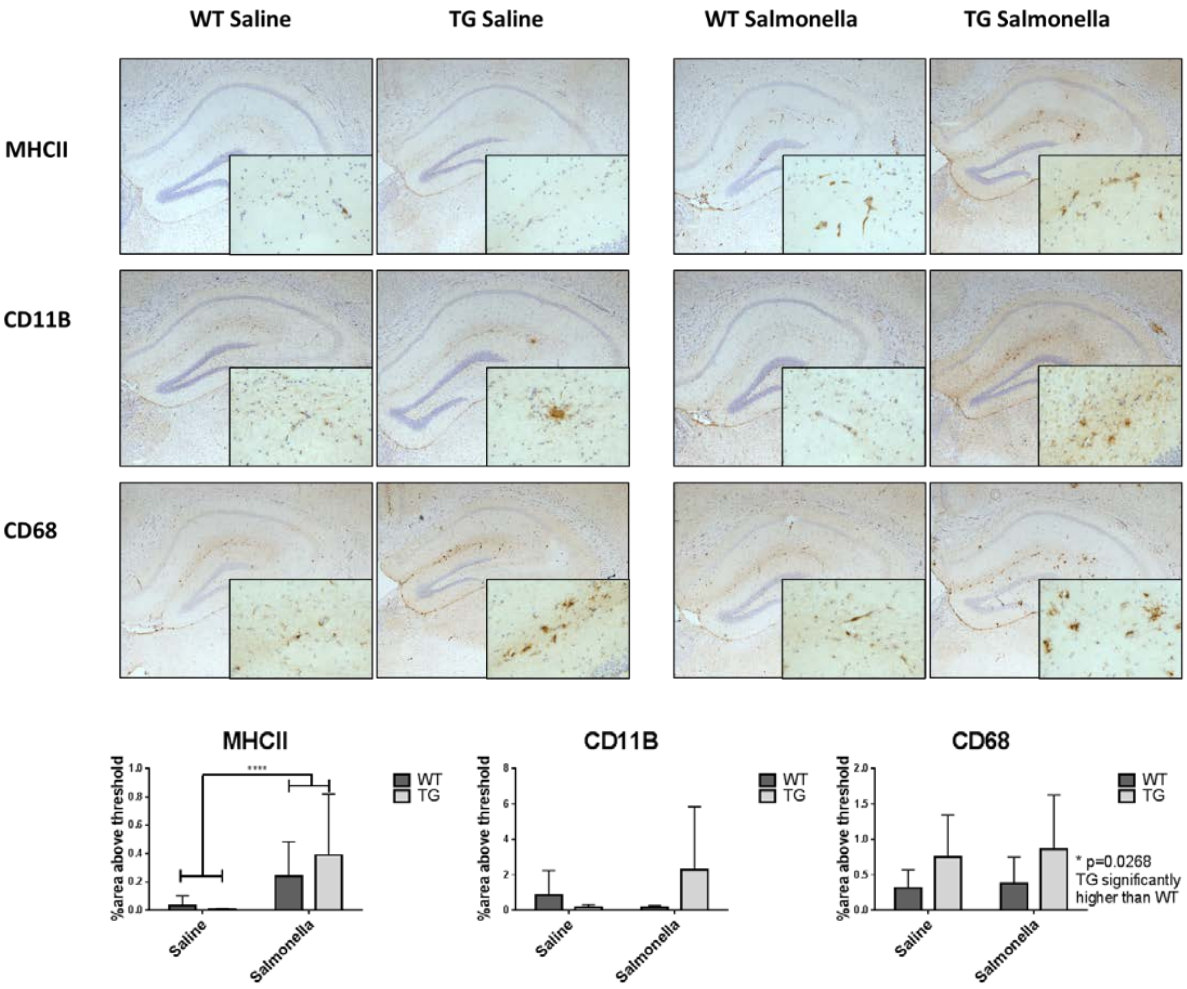

Figure 8. 6 Expression of MHCII, CD11b and CD68 in the hippocampus four weeks after *S. typhimurium* infection

The expression of: MHCII, CD11b and CD68 at one week post s.typhimurium infection. Pictures are taken with a 5x objective and 20x objective, scale bars are 500µm and 125µm respectively. *S.typhimurium* infection causes significant up-regulation of MHCII on brain endothelial cells ($p<0.0001$). There were no detectable changes in the expression of microglial markers CD11b or CD68. There were no significant differences between transgenic and wild type mice. Data analysed by 2-way ANOVA and Tukey post hoc test (n=8), graphs depict mean and standard deviation.

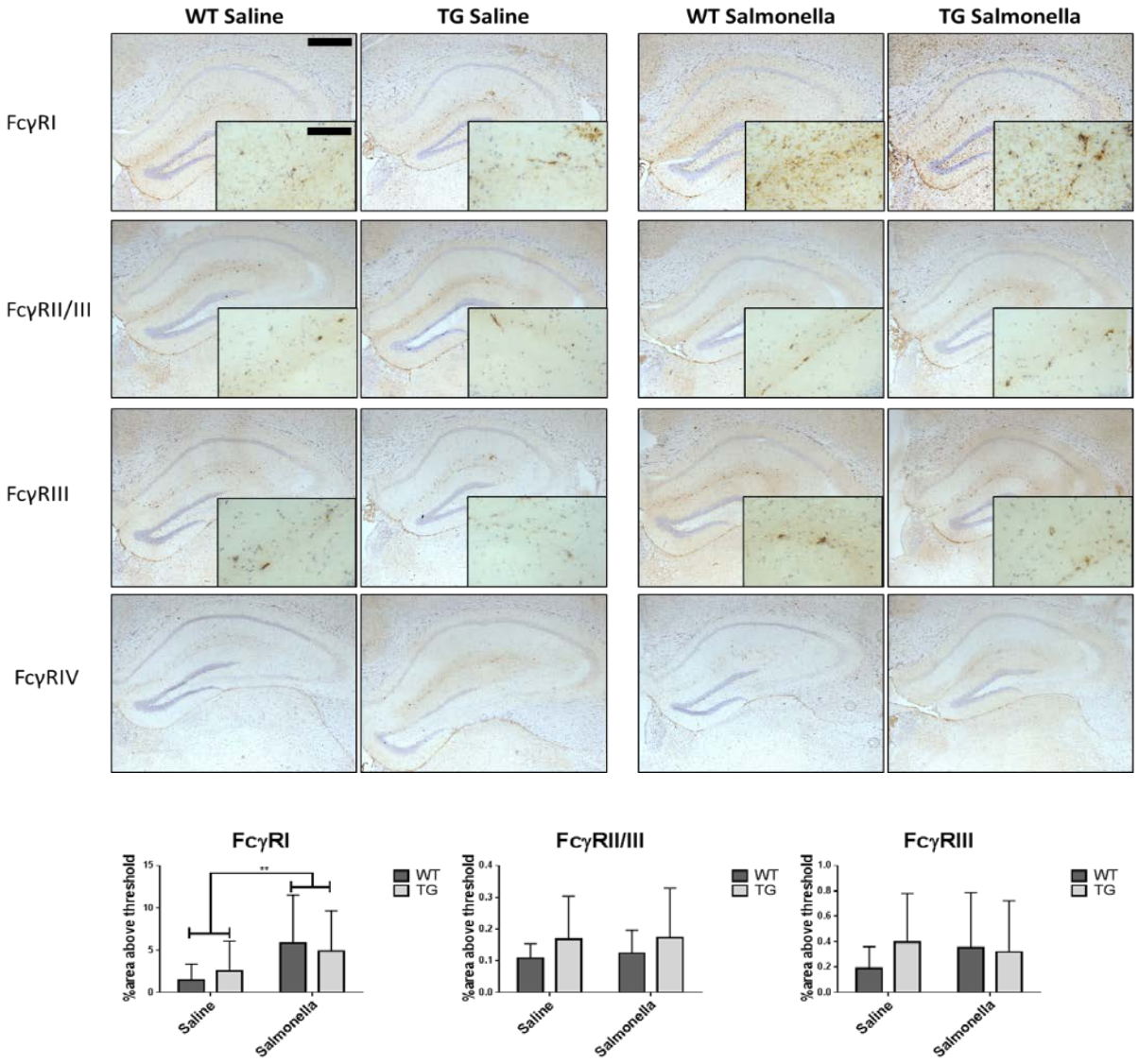

Figure 8. 7 Expression of FcγRs in the hippocampus at one week post infection with *S.typhimurium*

Expression of FcγRs one week after *S. typhimurium* infection. Pictures are taken with a 5x objective and 20x objective, scale bars are 500μm and 125μm respectively. *S. typhimurium* infection causes significant up-regulation of FcγRI ($p<0.01$) there was no difference in the response of TG2576 and WT animals. *S. typhimurium* did not affect the expression levels of FcγRII/III or FcγRIII, and there was no significant expression of FcγRIV in any group. Data analysed by 2-way ANOVA and Tukey post hoc test (n=8), graphs depict mean and standard deviation.

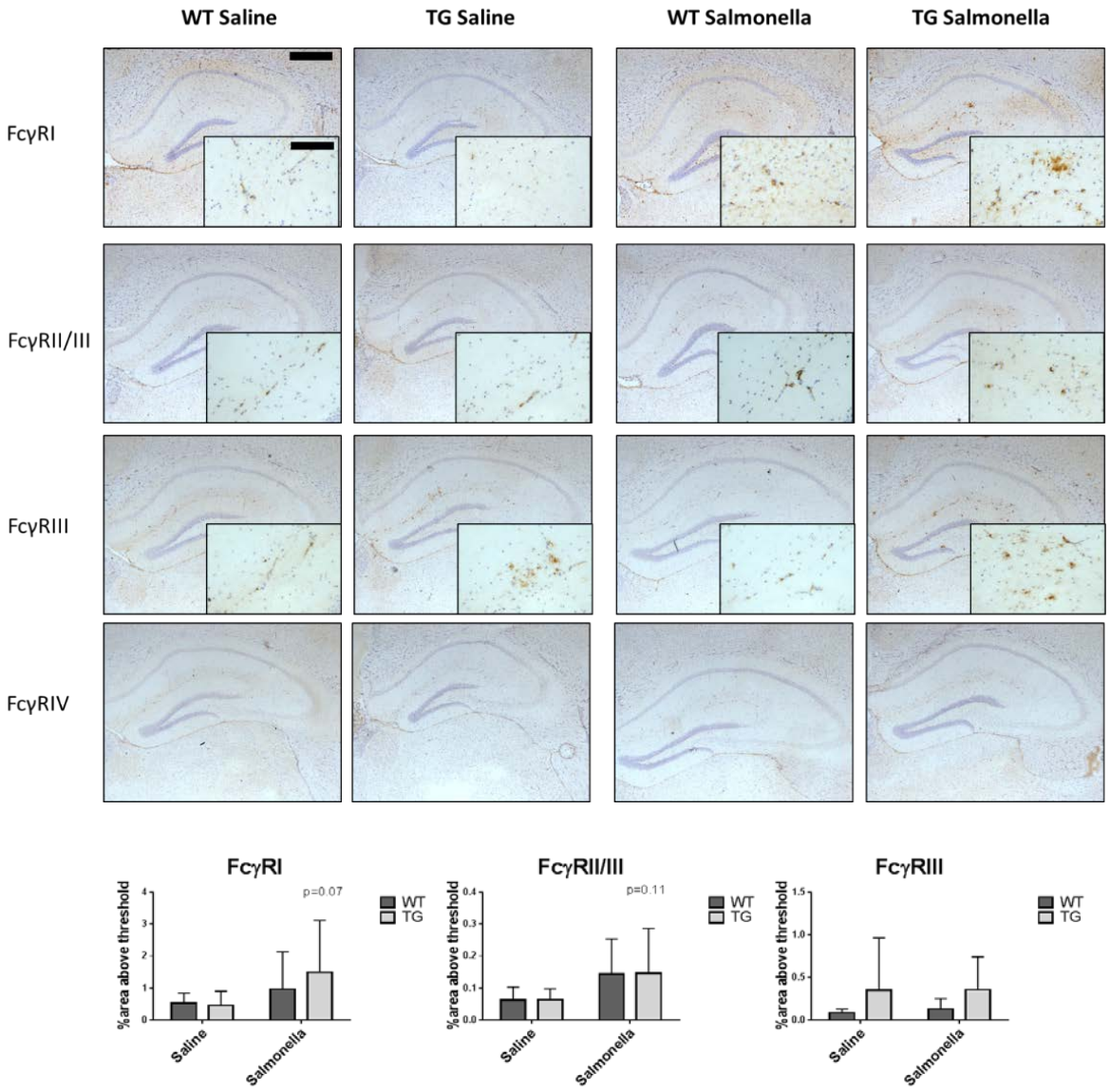

Figure 8. 8 Expression of FcγRs in the hippocampus at four weeks post infection with *S. typhimurium*

Expression of FcγRs four weeks after *S. typhimurium* infection. Pictures are taken with a 5x objective and 20x objective, scale bars are 500μm and 125μm respectively. The mean expression of FcγRI is higher in *S. typhimurium* infected mice than in saline injected controls, but this response is no statistically significant (p=0.07). There was also a non-significant increase in the expression of FcγRII/III (p=0.11). *S. typhimurium* had no effect on the expression of FcγRIII or FcγRIV, and there were no differences between TG2576 and WT mice for any of the FcγRs. Data analysed by 2-way ANOVA and Tukey post hoc test (n=8), graphs depict mean and standard deviation.

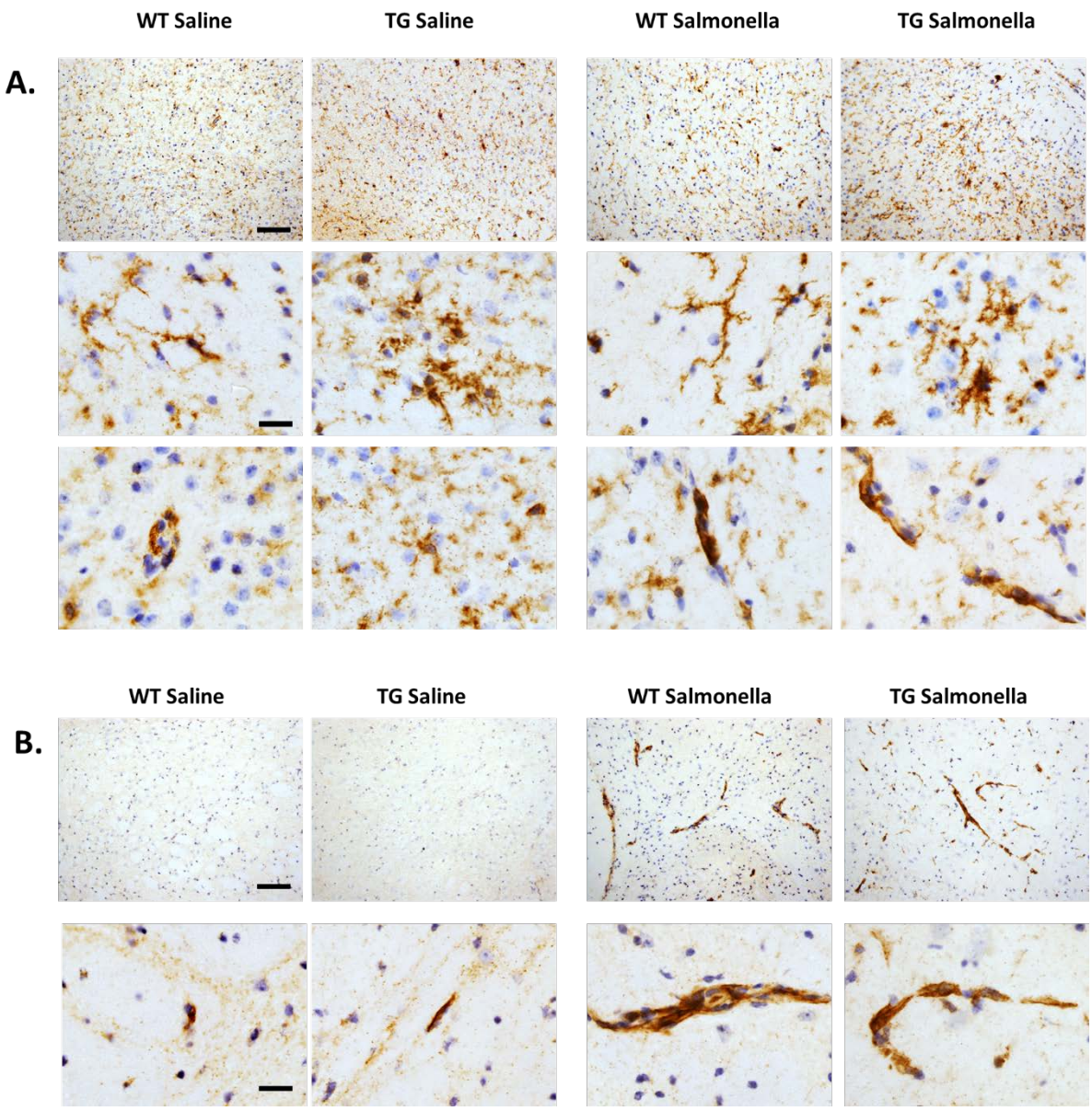

Figure 8. 9 High powered images of FcγRI and MHCII expression one week after *S. typhimurium* infection

A. Representative images of FcγRI expression one week after infection with *S. typhimurium* or saline. Images taken with a x20 or x100 objective (scale bars 100μm and 20μm respectively). **B.** Representative images of MHCII expression one week after infection with *S. typhimurium* or saline. Images taken with a x20 or x100 objective (scale bars 100μm and 20μm respectively).

8.3.3.2 Entry of plasma proteins and T-cells into the brain

S. typhimurium infection causes increased expression of MHCII on cells associated with the vasculature, therefore functional changes to the BBB were investigated. At one week post infection the levels of IgG in the brain were the same in all groups measured, however at four weeks *S. typhimurium* infection resulted in a significant increase in IgG levels in the brain ($p=0.0067$ fig. 8.9). This can be seen as increased IgG staining surrounding blood vessels, which appears to be leaking into the brain parenchyma.

Previous studies have reported increased numbers of T-cells entering the brain after infection with *Bordetella pertussis* (McManus et al., 2014), to test whether *S. typhimurium infection* also increased the numbers of T-cells in the brain, sections were stained for the T-cell receptor (CD3). The number of CD3 positive cells in the hippocampus were counted and normalised to hippocampal area. To find out if these T-cells were associated with blood vessels or had migrated into the brain parenchyma, sections were double stained for CD3 and the endothelial marker CD31, and the numbers of T-cells not associated with endothelial cells was counted. At one week post infection, the number of hippocampal T-cells were the same in all groups and there were no T-cells detected outside of blood vessels. At four post infection there were significantly more T-cells in the brains of mice infected with *S. typhimurium* compared to saline ($p<0.0001$), and a trend towards increased numbers in TG2576 mice infected with *S. typhimurium* compared to wild type ($p=0.15$). When the numbers of T-cellss were counted outside of blood vessels, there were significantly more in the parenchyma of TG2576 mice infected with *S. typhimurium* compared to TG2576 mice injected with saline ($p=0.003$), and again a trend towards increased numbers in *S. typhimurium* infected TG2576 compared to wild type ($p=0.07$).

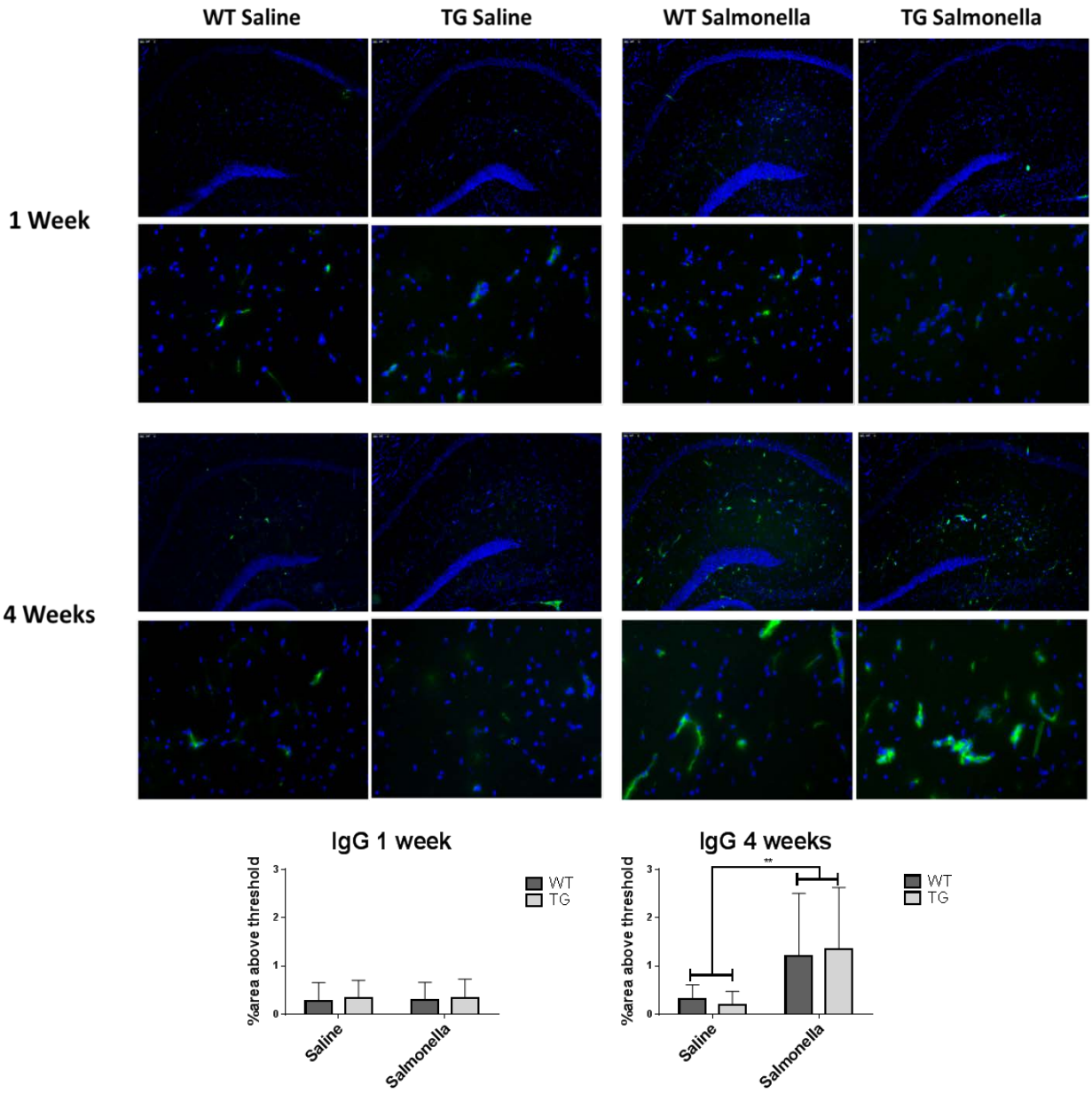

Figure 8. 10 Entry of IgG into the brain after infection with *S. typhimurium*

To detect changes in BBB permeability after *S. typhimurium*, brain sections were stained for mouse IgG. The levels of IgG in the hippocampus was quantified as area above threshold, and data analysed using 2-way ANOVA and Tukey post hoc test (n=8) and presented as mean and standard deviation. Four weeks after infection with *S. typhimurium* a statistically significant increase in the levels of IgG was observed in the brain (p=0.007).

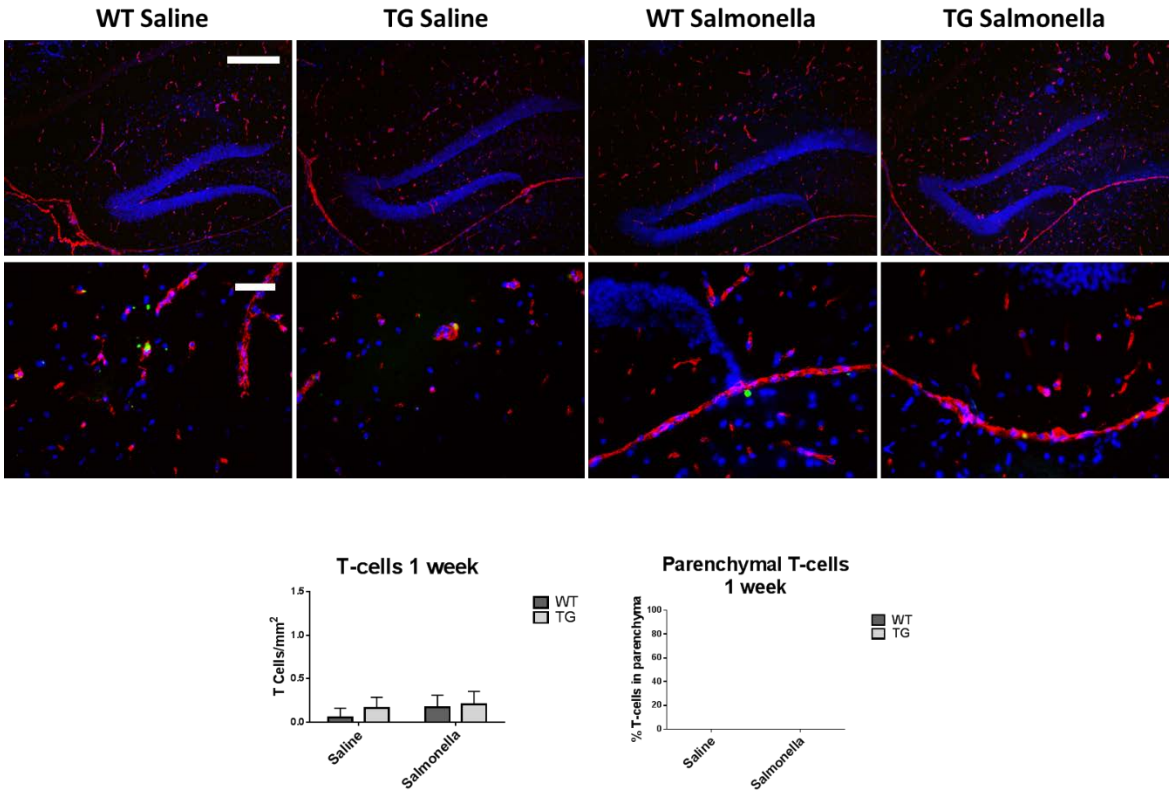

Figure 8. 11 T-cells in the brain one week after infection with *S. typhimurium*

To detect the number of T-cells in the brain parenchyma of TG2576 or WT mice one week after infection, 10µm brain sections were double immuno-stained for CD31 (endothelial cells) and CD3 (T-cells). The total number of CD3+ cells were counted and normalised to hippocampal area, expressed as T-cells/mm^2. Data were analysed by 2-way ANOVA and Tukey post hoc (n=8), and presented as mean and standard deviation. To determine the fraction of T-cells in the brain parenchyma, CD3+ cells that did not associate with endothelial cells (CD31), were counted and expressed as a percentage of total T-cells. These data were analysed using Krukal-wallis and Dunn's post hoc (n=8), and presented as mean and standard deviation. No significant changes were observed in the number of T-cells at one week post infection. This staining was performed by Miss Sophie Thornton.

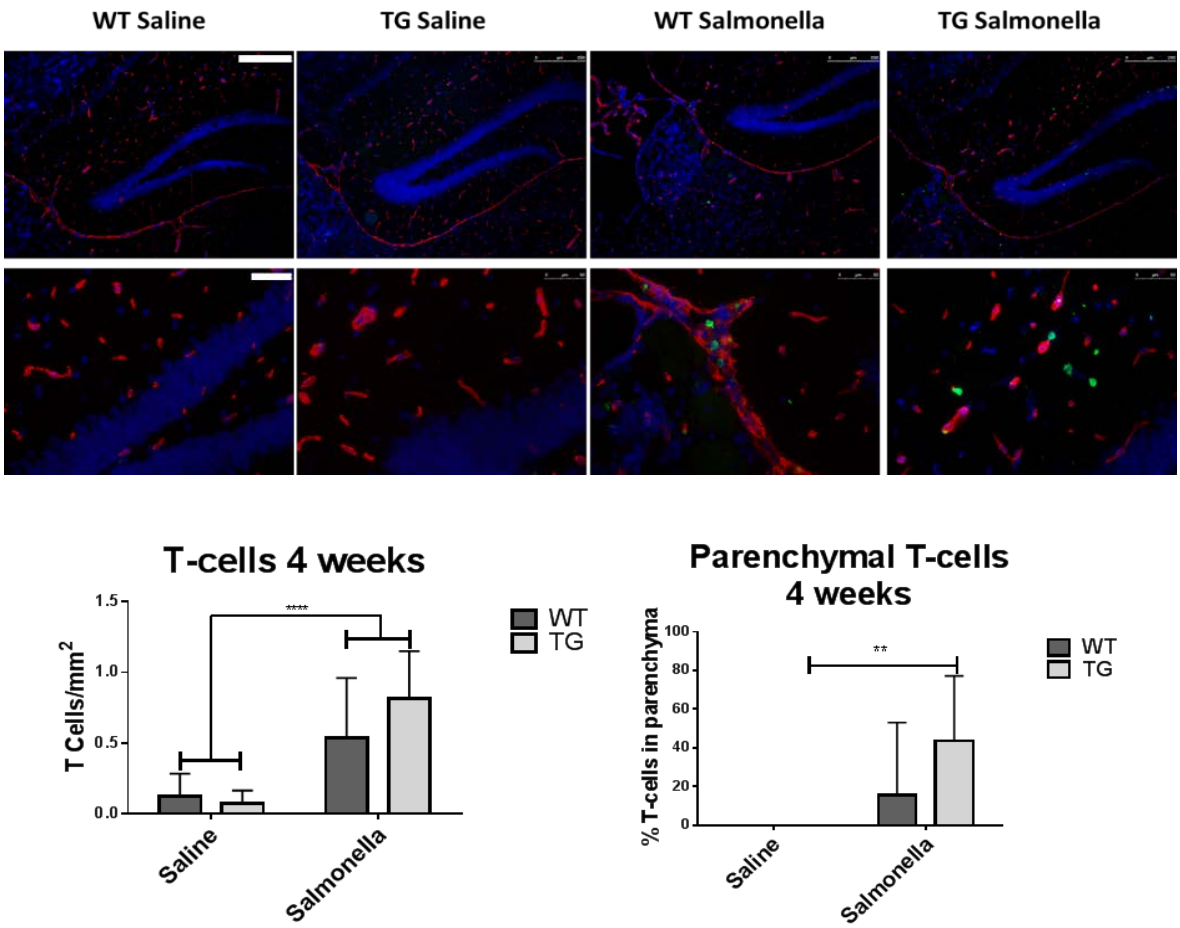

Figure 8. 12 T-cells in the brain four weeks after infection with *S. typhimurium*

To detect the number of T-cells in the brain parenchyma of TG2576 or WT mice four weeks after infection, 10µm brain sections were double immuno-stained for CD31 (endothelial cells) and CD3 (T-cells). The total number of CD3+ cells were counted and normalised to hippocampal area, expressed as T-cells/mm^2. Data were analysed by 2-way ANOVA and Tukey post hoc (n=8), and presented as mean and standard deviation. Infection with *S. typhimurium* results in a significant increase in the total number of T-cells in the brain ($p<0.0001$). To determine the fraction of T-cells in the brain parenchyma, CD3+ cells that did not associate with endothelial cells (CD31), were counted and expressed as a percentage of total T-cells. These data were analysed using Kruskal-wallis and Dunns post hoc and presented as mean and standard deviation (n=8). *S. typhimurium* results in a significant increase in the number of parenchymal T-cells in TG2576 mice. This staining was performed by Miss Sophie Thornton.

8.3.3.3 Brain cytokine levels

Mice infected with *S. typhimurium* have elevated cytokines in the brain at three weeks post infection (Puentener et al., 2012). To characterise the neuro-inflammatory response of TG2576 mice to *S. typhimurium*, we measured the levels of cytokines in brain tissue. At one week post infection, *S. typhimurium* causes increased levels of: IL-1β ($p<0.001$), IL-6 ($p<0.001$), KC ($p<0.001$) and a non-significant increase in TNFα ($p=0.06$) compared to saline injected control animals. Analysis indicates a significant interaction between genotype and *S. typhimurium* for the levels of the chemokine KC; post hoc tests shows that TG2576 mice infected with *S. typhimurium* have higher levels of KC compared to wild type littermates ($p=0.027$), there was also a non-significant increase in IL-6 ($p=0.15$) in the brains of TG2576 mice compared to wild type. Cytokine levels decrease in the brain at four weeks post infection, levels of IL-1β ($p<0.0001$), IL-6 ($p=0.03$) and TNFα ($p=0.028$) remain increased as compared to saline treatment. Of these cytokines, IL-1β levels were significantly elevated in *S. typhimurium* infected TG2576 mice compared to wild type littermates ($p=0.027$). These results confirm that *S. typhimurium* infection results in prolonged or exacerbated cytokine production in the brain of TG2576 mice compared to wild type mice.

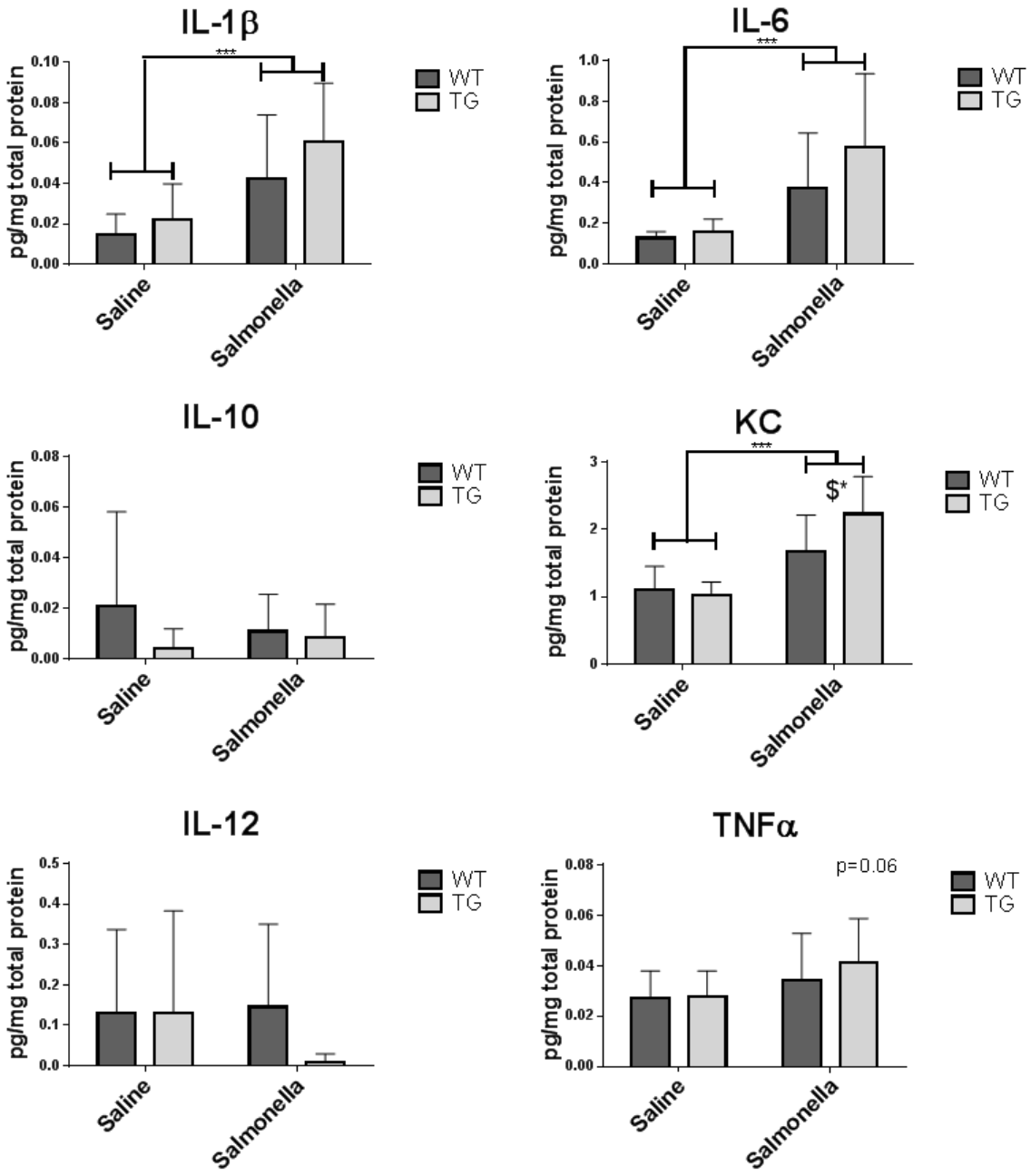

Figure 8. 13 Brain cytokine levels one week after *S. typhimurium* infection

The levels of cytokines were measured in the brain of TG2576 and wild type mice at one week post infection with *S. typhimurium* or saline using a multiplex immune assay (Mesoscale discovery). The levels of cytokines were normalised to total protein concentration, and expressed as pg/mg of total protein. Data sets were analysed using 2-way ANOVA, and Tukey post hoc test (n=8). *S. typhimurium* caused a significant increase in the levels of: IL-1β ($p<0.001$), IL-6 ($p<0.001$) and KC ($p<0.001$), and a trend towards increased TNFα ($p=0.06$). TG2576 mice infected with *S. typhimurium* had significantly higher levels of KC in their brain compared to *S. typhimurium* infected wild-type mice ($*, $p=0.0273$).

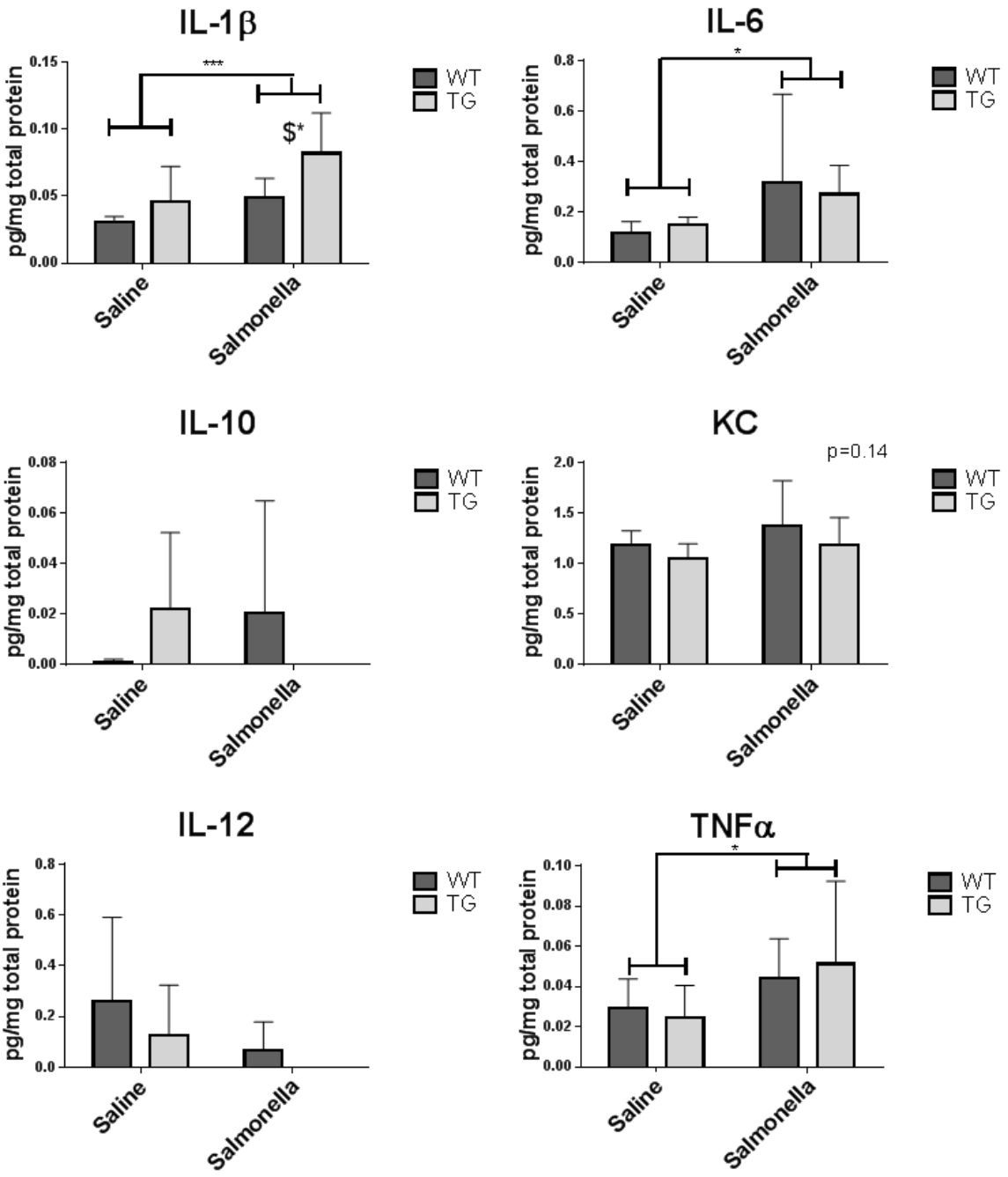

Figure 8. 14 Brain cytokine levels four weeks after infection with *S. typhimurium*

The levels of cytokines were measured in the brain of TG2576 and wild type mice at four weeks week post infection with *S. typhimurium* or saline using a multiplex immune assay (Mesoscale discovery). The levels of cytokines were normalised to total protein concentration, and expressed as pg/mg of total protein. Data sets were analysed using 2-way ANOVA, and Tukey post hoc test (n=8). *S. typhimurium* caused a significant increase in the levels of: IL-1β ($p<0.001$), IL-6 ($p=0.03$) and TNFα ($p=0.028$). TG2576 mice infected *S. typhimurium* also had significantly higher levels of IL-1β in their brain compared to *S. typhimurium* infected wild-type mice ($*, $p=0.020$).

8.3.4 The effect of s typhimurium on Aβ load

Previous studies have shown that repeated LPS injection or infection with *Bordetella pertussis* can lead to an increase in the levels of Aβ in the brains of transgenic APP mice (Lee et al., 2008; McManus et al., 2014; Sheng et al., 2003a). To investigate whether *S. typhimurium* infection induces a similar increase, the levels of Aβ were measured using a multiplex immune assay. Two different fractions of protein were obtained from brain homogenate, as described previously, gaining a triton soluble fraction and a formic acid soluble fraction. One week post infection, *S. typhimurium* has no effect on the levels of triton soluble Aβ compared to saline injected controls (figure 8.11). At four weeks, *S. typhimurium* infection caused a significant increase in the levels of triton soluble Aβ38 ($p=0.014$) and Aβ40 ($p=0.029$), and a non-statistically significant increase in Aβ42 ($p=0.06$). Conversely, at one week *S. typhimurium* infection caused a significant increase in formic acid soluble Aβ40 ($p=0.031$, fig. 8.12) and Aβ42 ($p=0.0019$) and a non-statistically significant increase in formic acid soluble Aβ38 ($p=0.0502$). These changes in formic acid soluble Aβ are transient, as there is no difference between saline and *S. typhimurium* treated mice at four weeks post infection.

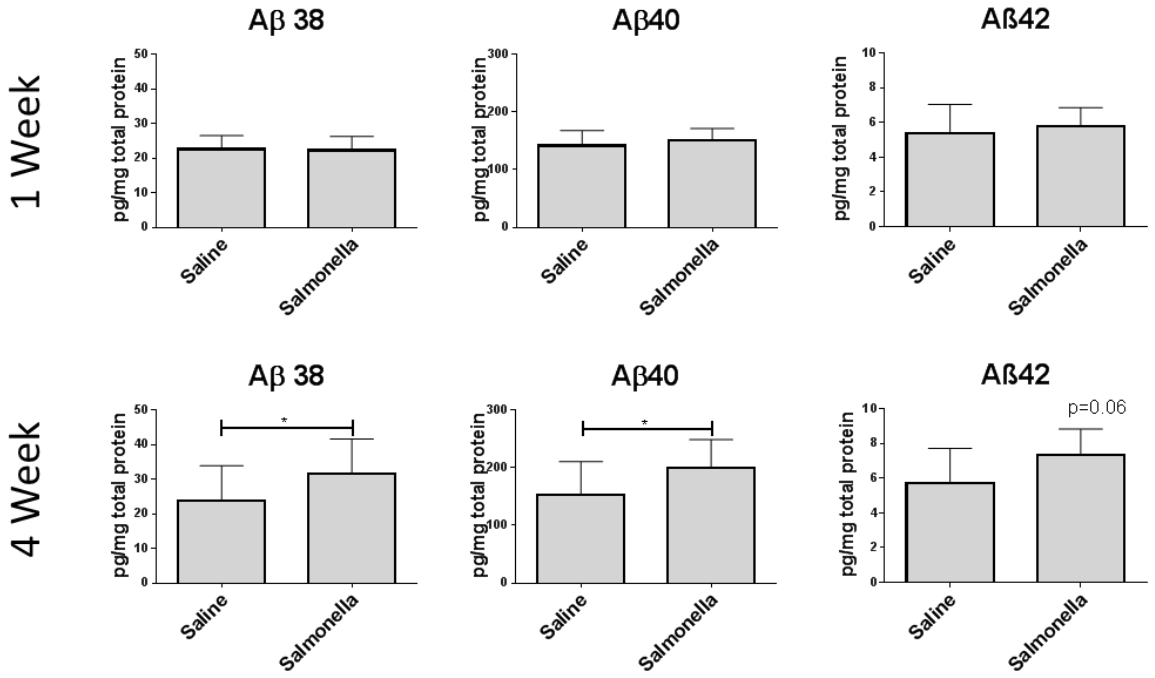

Figure 8. 15 *S. typhimurium* infection increases the levels of triton soluble Aβ at four weeks post infection

The concentration of Aβ38, Aβ40 and Aβ42 were measured in triton soluble brain extracts from TG2576 mice (n=8) injected with *S. typhimurium* or saline at one and four weeks post infection, using a multiplex immune assay (MSD). Data analysed by two tailed T-test (except Aβ38 1 week- Mann Whitney-U test) (n=8). Data presented as mean and standard deviation. The levels of Aβ38 (p=0.014) and Aβ40 (p=0.029) were significantly increased four weeks after infection with *S. typhimurium.*

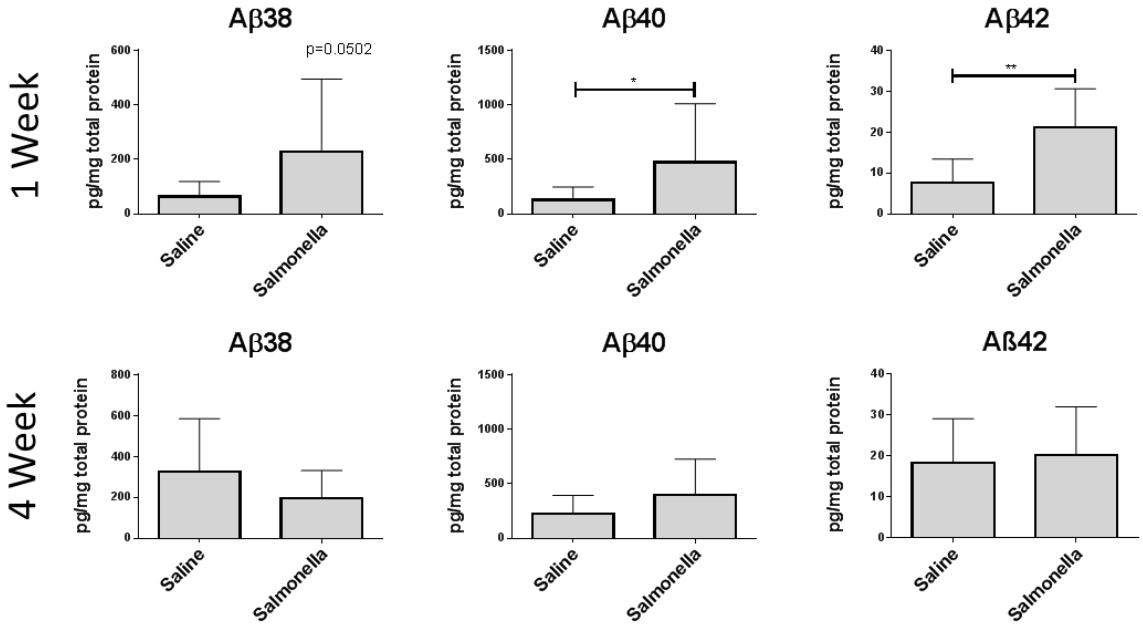

Figure 8. 16 *S. typhimurium* infection increases the levels of Formic acid soluble Aβ at 1 week post infection

The concentration of Aβ38, Aβ40 and Aβ42 were measured in formic acid soluble brain extracts from TG2576 mice injected with *S. typhimurium* or saline at one and four weeks post infection, using a multiplex immune assay (MSD). Data analysed by two tailed T test (Aβ40 four weeks, Aβ42 one week, Aβ42 four weeks), or Mann Whitney U test (Aβ38 one week, Aβ38 four weeks, Aβ40 one week) (n=8). Data presented as mean and standard deviation. The levels of Aβ40 (p=0.031) and Aβ40 (p=0.0019) were significantly increased one week after infection with *S. typhimurium.*

8.3.5 Nesting behaviour

S. typhimurium infection leads to increased neuro-inflammation measured by phenotype changes and increased cytokine concentration, and also is associated with increased concentration of Aβ peptide in the brains of TG2576 mice. To investigate changes to brain function, we used the well characterised nesting behaviour paradigm. Nesting is a normal behaviour of mice, essential for thermoregulation and reproduction, and has previously been shown to be dependent on the hippocampus. The ability of mice to build nests was scored on the morning of sacrifice. In spite of changes in neuro-inflammation and Aβ pathology, there were no changes in the ability of mice to build nests at one or four weeks post infection. All groups of mice scored an average of 4, which represents a normal score for healthy C57/BL6 mice (Deacon, 2006a).

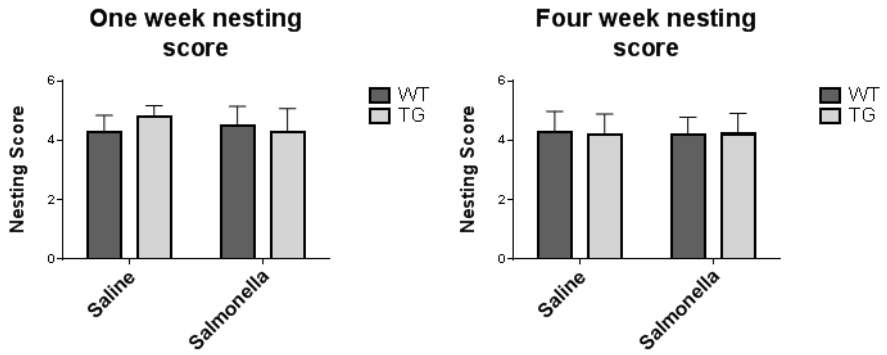

Figure 8. 17 *S. typhimurium* infection has no effect on nesting behaviour at one or four weeks

The night before sacrifice, mice infected with *S. typhimurium* or saline injected controls were tested for changes in nesting behaviour. Infection with *S. typhimurium* has no effect on the nesting behaviour score of mice at one or four weeks post infection. There was also no difference between TG2576 and wild type controls. Data were analysed by 2-way ANOVA and Tukey post hoc test (n=8), and presented as mean and standard deviation.

8.3.6 The relationship between cytokine levels and upregulation of immune receptors

Infection with *S. typhimurium* leads to a robust peripheral cytokine response including the 300-fold upregulation of IFNγ measured at one week post infection. The peripheral immune response is accompanied by a neuro-inflammatory changes including the increased expression of MHCII on cerebral vascular cells, increased expression of FcγRI on microglia and increased brain cytokine levels, with IL-1β higher (or prolonged) in TG2576 mice compared to wild type. The mechanism by which the peripheral inflammatory response is influencing brain immune receptor expression and cytokine production is currently unclear, as it is difficult to assess which cells are producing cytokines , or which are primed to respond in TG2576 mice compared to wild type. To understand the relationship between peripheral and neuro inflammation, data obtained from S. *typhimurium* infected mice were pooled (TG2576 and wild type) to allow correlation of systemic inflammation with changes in the brain. The levels of IFNγ in the serum positively correlate with the expression of MHCII on vascular cells in the brain (r^2=0.694, p<0.0001). The expression of MHCII also correlates with brain levels of IL-1β (r^2=0.296, p<0.026) and KC (r^2=0.291, p<0.031). Conversely, there is no relationship between IFNγ levels in the periphery and FcγRI expression in the brain. There is also no relationship between FcγRI expression and the levels of IL-1β and KC.

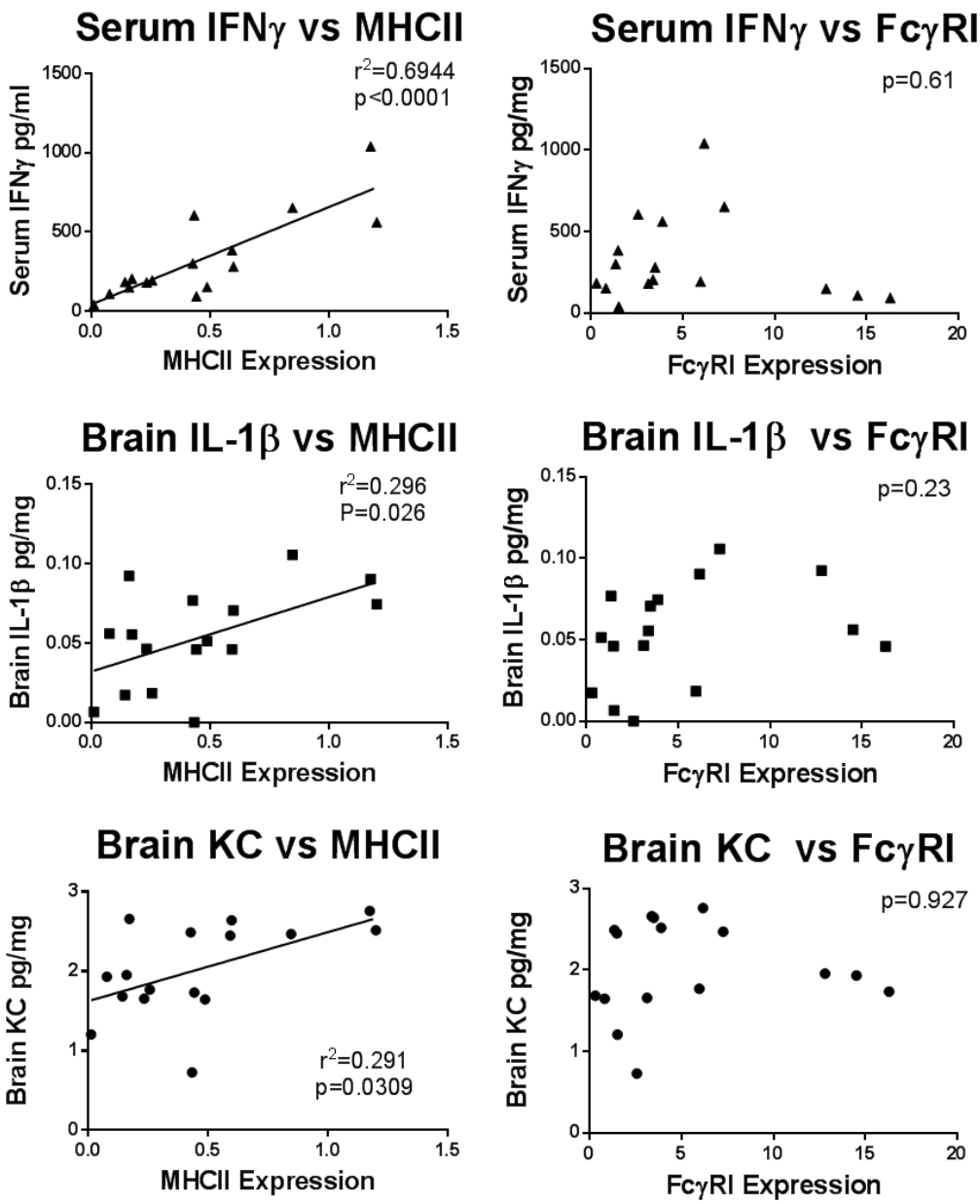

Figure 8. 18 Correlation between peripheral IFNγ and neuro-inflammatory changes

Data from *S. typhimurium* infected animals (n=16) (both TG2576 and WT) were pooled from the one week time point to allow analysis of the relationship between the peripheral immune response and neuro-inflammation. The peripheral concentration of IFNγ correlated with the expression of MHCII on endothelial cells (r^2=0.694, p=0.0001), however the expression of FcγRI did not (p=0.61). The expression levels of MHCII also correlated with the levels of brain IL-1β (r2= 0.296, p=0.026) and KC (r2= 0.291, p=0.309), FcγRI did not correlate with either (p=0.23) (p=0.927) respectively.

8.4 Discussion

The brain is able to respond to inflammatory changes in the periphery by adapting behaviour to prevent the spread of illness and enhance the body's ability to clear away the pathogens (Hart, 1988). In the diseased or ageing brain this response to peripheral inflammation can be detrimental, where an exacerbated response can cause enhanced cognitive decline (Holmes et al., 2009). There is also evidence that peripheral inflammation is involved in the development of AD (Carter, 2011; Hollingworth, 2011; Lambert et al., 2009; Stein et al., 2012; Stewart et al., 1997). The relationship between peripheral inflammation and neuro-inflammation/neuro-degeneration has mainly been studied using mimetics of infection such as LPS (Dantzer and Kelley, 2007). The response of animals to LPS is very different to a real bacterial infection (Puentener et al., 2012), and there is limited published work investigating the effect of real infections on the brain. In this chapter I have characterised the peripheral and central response of TG2576 mice to infection with the attenuated bacterium *Salmonella typhimurium* (SL3261) a close relative of the bacterium *Salmonella typhii* which causes human typhoid fever.

The brain mediates a number of behavioural changes in response to infection, collectively termed sickness behaviours, such as: feeling anti-social, lethargy or anorexia (Hart, 1988). *S. typhimurium* infection causes significant weight loss compared to saline injection. Peripheral inflammation can cause anorexia via a number of mechanisms: direct action of cytokines on the gastro-intestinal system, promoting the release of anorexogenic factors (i.e. leptin) or by affecting the signalling of neurons in the hypothalamus leading to central changes to appetite and metabolism(Plata-Salaman, 1998). Interestingly, the weight changes of TG2576 and wild type mice are significantly different. Both genotypes lose around 5% of body weight at one day post infection; TG2676 mice then begin to regain body weight after day two and return to starting body weight at seven days post infection. In contrast, wild type mice continue to lose weight on day two, and then do not return to starting body weight for the duration of the experiment. The response of the wild type mice is very similar to previous experiments where eighteen month old mice were given S. *typhimurium*, and lost weight for a pro-longed period of time compared to three month old mice (A. Hart unpublished data). The difference in weight recovery may be due to a different peripheral or central cytokine response to infection between TG2576 mice and WT, as cytokines are able to drive anorexia through the mechanisms described previously. However, in this experiment there was no difference in the peripheral cytokine response, and TG2576 mice presented with higher levels of cytokines in

the brain when compared to wild type mice. Therefore it seems unlikely that the differential weight recovery was due to different cytokine induced sickness behaviour. Another possibility is that TG2576 mice are metabolically different to wild type littermates. It has previously been shown that triple transgenic mice (APP/PS1/Tau) are metabolically different to their wild type littermates, and that injection of Aβ into the brain of rats results in changes in appetite and metabolism (James et al., 2014; Knight et al., 2012). Young triple transgenic mice have higher food intake than wild type, which results in a higher body weight at three months old. This higher food intake continues into adulthood, however due to their increased metabolism they weigh less than wild type mice by 12 months of age (Knight et al., 2012). The effect of Aβ on food intake and metabolism could explain the difference in weight recovery, as TG2576 mice may have a higher food intake when compared to wild type allowing a faster recovery of the lost weight. Unfortunately we did not measure food intake in this experiment, but it would be interesting to investigate how Aβ affects appetite and weight gain during infection. This is clinically relevant as patients with Alzheimer's disease are known to experience changes in metabolism and appetite (Cai et al., 2012).

Infection with *S. typhimurium* results in neuro-inflammation, measured by increased cytokine levels in brain tissue, and the up-regulation of MHCII on endothelial cells and FcγRI on microglia. The mechanism of this immune to brain communication is not clear, and it is not known what cell types in the brain are responsible for the cytokine production. Peripheral inflammation can cause changes in the brain through three known pathways: activation of the vagus nerve by increased inflammation in peripheral tissue (Berthoud and Neuhuber, 2000), the passage of cells and inflammatory mediators into the brain through circumventricular organs (Fry and Ferguson, 2007) or through the production of inflammatory mediators in the brain and the *de novo* production of pro-inflammatory mediators by the brain endothelium (Teeling et al., 2010). Up-regulation of MHCII on cerebral vascular cells demonstrates that they are responsive to peripheral infection. This is supported by the correlation between IFNγ levels in the serum and the expression levels of MHCII on the brain endothelium. The expression of FcγRI on microglia, is not related to the levels of circulating IFNγ and S. typhimurium does not affect the expression levels of other microglial markers, CD11b and CD68. These data suggest that microglial cells may not be responding directly to peripheral inflammation, whereas brain endothelial cells are. This is supported by correlations between MHCII expression and cytokine levels in the brain, whereas the expression of FcγRI has no relationship with brain cytokines. This does not prove that endothelial cells are the cells producing the cytokines, but gives strong evidence that they are involved in the neuro-

inflammatory response to infection. Further experiments are required to tease apart the individual roles of endothelial cells and microglia in response to peripheral infection.

Peripheral infection increases the levels of MHCII levels on cerebral vasculature, likely endothelial cells, and there are also changes in the integrity of the BBB. Under normal conditions, the BBB tightly regulates the entry of plasma proteins into the brain and therefore the levels of IgG are low (Zlokovic, 2008). Four weeks after *S. typhimurium* infection, the levels of IgG increase in the brain indicating a change in the permeability of the BBB. During infection there is also an increase in the expression of the activating FcγRI on microglial cells. The increase in activating FcγR expression, and increase in plasma protein entry into the brain could influence the response to anti-Aβ immunotherapy. AD patients treated with anti-Aβ immunotherapy experience cerebrovascular damage characterised by ARIA-E (Salloway et al., 2010), which are thought to be caused by FcγR mediated neuro-inflammation (Adolfsson et al., 2012; Wilcock et al., 2006). After *S. typhimurium* infection, there are increased levels of IgG in the brain and increased numbers of lymphocytes, indicating a loss of BBB integrity. If an AD patient were to contract a peripheral infection whilst being treated with anti-Aβ immunotherapy; the changes to BBB integrity caused by infection could worsen ARIA-E. Furthermore, the increased entry of anti-Aβ antibodies into the brain, coupled with increased FcγRI expression on effector cells, could drive an exacerbated inflammatory response to immunotherapy resulting in increased neuro-inflammation and more severe vascular damage. To test this hypothesis I would measure the neuro-inflammatory response of TG2576 mice to the antibody 3D6 IgG2a after infection with *S. typhimurium*. If peripheral inflammation increases the risk of inducing vascular side effects in patients, this should be considered when selecting treatments. For example, if a patient contracts a peripheral infection during treatment with anti-Aβ immunotherapy, to reduce side effects treatment could be withdrawn or replaced with an effector reduced antibody.

At one week post infection the levels of KC are significantly higher in TG2576 mice infected with *S. typhimurium* than wild type, and at four weeks the levels of IL-1β are also significantly higher in TG2576 mice. This response indicates that cells in the brain of TG2576 mice are primed to respond to an inflammatory stimulus, leading to increased cytokine production. Previous work has shown that microglia in the brains of mice with a neurodegenerative condition are primed to respond to a second immune stimulus. In this case, if endothelial cells are producing cytokines; either the endothelial cells are primed in the brains of TG2576 mice or the microglia are primed to respond to inflammatory mediators produced by the endothelium. Priming of the brain resulting in enhanced

cytokine production, in response to systemic inflammation, could explain the exacerbated sickness behaviour and cognitive decline observed in AD patients after peripheral inflammation (Holmes et al., 2009; Holmes et al., 2003).

Previous studies have shown that treatment with the bacterial mimetic LPS or *Bordetella pertussis* infection can cause an increased production of Aβ in the brain of transgenic APP mice via increased cleavage of APP by β-secretase (Lee et al., 2008; McManus et al., 2014; Sheng et al., 2003a). Here we show that infection with *S. typhimurium* can also cause increased brain Aβ; strengthening the hypothesis that inflammation plays an integral role in the development of AD. It is interesting to consider the possible reasons for increased Aβ levels in response to infection. Aβ has strong anti-microbial properties, and it has been proposed that in the event of infection neurons increase the cleavage of APP to Aβ to aid in the innate immune response to infection (Soscia et al., 2010). This is supported by studies showing that colonisation of the brain by *Chlamydia pneumoniae* leads to increased production of Aβ and the formation of plaques, which are also immuno-reactive for the bacterium (Little et al., 2004). Therefore, increased Aβ levels could form part of the brains natural protection from pathogens and this is why levels of Aβ increase in response to inflammation. However, the increase in triton soluble Aβ at four weeks post infection, also coincides with increased vascular permeability as measured by increased IgG. Therefore the accumulation of triton soluble Aβ at four weeks could also be explained by changes to the BBB, resulting in the dysfunction of Aβ clearance mechanisms. The low-density lipoprotein receptor related protein 1 (LRP1), is expressed by brain endothelial cells and mediates the efflux of Aβ from the brain (Deane et al., 2009; Jaeger et al., 2009a). Peripheral inflammation caused by LPS, results in decreased Aβ efflux from the brain via an LRP1 dependent mechanism (Erickson et al., 2012; Jaeger et al., 2009b). Therefore the increase in brain Aβ at four weeks post infection with *S. typhimurium* could be due to peripheral inflammation resulting in decreased LRP1 mediated Aβ efflux from the brain. Vascular dysfunction, resulting in increased BBB permeability is one of the first changes to occur in the prodromal stages of AD (MCI) (Montagne et al., 2015). Increased leakage of hippocampal blood vessels is observed in the brains of MCI patients, and correlates with cognitive decline. Therefore peripheral inflammation could result in increased brain Aβ by two distinct mechanisms: decreased LRP1 efflux of Aβ from the brain or increased production of Aβ by β-secretase. It is likely that in a healthy brain, once peripheral inflammation has been resolved that Aβ is cleared by normal mechanisms, for example LRP1 mediated efflux. However when a patient experiences prolonged inflammation or has genetic and environmental factors which affect the

clearance of Aβ from the brain (e.g. APOE4), this could lead to the pathological accumulation of Aβ and eventually lead to the development of other AD associated pathologies.

S. typhimurium infection causes increased neuro-inflammation and accumulation of Aβ; previous studies with LPS would suggest that this should cause measurable changes in behaviour (Dantzer and Kelley, 2007). We did not find any differences in nesting building between any experimental groups, which all scored an average of four representing healthy wild type mice. This can be explained by the difference between *S. typhimurium* and LPS; *S. typhimurium* only causes behavioural alterations (i.e., burrowing) at one day post infection, which is coincidently when there is highest serum LPS (Puentener et al., 2012). Another reason for the lack of behavioural alterations is that the nesting behaviour paradigm may not be sensitive enough to detect subtle changes in brain function. This is demonstrated by studies that show that lesions are required in both the anterior and posterior hippocampus to detect robust changes in the ability of mice to build nests (Deacon, 2006b). A more sensitive assay such as fear conditioning used in **chapter 6** may be able to pick up these subtle changes, however due to the limitations of the containment level 2 laboratory most behaviours analyses were not possible.

I propose that peripheral infection drives activation of the brain endothelium, leading to the up-regulation of MHCII and a decrease in the integrity of the BBB. The activated endothelium then produces inflammatory mediators such as: IL-1β, TNFα and KC. The decreased integrity of the BBB allows increased plasma proteins and lymphocytes into the brain, which could alter the microenvironment and augment the neuro-inflammatory response. Aβ levels in the brain are increased by two potential mechanisms: increased β-secretase cleavage of APP and/or decreased Aβ efflux by LRP1. In a healthy brain, the Aβ is then cleared away by normal mechanisms of efflux. However when a patient experiences chronic inflammation or has genetic or environmental risk factors which affect the clearance of Aβ, this could lead to Aβ accumulation. This accumulation could act as the precipitating factor for AD, driving the hyper-phosphorylation of tau and synaptic dysfunction. I also propose that changes in the BBB, and the increased expression of FcγRI on effector cells could influence the response to immunotherapy. A reduction in BBB integrity could exacerbate the vascular damage that patients experience during immunotherapy, and increased expression of FcγRI could exacerbate the inflammatory response.

Chapter 9: General discussion

AD is a chronic neurodegenerative condition that currently has no approved disease modifying therapeutics. Although the pathogenesis of AD is not completely understood, the accumulation and aggregation of the protein Aβ is thought to be important. As a result, the vast majority of drug discovery in recent years has centred on the removal of accumulated Aβ from the brain. One approach is to treat patients with antibodies specific for Aβ, which clears deposits from the brain and there is some evidence that this can improve cognition (Doody et al., 2014; Ostrowitzki et al., 2012; Salloway et al., 2014). However, these antibodies also cause damage to the cerebral vasculature, thought to be mediated by an inflammatory response to immunotherapy in the CNS (Ostrowitzki et al., 2012; Rinne et al., 2010; Salloway et al., 2010). These side effects have hampered clinical development of antibodies by limiting the top dose of antibody that can be safely administered, which could explain the lack of efficacy in certain clinical trials. The main aim of this thesis was to better understand the role of antibody effector function in the clearance of Aβ and the neuro-inflammatory response after treatment with anti-Aβ antibodies, enabling the development of antibodies with optimised effector function to reduce side effects or boost efficacy. We now propose a model with three factors that impact on the neuro-inflammatory response to anti-Aβ antibodies: antibody effector function, antibody specificity and the specific brain environment of the patient.

9.1.1 Antibody effector function

Antibody effector function is the ability of an antibody to ligate cellular receptors or complement proteins and to cause immune activation resulting in the clearance of an immune complex/opsonised cell (Ravetch and Bolland, 2001). The cellular receptors which bind to IgG are called FcγRs and are expressed by microglia and other cells in the brains of AD patients and transgenic APP mice. One mechanism of Aβ clearance after treatment with an anti-Aβ antibody is FcγR mediated phagocytosis, however the importance of antibody effector function in this clearance and the subsequent neuro-inflammatory response is not fully understood (Morgan, 2009). The response of effector cells to immune complexes is dependent on the type of FcγRs that are expressed by effector cells (Nimmerjahn and Ravetch, 2008), but limited information on such interactions in the brain is available in the literature. In **Chapter 4** I showed that activating FcγRI and FcγRIII were both expressed by microglia in the brains of 18 month old TG2576 mice,

particularly surrounding Aβ plaques; similar observations were made in the brains of AD patients, validating our animal data. Expression of the inhibitory receptor FcγRIIIb and the activating receptor FcγRIV was very low, almost undetectable, on microglial cells. Therefore, I conclude that FcγRI or FcγRIII are most likely the receptors that mediate plaque clearance and pro-inflammatory cytokine release after antibody treatment.

In **Chapter 5**, I compared IgG1 and IgG2a antibodies with identical target engagement for the efficacy to clear Aβ and the associated neuro-inflammatory response to this treatment. Intracranial injection with 3D6 IgG2a but not IgG1 led to plaque clearance and the release of the pro-inflammatory cytokine IL-1β. This study demonstrated that differential effector function of therapeutic antibodies resulted in a different neuro-inflammatory response and ability to clear plaques, this provides proof of principle that therapeutic antibodies can be engineered to reduce the inflammation or enhance plaque clearance. Both subclasses are able to ligate FcγRIII, but only IgG2a is able to bind to FcγRI, therefore it is likely that this clearance and inflammation is due to, or downstream of the engagement of FcγRI. This is a hypothesis that requires further testing to confirm, which could be achieved by crossing mice deficient for FcγRI with TG2576 mice and testing the efficacy to clear plaques following injection of 3D6 IgG2a. If the plaque clearance and IL-1β production are dependent on FcγRI activation, a reduction in cytokine production and plaque clearance would be observed. If FcγRI activation is important for clearance boosting the affinity of the constant region for FcγRI or making a constant region that binds specifically to FcγRI could improve efficacy of plaque clearance, however this may also worsen ARIA-E (Chan and Carter, 2010).

Therapeutic antibodies are given by systemic administration rather than injection directly to the brain, therefore in **chapter 6** I compared the effect of IgG subclass following systemic treatment. In contrast to intracranial injection of anti-Aβ antibodies, where 3D6 IgG1 failed to induce neuro-inflammation, peripheral treatment with both versions of mC2 resulted in the increased levels of four cytokines: IL-1β, TNFα, KC and IL-6 with no difference between IgG subclass. Since the response to mC2 IgG1 and mC2 IgG2a was similar, the increased cytokine production is unlikely to result from FcγRI ligation, since IgG1 cannot ligate this receptor (Bruhns, 2012). Both antibodies are able to ligate FcγRIII with comparable affinity, and based on these results I hypothesise that mC2 IgG1 and IgG2a activate microglial cells through FcγRIII resulting in increased cytokine production. Indeed, small immune complexes were formed in the brain parenchyma after systemic administration of mC2, rather than binding to plaques. This hypothesis requires further testing,

using FcγRIII knockout animals to determine the importance of FcγRIII. Our lab previously showed that reduced inflammation in the brain of FcγRIII deficient mice following experimental immune complex formation (Carare et al., 2013), but this has not yet been shown for anti-Aβ antibodies. It is also not clear whether FcγR mediated phagocytosis of immune complexes is required for antibody efficacy as both subclasses were able to reverse behavioural deficits without significant clearance of Aβ. It may be sufficient for an antibody to bind to toxic Aβ and block their interactions with neuronal receptors-preventing synaptic dysfunction. In this case antibody effector function could be unnecessary or even damaging.

These findings raise the interesting question: do 3D6 and mC2 promote cytokine release through different FcγRs? The route of administration was different in these experiments, 3D6 was injected directly into the hippocampus, whereas mC2 was given systemically. This could influence the response to antibody treatment in a number of ways, which have been discussed in previous chapters. FcγRI has high affinity for IgG, allowing it to ligate monomeric IgG whereas other FcγRs require the enhanced avidity of immune complexes (Bruhns, 2012). This means that in the periphery FcγRI is normally occupied by monomeric IgG preventing the ligation of immune complexes (Allen and Seed, 1989; van der Poel et al., 2011). In spite of this, FcγRI plays a role in a range of auto-immune conditions and in the effector function of therapeutic antibodies (Barnes et al., 2002; Bevaart et al., 2006; Mancardi et al., 2013). This is achieved by the displacement of monomeric IgG by immune complexes due to re-localisation of the receptor, and the increased avidity of immune complexes allowing them to outcompete monomeric IgG for binding to FcγRI (van der Poel et al., 2010). Even though IgG levels are lower in the CNS, some IgG still diffuses into the brain. It is therefore likely that FcγRI expressed on microglia is at least partially occupied by monomeric IgG. This could explain the apparent FcγRI dependent cytokine release after intracranial injection, but not after systemic treatment. Intracranial injection of 3D6 results in a high localised concentration of antibody. High 3D6 concentration would opsonise plaques with a high density of IgG, this opsonised plaque would have high avidity and therefore could out-compete the monomeric IgG bound to microglial FcγRI, causing the production of IL-1β. The BBB tightly regulates the entry of IgG into the brain (Banks, 2012), and therefore the local concentration of IgG after systemic treatment will be much lower than after intracranial administration. The lower levels of IgG would reduce the density bound to deposits of Aβ, and therefore not engage FcγRI as strongly. This cannot be proven with the comparison between mC2 and 3D6, as mC2 does

not bind to plaques as strongly. To test this hypothesis systemic treatment with 3D6 is required, but unfortunately this was not possible due to the limited production of this antibody.

Comparing the efficacy of the antibodies 3D6 and mC2 in the studies so far described is difficult due to the difference in route of administration, however when mC2 was given by intracranial injection described in **chapter 6** confirmed there was no difference in cytokine levels between IgG1 and IgG2a subclasses. A likely explanation for these differences is the antibody specificity, 3D6 can bind plaques effectively whereas mC2 cannot. It is possible that dependent on the species of Aβ targeted, and therefore size of immune complex, different brain FcγRs are involved in the production of pro-inflammatory cytokines. *In vitro* it has previously been shown that the size of immune complex affects the affinity for different FcγRs (Lux et al., 2013). Based on these observation, I predict that FcγRI is involved in the clearance of plaques, but not in the removal of soluble immune complexes. These differences could again be explained by avidity. Plaques are large insoluble deposits and therefore their opsonisation with IgG would result in a structure with higher avidity for FcγRs than smaller soluble immune complexes. This high avidity could enable the opsonised plaques to outcompete monomeric IgG already bound to microglial FcγRI. This explains the enhanced ability of 3D6 IgG2a to clear Aβ plaques and the increased IL-1β production compared to 3D6 IgG1 which cannot bind FcγRI. Small soluble immune complexes produced by the binding of Aβ oligomers by mC2 after systemic treatment, may not be able to bind to occupied FcγRI. Instead these immune complexes ligate FcγRIII which is expressed by microglia (which is not occupied by monomeric IgG), explaining the equivalent cytokine production after treatment with mC2 IgG1 or IgG2a. Therefore depending on the target of the antibody developed, different effector functions may be required. This hypothesis is outlined in figure 9.1.

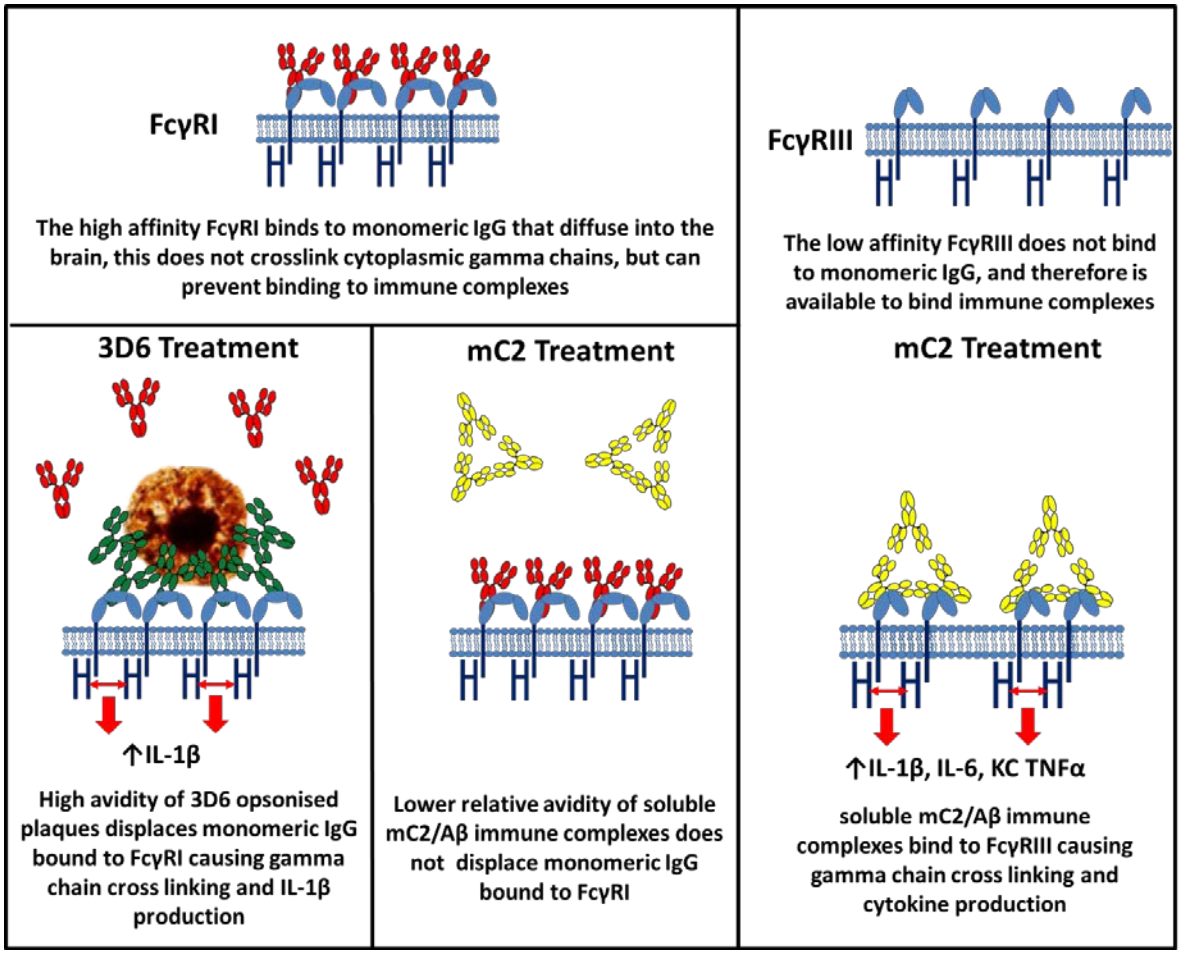

Figure 9. 1 Proposed mechanism of differential FcyR activation by 3D6 and mC2

Hypothesised mechanism by which the specificity of anti-Aβ antibodies could determine the FcyR activated. FcyRI is a high affinity receptor that is able to bind to monomeric IgG, this does not result in the cross-linking and activation of cytoplasmic gamma chains but can prevent ligation of immune complexes. FcyRIII is a low affinity receptor that does not bind monomeric IgG, but can ligate immune complexes. Treatment with the plaque binding antibody 3D6, results in the opsonisation of plaques forming structures with high avidity for FcyRs. This high avidity causes the displacement of monomeric IgG that is occupying FcyRI, resulting in the cross-linking of cytoplasmic gamma chains and production of IL-1β/clearance of plaques. Treatment with an antibody such as mC2 which binds to smaller soluble forms of Aβ, results in the formation of smaller immune complexes with lower avidity than 3D6 opsonised plaques. This prevents the displacement of the monomeric IgG occupying FcyRI.However, FcyRIII is not occupied by monomeric IgG and therefore soluble immune complexes are able to cross link gamma chains, resulting in the production of pro-inflammatory cytokines.

9.1.2 Antibody specificity

Anti-Aβ antibodies have been developed which bind to: the N-terminus, mid domain or the C-terminus (Fuller et al., 2014). Differences in subclass, pre-clinical model, time course or dose make it difficult to compare previous pre-clinical studies and to determine the importance of antibody epitope in the clearance of plaques and induction of a neuro-inflammatory response. In **chapter 7** we compared three murine versions of antibodies which have all been tested in phase III clinical trials for AD: Bapineuzumab, Crenezumab and Gantenerumab, importantly, all antibodies in my study share the same IgG2a constant region. 3D6, the murine version of Bapineuzumab, recognises the N-terminus of Aβ and binds strongly to plaques and recombinant Aβ *in vitro*. This translated into 3D6 clearing plaques effectively *in vivo*, but this was accompanied by increased neuro-inflammation. Gantenerumab binds to an N-terminus conformation epitope, and was able to bind to recombinant Aβ and plaques, but not as potently as 3D6. Gantenerumab was unable to clear plaques at the time point measured, however there was clear evidence of plaque binding which was accompanied by increased neuro-inflammation. The antibody mC2 is the murine version of Crenezumab and recognises the mid domain of Aβ, *in vitro* mC2 was able to bind to recombinant peptide but did not label plaques strongly without formic acid treatment. *In vivo* Crenezumab did not clear plaques or cause neuroinflammation. Therefore, the strength of the neuro-inflammatory response to antibody treatment seems to be dependent on the ability of an antibody to bind to plaques.

Eight weeks of treatment with mC2 does not clear plaques from the brains of 18 month old TG2576 mice, but treatment does reverse cognitive deficits as measured by the well characterised fear conditioning test. This raises the question-do we need to clear plaques to treat AD? I propose that this is dependent on the stage of AD that is treated. It is thought that accumulation and aggregation of Aβ are one of the first events that occurs in AD, and this process occurs many years before the disease clinically manifests. This accumulation is then thought to 'kick start' other pathologies such as tau accumulation and spreading, and neuro-inflammation which then lead to cognitive decline (Perrin et al., 2009). This theory is supported by data from the post mortem analysis of patients immunised against Aβ in the AN1792 trial. Patients with established AD that generated sufficient titres of anti-Aβ antibodies had widespread clearance of plaques from the brain (Nicoll et al., 2006).

This clearance of plaques removed one element of tau pathology-dystrophic neurites and also reduced the expression of immune receptors on microglial cells in regions of Aβ clearance (Boche et al., 2010; Zotova et al., 2013; Zotova et al., 2011). This finding demonstrates a link between the accumulation of Aβ and the accumulation of tau, and that clearance of Aβ may resolve inflammation. In the same study it was found that other tau pathology such as tangles continued to propagate in a normal fashion as described by Braak staging, demonstrating that once started some tau pathology is independent from Aβ. Therefore to treat a patient early in the pathology of the disease, targeting plaques may be beneficial as this may prevent the development of other pathologies. This is supported by data from the clinical trial for Aducanumab, an antibody which specifically recognises aggregated Aβ, and is able to improve cognition in mild AD. However, targeting plaques later on may be ineffectual or even dangerous as the vascular damage caused by plaque binding antibodies Bapineuzumab and Gantenerumab suggest (Bohrmann et al., 2012; Rinne et al., 2010). During the late stages of AD, the actual levels of Aβ in the brain remain fairly unchanged, but as mentioned previously it is thought that certain species of Aβ cause neuronal dysfunction. Therefore to treat the disease at later stages, targeting these soluble oligomeric forms could be beneficial in improving brain function. This is supported by data in this thesis but also by clinical trials for Solanezumab, an antibody which targets soluble Aβ, which is able to improve cognition of AD patients without causing vascular damage (Doody et al., 2014).

9.1.3 Patient inflammatory state

The third factor important for the neuro-inflammatory response to anti-Aβ immunotherapy is the individual patient's brain microenvironment at the time of therapy. It is well characterised that microglia in the brain of mice with neurodegenerative disease are primed to respond to systemic immune challenges (Combrinck et al., 2002; Cunningham et al., 2005; Lunnon et al., 2011). Systemic infection can also prime the brain to respond to a second immune challenge (Puentener et al., 2012). In **Chapter 8** I show that cells in the brain of TG2576 mice are primed to respond to systemic inflammation, shown by exacerbated cytokine production and increased Aβ load compared to wild type mice following exposure to a real systemic infection. Similar observations were made in studies using LPS, which mimics aspect of a bacterial infection (Jaeger et al., 2009b; Lee et al., 2008; Sheng et al., 2003b). As a real infection activates a range of innate immune receptors as well as an adaptive immune response, I believe this to be a more accurate model to test the effect of systemic infection on the AD affected brain. One of the observations following

systemic infection was the increased expression of FcγRI in the brains of TG2576 mice after infection with *S. typhimurium*. Due to the predicted involvement of FcγRI on the detrimental neuro-inflammatory response to 3D6 , we hypothesise that mice infected with *S. typhimurium* will have an exacerbated neuro-inflammatory response to 3D6 IgG2a. This could have important implications for patients treated with anti-Aβ antibodies as systemic inflammation, a common risk factor for AD progression, could increase the neuro-inflammation caused by immunotherapy, which could increase the severity of ARIA-E.

The effector function of anti-Aβ antibodies could also be determined by the individual genetics of a patient. There are several polymorphisms which have been identified in human FcγRs, changing the affinity for IgG or their ability to function (Bournazos et al., 2009b). These polymorphisms not only increase the risk of developing auto-immune disease, but can also change the response of a patient to immunotherapy. Single nucleotide polymorphisms (SNPs) have been discovered in FcγRIIa and FcγRIIIa have been found which increase their affinity for certain IgG subclasses, for example the SNP V158F in FcγRIIIa increases the affinity of the receptor for human IgG1 and IgG3 (Koene et al., 1997). Patients with B-cell lymphoma who have this SNP, respond better to anti-CD20 immunotherapy due to enhanced effector function which increases ADCC (Cartron, 2002). This could have relevance to AD, as microglia in the brains of AD patients express FcγRIIIa, and therefore AD patients possessing the V158F polymorphism could have a stronger neuro-inflammatory response anti-Aβ immunotherapy. This could enable enhanced plaque clearance but increased likelihood of developing ARIA-E.

9.1.4 How does neuro-inflammation induce vascular dysfunction?

ARIA-E is the leakage of fluid and plasma proteins into the parenchyma due to dysfunction of the BBB and although this is a well described side effect of immunotherapy, the exact mechanisms are not fully understood. *In vivo* experimental studies have shown that anti-Aβ immunotherapy causes increased activity of MMPs 2 and 9, providing a potential mechanism for the side effects associated with immunotherapy (Wilcock et al., 2011a). Research into the effect of inflammation on ischemic stroke has shown that central or peripheral administered IL-1β can stimulate the release of MMP-9 from astrocytes or neutrophils. Neutrophils may adhere to activated endothelium and MMP-9 released by these cells cleaves the tight junction protein claudin-5 expressed by brain endothelial

cells, disrupting BBB integrity and increasing vascular permeability (McColl et al., 2008; Thornton et al., 2008). This reduction in the integrity of the BBB could also explain the incidence of ARIA-E after anti-Aβ immunotherapy, where FcγR-mediated inflammation may lead to increased IL-1β, and MMP-9 activity. A summary of this proposed mechanism is shown in figure 9.2A. Antibodies that can bind to plaques, i.e. 3D6 and Gantenerumab, are associated with increased neuro-inflammation compared to antibodies which do not bind to plaques i.e. mC2. If neuro-inflammation is the driver of ARIA-E, treatment with a plaque binding antibody would induce ARIA-E but treatment with an antibody targeting soluble forms would not. In support of this hypothesis, the antibodies: Bapineuzumab, Gantenerumab and Aducanumab all bind to plaques and have been shown to induce ARIA-E, but antibodies which cannot bind to plaques such as Solanezumab and Crenezumab do not (Adolfsson et al., 2012; Doody et al., 2014; Ostrowitzki et al., 2012; Rinne et al., 2010). In this thesis I show that Infection of TG2576 with *S. typhimurium* results in increased brain IL-1β and KC, this is accompanied by increased vascular permeability and entry of T-cells into the brain parenchyma. Studies investigating stroke, demonstrate that increased vascular permeability after systemic inflammation is due to cleavage of the tight junction protein claudin-5 by MMP-9, which is released after stimulation with IL-1β (McColl et al., 2008; Thornton et al., 2008). The proposed mechanism for changes in vascular permeability and neuro-inflammation after peripheral infection are shown in figure 9.2B. Therefore, peripheral inflammation could increase the severity of ARIA-E through both FcγR dependent and independent mechanisms. As previously discussed, increased FcγR expression of effector cells in the brain could result in an exacerbated inflammatory response to immunotherapy causing increased vascular permeability by the decrease of tight junction integrity. Systemic inflammation could also mediate increased vascular permeability directly by the increased production of cytokines by the activated endothelium/microglia, and therefore this could worsen ARIA-E by independently increasing vascular permeability. The proposed mechanisms of ARIA-E exacerbation by peripheral inflammation are shown in figure 9.2C.

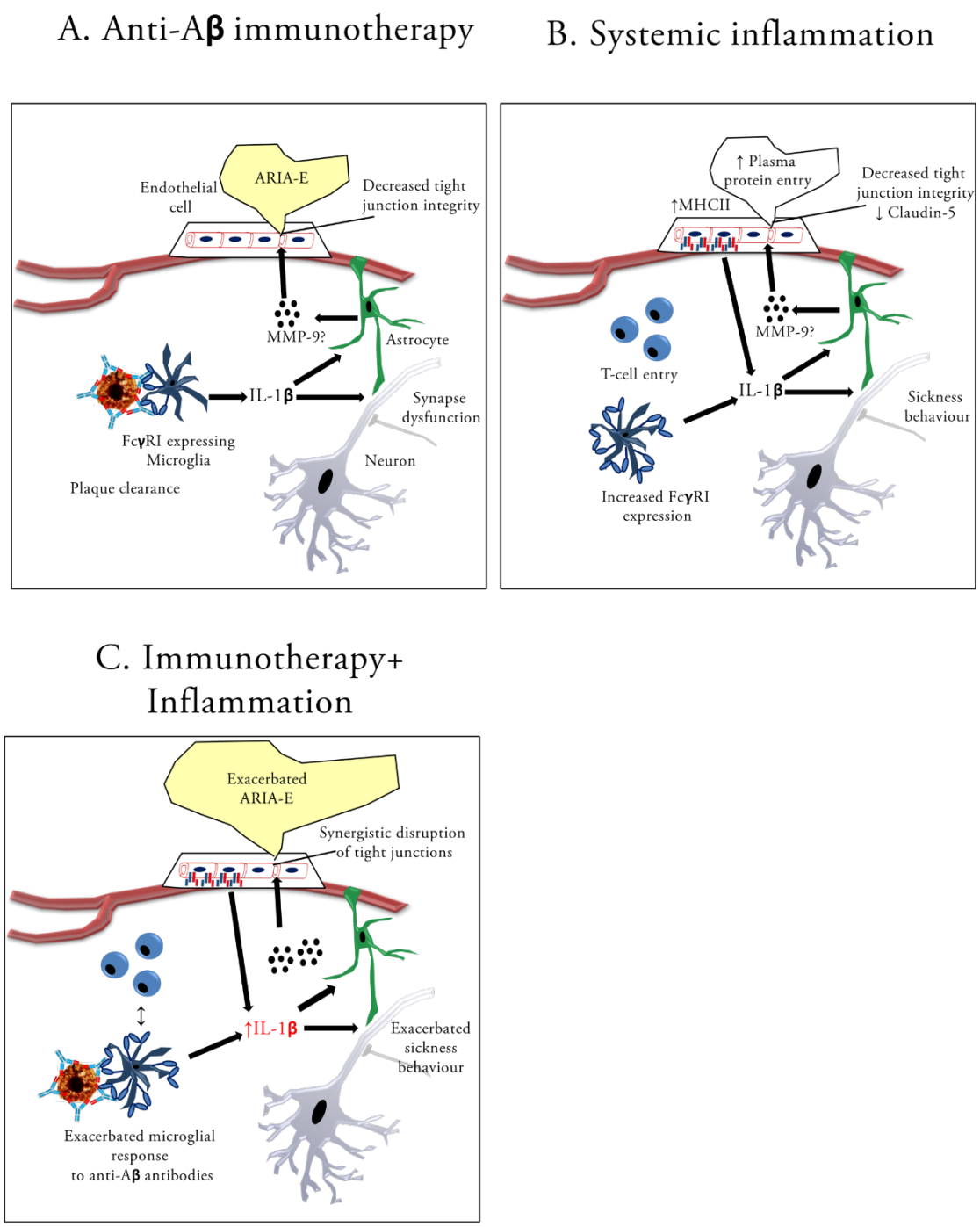

Figure 9. 2 Proposed mechanisms for ARIA-E and exacerbation by systemic inflammation

A. Immunotherapy causes increased levels of the cytokine IL-1β by activation of microglial FcγRI. IL-1β promotes the release of MMP-9 from astrocytes or other cell types, resulting in the cleavage of tight junction proteins and ARIA-E. **B.** Systemic infection causes: the activation of endothelial cells, the upregulation of FcγRI on microglia and the increased levels of IL-1β in the brain. This also induces cleavage of tight junction proteins by MMPs and increased vascular permeability. **C.** Systemic inflammation could exacerbate ARIA-E either by increasing FcγRI causing increased cytokine release, or by independently increasing vascular permeability.

Anti-Aβ immunotherapy can cause damage to the cerebral vasculature, likely through FcγR mediated inflammation. However, the effect of altered microenvironment, microglial priming, increased neuro-inflammation and the influx of plasma on the function of neurons has not been thoroughly discussed. It is well established that inflammation is a key neuropathological feature of AD, and there is a growing body of evidence implicating FcγRs themselves in the pathology of numerous neurodegenerative conditions (Fuller et al., 2014). Thus, it is important to consider the consequences of altered FcγR expression and activation through immunotherapy and/or other factors, such as systemic infections. We and others have now shown that inflammation driven by infection or mimetics of infection, can lead to the increased accumulation of Aβ and tau (Kitazawa et al., 2005; Lee et al., 2008; Sheng et al., 2003a). Therefore increasing the levels of inflammation in the brain of AD patients could have deleterious effects. Soluble inflammatory mediators such as TNFα and IL-1β have divergent roles within the CNS and regulate the function of neurons. Intracranial administration of these mediators causes changes in neuronal function (Ross et al., 2003; Stellwagen and Malenka, 2006), and therefore increased CNS levels of these cytokines as a result of immunotherapy could further disrupt synaptic function in AD patients. Furthermore plasma proteins such as IgG have been shown to be neurotoxic in a variety of disease models (Fernandez-Vizarra et al., 2012). Arguably increased levels of neuro-inflammation and plasma proteins after immunotherapy could lead to neuronal dysfunction or loss. Supporting this hypothesis, AD patients treated with Bapineuzumab actually had decreased brain volume compared to those given control antibody. This could suggest that the increased inflammation or the breakdown of the BBB caused by Bapineuzumab, could result in the loss of neurons and reduction in brain volume (Salloway et al., 2014).

9.2 Future directions

9.2.1 Systemic treatment with a plaque binding antibody

The results in this thesis show that intracranial administration of 3D6 IgG2a is associated with increased IL-1β compared to 3D6 IgG1 or isotype controls. Comparison with data from mC2 treatment, lead to the conclusion that IgG2a antibodies that target plaques, cause increased neuro-inflammation likely through activation of FcγRI. Unfortunately, due to the low antibody expression of recombinant 3D6 it was not possible to produce sufficient antibody to compare and confirm these findings after systemic treatment. It is therefore possible that this result was due to the administration route rather than the antibody specificity. To test the role of effector function after systemic treatment with a plaque binding antibody, I would treat TG2576 mice with IgG1 and IgG2a versions of a plaque binding antibody, for example Gantenerumab, which produced well after transfection. Alternatively, to circumvent the problems with expression levels of 3D6, I would produce a chimeric version of Bapineuzumab, the clinical candidate derived from 3D6, using the variable domains from Bapineuzumab and mouse constant regions. This strategy worked well in the production of Gantenerumab, which had a yield 300-fold higher than 3D6. If chimeric Bapineuzumab also does not produce at a sufficient level in our expression system, I would instead produce a chimeric version of the fully human antibody, Aducanumab, which specifically recognises aggregated Aβ and therefore plaques. I would hypothesise that treatment with the IgG2a version would clear plaques more effectively and cause more neuro-inflammation than the IgG1. It would be interesting to compare the ability of an antibody like 3D6 to reverse cognitive deficits directly with mC2. This would give insight into which species of Aβ should be targeted in clinical trials.

9.2.2 Elucidating the specific FcγRs involved in anti-Aβ antibody effector function and optimisation of the antibody Fc region

Although experiments in this thesis provide indications of the FcγRs that are likely to be involved in the effector function of anti-Aβ antibodies, further experiments are required to confirm these hypotheses. To test the importance of individual FcγRs in the effector function of anti-Aβ antibodies, I would cross TG2576 mice with mice deficient for either FcγRI or FcγRIII. This would produce a mouse model which accumulates Aβ but lacks the expression of either FcγRI or FcγRIII. It would first be necessary to characterise the pathology in the new strains of mice to ensure that the accumulation of Aβ, or the cognitive deficits associated with this model are not altered by FcγR deficiency. The data from this thesis suggest that dependent of the species of Aβ targeted, antibodies may require different effector functions. I hypothesise that FcγRI is responsible for plaque clearance and neuro-inflammation after treatment with 3D6 IgG2a. To test this I would repeat intracranial injections of the antibody 3D6 IgG2a into WT TG2576 and FcγRI deficient TG2576, measuring cytokine levels and Aβ clearance. If FcγRI mediates the effector function of 3D6, the clearance of plaques and release of IL-1β would be reduced in the FcγRI deficient mice. This information could inform the Fc engineering of therapeutic antibodies to reduce neuro-inflammation or increase plaque clearance.

My data suggest that FcγRIII mediates neuro-inflammation after systemic antibody treatment, however it is unclear whether FcγRs are required to reverse cognitive deficits. To determine the importance of effector function in the reversal of cognitive deficits by mC2 treatment, I would generate mC2 IgG2a with the amino acid substitution D265A which reduces binding to all mouse FcγRs (Baudino et al., 2008). I would repeat systemic treatment of TG2576 mice and FcγRIII deficient TG2576 mice with either mC2 IgG2a or mC2 $IgG2a_{D265A}$, measuring cognitive deficit and brain cytokine levels. If the FcγRIII is not important for the reversal of cognitive deficits in TG2576 after mC2 treatment, FcγRIII deficient mice treated with mC2 IgG2a or TG2576 mice treated with $IgG2a_{D265A}$ would both show the same improvement in cognition as WT TG2576 mice treated with mC2IgG2a. If the neuro-inflammation after treatment with mC2 is mediated through FcγRIII, FcγRIII deficient mice treated with mC2 IgG2a or TG2576 mice treated with $IgG2a_{D265A}$ would have

reduced cytokine levels compared to WT TG2576 mice treated with mC2IgG2a. This information could inform the engineering of Fc regions for clinical trials of antibodies such as Solanezumab which bind to soluble forms of Aβ (Doody et al., 2014).

Previous studies have shown that the removal of Aβ by immunotherapy is partially dependent on FcRn mediated efflux from the brain, which is expressed by brain endothelial cells (Deane et al., 2005). Fc regions of therapeutic antibodies have been mutated to increase their affinity for FcRn, resulting in increased serum half-life of therapeutic antibodies and therefore reduces the length of time needed between doses (Ghetie et al., 1997). These mutants could be of interest for the optimisation of anti-Aβ antibodies, as they would not only increase the serum persistence but could also enhance FcRn mediated efflux from the brain. I hypothesise that the increased affinity for FcRn would enhance FcRn mediated efflux, and therefore improve Aβ elimination from the brain. To test this hypothesis I would generate 3D6 IgG2a with mutations associated with increased or loss of FcRn binding affinity, and inject directly into the hippocampus of 18 month old TG2576 mice and measure Aβ clearance from the brain.

9.2.3 Determining the levels of functional IL-1β and its effect on neuronal function

Treatment with anti-Aβ antibodies or infection with *S. typhimurium* results in the increased production of central IL-1β. This cytokine is reported to be up-regulated in a number of models of disease, and induces the release of MMPs from astrocytes or neutrophils in the brain (McColl et al., 2008; Thornton et al., 2008). This could have important consequences for BBB permeability, particularly in the context of ARIA-E after immunotherapy. However, IL-1β is expressed as a pro-form and requires post-translational cleavage to produce mature and active IL-1β (Netea et al., 2015). To determine whether the IL-1β measured has been cleaved to form mature IL-1β I would use western blotting in brain homogenate of animals injected with 3D6 IgG2a. Western blotting is able to distinguish the larger pro-IL-1β from the mature and smaller IL-1β by size, and this would give a better indication of the potential of IL-1β production to alter brain function. The IL-1 receptor is expressed by neurons, and IL-1β can modify neuronal function (Bellinger et al., 1993; Katsuki et al., 1990). This is illustrated by the induction of sickness behaviours after intracranial

injection (Dantzer and Kelley, 2007). I hypothesise that the increased levels of IL-1β after treatment with 3D6 IgG2a could cause changes in the function of neurons. Testing this hypothesis is technically challenging, and would require a combination of behavioural assessment and direct measurement of neuronal function. I would use a behaviour that has previously been shown to be sensitive to cytokine induced sickness behaviour, such as the burrowing assay (Dantzer and Kelley, 2007). Seven days after intracranial injection with 3D6 IgG1 and IgG2a or isotype controls I would measure changes in burrowing activity. I would hypothesise that the increased levels of IL-1β in the brains of mice injected with 3D6 IgG2a would lead to a decrease in burrowing activity compared to 3D6 IgG1 injected mice, but this effect may be difficult to separate from the benefit of clearing Aβ. To measure direct changes in neuronal function I would use *in vivo* electrophysiology, a technique which can measure synaptic activity in the hippocampus in live anaesthetised mice. For both of these experiments, intracranial IL-1β injection would serve as a good positive control.

9.2.4 Characterisation of ARIA-E, and exacerbation mediated by peripheral inflammation

ARIA-E remains a problem for current antibodies in clinical trials, and is thought to be caused by neuro-inflammation resulting in a reduction of BBB integrity. A limitation of this thesis is the lack of a reliable method to detect this BBB dysfunction after immunotherapy, linking the neuro-inflammation seen after antibody treatment with actual BBB changes. Previous studies *in vivo* have shown that immunotherapy can cause the release of MMP-9, which could in turn cause ARIA-E by cleavage of tight junction proteins (Wilcock et al., 2011a). In the general discussion I proposed three factors important for the level of neuro-inflammation after anti-Aβ immunotherapy. I hypothesise that antibodies with stronger effector function associated with a stronger neuro-inflammatory response *in vivo*, would also cause increased MMP activity. To test this hypothesis, I would repeat intracranial injections of 3D6 IgG1 and IgG2a into 18 month old TG2576 mice, taking tissue for IHC and for homogenate. In brain sections I would stain for the expression of tight junction proteins, such as claudin-5, measuring the integrity of tight junctions. In the homogenate I would measure the activity of MMPs by zymography. These experiments could provide evidence of a link between the effector function of antibodies and the likelihood of inducing ARIA-E in patients.

I hypothesise that infection with *S. typhimurium* could lead to the exacerbation of neuro-inflammation and BBB dysfunction after antibody treatment via FcγR dependent and independent mechanisms. To test this hypothesis I would infect TG2576 mice with *S. typhimurium* or inject with saline. Then at one or four weeks post infection I would inject 3D6 IgG2a or IgG2a isotype control into the hippocampus. To test exacerbation of inflammation I would then measure the levels of pro-inflammatory cytokines a week after injection with 3D6, and again measure the activity of MMPs and tight junction integrity to test for increased BBB dysfunction. These mechanisms could be important for other conditions that result in increased expression of FcγRs in the brain and disruption of the BBB, for example obesity. Mice given a high fat diet exhibit: increased activating FcγR expression in the brain, decreased expression of tight junction proteins and increased parenchymal IgG (Tucsek et al., 2014). Therefore obesity could worsen the side effects of anti-Aβ immunotherapy through the same mechanisms as systemic infection. If *S.typhimurium* does cause an exacerbated neuro-inflammatory response to immunotherapy and increased BBB dysfunction, I would test this hypothesis by giving TG2576 mice a high fat diet before treatment with 3D6 IgG2a and measure the same read outs as previously described. It would also be interesting to investigate the effects of peripheral inflammation on the response of AD patients to anti-Aβ immunotherapy. Patients with higher levels of serum cytokines may be at greater risk of developing ARIA-E. FcγR polymorphisms could also affect the neuro-inflammatory response to immunotherapy, and it would therefore be interesting to compare FcγR polymorphisms with the clearance of Aβ and the development of ARIA-E after immunotherapy. The enhanced affinity of the $FcγRIII_{V158F}$ polymorphism for example, could enhance the ability of microglia to clear plaques but also increase the risk of causing ARIA-E (Bournazos et al., 2009b).

9.2.5 Tau as a target for immunotherapy, and combination trials

Neurodegenerative diseases are almost all associated with the accumulation of a misfolded protein in a specific area of the CNS. Antibodies are in development for the treatment of other misfolded proteins for the treatment of neurodegenerative disease, for example the second pathological hallmark of AD-tau. Mice transgenic for human tau, with mutations associated with tauopathies, accumulate tau in the brain causing neuronal dysfunction and cognitive deficits (SantaCruz et al., 2005). Immunisation against tau can clear deposits and reverse cognitive deficits in transgenic tau

models (Boutajangout et al., 2010). Recently it has been shown that tau immunotherapy is dependent on the FcγRs expressed on microglia and on neurons (Congdon et al., 2013; Luo et al., 2015). To optimise immunotherapy for the treatment of tau I would first characterise the FcγRs important for the removal of tau and reversal of cognitive deficits. I would do this as previously described for transgenic APP mice, by breeding transgenic tau mice with mice deficient for individual FcγRs.

AD is a complex disease that develops over decades, and is associated with numerous neuropathological changes. It has already been shown that complete clearance Aβ from the brains of AD patients late in the disease is unable to affect some tau pathology(Boche et al., 2010). Therefore patients could benefit from combination treatment with both anti-Aβ and anti-tau antibodies. Preclinical testing of combination therapies is challenging due to a lack of models fully recapitulating AD pathology. However, the 3xTG model is transgenic for both human Aβ and human tau. I would treat these mice systemically with anti-Aβ and anti-tau antibodies, measuring the clearance of both peptides and improvements in cognition.

9.3 Summary

Immunotherapy is a promising strategy for the treatment of AD, anti-Aβ antibodies are able to clear Aβ deposits and reverse cognitive decline in AD patients. The development of these antibodies has been hampered by side effects, thought to be caused by a pro-inflammatory response to antibody coated plaques. In this thesis we provide the first proof of principle evidence that engineering the Fc region of therapeutic anti-Aβ antibodies can modify the neuro-inflammatory response *in vivo*. We also provide evidence that neuro-inflammation is dependent on the species of Aβ targeted. Finally we propose systemic inflammation may contribute to side effect severity through FcγR dependent and independent mechanisms. Therefore, during the development of new clinical candidate antibodies the effector function should be designed based on the species of Aβ targeted, and the function the antibody is required to perform. To fully optimise immunotherapy for AD further research is required to understand the specific FcγRs that are involved in neuro-inflammation and plaque clearance.

Appendices

Appendix A

Avertin for terminal anaethesia

250ml 0.9% saline (autoclaved)

20ml analytical grade absolute alcohol (Fisher, Loughborough, UK)

5ml avertin concentrate (25g tri bromo-ethanol+ 15.5ml tertiary amy alcohol)

Sterile filtered

Congo red

Staining solution:

0.3g Congo red (Sigma, Dorset, UK)

0.3g NaCl

80ml Ethanol

20ml dH_2O

1ml 1% NaOH

Destain:

50ml Ethanol

50ml dH_2O

2ml 1% NaOH

Phosphate Buffer saline

NaCl 8g

KCl 0.2g

KH_2PO_4 0.24g

Na_2PO_4 1.44

Up to 1 litre in distilled water

Elisa coating buffer

0.1M carbonate/bicarbonate buffer

5.3g Na_2CO_3

4.2g $NaHCO_3$

0.2g NaN_3

Up to 1 litre in distilled water

Elisa Wash Buffer

1 Litre PBS

0.5ml Tween 20 (sigma, Poole, Dorset)

Elisa substrate buffer 1

9ml 0.05M phosphate-citrate buffer (Sigma, Dorset, UK)

1 TMB tablet (Sigma, Dorset, UK) dissolved in 1ml DMSO (Fisher, Loughborough, UK)

2 µl of Hydrogen peroxide added at the last minute

TAE (50x stock)

242g Tris Base

57.1ml Acetic acid

100ml 0.5M EDTA

Up to 1 litre in distilled water

APS coated slides

Wash slides in 10% Decon 90 for 1 hour. Wash slides under tap water, and two rinses in distilled water. Dry slides overnight in 60^0C oven. Place in 2% APS(Sigma, 3-Aminopropyltriethoxy-silane) in methanol for 15 seconds, then rinse in methanol. Wash slides in distilled water and allow to dry overnight.

3,3 Di-amino Benzidine (DAB) substrate solution

5ml 2.5% DAB (Sigma, Dorset, UK)

125ml phosphate buffer

125ml distilled water

125µl 30% H202 (Sigma, Dorset, UK)

Glycine

2.5M Glycine adjusted to pH3

TRIS pH8

1 Litre sterile endotoxin free water

11.7g NaCl

4.84g TRIS

0.75g EDTA

4ml 5M HCL

Appendix B

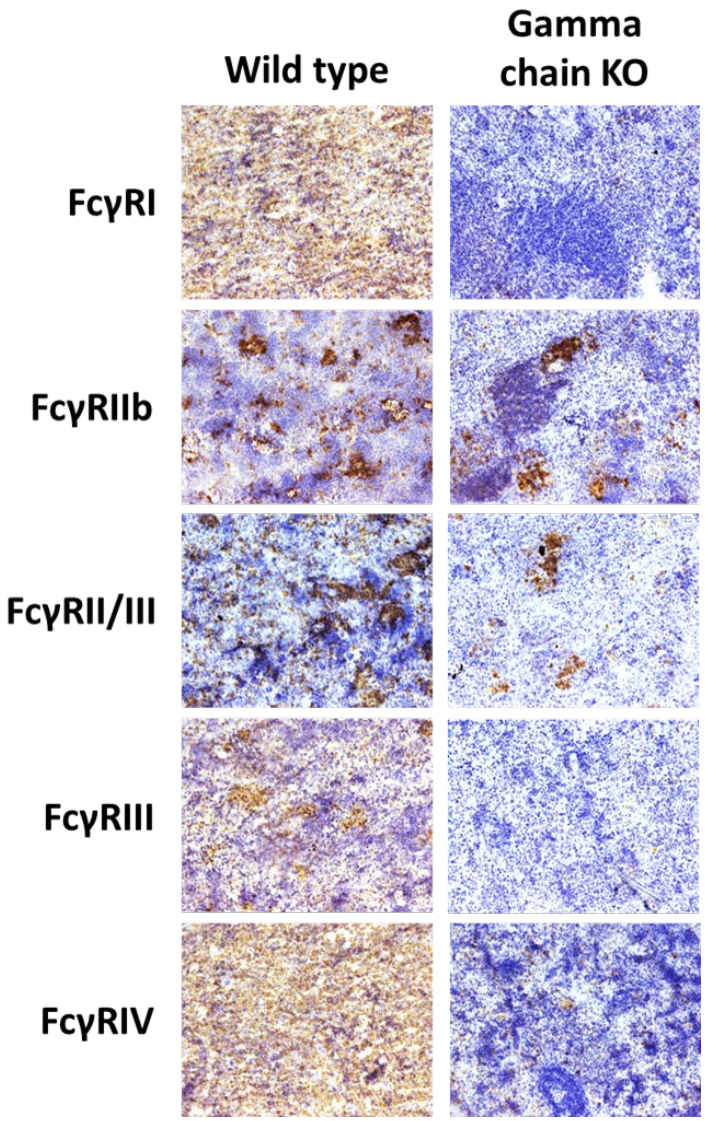

Figure Appendix 1 Validation of in house FcγR antibodies in wild type and gamma chain KO spleen

Antibodies which have been generated in house for the detection of mouse FcγRs were validated by staining spleen sections from wild type and gamma chain KO animals.

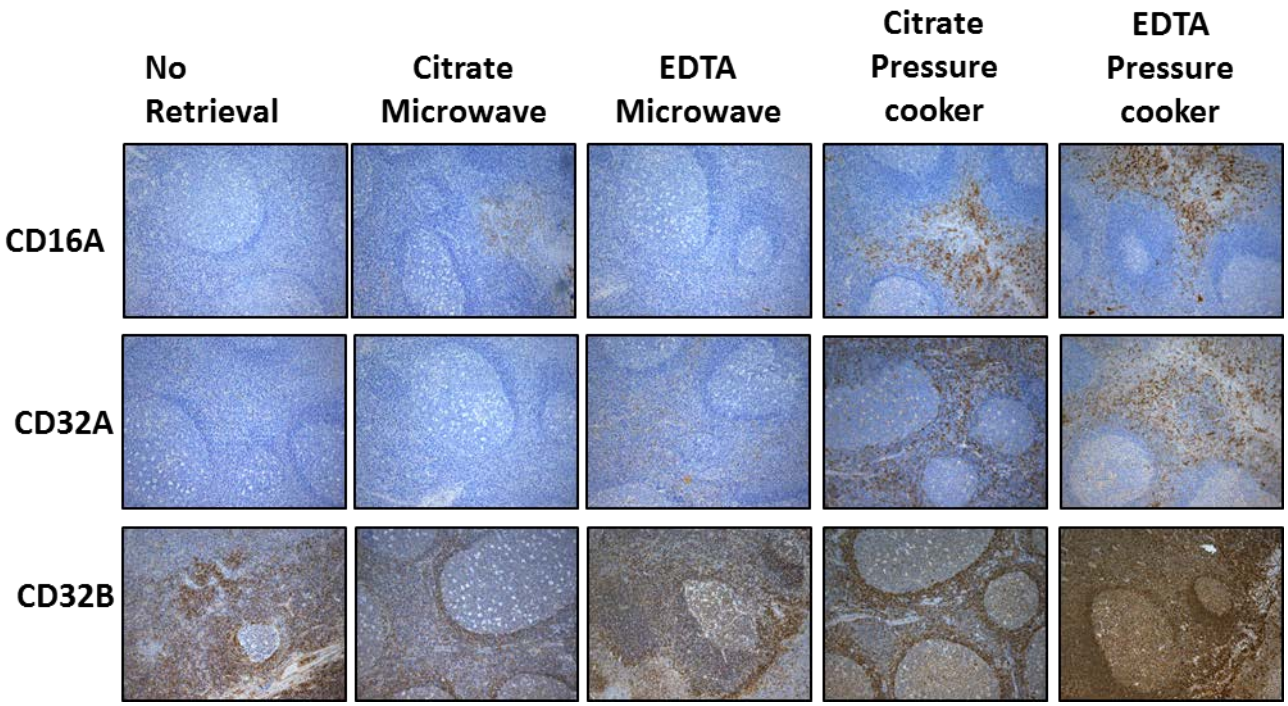

Figure Appendix 2 Optimisation of anti human FcyR antibodies in human tonsil

Antibodies against: CD16A, CD32A and Cd32B were optimised in human tonsil tissue. Two different antigenic retrieval methods and two different buffers were tried in combination: Citrate or EDTA and pressure cooker or microwave.

List of References

Abbas, N., Bednar, I., Mix, E., Marie, S., Paterson, D., Ljungberg, A., Morris, C., Winblad, B., Nordberg, A. and Zhu, J. (2002). Up-regulation of the inflammatory cytokines IFN-γ and IL-12 and down-regulation of IL-4 in cerebral cortex regions of APPSWE transgenic mice. *Journal of Neuroimmunology* **126**, 50-57.

Adolfsson, O., Pihlgren, M., Toni, N., Varisco, Y., Buccarello, A. L., Antoniello, K., Lohmann, S., Piorkowska, K., Gafner, V., Atwal, J. K. et al. (2012). An Effector-Reduced Anti-β-Amyloid (Aβ) Antibody with Unique Aβ Binding Properties Promotes Neuroprotection and Glial Engulfment of Aβ. *The Journal of Neuroscience* **32**, 9677-9689.

Allen, J. M. and Seed, B. (1989). ISOLATION AND EXPRESSION OF FUNCTIONAL HIGH-AFFINITY FC RECEPTOR COMPLEMENTARY DNAS. *Science* **243**, 378-381.

Allsop, D., Wong, C. W., Ikeda, S., Landon, M., Kidd, M. and Glenner, G. G. (1988). Evidence for the origin of cerebral amyloid in Alzheimer's disease drom A Beta protein precursor. *Neuropathol Appl Neurobiol* **14**, 254-255.

Almkvist, O. (1996). Neuropsychological features of early Alzheimer's disease: Preclinical and clinical stages. *Acta Neurologica Scandinavica* **93**, 63-71.

Amaral, D. G. and Lavenex, P. (2007). The Hippocampus Book, pp. 37-114.

Andoh, T. and Kuraishi, Y. (2004). Primary sensory neurons express the high affinity IgG Fc gamma RI receptor and responds to IgG-antigen complex. *Journal of Pharmacological Sciences* **94**, 74P-74P.

Andreasen, N., Simeoni, M., Ostlund, H., Lisjo, P. I., Fladby, T., Loercher, A. E., Byrne, G. J., Murray, F., Scott-Stevens, P. T., Wallin, A. et al. (2015). First Administration of the Fc-Attenuated Anti-β Amyloid Antibody GSK933776 to Patients with Mild Alzheimer's Disease: A Randomized, Placebo-Controlled Study. *PLoS One* **10**, e0098153.

Apelt, J. and Schliebs, R. (2001). β-Amyloid-induced glial expression of both pro- and anti-inflammatory cytokines in cerebral cortex of aged transgenic Tg2576 mice with Alzheimer plaque pathology. *Brain Res* **894**, 21-30.

Arendash, G. W., Gordon, M. N., Diamond, D. M., Austin, L. A., Hatcher, J. M., Jantzen, P., DiCarlo, G., Wilcock, D. and Morgan, D. (2001). Behavioral assessment of Alzheimer's transgenic mice following long-term Abeta vaccination: task specificity and correlations between Abeta deposition and spatial memory. *DNA Cell Biol* **20**, 737-44.

Arlaud, G. J., Gaboriaud, C., Thielens, N. M., Budayova-Spano, M., Rossi, V. and Fontecilla-Camps, J. C. (2002). Structural biology of the C1 complex of complement unveils the mechanisms of its activation and proteolytic activity. *Molecular Immunology* **39**, 383-394.

Bacskai, B. J., Kajdasz, S. T., McLellan, M. E., Games, D., Seubert, P., Schenk, D. and Hyman, B. T. (2002). Non-Fc-mediated mechanisms are involved in clearance of amyloid-beta in vivo by immunotherapy. *Journal of Neuroscience* **22**, 7873-7878.

Bales, K. R., Verina, T., Dodel, R. C., Du, Y. S., Altstiel, L., Bender, M., Hyslop, P., Johnstone, E. M., Little, S. P., Cummins, D. J. et al. (1997). Lack of apolipoprotein E dramatically reduces amyloid beta-peptide deposition. *Nature Genetics* **17**, 263-264.

Banks, W. A. (2012). Drug delivery to the brain in Alzheimer's disease: Consideration of the blood-brain barrier. *Advanced Drug Delivery Reviews* **64**, 629-639.

Bard, F., Cannon, C., Barbour, R., Burke, R. L., Games, D., Grajeda, H., Guido, T., Hu, K., Huang, J. P., Johnson-Wood, K. et al. (2000). Peripherally administered antibodies against amyloid beta-peptide enter the central nervous system and reduce pathology in a mouse model of Alzheimer disease. *Nature Medicine* **6**, 916-919.

Barnes, N., Gavin, A. L., Tan, P. S., Mottram, P., Koentgen, F. and Hogarth, P. M. (2002). FcγRI-Deficient Mice Show Multiple Alterations to Inflammatory and Immune Responses. *Immunity* **16**, 379-389.

Baudino, L., Shinohara, Y., Nimmerjahn, F., Furukawa, J. I., Nakata, M., Martinez-Soria, E., Petry, F., Ravetch, J. V., Nishimura, S. I. and Izui, S. (2008). Crucial Role of Aspartic Acid at Position 265 in the CH2 Domain for Murine IgG2a and IgG2b Fc-Associated Effector Functions. *Journal of Immunology* **181**, 6664-6669.

Bellinger, F. P., Madamba, S. and Siggins, G. R. (1993). Interleukin 1 Beta inhibits synaptic strength and lon-term potentiation in the rat CA1 hippocampus. *Brain Res* **628**, 227-234.

Benzing, W. C., Wujek, J. R., Ward, E. K., Shaffer, D., Ashe, K. H., Younkin, S. G. and Brunden, K. R. (1999). Evidence for glial-mediated inflammation in aged APP(SW) transgenic mice. *Neurobiol Aging* **20**, 581-9.

Berthoud, H.-R. and Neuhuber, W. L. (2000). Functional and chemical anatomy of the afferent vagal system. *Autonomic Neuroscience* **85**, 1-17.

Bevaart, L., Jansen, M. J. H., van Vugt, M. J., Verbeek, J. S., van de Winkel, J. G. J. and Leusen, J. H. W. (2006). The High-Affinity IgG Receptor, FcγRI, Plays a Central Role in Antibody Therapy of Experimental Melanoma. *Cancer Res* **66**, 1261-1264.

Bie, B. W., Jiang; Yang, Hui; Xu, Jijun J; Brown, David L Naguib, Mohamed. (2014). Epigentic suppresion of neuroligin 1 underlies amyloid induced memory deficiency. *Nat Neuroscience* **17**, 223-231.

Boche, D., Denham, N., Holmes, C. and Nicoll, J. A. R. (2010). Neuropathology after active A beta 42 immunotherapy: implications for Alzheimer's disease pathogenesis. *Acta Neuropathol* **120**, 369-384.

Boche, D., Zotova, E., Weller, R. O., Love, S., Neal, J. W., Pickering, R. M., Wilkinson, D., Holmes, C. and Nicoll, J. A. (2008). Consequence of Abeta immunization on the vasculature of human Alzheimer's disease brain. *Brain* **131**, 3299-310.

Bohrmann, B., Baumann, K., Benz, J., Gerber, F., Huber, W., Knoflach, F., Messer, J., Oroszlan, K., Rauchenberger, R., Richter, W. F. et al. (2012). Gantenerumab: A Novel Human Anti-A beta Antibody Demonstrates Sustained Cerebral Amyloid-beta Binding and Elicits Cell-Mediated Removal of Human Amyloid-beta. *Journal of Alzheimers Disease* **28**, 49-69.

Boulianne, G. L., Hozumi, N. and Shulman, M. J. (1984). PRODUCTION OF FUNCTIONAL CHIMAERIC MOUSE HUMAN-ANTIBODY. *Nature* **312**, 643-646.

Bouras, C., Riederer, B. M., Kovari, E., Hof, P. R. and Giannakopoulos, P. (2005). Humoral immunity in brain aging and Alzheimer's disease. *Brain Research Reviews* **48**, 477-487.

Bournazos, S., Hart, S. P., Chamberlain, L. H., Glennie, M. J. and Dransfield, I. (2009a). Association of FcγRIIa (CD32a) with Lipid Rafts Regulates Ligand Binding Activity. *The Journal of Immunology* **182**, 8026-8036.

Bournazos, S., Woof, J. M., Hart, S. P. and Dransfield, I. (2009b). Functional and clinical consequences of Fc receptor polymorphic and copy number variants. *Clinical & Experimental Immunology* **157**, 244-254.

Boutajangout, A., Quartermain, D. and Sigurdsson, E. M. (2010). Immunotherapy Targeting Pathological Tau Prevents Cognitive Decline in a New Tangle Mouse Model. *The Journal of Neuroscience* **30**, 16559-16566.

Bowles, J. A., Wang, S. Y., Link, B. K., Allan, B., Beuerlein, G., Campbell, M. A., Marquis, D., Ondek, B., Wooldridge, J. E., Smith, B. J. et al. (2006). Anti-CD20 monoclonal antibody with enhanced affinity for CD16 activates NK cells at lower concentrations and more effectively than rituximab. *Blood* **108**, 2648-54.

Braak, H. and Braak, E. (1991). Neuropathological stageing of Alzheimer-related changes. *Acta Neuropathol* **82**, 239-259.

Broz, P., Ohlson, M. B. and Monack, D. M. (2012). Innate immune response to Salmonella typhimurium, a model enteric pathogen. *Gut Microbes* **3**, 62-70.

Bruhns, P. (2012). Properties of mouse and human IgG receptors and their contribution to disease models. *Blood* **119**, 5640-5649.

Bruhns, P., Iannascoli, B., England, P., Mancardi, D. A., Fernandez, N., Jorieux, S. and Daeron, M. (2009). Specificity and affinity of human Fc gamma receptors and their polymorphic variants for human IgG subclasses. *Blood* **113**, 3716-3725.

Burmeister, W. P., Huber, A. H. and Bjorkman, P. J. (1994). Crystal structure of the complex of rat neonatal Fc receptor with Fc. *Nature* **372**, 379-383.

Burstein, A. H., Zhao, Q., Ross, J., Styren, S., Landen, J. W., Ma, W. W., McCush, F., Alvey, C., Kupiec, J. W. and Bednar, M. M. (2013). Safety and Pharmacology of Ponezumab (PF-04360365) After a Single 10-Minute Intravenous Infusion in Subjects With Mild to Moderate Alzheimer Disease. *Clinical Neuropharmacology* **36**, 8-13.

Butchart, J., Brook, L., Hopkins, V., Teeling, J., Puentener, U., Culliford, D., Sharples, R., Sharif, S., McFarlane, B., Raybould, R. et al. (2015). Etanercept in Alzheimer disease: A randomized, placebo-controlled, double-blind, phase 2 trial. *Neurology* **84**, 2161-2168.

Cabezas, R., Avila, M., Gonzalez, J., El-Bachá, R. S., Baez, E., Garcia-Segura, L. M., Jurado Coronel, J. C., Capani, F., Cardona Gomez, G. P. and Barreto, G. E. (2014). Astrocytic modulation of Blood Brain Barrier: Perspectives on Parkinson´s Disease. *Frontiers in Cellular Neuroscience* **8**.

Cai, H., Cong, W.-n., Ji, S., Rothman, S., Maudsley, S. and Martin, B. (2012). Metabolic Dysfunction in Alzheimer's Disease and Related Neurodegenerative Disorders. *Current Alzheimer Research* **9**, 5-17.

Cao, S., Standaert, D. G. and Harms, A. S. (2012). The gamma chain subunit of Fc receptors is required for alpha-synuclein-induced pro-inflammatory signaling in microglia. *J Neuroinflammation* **9**.

Cao, S., Theodore, S. and Standaert, D. G. (2010). Fc gamma receptors are required for NF-kappa B signaling, microglial activation and dopaminergic neurodegeneration in an AAV-synuclein mouse model of Parkinson's disease. *Mol Neurodegener* **5**.

Carare, R. O., Teeling, J. L., Hawkes, C. A., Püntener, U., Weller, R. O., Nicoll, J. A. R. and Perry, V. H. (2013). Immune complex formation impairs the elimination of solutes from the brain: implications for immunotherapy in Alzheimer's disease. *Acta Neuropathologica Communications* **1**, 48-48.

Carter, C. (2011). Alzheimer's Disease: APP, Gamma Secretase, APOE, CLU, CR1, PICALM, ABCA7, BIN1, CD2AP, CD33, EPHA1, and MS4A2, and Their Relationships with Herpes Simplex, C. Pneumoniae, Other Suspect Pathogens, and the Immune System. *Int J Alzheimers Dis* **2011**, 501862.

Carter, P. B. and Collins, F. M. (1974). THE ROUTE OF ENTERIC INFECTION IN NORMAL MICE. *The Journal of Experimental Medicine* **139**, 1189-1203.

Cartron, G. (2002). Therapeutic activity of humanized anti-CD20 monoclonal antibody and polymorphism in IgG Fc receptor Fcgamma RIIIa gene. *Blood* **99**, 754-758.

Carty, N. C., Wilcock, D. M., Rosenthal, A., Grimm, J., Pons, J., Ronan, V., Gottschall, P. E., Gordon, M. N. and Morgan, D. (2006). Intracranial administration of deglycosylated C-terminal-specific anti-Abeta antibody efficiently clears amyloid plaques without activating microglia in amyloid-depositing transgenic mice. *J Neuroinflammation* **3**, 11.

Chan, A. C. and Carter, P. J. (2010). Therapeutic antibodies for autoimmunity and inflammation. *Nature Reviews Immunology* **10**, 301-316.

Chen, L. H., Kao, P. Y., Fan, Y. H., Ho, D. T., Chan, C. S., Yik, P. Y., Ha, J. C., Chu, L. W. and Song, Y. Q. (2012). Polymorphisms of CR1, CLU and PICALM confer susceptibility of Alzheimer's disease in a southern Chinese population. *Neurobiol Aging* **33**, 210 e1-7.

Chothia, C. and Lesk, A. M. (1987). Canonical structures for the hypervariable regions of immunoglobulins. *J Mol Biol* **196**, 901-917.

Chothia, C., Lesk, A. M., Tramontano, A., Levitt, M., Smith-Gill, S. J., Air, G., Sheriff, S., Padlan, E. A., Davies, D., Tulip, W. R. et al. (1989). Conformations of immunoglobulin hypervariable regions. *Nature* **342**, 877-883.

Chung, E., Ji, Y., Sun, Y., Kascsak, R. J., Kascsak, R. B., Mehta, P. D., Strittmatter, S. M. and Wisniewski, T. (2010). Anti-PrPC monoclonal antibody infusion as a novel treatment for cognitive deficits in an alzheimer's disease model mouse. *BMC Neurosci* **11**.

Citron, M., Oltersdorf, T., Haass, C., McConlogue, L., Hung, A. Y., Seubert, P., Vigopelfrey, C., Lieberburg, I. and Selkoe, D. J. (1992). MUTATION OF THE BETA-AMYLOID PRECURSOR PROTEIN IN FAMILIAL ALZHEIMERS-DISEASE INCREASES BETA-PROTEIN PRODUCTION. *Nature* **360**, 672-674.

Clynes, R., Maizes, J. S., Guinamard, R., Ono, M., Takai, T. and Ravetch, J. V. (1999). Modulation of immune complex-induced inflammation in vivo by the coordinate expression of activation and inhibitory Fc receptors. *Journal of Experimental Medicine* **189**, 179-185.

Coburn, B., Grassl, G. A. and Finlay, B. B. (2006). Salmonella, the host and disease: a brief review. *Immunol Cell Biol* **85**, 112-118.

Cohen, S. I. A., Linse, S., Luheshi, L. M., Hellstrand, E., White, D. A., Rajah, L., Otzen, D. E., Vendruscolo, M., Dobson, C. M. and Knowles, T. P. J. (2013). Proliferation of amyloid-beta 42 aggregates occurs through a secondary nucleation mechanism. *Proceedings of the National Academy of Sciences of the United States of America* **110**, 9758-9763.

Cole, S. L. and Vassar, R. (2008). The Role of Amyloid Precursor Protein Processing by BACE1, the β-Secretase, in Alzheimer Disease Pathophysiology. *Journal of Biological Chemistry* **283**, 29621-29625.

Combrinck, M. I., Perry, V. H. and Cunningham, C. (2002). Peripheral infection evokes exaggerated sickness behaviour in pre-clinical murine prion disease. *Neuroscience* **112**, 7-11.

Congdon, E. E., Gu, J. P., Sait, H. B. R. and Sigurdsson, E. M. (2013). Antibody Uptake into Neurons Occurs Primarily via Clathrin-dependent Fc gamma Receptor Endocytosis and Is a Prerequisite for Acute Tau Protein Clearance. *Journal of Biological Chemistry* **288**, 35452-35465.

Cooper, P. R., Ciambrone, G. J., Kliwinski, C. M., Maze, E., Johnson, L., Li, Q., Feng, Y. and Hornby, P. J. (2013). Efflux of monoclonal antibodies from rat brain by neonatal Fc receptor, FcRn. *Brain Res* **1534**, 13-21.

Cribbs, D. H., Berchtold, N. C., Perreau, V., Coleman, P. D., Rogers, J., Tenner, A. J. and Cotman, C. W. (2012). Extensive innate immune gene activation accompanies brain aging, increasing vulnerability to cognitive decline and neurodegeneration: a microarray study. *J Neuroinflammation* **9**.

Crump, J. A., Luby, S. P. and Mintz, E. D. (2004). The global burden of typhoid fever. *Bulletin of the World Health Organization* **82**, 346-353.

Cruts, M. and Van Broeckhoven, C. (1998). Presenilin mutations in Alzheimer's disease. *Human Mutation* **11**, 183-190.

Cunningham, C., Wilcockson, D. C., Campion, S., Lunnon, K. and Perry, V. H. (2005). Central and Systemic Endotoxin Challenges Exacerbate the Local Inflammatory Response and Increase Neuronal Death during Chronic Neurodegeneration. *The Journal of Neuroscience* **25**, 9275-9284.

D'Andrea, M. R. (2003). Evidence linking neuronal cell death to autoimmunity in Alzheimer's disease. *Brain Res* **982**, 19-30.

Dagher, N. N., Najafi, A. R., Kayala, K. M. N., Elmore, M. R. P., White, T. E., Medeiros, R., West, B. L. and Green, K. N. (2015). Colony-stimulating factor 1 receptor inhibition prevents microglial plaque association and improves cognition in 3xTg-AD mice. *J Neuroinflammation* **12**, 139.

Dantzer, R. and Kelley, K. W. (2007). Twenty Years of Research on Cytokine-Induced Sickness Behavior. *Brain, behavior, and immunity* **21**, 153-160.

Deacon, R. M. J. (2006a). Assessing nest building in mice. *Nat. Protocols* **1**, 1117-1119.

Deacon, R. M. J. (2006b). Assessing nest building in mice. *Nat Protoc* **1**, 1117-1119.

Deane, R., Bell, R. D., Sagare, A. and Zlokovic, B. V. (2009). Clearance of amyloid-β peptide across the blood-brain barrier: Implication for therapies in Alzheimer's disease. *CNS Neurol Disord Drug Targets* **8**, 16-30.

Deane, R., Sagare, A., Hamm, K., Parisi, M., LaRue, B., Guo, H., Wu, Z., Holtzman, D. M. and Zlokovic, B. V. (2005). IgG-assisted age-dependent clearance of Alzheimer's amyloid beta peptide by the blood-brain barrier neonatal Fc receptor. *J Neurosci* **25**, 11495-503.

DellaGioia, N., Devine, L., Pittman, B. and Hannestad, J. (2013). Bupropion pre-treatment of endotoxin-induced depressive symptoms. *Brain, behavior, and immunity* **31**, 197-204.

DeMattos, R. B., Bales, K. R., Cummins, D. J., Dodart, J. C., Paul, S. M. and Holtzman, D. M. (2001). Peripheral anti-A beta antibody alters CNS and plasma A beta clearance and decreases brain A beta burden in a mouse model of Alzheimer's disease. *Proc Natl Acad Sci U S A* **98**, 8850-5.

DeMattos, Ronald B., Lu, J., Tang, Y., Racke, Margaret M., DeLong, Cindy A., Tzaferis, John A., Hole, Justin T., Forster, Beth M., McDonnell, Peter C., Liu, F. et al. (2012). A Plaque-Specific Antibody Clears Existing β-amyloid Plaques in Alzheimer's Disease Mice. *Neuron* **76**, 908-920.

Diamond, B., Kowal, C., Huerta, P. T., Aranow, C., Mackay, M., DeGiorgio, L. A., Lee, J., Triantaylopoulou, A., Cohen-Solal, J. and Volpe, B. T. (2006). Immunity and acquired alterations in cognition and emotion: Lessons from SLE. In *Advances in Immunology, Vol 89*, vol. 89 (ed. F. W. Alt), pp. 289-320.

DiCarlo, G., Wilcock, D., Henderson, D., Gordon, M. and Morgan, D. (2001). Intrahippocampal LPS injections reduce Abeta load in APP+PS1 transgenic mice. *Neurobiol Aging* **22**, 1007-12.

Dickson, T. C. and Vickers, J. C. (2001). The morphological phenotype of β-amyloid plaques and associated neuritic changes in Alzheimer's disease. *Neuroscience* **105**, 99-107.

Dodart, J. C., Bales, K. R., Gannon, K. S., Greene, S. J., DeMattos, R. B., Mathis, C., DeLong, C. A., Wu, S., Wu, X., Holtzman, D. M. et al. (2002). Immunization reverses memory deficits without reducing brain A beta burden in Alzheimer's disease model. *Nature Neuroscience* **5**, 452-457.

Doody, R. S., Thomas, R. G., Farlow, M., Iwatsubo, T., Vellas, B., Joffe, S., Kieburtz, K., Raman, R., Sun, X., Aisen, P. S. et al. (2014). Phase 3 Trials of Solanezumab for Mild-to-Moderate Alzheimer's Disease. *New England Journal of Medicine* **370**, 311-321.

Drew, L. J., Fusi, S. and Hen, R. (2013). Adult neurogenesis in the mammalian hippocampus: Why the dentate gyrus? *Learning & Memory* **20**, 710-729.

Dunlap, N. E., Benjamin, W. H., Berry, A. K., Eldridge, J. H. and Briles, D. E. (1992). A 'safe-site' for Salmonella typhimurium is within splenic polymorphonuclear cells. *Microbial Pathogenesis* **13**, 181-190.

Edison, P., Archer, H. A., Gerhard, A., Hinz, R., Pavese, N., Turkheimer, F. E., Hammers, A., Tai, Y. F., Fox, N., Kennedy, A. et al. (2008). Microglia, amyloid, and cognition in Alzheimer's disease: An 11C (R)PK11195-PET and 11C PIB-PET study. *Neurobiol Dis* **32**, 412-419.

Engelhardt, J. I., Le, W. D., Siklos, L., Obal, I., Boda, K. and Appel, S. H. (2000). Stereotaxic injection of IgG from patients with Alzheimer disease initiates injury of cholinergic neurons of the basal forebrain. *Archives of Neurology* **57**, 681-686.

Erickson, M. A., Hartvigson, P. E., Morofuji, Y., Owen, J. B., Butterfield, D. A. and Banks, W. A. (2012). Lipopolysaccharide impairs amyloid beta efflux from brain: altered vascular sequestration, cerebrospinal fluid reabsorption, peripheral clearance and transporter function at the blood–brain barrier. *J Neuroinflammation* **9**, 150-150.

Farr, S. A., Erickson, M. A., Niehoff, M. L., Banks, W. A. and Morley, J. E. (2014). Central and Peripheral Administration of Antisense Oligonucleotide Targeting Amyloid Precursor Protein Improves Learning and Memory and Reduces Neuroinflammatory Cytokines in Tg2576 (APPswe) Mice. *J Alzheimers Dis* **40**, 1005-1016.

Feng, X., Chen, A., Zhang, Y., Wang, J., Shao, L. and Wei, L. (2015). Application of dental nanomaterials: potential toxicity to the central nervous system. *International Journal of Nanomedicine* **10**, 3547-3565.

Fernandez-Vizarra, P., Lopez-Franco, O., Mallavia, B., Higuera-Matas, A., Lopez-Parra, V., Ortiz-Munoz, G., Ambrosio, E., Egido, J., Almeida, O. F. X. and Gomez-Guerrero, C. (2012). Immunoglobulin G Fc receptor deficiency prevents Alzheimer-like pathology and cognitive impairment in mice. *Brain* **135**, 2826-2837.

Freeman, G. B., Brown, T. P., Wallace, K. and Bales, K. R. (2012). Chronic Administration of an Aglycosylated Murine Antibody of Ponezumab Does Not Worsen Microhemorrhages in Aged Tg2576 Mice. *Current Alzheimer Research* **9**, 1059-1068.

Frenkel, D., Katz, O. and Solomon, B. (2000). Immunization against Alzheimer's β-amyloid plaques via EFRH phage administration. *Proceedings of the National Academy of Sciences of the United States of America* **97**, 11455-11459.

Friedman, R. L. and Moon, R. J. (1977). Hepatic clearance of Salmonella typhimurium in silica-treated mice. *Infection and Immunity* **16**, 1005-1012.

Fry, M. and Ferguson, A. V. (2007). The sensory circumventricular organs: Brain targets for circulating signals controlling ingestive behavior. *Physiology & Behavior* **91**, 413-423.

Fukuchi, K.-i., Tahara, K., Kim, H.-D., Maxwell, J. A., Lewis, T. L., Accavitti-Loper, M. A., Kim, H., Ponnazhagan, S. and Lalonde, R. (2006). Anti-Aβ single chain antibody delivery via adeno-associated virus for treatment of Alzheimer's disease. *Neurobiol Dis* **23**, 502-511.

Fuller, J. P., Stavenhagen, J. B. and Teeling, J. L. (2014). New roles for Fc receptors in neurodegeneration-the impact on Immunotherapy for Alzheimer's Disease. *Frontiers in Neuroscience* **8**.

Games, D., Adams, D., Alessandrini, R., Barbour, R., Berthelette, P., Blackwell, C., Carr, T., Clemens, J., Donaldson, T., Gillespie, F. et al. (1995). ALZHEIMER-TYPE NEUROPATHOLOGY IN TRANSGENIC MICE OVEREXPRESSING V717F BETA-AMYLOID PRECURSOR PROTEIN. *Nature* **373**, 523-527.

Garden, G. A. (2002). Microglia in human immunodeficiency virus-associated neurodegeneration. *Glia* **40**, 240-251.

Ghetie, V., Popov, S., Borvak, J., Radu, C., Matesoi, D., Medesan, C., Ober, R. J. and Ward, E. S. (1997). Increasing the serum persistence of an IgG fragment by random mutagenesis. *Nature Biotechnology* **15**, 637-640.

Giannakopoulos, P., Herrmann, F. R., Bussiere, T., Bouras, C., Kovari, E., Perl, D. P., Morrison, J. H., Gold, G. and Hof, P. R. (2003). Tangle and neuron numbers, but not amyloid load, predict cognitive status in Alzheimer's disease. *Neurology* **60**, 1495-1500.

Ginhoux, F., Greter, M., Leboeuf, M., Nandi, S., See, P., Gokhan, S., Mehler, M. F., Conway, S. J., Ng, L. G., Stanley, E. R. et al. (2010). Fate Mapping Analysis Reveals That Adult Microglia Derive from Primitive Macrophages. *Science* **330**, 841-845.

Goate, A., Chartier-Harlin, M.-C., Mullan, M., Brown, J., Crawford, F., Fidani, L., Giuffra, L., Haynes, A., Irving, N., James, L. et al. (1991). Segregation of a missense mutation in the amyloid precursor protein gene with familial Alzheimer's disease. *Nature* **349**, 704-706.

Guerreiro, R., Wojtas, A., Bras, J., Carrasquillo, M., Rogaeva, E., Majounie, E., Cruchaga, C., Sassi, C., Kauwe, J. S. K., Younkin, S. et al. (2013). TREM2 Variants in Alzheimer's Disease. *New England Journal of Medicine* **368**, 117-127.

Hammond, C. J., Hallock, L. R., Howanski, R. J., Appelt, D. M., Little, C. S. and Balin, B. J. (2010). Immunohistological detection of Chlamydia pneumoniae in the Alzheimer's disease brain. *BMC Neurosci* **11**, 121-121.

Hardy, J. and Selkoe, D. J. (2002). Medicine - The amyloid hypothesis of Alzheimer's disease: Progress and problems on the road to therapeutics. *Science* **297**, 353-356.

Hart, A. D., Wyttenbach, A., Perry, V. H. and Teeling, J. L. (2012). Age related changes in microglial phenotype vary between CNS regions: Grey versus white matter differences. *Brain Behavior and Immunity* **26**, 754-765.

Hart, B. L. (1988). Biological basis of the behavior of sick animals. *Neuroscience & Biobehavioral Reviews* **12**, 123-137.

Hawkins, B. T. and Davis, T. P. (2005). The blood-brain barrier/neurovascular unit in health and disease. *Pharmacological Reviews* **57**, 173-185.

He, Y., Le, W.-D. and Appel, S. H. (2002). Role of Fcγ Receptors in Nigral Cell Injury Induced by Parkinson Disease Immunoglobulin Injection into Mouse Substantia Nigra. *Exp Neurol* **176**, 322-327.

Hess, J., Ladel, C., Miko, D. and Kaufmann, S. H. (1996). Salmonella typhimurium aroA- infection in gene-targeted immunodeficient mice: major role of CD4+ TCR-alpha beta cells and IFN-gamma in bacterial clearance independent of intracellular location. *The Journal of Immunology* **156**, 3321-6.

Hoiseth, S. K. and Stocker, B. A. D. (1981). Aromatic-dependent Salmonella typhimurium are non-virulent and effective as live vaccines. *Nature* **291**, 238-239.

Holcomb, L., Gordon, M. N., McGowan, E., Yu, X., Benkovic, S., Jantzen, P., Wright, K., Saad, I., Mueller, R., Morgan, D. et al. (1998). Accelerated Alzheimer-type phenotype in transgenic mice carrying both mutant amyloid precursor protein and presenilin 1 transgenes. *Nature Medicine* **4**, 97-100.

Hollingworth, P. Harold, D. Sims, R. Gerrish, A. Lambert, J.-C. Carrasquillo, M. M. Abraham, R. Hamshere, M. L. Pahwa, J. S. Moskvina, V. et al. (2011). Common variants at ABCA7, MS4A6A/MS4A4E, EPHA1, CD33 and CD2AP are associated with Alzheimer's disease. *Nature Genetics* **43**, 429-+.

Hollingworth, P. H., Denise; Sims, Rebecca; Gerrish, Amy; Lambert, J.C. (2011). Common variants at ABCA7, MS4A6A/MS4A4E, EPHA1, CD33 and CD2AP are associated with Alzheimer's disease. *Nat Genet* **43**, 429-35.

Holmes, C., Boche, D., Wilkinson, D., Yadegarfar, G., Hopkins, V., Bayer, A., Jones, R. W., Bullock, R., Love, S., Neal, J. W. et al. (2008). Long-term effects of A beta(42) immunisation in Alzheimer's disease: follow-up of a randomised, placebo-controlled phase I trial. *Lancet* **372**, 216-223.

Holmes, C., Cunningham, C., Zotova, E., Culliford, D. and Perry, V. H. (2011). Proinflammatory cytokines, sickness behavior, and Alzheimer disease. *Neurology* **77**, 212-218.

Holmes, C., Cunningham, C., Zotova, E., Woolford, J., Dean, C., Kerr, S., Culliford, D. and Perry, V. H. (2009). Systemic inflammation and disease progression in Alzheimer disease. *Neurology* **73**, 768-774.

Holmes, C., El-Okl, M., Williams, A., Cunningham, C., Wilcockson, D. and Perry, V. (2003). Systemic infection, interleukin 1ß, and cognitive decline in Alzheimer's disease. *J Neurol Neurosurg Psychiatry* **74**, 788-789.

Holtzman, D. M., Fagan, A. M., Mackey, B., Tenkova, T., Sartorius, L., Paul, S. M., Bales, K., Ashe, K. H., Irizarry, M. C. and Hyman, B. T. (2000). Apolipoprotein E facilitates neuritic and cerebrovascular plaque formation in an Alzheimer's disease model. *Ann Neurol* **47**, 739-747.

Horton, H. M., Chu, S. Y., Ortiz, E. C., Pong, E., Cemerski, S., Leung, I. W. L., Jacob, N., Zalevsky, J., Desjarlais, J. R., Stohl, W. et al. (2011). Antibody-Mediated Coengagement of FcγRIIb and B Cell Receptor Complex Suppresses Humoral Immunity in Systemic Lupus Erythematosus. *The Journal of Immunology* **186**, 4223-4233.

Hsiao, K., Chapman, P., Nilsen, S., Eckman, C., Harigaya, Y., Younkin, S., Yang, F. and Cole, G. (1996). Correlative memory deficits, Abeta elevation, and amyloid plaques in transgenic mice. *Science* **274**, 99-102.

Huber, R., Deisenhofer, J., Colman, P. M., Matsushima, M. and Palm, W. (1976). Crystallographic structure studies of an IgG molecule and an Fc fragment. *Nature* **264**, 415-420.

Hulse, R. E., Swenson, W. G., Kunkler, P. E., White, D. M. and Kraig, R. P. (2008). Monomeric IgG Is Neuroprotective via Enhancing Microglial Recycling Endocytosis and TNF-alpha. *Journal of Neuroscience* **28**, 12199-12211.

Imbimbo, B. P., Ottonello, S., Frisardi, V., Solfrizzi, V., Greco, A., Seripa, D., Pilotto, A. and Panza, F. (2012). Solanezumab for the treatment of mild-to-moderate Alzheimer's disease. *Expert Review of Clinical Immunology* **8**, 135-149.

Jack, C. R., Lowe, V. J., Weigand, S. D., Wiste, H. J., Senjem, M. L., Knopman, D. S., Shiung, M. M., Gunter, J. L., Boeve, B. F., Kemp, B. J. et al. (2009). Serial PIB and MRI in normal, mild cognitive impairment and Alzheimer's disease: implications for sequence of pathological events in Alzheimer's disease. *Brain* **132**, 1355-1365.

Jaeger, L. B., Dohgu, S., Hwang, M. C., Farr, S. A., Murphy, M. P., Fleegal-DeMotta, M. A., Lynch, J. L., Robinson, S. M., Niehoff, M. L., Johnson, S. N. et al. (2009a). Testing the Neurovascular Hypothesis of Alzheimer's Disease: LRP-1 Antisense Reduces Blood-Brain Barrier Clearance, Increases Brain Levels of Amyloid-beta Protein, and Impairs Cognition. *Journal of Alzheimers Disease* **17**, 553-570.

Jaeger, L. B., Dohgu, S., Sultana, R., Lynch, J. L., Owen, J. B., Erickson, M. A., Shah, G. N., Price, T. O., Fleegal-Demotta, M. A., Butterfiled, D. A. et al. (2009b). Lipopolysaccharide alters the blood-brain barrier transport of amyloid beta protein: A mechanism for inflammation in the progression of Alzheimer's disease. *Brain Behavior and Immunity* **23**, 507-517.

James, D., Kang, S. and Park, S. (2014). Injection of β-amyloid into the hippocampus induces metabolic disturbances and involuntary weight loss which may be early indicators of Alzheimer's disease. *Aging Clinical and Experimental Research* **26**, 93-98.

Jefferis, R. and Lund, J. (2002). Interaction sites on human IgG-Fc for FcγR: current models. *Immunology Letters* **82**, 57-65.

Jones, P. T., Dear, P. H., Foote, J., Neuberger, M. S. and Winter, G. (1986). Replacing the complementarity-determining regions in a human antibody with those from a mouse. *Nature* **321**, 522-525.

Jonsson, T., Atwal, J. K., Steinberg, S., Snaedal, J., Jonsson, P. V., Bjornsson, S., Stefansson, H., Sulem, P., Gudbjartsson, D., Maloney, J. et al. (2012). A mutation in APP protects against Alzheimer's disease and age-related cognitive decline. *Nature* **488**, 96-99.

Josephs, K. A., Whitwell, J. L., Ahmed, Z., Shiung, M. M., Weigand, S. D., Knopman, D. S., Boeve, B. F., Parisi, J. E., Petersen, R. C., Dickson, D. W. et al. (2008). Beta-amyloid burden is not associated with rates of brain atrophy. *Ann Neurol* **63**, 204-12.

Jung, S. T., Reddy, S. T., Kang, T. H., Borrok, M. J., Sandlie, I., Tucker, P. W. and Georgiou, G. (2010). Aglycosylated IgG variants expressed in bacteria that selectively bind FcγRI potentiate tumor cell killing by monocyte-dendritic cells. *Proceedings of the National Academy of Sciences* **107**, 604-609.

Kam, T.-I., Song, S., Gwon, Y., Park, H., Yan, J.-J., Im, I., Choi, J.-W., Choi, T.-Y., Kim, J., Song, D.-K. et al. (2013). FcγRIIb mediates amyloid-β neurotoxicity and memory impairment in Alzheimer's disease. *The Journal of Clinical Investigation* **123**, 2791-2802.

Kathryn, S. (2002). Dosing in phase II trial of Alzheimer's vaccine suspended. *The Lancet Neurology* **1**, 3.

Katsuki, H., Nakai, S., Hirai, Y., Akaji, K., Kiso, Y. and Satoh, M. (1990). Interleukin-1-Beta inhibits long-term potentiation in the CA3 region of mouse hippocampal slices. *Eur J Pharmacol* **181**, 323-326.

Kawarabayashi, T., Younkin, L. H., Saido, T. C., Shoji, M., Ashe, K. H. and Younkin, S. G. (2001). Age-dependent changes in brain, CSF, and plasma amyloid beta protein in the Tg2576 transgenic mouse model of Alzheimer's disease. *Journal of Neuroscience* **21**, 372-381.

Kelly R, B. (2010). Brain lipid metabolism, apolipoprotein E and the pathophysiology of Alzheimer's disease. *Neuropharmacology* **59**, 295-302.

Kim, J.-K., Tsen, M.-F., Ghetie, V. and Ward, E. S. (1994). Localization of the site of the murine IgG1 molecule that is involved in binding to the murine intestinal Fc receptor. *European Journal of Immunology* **24**, 2429-2434.

Kim, J. K., Firan, M., Radu, C. G., Kim, C. H., Ghetie, V. and Ward, E. S. (1999). Mapping the site on human IgG for binding of the MHC class I-related receptor, FcRn. *European Journal of Immunology* **29**, 2819-2825.

Kitazawa, M., Oddo, S., Yamasaki, T. R., Green, K. N. and LaFerla, F. M. (2005). Lipopolysaccharide-Induced Inflammation Exacerbates Tau Pathology by a Cyclin-Dependent Kinase 5-Mediated Pathway in a Transgenic Model of Alzheimer's Disease. *The Journal of Neuroscience* **25**, 8843-8853.

Klyubin, I., Betts, V., Welzel, A. T., Blennow, K., Zetterberg, H., Wallin, A., Lemere, C. A., Cullen, W. K., Peng, Y., Wisniewski, T. et al. (2008). Amyloid beta protein dimer-containing human CSF disrupts synaptic plasticity: Prevention by systemic passive immunization. *Journal of Neuroscience* **28**, 4231-4237.

Knight, E. M., Verkhratsky, A., Luckman, S. M., Allan, S. M. and Lawrence, C. B. (2012). Hypermetabolism in a triple-transgenic mouse model of Alzheimer's disease. *Neurobiol Aging* **33**, 187-193.

Koene, H. R., Kleijer, M., Algra, J., Roos, D., E.G.Kr. von dem Borne, A. and de Haas, M. (1997). FcγRIIIa-158V/F Polymorphism Influences the Binding of IgG by Natural Killer Cell FcγRIIIa, Independently of the FcγRIIIa-48L/R/H Phenotype.

Koenigsknecht-Talboo, J., Meyer-Luehmann, M., Parsadanian, M., Garcia-Alloza, M., Finn, M. B., Hyman, B. T., Bacskai, B. J. and Holtzman, D. M. (2008). Rapid Microglial Response Around Amyloid Pathology after Systemic Anti-A beta Antibody Administration in PDAPP Mice. *Journal of Neuroscience* **28**, 14156-14164.

Komine-Kobayashi, M., Chou, N., Mochizuki, H., Nakao, A., Mizuno, Y. and Urabe, T. (2004). Dual Role of Fcγ Receptor in Transient Focal Cerebral Ischemia in Mice. *Stroke* **35**, 958-963.

Krabbe, K. S., Reichenberg, A., Yirmiya, R., Smed, A., Pedersen, B. K. and Bruunsgaard, H. (2005). Low-dose endotoxemia and human neuropsychological functions. *Brain, behavior, and immunity* **19**, 453-460.

Krstic, D., Madhusudan, A., Doehner, J., Vogel, P., Notter, T., Imhof, C., Manalastas, A., Hilfiker, M., Pfister, S., Schwerdel, C. et al. (2012). Systemic immune challenges trigger and drive Alzheimer-like neuropathology in mice. *J Neuroinflammation* **9**, 151-151.

Lacroix, S., Feinstein, D. and Rivest, S. (1998). The Bacterial Endotoxin Lipopolysaccharide has the Ability to Target the Brain in Upregulating Its Membrane CD14 Receptor Within Specific Cellular Populations. *Brain Pathology* **8**, 625-640.

Lai, A. Y. and McLaurin, J. (2010). Mechanisms of amyloid-Beta Peptide uptake by neurons: the role of lipid rafts and lipid raft-associated proteins. *Int J Alzheimers Dis* **2011**, 548380-548380.

Lambert, J. C., Heath, S., Even, G., Campion, D., Sleegers, K., Hiltunen, M., Combarros, O., Zelenika, D., Bullido, M. J., Tavernier, B. et al. (2009). Genome-wide association study identifies variants at CLU and CR1 associated with Alzheimer's disease. *Nat Genet* **41**, 1094-9.

Lambert, J. C. A. I.-V., Carla; Harold Denise, et al. (2013). Meta-analysis of 74,046 individuals identifies 11 new susceptibility loci for Alzheimer's disease. *Nat Genet*.

Landen, J. W., Zhao, Q., Cohen, S., Borrie, M., Woodward, M., Billing, C. B., Jr., Bales, K., Alvey, C., McCush, F., Yang, J. et al. (2013). Safety and Pharmacology of a Single Intravenous Dose of Ponezumab in Subjects With Mild-to-Moderate Alzheimer Disease: A Phase I, Randomized, Placebo-Controlled, Double-Blind, Dose-Escalation Study. *Clinical Neuropharmacology* **36**, 14-23.

Lazar, G. A., Dang, W., Karki, S., Vafa, O., Peng, J. S., Hyun, L., Chan, C., Chung, H. S., Eivazi, A., Yoder, S. C. et al. (2006). Engineered antibody Fc variants with enhanced effector function. *Proceedings of the National Academy of Sciences of the United States of America* **103**, 4005-4010.

Le, W. D., Rowe, D., Xie, W. J., Ortiz, I., He, Y. and Appel, S. H. (2001). Microglial activation and dopaminergic cell injury: An in vitro model relevant to Parkinson's disease. *Journal of Neuroscience* **21**, 8447-8455.

Lee, J., Lee, Y., Yuk, D., Choi, D., Ban, S., Oh, K. and Hong, J. (2008). Neuro-inflammation induced by lipopolysaccharide causes cognitive impairment through enhancement of beta-amyloid generation. *J Neuroinflammation* **5**, 37.

Li, Y. N., Qin, X. J., Kuang, F., Wu, R., Duan, M. L., Ju, G. and Wang, B. R. (2008). Alterations of Fc Gamma Receptor I and Toll-Like Receptor 4 Mediate the Antiinflammatory Actions of Microglia and Astrocytes After Adrenaline-Induced Blood-Brain Barrier Opening in Rats. *J Neurosci Res* **86**, 3556-3565.

Little, C. S., Hammond, C. J., MacIntyre, A., Balin, B. J. and Appelt, D. M. (2004). Chlamydia pneumoniae induces Alzheimer-like amyloid plaques in brains of BALB/c mice. *Neurobiol Aging* **25**, 419-429.

Liu, R., Yuan, B., Emadi, S., Zameer, A., Schulz, P., McAllister, C., Lyubchenko, Y., Goud, G. and Sierks, M. R. (2004). Single Chain Variable Fragments against β-Amyloid (Aβ) Can Inhibit Aβ Aggregation and Prevent Aβ-Induced Neurotoxicity†. *Biochemistry* **43**, 6959-6967.

Liu, S., Agalliu, D., Yu, C. and Fisher, M. (2012). The Role of Pericytes in Blood-Brain Barrier Function and Stroke. *Current Pharmaceutical Design* **18**, 3653-3662.

Lonberg, N., Taylor, L. D., Harding, F. A., Trounstine, M., Higgins, K. M., Schramm, S. R., Kuo, C.-C., Mashayekh, R., Wymore, K., McCabe, J. G. et al. (1994). Antigen-specific human antibodies from mice comprising four distinct genetic modifications. *Nature* **368**, 856-859.

Lu, J., Moochhala, S., Kaur, C. and Ling, E. A. (2001). Cellular inflammatory response associated with breakdown of the blood-brain barrier after closed head injury in rats. *J Neurotrauma* **18**, 399-408.

Lubec, G. and Engidawork, E. (2002). The brain in Down syndrome (TRISOMY 21). *Journal of Neurology* **249**, 1347-1356.

Lunnon, K., Teeling, J. L., Tutt, A. L., Cragg, M. S., Glennie, M. J. and Perry, V. H. (2011). Systemic inflammation modulates Fc receptor expression on microglia during chronic neurodegeneration. *J Immunol* **186**, 7215-24.

Luo, W., Liu, W., Hu, X., Hanna, M., Caravaca, A. and Paul, S. M. (2015). Microglial internalization and degradation of pathological tau is enhanced by an anti-tau monoclonal antibody. *Scientific Reports* **5**, 11161.

Lux, A., Yu, X., Scanlan, C. N. and Nimmerjahn, F. (2013). Impact of Immune Complex Size and Glycosylation on IgG Binding to Human FcγRs. *The Journal of Immunology* **190**, 4315-4323.

Maier, M., Seabrook, T. J., Lazo, N. D., Jiang, L. Y., Das, P., Janus, C. and Lemere, C. A. (2006). Short amyloid-beta(A beta) immunogens reduce cerebral A beta load and learning deficits in an Alzheimer's disease mouse model in the absence of an A beta-specific cellular immune response. *Journal of Neuroscience* **26**, 4717-4728.

Mancardi, D. A., Albanesi, M., Joensson, F., Iannascoli, B., Van Rooijen, N., Kang, X., England, P., Daeron, M. and Bruhns, P. (2013). The high-affinity human IgG receptor Fc gamma RI (CD64) promotes IgG-mediated inflammation, anaphylaxis, and antitumor immunotherapy. *Blood* **121**, 1563-1573.

Manos, P. J. and Wu, R. (1997). The duration of delirium in medical and postoperative patients referred for psychiatric consultation. *Annals of clinical psychiatry : official journal of the American Academy of Clinical Psychiatrists* **9**, 219-26.

Martin, J. B. (1999). Molecular Basis of the Neurodegenerative Disorders. *New England Journal of Medicine* **340**, 1970-1980.

Masliah, E., Hansen, L., Albright, T., Mallory, M. and Terry, R. D. (1991). Immunoelectron Microscopic Study of Synaptic Pathology in Alzheimers-Disease. *Acta Neuropathol* **81**, 428-433.

Masliah, E., Mallory, M., Alford, M., DeTeresa, R., Hansen, L. A., McKeel, D. W. and Morris, J. C. (2001). Altered expression of synaptic proteins occurs early during progression of Alzheimer's disease. *Neurology* **56**, 127-129.

Masters, C. L., Simms, G., Weinman, N. A., Multhaup, G., McDonald, B. L. and Beyreuther, K. (1985). Amyloid plaque core protein in alzheimer-disease and down syndrome. *Proceedings of the National Academy of Sciences of the United States of America* **82**, 4245-4249.

McCafferty, J., Griffiths, A. D., Winter, G. and Chiswell, D. J. (1990). Phage antibodies: filamentous phage displaying antibody variable domains. *Nature* **348**, 552-554.

McColl, B. W., Rothwell, N. J. and Allan, S. M. (2008). Systemic Inflammation Alters the Kinetics of Cerebrovascular Tight Junction Disruption after Experimental Stroke in Mice. *The Journal of Neuroscience* **28**, 9451-9462.

McManus, R. M., Higgins, S. C., Mills, K. H. G. and Lynch, M. A. (2014). Respiratory infection promotes T cell infiltration and amyloid-β deposition in APP/PS1 mice. *Neurobiol Aging* **35**, 109-121.

Mehlhorn, G., Hollborn, M. and Schliebs, R. (2000). Induction of cytokines in glial cells surrounding cortical β-amyloid plaques in transgenic Tg2576 mice with Alzheimer pathology. *International Journal of Developmental Neuroscience* **18**, 423-431.

Mittrücker, H. W. and Kaufmann, S. H. (2000). Immune response to infection with Salmonella typhimurium in mice. *Journal of Leukocyte Biology* **67**, 457-63.

Mohamed, H. A., Mosier, D. R., Zou, L. L., Siklos, L., Alexianu, M. E., Engelhardt, J. I., Beers, D. R., Le, W. D. and Appel, S. H. (2002). Immunoglobulin Fc gamma receptor promotes immunoglobulin uptake, immunoglobulin-mediated calcium increase, and neurotransmitter release in motor neurons. *J Neurosci Res* **69**, 110-116.

Montagne, A., Barnes, Samuel R., Sweeney, Melanie D., Halliday, Matthew R., Sagare, Abhay P., Zhao, Z., Toga, Arthur W., Jacobs, Russell E., Liu, Collin Y., Amezcua, L. et al. (2015). Blood-Brain Barrier Breakdown in the Aging Human Hippocampus. *Neuron* **85**, 296-302.

Montoyo, H. P., Vaccaro, C., Hafner, M., Ober, R. J., Mueller, W. and Ward, E. S. (2009). Conditional deletion of the MHC class I-related receptor FcRn reveals the sites of IgG homeostasis in mice. *Proceedings of the National Academy of Sciences of the United States of America* **106**, 2788-2793.

Morgan, D. (2009). The Role of Microglia in Antibody-Mediated Clearance of Amyloid-Beta from the Brain. *Cns & Neurological Disorders-Drug Targets* **8**, 7-15.

Morgan, D., Diamond, D. M., Gottschall, P. E., Ugen, K. E., Dickey, C., Hardy, J., Duff, K., Jantzen, P., DiCarlo, G., Wilcock, D. et al. (2000). A beta peptide vaccination prevents memory loss in an animal model of Alzheimer's disease. *Nature* **408**, 982-5.

Morgan, D., Gordon, M. N., Tan, J., Wilcock, D. and Rojiani, A. M. (2005). Dynamic complexity of the microglial activation response in transgenic models of amyloid deposition: implications for Alzheimer therapeutics. *J Neuropathol Exp Neurol* **64**, 743-53.

Mosser, D. M. and Edwards, J. P. (2008). Exploring the full spectrum of macrophage activation. *Nat Rev Immunol* **8**, 958-969.

Murinello, S., Mullins, R. F., Lotery, A. J., Perry, V. H. and Teeling, J. L. (2014). Fc gamma Receptor Upregulation Is Associated With Immune Complex Inflammation in the Mouse Retina and Early Age-Related Macular Degeneration. *Invest Ophthalmol Vis Sci* **55**, 247-258.

Nakahara, J., Tan-Takeuchi, K., Seiwa, C., Gotoh, M., Kaifu, T., Ujike, A., Inui, M., Yagi, T., Ogawa, M., Aiso, S. et al. (2003). Signaling via immunoglobulin Fc receptors induces oligodendrocyte precursor cell differentiation. *Dev Cell* **4**, 841-852.

Nakamura, K., Hirai, H., Torashima, T., Miyazaki, T., Tsurui, H., Xiu, Y., Ohtsuji, M., Lin, Q. S., Tsukamoto, K., Nishimura, H. et al. (2007). CD3 and immunoglobulin G Fc receptor regulate cerebellar functions. *Mol Cell Biol* **27**, 5128-5134.

Netea, M. G., van de Veerdonk, F. L., van der Meer, J. W. M., Dinarello, C. A. and Joosten, L. A. B. (2015). Inflammasome-Independent Regulation of IL-1-Family Cytokines. *Annual Review of Immunology* **33**, 49-77.

Neves, G., Cooke, S. F. and Bliss, T. V. P. (2008). Synaptic plasticity, memory and the hippocampus: a neural network approach to causality. *Nat Rev Neurosci* **9**, 65-75.

Nicolakakis, N. and Hamel, E. (2011). Neurovascular function in Alzheimer's disease patients and experimental models. *J Cereb Blood Flow Metab* **31**, 1354-1370.

Nicoll, J. A. R., Barton, E., Boche, D., Neal, J. W., Ferrer, I., Thompson, P., Vlachouli, C., Wilkinson, D., Bayer, A., Games, D. et al. (2006). A beta species removal after A beta(42) immunization. *J Neuropathol Exp Neurol* **65**, 1040-1048.

Nicoll, J. A. R., Wilkinson, D., Holmes, C., Steart, P., Markham, H. and Weller, R. O. (2003). Neuropathology of human Alzheimer disease after immunization with amyloid-beta peptide: a case report. *Nature Medicine* **9**, 448-452.

Nilsberth, C., Westlind-Danielsson, A., Eckman, C. B., Condron, M. M., Axelman, K., Forsell, C., Stenh, C., Luthman, J., Teplow, D. B., Younkin, S. G. et al. (2001). The 'Arctic' APP mutation (E693G) causes Alzheimer's disease by enhanced A beta protofibril formation. *Nature Neuroscience* **4**, 887-893.

Nimmerjahn, A., Kirchhoff, F. and Helmchen, F. (2005a). Resting microglial cells are highly dynamic surveillants of brain parenchyma in vivo. *Science* **308**, 1314-1318.

Nimmerjahn, F., Bruhns, P., Horiuchi, K. and Ravetch, J. V. (2005b). FcγRIV: A Novel FcR with Distinct IgG Subclass Specificity. *Immunity* **23**, 41-51.

Nimmerjahn, F. and Ravetch, J. V. (2005). Divergent immunoglobulin g subclass activity through selective Fc receptor binding. *Science* **310**, 1510-2.

Nimmerjahn, F. and Ravetch, J. V. (2008). Fcgamma receptors as regulators of immune responses. *Nat Rev Immunol* **8**, 34-47.

Nitsch, R. M. and Hock, C. (2008). Targeting beta-amyloid pathology in Alzheimer's disease with A beta immunotherapy. *Neurotherapeutics* **5**, 415-420.

Nyland, H., Mork, S. and Matre, R. (1984). Fc gamma receptors in multiple sclerosis brains. *Ann N Y Acad Sci* **436**, 476-479.

Ober, R. J., Martinez, C., Lai, X., Zhou, J. and Ward, E. S. (2004). Exocytosis of IgG as mediated by the receptor, FcRn: An analysis at the single-molecule level. *Proceedings of the National Academy of Sciences of the United States of America* **101**, 11076-11081.

Obregon, D., Hou, H., Bai, Y., Nikolic, W. V., Mori, T., Luo, D., Zeng, J., Ehrhart, J., Fernandez, F., Morgan, D. et al. (2008). CD40L disruption enhances A beta vaccine-mediated

reduction of cerebral amyloidosis while minimizing cerebral amyloid angiopathy and inflammation. *Neurobiol Dis* **29**, 336-353.

Oganesyan, V., Gao, C., Shirinian, L., Wu, H. and Dall'Acqua, W. F. (2008). Structural characterization of a human Fc fragment engineered for lack of effector functions. *Acta Crystallographica Section D: Biological Crystallography* **64**, 700-704.

Orgogozo, J. M., Gilman, S., Dartigues, J. F., Laurent, B., Puel, M., Kirby, L. C., Jouanny, P., Dubois, B., Eisner, L., Flitman, S. et al. (2003). Subacute meningoencephalitis in a subset of patients with AD after A beta 42 immunization. *Neurology* **61**, 46-54.

Orr, C. F., Rowe, D. B., Mizuno, Y., Mori, H. and Halliday, G. M. (2005). A possible role for humoral immunity in the pathogenesis of Parkinson's disease. *Brain* **128**, 2665-2674.

Ostrowitzki, S., Deptula, D., Thurfjell, L. and et al. (2012). MEchanism of amyloid removal in patients with alzheimer disease treated with gantenerumab. *Archives of Neurology* **69**, 198-207.

Paolicelli, R. C., Bolasco, G., Pagani, F., Maggi, L., Scianni, M., Panzanelli, P., Giustetto, M., Ferreira, T. A., Guiducci, E., Dumas, L. et al. (2011). Synaptic Pruning by Microglia Is Necessary for Normal Brain Development. *Science* **333**, 1456-1458.

Parekh, R. B., Dwek, R. A., Sutton, B. J., Fernandes, D. L., Leung, A., Stanworth, D., Rademacher, T. W., Mizuochi, T., Taniguchi, T., Matsuta, K. et al. (1985). ASSOCIATION OF RHEUMATOID-ARTHRITIS AND PRIMARY OSTEO-ARTHRITIS WITH CHANGES IN THE GLYCOSYLATION PATTERN OF TOTAL SERUM IGG. *Nature* **316**, 452-457.

Peress, N. S., Fleit, H. B., Perillo, E., Kuljis, R. and Pezzullo, C. (1993). Identifcation of Fc gamma RI, II and III on normal human brain ramified microglia in senile plaques in Alzheimer's Disease. *Journal of Neuroimmunology* **48**, 71-80.

Perl, D. P. (2010). Neuropathology of Alzheimer's Disease. *Mount Sinai Journal of Medicine* **77**, 32-42.

Perrin, R. J., Fagan, A. M. and Holtzman, D. M. (2009). Multimodal techniques for diagnosis and prognosis of Alzheimer's disease. *Nature* **461**, 916-922.

Pfeifer, M., Boncristiano, S., Bondolfi, L., Stalder, A., Deller, T., Staufenbiel, M., Mathews, P. M. and Jucker, M. (2002). Cerebral hemorrhage after passive anti-A beta immunotherapy. *Science* **298**, 1379-1379.

Plata-Salaman, C. R. (1998). Cytokine-Induced Anorexia: Behavioral, Cellular, and Molecular Mechanismsa. *Ann N Y Acad Sci* **856**, 160-170.

Poduslo, J. F., Curran, G. L. and Berg, C. T. (1994). MACROMOLECULAR PERMEABILITY ACROSS THE BLOOD-NERVE AND BLOOD-BRAIN BARRIERS. *Proceedings of the National Academy of Sciences of the United States of America* **91**, 5705-5709.

Puentener, U., Booth, S. G., Perry, V. H. and Teeling, J. L. (2012). Long-term impact of systemic bacterial infection on the cerebral vasculature and microglia. *J Neuroinflammation* **9**.

Raghavan, M., Bonagura, V. R., Morrison, S. L. and Bjorkman, P. J. (1995). Analysis of the pH Dependence of the Neonatal Fc Receptor/Immunoglobulin G Interaction Using Antibody and Receptor Variants. *Biochemistry* **34**, 14649-14657.

Ravetch, J. V. and Bolland, S. (2001). IgG Fc receptors. *Annual Review of Immunology* **19**, 275-290.

Reisberg, B., Doody, R., Stoffler, A., Schmitt, F., Ferris, S., Mobius, H. J. and Memantine Study, G. (2003). Memantine in moderate-to-severe Alzheimer's disease. *New England Journal of Medicine* **348**, 1333-1341.

Richards, J. O., Karki, S., Lazar, G. A., Chen, H., Dang, W. and Desjarlais, J. R. (2008). Optimization of antibody binding to FcγRIIa enhances macrophage phagocytosis of tumor cells. *Molecular Cancer Therapeutics* **7**, 2517-2527.

Rinne, J. O., Brooks, D. J., Rossor, M. N., Fox, N. C., Bullock, R., Klunk, W. E., Mathis, C. A., Blennow, K., Barakos, J., Okello, A. A. et al. (2010). (11)C-PiB PET assessment of change in fibrillar amyloid-beta load in patients with Alzheimer's disease treated with bapineuzumab: a phase 2, double-blind, placebo-controlled, ascending-dose study. *Lancet Neurology* **9**, 363-372.

Rogers, J., Lubernarod, J., Styren, S. D. and Civin, W. H. (1988). EXPRESSION OF IMMUNE SYSTEM-ASSOCIATED ANTIGENS BY CELLS OF THE HUMAN CENTRAL NERVOUS-SYSTEM - RELATIONSHIP TO THE PATHOLOGY OF ALZHEIMERS-DISEASE. *Neurobiol Aging* **9**, 339-349.

Rogers, J., Mastroeni, D., Leonard, B., Joyce, J. and Grover, A. (2007). Neuroinflammation in alzheimer's disease and Parkinson's disease: Are microglia pathogenic in either disorder? In *Neuroinflammation in Neuronal Death and Repair*, vol. 82 (ed. G. C. M. T. L. S. A. Bagetta), pp. 235-246.

Roopenian, D. C. and Akilesh, S. (2007). FcRn: the neonatal Fc receptor comes of age. *Nat Rev Immunol* **7**, 715-25.

Ross, F. M., Allan, S. M., Rothwell, N. J. and Verkhratsky, A. (2003). A dual role for interleukin-1 in LTP in mouse hippocampal slices. *Journal of Neuroimmunology* **144**, 61-67.

Rother, R. P., Rollins, S. A., Mojcik, C. F., Brodsky, R. A. and Bell, L. (2007). Discovery and development of the complement inhibitor eculizumab for the treatment of paroxysmal nocturnal hemoglobinuria. *Nat Biotech* **25**, 1256-1264.

Sagar, S. M., Price, K. J., Kasting, N. W. and Sharp, F. R. (1995). Anatomic patterns of FOS immunostaining in rat brain following systemic endotoxin administration. *Brain Res Bull* **36**, 381-392.

Salloway, S., Sperling, R., Fox, N. C., Blennow, K., Klunk, W., Raskind, M., Sabbagh, M., Honig, L. S., Porsteinsson, A. P., Ferris, S. et al. (2014). Two Phase 3 Trials of Bapineuzumab in Mild-to-Moderate Alzheimer's Disease. *New England Journal of Medicine* **370**, 322-333.

Salloway, S. P., Black, R., Sperling, R., Fox, N., Gilman, S., Schenk, D. and Grundman, M. (2010). A phase 2 multiple ascending dose trial of bapineuzumab in mild to moderate Alzheimer Disease Reply. *Neurology* **74**, 2026-2027.

SantaCruz, K., Lewis, J., Spires, T., Paulson, J., Kotilinek, L., Ingelsson, M., Guimaraes, A., DeTure, M., Ramsden, M., McGowan, E. et al. (2005). Tau suppression in a neurodegenerative mouse model improves memory function. *Science* **309**, 476-481.

Schenk, D. (2002). Amyloid-beta immunotherapy for Alzheimer's disease: the end of the beginning. *Nature Reviews Neuroscience* **3**, 824-828.

Schenk, D., Barbour, R., Dunn, W., Gordon, G., Grajeda, H., Guido, T., Hu, K., Huang, J. P., Johnson-Wood, K., Khan, K. et al. (1999). Immunization with amyloid-beta attenuates Alzheimer disease-like pathology in the PDAPP mouse. *Nature* **400**, 173-177.

Schlachetzki, F., Zhu, C. N. and Pardridge, W. M. (2002). Expression of the neonatal Fc receptor (FcRn) at the blood-brain barrier. *J Neurochem* **81**, 203-206.

Senechal, Y., Kelly, P. H. and Dev, K. K. (2008). Amyloid precursor protein knockout mice show age-dependent deficits in passive avoidance learning. *Behavioural Brain Research* **186**, 126-132.

Serpell, L. C. (2000). Alzheimer's amyloid fibrils: structure and assembly. *Biochimica et Biophysica Acta (BBA) - Molecular Basis of Disease* **1502**, 16-30.

Sheng, J., Bora, S., Xu, G., Borchelt, D., Price, D. and Koliatsos, V. (2003a). Lipopolysaccharide-induced-neuroinflammation increases intracellular accumulationof amyloid precursor protein and amyloid beta peptide in APPswe transgenic mice. *Neurobiol Dis* **14**, 133 - 145.

Sheng, J. G., Bora, S. H., Xu, G., Borchelt, D. R., Price, D. L. and Koliatsos, V. E. (2003b). Lipopolysaccharide-induced-neuroinflammation increases intracellular accumulation of amyloid precursor protein and amyloid β peptide in APPswe transgenic mice. *Neurobiol Dis* **14**, 133-145.

Shields, R. L., Lai, J., Keck, R., O'Connell, L. Y., Hong, K., Meng, Y. G., Weikert, S. H. A. and Presta, L. G. (2002). Lack of fucose on human IgG1 N-linked oligosaccharide improves binding to human Fc gamma RIII and antibody-dependent cellular toxicity. *Journal of Biological Chemistry* **277**, 26733-26740.

Shields, R. L., Namenuk, A. K., Hong, K., Meng, Y. G., Rae, J., Briggs, J., Xie, D., Lai, J., Stadlen, A., Li, B. et al. (2001). High Resolution Mapping of the Binding Site on Human IgG1 for FcγRI, FcγRII, FcγRIII, and FcRn and Design of IgG1 Variants with Improved Binding to the FcγR. *Journal of Biological Chemistry* **276**, 6591-6604.

Shinkawa, T., Nakamura, K., Yamane, N., Shoji-Hosaka, E., Kanda, Y., Sakurada, M., Uchida, K., Anazawa, H., Satoh, M., Yamasaki, M. et al. (2003). The absence of fucose but not the presence of galactose or bisecting N-acetylglucosamine of human IgG1 complex-type oligosaccharides shows the critical role of enhancing antibody-dependent cellular cytotoxicity. *Journal of Biological Chemistry* **278**, 3466-3473.

Shoji, M., Harigaya, Y., Matsubara, E., Kawarabayashi, T., Murakami, T., Oomori, N., Sato, K., Nagano, I. and Abe, K. (2003). A beta 42 vaccine on the Tg2576 Alzheimer model mice. *Molecular Mechanisms and Epochal Therapeutics of Ischemic Stroke and Dementia* **1252**, 399-403.

Sly, L. M., Krzesicki, R. F., Brashler, J. R., Buhl, A. E., McKinley, D. D., Carter, D. B. and Chin, J. E. (2001). Endogenous brain cytokine mRNA and inflammatory responses to lipopolysaccharide are elevated in the Tg2576 transgenic mouse model of Alzheimer's disease. *Brain Res Bull* **56**, 581-588.

Solomon, B., Koppel, R., Hanan, E. and Katzav, T. (1996). Monoclonal antibodies inhibit in vitro fibrillar aggregation of the Alzheimer beta-amyloid peptide. *Proceedings of the National Academy of Sciences of the United States of America* **93**, 452-455.

Sondermann, P., Huber, R., Oosthuizen, V. and Jacob, U. (2000). The 3.2-[angst] crystal structure of the human IgG1 Fc fragment-Fc[gamma]RIII complex. *Nature* **406**, 267-273.

Soscia, S. J., Kirby, J. E., Washicosky, K. J., Tucker, S. M., Ingelsson, M., Hyman, B., Burton, M. A., Goldstein, L. E., Duong, S., Tanzi, R. E. et al. (2010). The Alzheimer's Disease-Associated Amyloid β-Protein Is an Antimicrobial Peptide. *PLoS One* **5**, e9505.

Stein, P. S., Steffen, M. J., Smith, C., Jicha, G., Ebersole, J. L., Abner, E. and Dawson, D. (2012). Serum antibodies to periodontal pathogens are a risk factor for Alzheimer's disease. *Alzheimers Dement* **8**, 196-203.

Stellwagen, D. and Malenka, R. C. (2006). Synaptic scaling mediated by glial TNF-alpha. *Nature* **440**, 1054-1059.

Stewart, W. F., Kawas, C., Corrada, M. and Metter, E. J. (1997). Risk of Alzheimer's disease and duration of NSAID use. *Neurology* **48**, 626-632.

Storandt, M., Head, D., Fagan, A. M., Holtzman, D. M. and Morris, J. C. Toward a multifactorial model of Alzheimer disease. *Neurobiol Aging*.

Strittmatter, W. J. and Roses, A. D. (1995). Apolipoprotein E and Alzheimer's disease. *Proceedings of the National Academy of Sciences of the United States of America* **92**, 4725-4727.

SturchlerPierrat, C., Abramowski, D., Duke, M., Wiederhold, K. H., Mistl, C., Rothacher, S., Ledermann, B., Burki, K., Frey, P., Paganetti, P. A. et al. (1997). Two amyloid precursor protein transgenic mouse models with Alzheimer disease-like pathology. *Proceedings of the National Academy of Sciences of the United States of America* **94**, 13287-13292.

Sudduth, T. L., Greenstein, A. and Wilcock, D. M. (2013). Intracranial Injection of Gammagard, a Human IVIg, Modulates the Inflammatory Response of the Brain and Lowers A beta in APP/PS1 Mice Along a Different Time Course than Anti-A beta Antibodies. *Journal of Neuroscience* **33**, 9684-9692.

Suzuki, N., Cheung, T. T., Cai, X. D., Odaka, A., Otvos, L., Eckman, C., Golde, T. E. and Younkin, S. G. (1994). AN INCREASED PERCENTAGE OF LONG AMYLOID-BETA PROTEIN SECRETED BY FAMILIAL AMYLOID-BETA PROTEIN-PRECURSOR (BETA-APP(717)) MUTANTS. *Science* **264**, 1336-1340.

Szekely, C. A., Thorne, J. E., Zandi, P. P., Ek, M., Messias, E., Breitner, J. C. S. and Goodman, S. N. (2004). Nonsteroidal anti-inflammatory drugs for the prevention of Alzheimer's disease: a systematic review. *Neuroepidemiology* **23**, 159-169.

Takai, T., Li, M., Sylvestre, D., Clynes, R. and Ravetch, J. V. (1994). FCR GAMMA-CHAIN DELETION RESULTS IN PLEIOTROPIC EFFECTOR CELL DEFECTS. *Cell* **76**, 519-529.

Tariot Pn, F. M. R. G. G. T. (2004). Memantine treatment in patients with moderate to severe alzheimer disease already receiving donepezil: A randomized controlled trial. *JAMA* **291**, 317-324.

Teeling, J. L., Carare, R. O., Glennie, M. J. and Perry, V. H. (2012). Intracerebral immune complex formation induces inflammation in the brain that depends on Fc receptor interaction. *Acta Neuropathol* **124**, 479-490.

Teeling, J. L., Cunningham, C., Newman, T. A. and Perry, V. H. (2010). The effect of non-steroidal anti-inflammatory agents on behavioural changes and cytokine production following systemic inflammation: Implications for a role of COX-1. *Brain, behavior, and immunity* **24**, 409-419.

Thornton, P., Pinteaux, E., Allan, S. M. and Rothwell, N. J. (2008). Matrix metalloproteinase-9 and urokinase plasminogen activator mediate interleukin-1-induced neurotoxicity. *Molecular and Cellular Neuroscience* **37**, 135-142.

Tilling, T., Korte, D., Hoheisel, D. and Galla, H.-J. (1998). Basement Membrane Proteins Influence Brain Capillary Endothelial Barrier Function In Vitro. *J Neurochem* **71**, 1151-1157.

Tolnay, M. and Probst, A. (1999). REVIEW: tau protein pathology in Alzheimer's disease and related disorders. *Neuropathol Appl Neurobiol* **25**, 171-187.

Tucsek, Z., Toth, P., Sosnowska, D., Gautam, T., Mitschelen, M., Koller, A., Szalai, G., Sonntag, W. E., Ungvari, Z. and Csiszar, A. (2014). Obesity in Aging Exacerbates Blood–Brain Barrier Disruption, Neuroinflammation, and Oxidative Stress in the Mouse Hippocampus: Effects on Expression of Genes Involved in Beta-Amyloid Generation and Alzheimer's Disease. *The Journals of Gerontology Series A: Biological Sciences and Medical Sciences* **69**, 1212-1226.

Ulvestad, E., Williams, K., Vedeler, C., Antel, J., Nyland, H., Mork, S. and Matre, R. (1994). Reactive microglia in multiple sclerosis lesions have an increased expression of receptors for the Fc part of IgG. *J Neurol Sci* **121**, 125-131.

Um, J. W., Nygaard, H. B., Heiss, J. K., Kostylev, M. A., Stagi, M., Vortmeyer, A., Wisniewski, T., Gunther, E. C. and Strittmatter, S. M. (2012). Alzheimer amyloid-beta oligomer bound to postsynaptic prion protein activates Fyn to impair neurons. *Nature Neuroscience* **15**, 1227-U85.

van der Poel, C. E., Karssemeijer, R. A., Boross, P., van der Linden, J. A., Blokland, M., van de Winkel, J. G. J. and Leusen, J. H. W. (2010). Cytokine-induced immune complex binding to the high-affinity IgG receptor, FcγRI, in the presence of monomeric IgG.

van der Poel, C. E., Spaapen, R. M., van de Winkel, J. G. J. and Leusen, J. H. W. (2011). Functional Characteristics of the High Affinity IgG Receptor, FcγRI. *The Journal of Immunology* **186**, 2699-2704.

van Vugt, M. J., Kleijmeer, M. J., Keler, T., Zeelenberg, I., van Dijk, M. A., Leusen, J. H. W., Geuze, H. J. and van de Winkel, J. G. J. (1999). The FcγRIa (CD64) Ligand Binding Chain Triggers Major Histocompatibility Complex Class II Antigen Presentation Independently of Its Associated FcR γ-Chain.

Vassiloyanakopoulos, A. P., Okamoto, S. and Fierer, J. (1998). The crucial role of polymorphonuclear leukocytes in resistance to Salmonella dublin infections in genetically susceptible and resistant mice. *Proceedings of the National Academy of Sciences of the United States of America* **95**, 7676-7681.

Wang, H., Yu, M., Ochani, M., Amella, C. A., Tanovic, M., Susarla, S., Li, J. H., Wang, H., Yang, H., Ulloa, L. et al. (2003). Nicotinic acetylcholine receptor [alpha]7 subunit is an essential regulator of inflammation. *Nature* **421**, 384-388.

Watkins, L. R., Goehler, L. E., Relton, J. K., Tartaglia, N., Silbert, L., Martin, D. and Maier, S. F. (1995). Blockade of interleukin-1 induced hyperthermia by subdiaphragmatic vagotomy: evidence for vagal mediation of immune-brain communication. *Neurosci Lett* **183**, 27-31.

Watt, A. D., Crespi, G. A. N., Down, R. A., Ascher, D. B., Gunn, A., Perez, K. A., McLean, C. A., Villemagne, V. L., Parker, M. W., Barnham, K. J. et al. (2014). Do current therapeutic anti-A beta antibodies for Alzheimer's disease engage the target? *Acta Neuropathol* **127**, 803-810.

Westerman, M. A., Cooper-Blacketer, D., Mariash, A., Kotilinek, L., Kawarabayashi, T., Younkin, L. H., Carlson, G. A., Younkin, S. G. and Ashe, K. H. (2002). The relationship between A beta and memory in the Tg2576 mouse model of Alzheimer's disease. *Journal of Neuroscience* **22**, 1858-1867.

Wilcock, D. M., Alamed, J., Gottschall, P. E., Grimm, J., Rosenthal, A., Pons, J., Ronan, V., Symmonds, K., Gordon, M. N. and Morgan, D. (2006). Deglycosylated anti-amyloid-beta antibodies eliminate cognitive deficits and reduce parenchymal amyloid with minimal vascular consequences in aged amyloid precursor protein transgenic mice. *J Neurosci* **26**, 5340-6.

Wilcock, D. M., DiCarlo, G., Henderson, D., Jackson, J., Clarke, K., Ugen, K. E., Gordon, M. N. and Morgan, D. (2003). Intracranially administered anti-Abeta antibodies reduce beta-amyloid deposition by mechanisms both independent of and associated with microglial activation. *J Neurosci* **23**, 3745-51.

Wilcock, D. M., Morgan, D., Gordon, M. N., Taylor, T. L., Ridnour, L. A., Wink, D. A. and Colton, C. A. (2011a). Activation of matrix metalloproteinases following anti-Abeta immunotherapy; implications for microhemorrhage occurrence. *J Neuroinflammation* **8**, 115.

Wilcock, D. M., Munireddy, S. K., Rosenthal, A., Ugen, K. E., Gordon, M. N. and Morgan, D. (2004a). Microglial activation facilitates Abeta plaque removal following intracranial anti-Abeta antibody administration. *Neurobiol Dis* **15**, 11-20.

Wilcock, D. M., Rojiani, A., Rosenthal, A., Levkowitz, G., Subbarao, S., Alamed, J., Wilson, D., Wilson, N., Freeman, M. J., Gordon, M. N. et al. (2004b). Passive amyloid immunotherapy clears amyloid and transiently activates microglia in a transgenic mouse model of amyloid deposition. *J Neurosci* **24**, 6144-51.

Wilcock, D. M., Rojiani, A., Rosenthal, A., Subbarao, S., Freeman, M. J., Gordon, M. N. and Morgan, D. (2004c). Passive immunotherapy against Abeta in aged APP-transgenic mice reverses cognitive deficits and depletes parenchymal amyloid deposits in spite of increased vascular amyloid and microhemorrhage. *J Neuroinflammation* **1**, 24.

Wilcock, D. M., Zhao, Q., Morgan, D., Gordon, M. N., Everhart, A., Wilson, J. G., Lee, J. E. and Colton, C. A. (2011b). Diverse inflammatory responses in transgenic mouse models of Alzheimer's disease and the effect of immunotherapy on these responses. *ASN Neuro* **3**, 249-58.

Wisniewski, H. M., Bancher, C., Barcikowska, M., Wen, G. Y. and Currie, J. (1989). Spectrum of morphological appearance of amyloid deposits in Alzheimer's disease. *Acta Neuropathol* **78**, 337-347.

Wolak, D. J., Pizzo, M. E. and Thorne, R. G. (2015). Probing the extracellular diffusion of antibodies in brain using in vivo integrative optical imaging and ex vivo fluorescence imaging. *Journal of Controlled Release* **197**, 78-86.

Yang, L., Lindholm, K., Konishi, Y., Li, R. and Shen, Y. (2002). Target Depletion of Distinct Tumor Necrosis Factor Receptor Subtypes Reveals Hippocampal Neuron Death and Survival through Different Signal Transduction Pathways. *The Journal of Neuroscience* **22**, 3025-3032.

Yuasa, T., Kubo, S., Yoshino, T., Ujike, A., Matsumura, K., Ono, M., Ravetch, J. V. and Takai, T. (1999). Deletion of Fc gamma receptor IIB renders H-2(b) mice susceptible to collagen-induced arthritis. *Journal of Experimental Medicine* **189**, 187-194.

Zago, W., Buttini, M., Comery, T. A., Nishioka, C., Gardai, S. J., Seubert, P., Games, D., Bard, F., Schenk, D. and Kinney, G. G. (2012). Neutralization of Soluble, Synaptotoxic Amyloid β Species by Antibodies Is Epitope Specific. *The Journal of Neuroscience* **32**, 2696-2702.

Zago, W., Schroeter, S., Guido, T., Khan, K., Seubert, P., Yednock, T., Schenk, D., Gregg, K. M., Games, D., Bard, F. et al. (2013). Vascular alterations in PDAPP mice after anti-Aβ immunotherapy: Implications for amyloid-related imaging abnormalities. *Alzheimer's & Dementia*.

Zhang, Y. and Pardridge, W. M. (2001). Mediated efflux of IgG molecules from brain to blood across the blood-brain barrier. *Journal of Neuroimmunology* **114**, 168-172.

Zlokovic, B. V. (2008). The Blood-Brain Barrier in Health and Chronic Neurodegenerative Disorders. *Neuron* **57**, 178-201.

Zotova, E., Bharambe, V., Cheaveau, M., Morgan, W., Holmes, C., Harris, S., Neal, J. W., Love, S., Nicoll, J. A. R. and Boche, D. (2013). Inflammatory components in human Alzheimer's disease and after active amyloid-beta(42) immunization. *Brain* **136**, 2677-2696.

Zotova, E., Holmes, C., Johnston, D., Neal, J. W., Nicoll, J. A. and Boche, D. (2011). Microglial alterations in human Alzheimer's disease following Abeta42 immunization. *Neuropathol Appl Neurobiol* **37**, 513-24.